Michaël Becidan

Experimental Studies on Municipal Solid Waste and Biomass Pyrolysis

Thesis for the degree of doctor philosophiae

Trondheim, May 2007

Norwegian University of
Science and Technology
Faculty of Engineering Science and Technology
Department of Energy and Process Technology

NTNU
Innovation and Creativity

NTNU
Norwegian University of Science and Technology

Thesis for the degree of doctor philosophiae

Faculty of Engineering Science and Technology
Department of Energy and Process Technology

ISBN 978-82-471-2744-5 (printed ver.)
ISBN 978-82-471-2758-2 (electronic ver.)
ISSN 1503-8181

Theses at NTNU, 2007:125

Printed by Tapir Uttrykk

Preface

This thesis is submitted in partial fulfilment of the requirements for the degree “Doctor of Philosophy” at the Norwegian University of Science and Technology (NTNU), Trondheim, Norway.

The work was carried out at the Faculty of Engineering Science and Technology at the Department of Energy and Process Engineering, with Professor Johan E. Hustad and Dr. Øyvind Skreiberg as supervisors.

This work has been part of the “Environment and Process Management” research program funded by the Research Council of Norway and carried out in cooperation with SINTEF Energy Research, SINTEF Materials and Chemistry and several industrial partners. The author also expresses his gratitude to the Nordic Graduate School of Biofuels Science and Technology (biofuelsGS) for providing financial support.

Acknowledgements

I would like to thank my supervisors Johan E. Hustad and Øyvind Skreiberg. Through these years, your guidance, your support, your thoroughness and your kindness have been constant. You were always there for me when I needed you. A big thank to my co-workers in the laboratory, Willy Horrigmo and Roger Khalil, your professionalism and your expertise are deeply appreciated. I also want to thank Professor Gábor Várhegyi warmly; I learned a lot working with you.

A special thanks to my best friend Dr. Rehan Naqvi. Without your presence, this endeavour would not have been the same.

I would like to express my gratitude to my family in France, my mother Gisèle, my father Simon and my beloved brothers David and Benjamin. Nothing would be possible without you.

Finally, thousand thanks to my Norwegian family: Maria, the woman in my life, and Ava, our daughter, who luckily decided to sleep and smile through most of 2006-2007.

Pour ma maman, Gisèle

Table of Contents

Motivation and Methodology

MSW and biomass are seen as alternatives to fossil fuels because they are sustainable and CO_2-neutral. However, technical, operating and environmental challenges remain to further optimise thermal processes so that bioenergy can be extensively implemented at a large industrial scale.
Different aspects of MSW/biomass thermal treatment have been investigated in a series of papers in this thesis in addition to the introduction given in Chapters 1-9.
In order to study several of these challenges, an in-house designed experimental set-up was developed and associated with advanced measurement techniques (FTIR and GC). The results addressed can be grouped into three areas (Chapters 6, 7 and 8): N-chemistry, pyrolysis and degradation characteristics. These areas were discussed in a series of 6 papers (referred to as Paper I, II, III, IV, V and VI).
The introductory part of this thesis also contains an extensive and critical literature study, with a focus on nitrogen (N).

Executive Summary

The **introduction of this thesis** (Chapters 1-9) presents the broader picture of waste management and thermal treatments (situation, trends and novel concepts) with a strong focus on nitrogen (N) in Chapter 6 (a summary of this chapter can be found on page 42). A new insight on N-functionalities is presented, mostly based on plant physiology publications widely ignored by the bioenergy world. N in biomass is found in a variety of chemical compounds and not only in protein compounds. An extensive literature survey concerning N-chemistry during pyrolysis of model compounds and biomass has also been done. A critical light is cast on these studies.

Paper I (or P-I) ([Becidan 2004]) presents preliminary results using the experimental set-up and shows its potential in thermal studies. The study of N-release was twofold: NOx release during combustion of biomass and NOx precursors (NH_3 and HCN) release during pyrolysis of sewage sludge. The main results confirm known trends: N-release during combustion decreases with increasing fuel-N content; N-release as NH_3 and HCN during pyrolysis is clearly dependent on temperature with increasing release with increasing temperature and NH_3 as the main component at all conditions.

Paper II (or P-II) ([Skreiberg 2004]) presents modelling work realised to assess the potential for reduction of NOx emission formed from fuel-N by implementing staged air combustion. The results obtained from these chemical analysis of ideal reactors (Plug Flow Reactor and Perfectly Stirred Reactor) can be seen as a simplified CFD approach. The reduction potential is depending on a variety of factors and will therefore have to be assessed on a case-to-case basis. However, some conclusions can be drawn: (1) PSR mixing conditions are more favourable than PFR flow; (2) increasing fuel-N content will increase the relative NOx reduction potential; (3) increasing fuel-N fraction of NH_3, or HNCO, compared to HCN will increase the NOx reduction potential; (4) increasing amounts of CO, and H_2, will increase the NOx reduction potential, but it depends also on the fuel-N compounds; (5) one primary air stage is sufficient, unless also the fuel supply

is staged. It is possible to further increase the NOx reduction with more primary air stages at some conditions, but the increase is limited; (6) increasing overall excess air ratio will decrease the NOx reduction potential; (7) increasing residence time will only significantly increase the NOx reduction potential until the main chemistry is completed. However, the time for completion of the main chemistry is significantly longer in a PSR compared to a PFR, and the effect of an increasing residence time is much more pronounced at optimum conditions in a PSR; (8) temperature is an important parameter. However, for a specific set of other parameters there exists an optimum temperature. The temperature in the primary air stage should be high enough to complete the main chemistry. The temperature needed to complete the main chemistry, and the fuel-N chemistry, in a PSR is higher than in a PFR for the same residence time. The temperature in the secondary air stage should be as low as possible, but high enough to ensure complete combustion.

Paper III (or P-III) ([Becidan 2007a]) looks at the products distribution and the main pyrolysis products of thermally thick and scarcely studied biomass residues samples. For all fuels, higher temperatures favour gas yield at the expense of char and liquid yields. High heating rate also promotes gas yield. The main gas components were CO_2, CO, CH_4, H_2, C_2H_2, C_2H_6 and C_2H_4. An increase in temperature and heating rate leads to increasing yields for all the gases up to 825-900°C where CO_2 and hydrocarbons yields show a clear tendency to stabilise, increase slightly or decrease slightly depending on the fuel. The gas release dynamics reveal important information about the thermal behaviour of the various components (cellulose, hemicellulose and lignin) of the biomass and are consistent with studies using TGA. The gross calorific value of the gas produced increases with increasing temperature reaching a plateau at 750-900°C. This study provides valuable data of the thermal behaviour of thermally thick biomass samples which is of interest for further work in the area of combustion, gasification and pyrolysis in fixed beds. The study confirms the potential of those unexploited residues for production of energy carriers through pyrolysis.

Paper IV (or P-IV) ([Becidan 2007b]) proposes a more extensive study of N-release from 3 biomass residues (coffee waste, brewer spent grains, fibreboard). This study of N-behaviour during biomass pyrolysis of thermally thick samples provided several findings. At high heating rate, NH_3 and HCN are the two N-containing compounds, NH_3 being the main one at all conditions; NH_3 release increases with increasing heating rate and temperature to reach a maximum at 825-900°C while HCN yield increases sharply with temperature without reaching a plateau in the temperature range studied. N-selectivity, N release pattern and N-compounds thermal behaviour are affected by the fuel properties, in all probability including N-functionalities. While the total N-conversion levels to ($HCN+NH_3$) are similar for all fuels at high heating rate, the differences are very significant at low heating rate (more than 2-fold for NH_3 and 3-fold for HCN). This can be related to the different fuel properties including N-functionalities. Several attempts have been made previously to correlate N-functionalities and N-release during pyrolysis. However no clear dependence has ever been established for biomass. Furthermore, the intricate and versatile nature of N in biomass samples and its interactions with hemicellulose, cellulose and lignin prior to and during pyrolysis are difficult to elucidate.

A mechanism of cross-linking between a protein side group and cellulose during pyrolysis was proposed. Further work should focus on the use of the data obtained for improved modelling of biomass pyrolysis. In order to obtain more mechanistic insights the study of model compounds seems more appropriate but may have limited validity because of the intricate structure of "real" biomass. These two types of studies are therefore complementary to obtain a good overview of N-release.

Paper V (or P-V) ([Becidan 2007c]) presents the kinetics of decomposition of the three afore-mentioned biomass residues. The results can be summarised as such:
(1) The samples were studied at five different *T(t)* temperature programs. The temperature programs covered a wide range of experimental conditions: the experiments exhibited 10 – 14 times variation in time span, mean reaction rate and peak reaction rate. The experiments on a given sample were described by the same set of model parameters. The optimal parameters were determined by the method of least squares. Three models were proposed that described equally well the behavior of the samples in the range of observations.
(2) A model built from three distributed activation energy reactions was suitable to describe the devolatilisation at the highly different *T(t)* functions of our study with only 12 adjustable parameters. The other two models contained simpler mathematical equations (first order and *n*th order partial reactions, respectively), accordingly their use may be more convenient when the coupling of kinetic and transport equations are needed. On the other hand, the simpler models needed higher numbers of parameters to describe the complexity of these wastes
(3) The reliability of the proposed models was tested in three ways: (i) the models provided good fits for all the five experiments of a sample; (ii) the evaluation of a narrower subset of the experiments (the three slowest experiments) provided approximately the same parameters as the evaluation of the whole series of experiments; (iii) the models proved to be suitable to predict the behavior of the samples outside of those experimental conditions at which the model parameters were determined. Check (iii) corresponded to an extrapolation to ca. four-time higher reaction rates from the domain of the three slowest experiments.
(4) The evaluated experiments included "constant reaction rate" (CRR) measurements. This type of temperature control involves a continuously changing heating rate. The simultaneous evaluation of linear, stepwise and CRR experiments proved to be advantageous in the determination of reliable kinetic models.
(5) The samples had very different chemical compositions. Nevertheless, the same models described them equally well. Accordingly, the models and the strategies for their evaluation and validation can be recommended for a wider range of biomass studies.

Paper VI (or P-VI) ([Becidan 2007d]), this study on thermally thick biomass samples pyrolysis has investigated (1) temperature field, (2) weight loss at two scales (TGA and macro-TGA). The main findings are:
(a) Qualitative evaluation of the thermal history: three temperature regimes have been identified: (1) exponentially increasing temperature, (2) linearly increasing temperature (3) 2-slope increasing temperature with a flattening period. The regime at a given point will depend on the sample weight, the reactor temperature and the location in the sample.

(b) Quantitative evaluation of the thermal history: significant temperature gradients were measured, with a maximum radial gradient of 167°C/cm for coffee waste at a reactor temperature of 900°C. This will affect the pyrolysis process.
(c) The step-by-step pyrolysis chemistry was described and discussed (10°C/min heating rate). By use of a novel concept, i.e. intra-sample heating rate, the exothermic step of pyrolysis was shown. It is related to char and/or char-forming reactions.
(d) The comparative study of weight loss in TGA and macro-TGA (10°C/min heating rate, never done before to our knowledge) was performed to investigate the "scaling effect". Pyrolysis time and pyrolysis rate differences were characterised and quantified.

Abbreviations

A	Absorbance
a.a.	Amino Acids
BAT	Best Available Technique
daf	dry ash free
DKP	Diketopiperazine
DNA	Deoxyribonucleic Acid
E	Activation Energy
EPA	Environmental Protection Agency
EU	European Union
FC	Fixed Carbon
FTIR	Fourier Transform Infra Red
GC	Gas Chromatography
GDP	Gross Domestic Product
HDI	Human Development Index
HDPE	High Density Polyethylene
HHW	Hazardous Household Waste
IUPAC	International Union of Pure and Applied Chemistry
LDPE	Low Density Polyethylene
logA	Logarithm of the frequency factor
MS	Mass Spectrometry
MSW	Municipal Solid Waste
N	Nitrogen
[N]	Nitrogen Concentration
NPN	Non Protein Nitrogen
P-I, P-II, P-III, P-IV, P-V, P-VI	Published Papers I-VI
PA	Polyamide
PET	Polyethylene Terephthalate
PN	Protein Nitrogen
PP	Poly Propylene
PS	Polystyrene
PVC	Polyvinyl Chloride
Q-N	Quaternary-Nitrogen
RDF	Refused Derived Fuel
RNA	Ribonucleic Acid
SC	Short Communication
SDT 2960	TGA apparatus
TCD	Thermal Conductivity Detector
TGA	Thermogravimetric Analysis
TN	Total Nitrogen
VM	Volatile Matter
wt%	weight %

1 Municipal Solid Waste worldwide generation: situation and trends

Municipal solid waste (MSW) management is an intensifying challenge on a global level. Even though reliable data are difficult to obtain in this field and large variations occur, current trends show that MSW generation is growing worldwide. This growth is observed not only on the total MSW generation but also on the per capita generation. Figure 1.1 shows these trends for the EU 25 with a constant increase for the last decade. For comparison, the USA was producing about 740 kg/year per capita (highest generation rate in the world) and India (representative of developing countries) 150-200 kg/year in 2003.

The main reason for the increasing MSW amounts "produced" are mainly two:

1. The increasing world population.

2. The propagation and intensification of a modern style of living (increased worldwide industrialisation) as it is strongly correlated with enlarged MSW production per capita. Figure 1.2 and Figure 1.3 show the increasing amount of MSW generation per capita as a function of the Gross Domestic Product (or GDP, total annual value of goods and services produced by a country), indicator of the wealth of a society and as a function of the HDI (or Human Development Index, a measurement of human progress obtained by combining indicators of real purchasing power, education, and health) used to evaluate the development of a society.

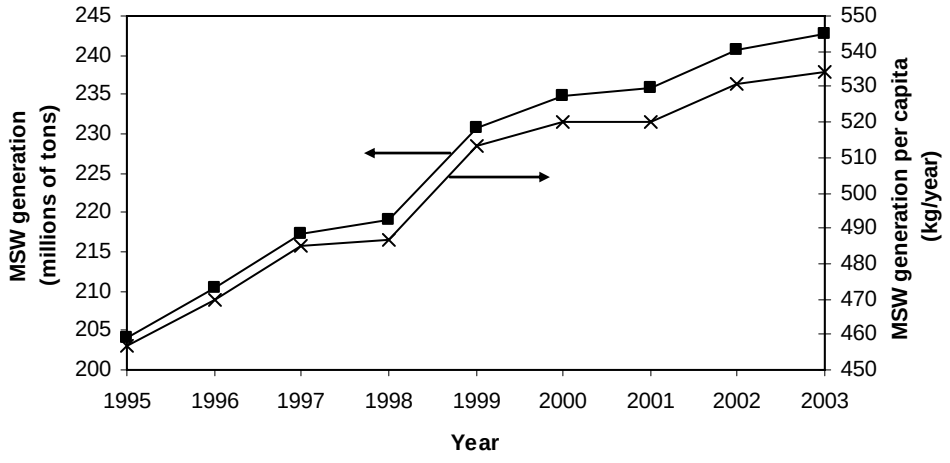

Figure 1.1. MSW generation in the EU 25 [EUROSTAT 2006].

The efficient disposal of growing MSW amounts are an urgent challenge for all societies as they pose a potential threat to the environment and to public health. However, the social acceptability of the MSW disposal routes is greatly depending on the public environmental awareness. Waste management is a people issue, in other words largely dictated by political decisions (i.e. control organs and legislation). EU directives are setting up regulations, standards and targets/strategies that member states have to comply with. International protocols and directives to global issues are to be required but not easy to achieve as revealed by the long and difficult ratification of the Kyoto Protocol.

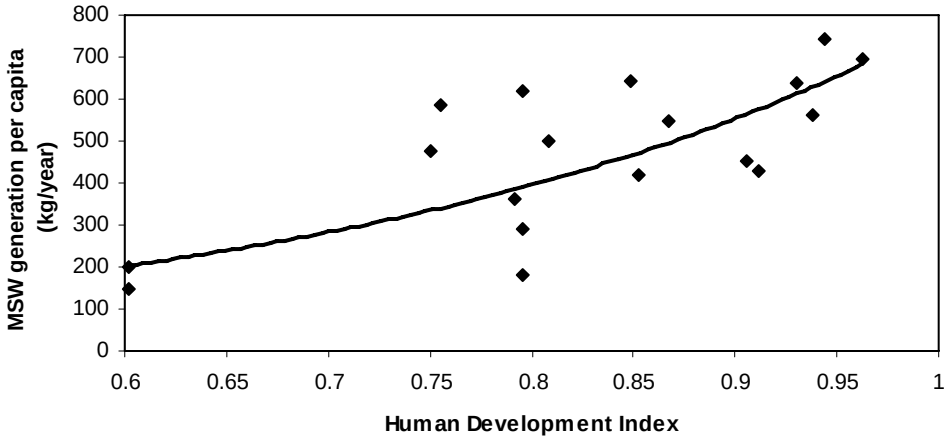

Figure 1.2. MSW generation against HDI. 2003. Countries not specified [HDR 2003; NEA 2006].

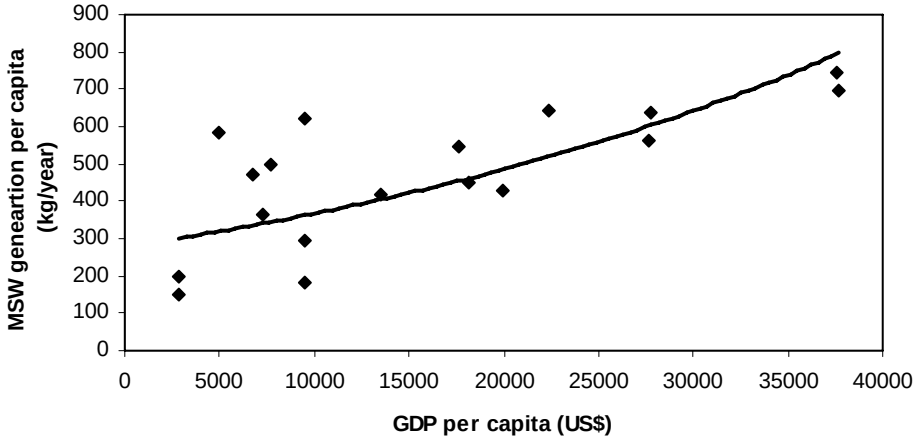

Figure 1.3. MSW generation against GDP. 2003. Countries not specified [CIA 2003; NEA 2006].

This dissertation will present a broad picture of the MSW issue from the cradle (trash bin) to the grave (after treatment) with focus on three specific issues (i.e. pyrolysis, N-chemistry and degradation characteristics) that were investigated in a series of articles.

First, definitions of MSW will be discussed and especially how regulations and standards define MSW in order to obtain reliable data and efficient treatment strategies. Secondly, the nature of MSW will be presented qualitatively and quantitatively from the main categories to the elemental composition of MSW as an in-depth knowledge of MSW is a key-feature of a well-adapt management strategy. Thirdly, the present situation of waste treatment technologies will be discussed together with the foreseeable trends and the set targets. Each method will be evaluated through its possible applications but also the major unresolved challenges (technical, environmental, etc) and needed optimisation.

2 What is MSW?

Waste is generally associated with the image of a heap of rubbish waiting to be picked up and carried away. Far, far away because of its scent and its appeal to rodents. But as soon as one approaches the trash bin and take a look at the content, its variety and heterogeneity strikes you immediately. This complexity calls for a proper waste regulation in order to have good data quality about waste, a pre-requisite to efficient waste management.

First and foremost, defining with accuracy the different types/categories of waste produced is crucial and is not as straight forward as it seems because it exists many definitions/classifications. The lack of clear definitions is in fact the first obstacle in the immense waste management challenge (strategy/optimisation). Tchobanoglous et al. [2002] lists 10 main sources of solid wastes: residential, commercial, institutional, industrial (non-process wastes), construction and demolition, municipal solid waste (MSW), municipal services, treatment facilities, industrial and agricultural. Tchobanoglous et al. [2002] specify that MSW "is normally assumed to include all the wastes generated in a community, with the exception of waste generated by municipal services, treatment plants, and industrial and agricultural processes". In other words, the term MSW covers the waste produced by households and commercial activities and small non-process industries located in urban areas. The US Environmental Protection Agency (EPA) simply defines MSW as "more commonly known as trash or garbage – consists of everyday items thrown away by US residents, businesses and institutions". The importance of MSW originated from other sources than households is dependent on the degree to which waste from these sources is performed by municipal waste collection and co-collected with household waste. The percentage of commercial waste in MSW ranges from 10 to 35% for most EU countries [EUROSTAT 2005]. Any MSW data interpretation (content and amount) should be done carefully as not all countries collect (and therefore classify) waste in the same way. Furthermore, some countries are not able to report the share of MSW from different sources.

However, in order to collect statistically-sound data, which can be further used to design management strategies, a more detailed and systematic method is necessary. For this purpose, the Irish EPA published in 2002 the "European Waste Catalogue and Hazardous Waste List" which is a consolidated version of the EU legislation concerning listing and classification of waste. Waste is defined as such: "Waste is defined in Section 4(1) of the Waste Management Acts 1996 and 2001 as "any substance or object belonging to a category of waste specified in the First Schedule [of the Waste Management Act] or for the time being included in the European Waste Catalogue which the holder discards or intends or is required to discard, and anything which is discarded or otherwise dealt with as if it were waste shall be presumed to be waste until the contrary is proved."". Beyond this technocratic definition, waste is divided into 20 categories, each category is then sub-divided, the full classification covering 30 pages. MSW is here referred to as "municipal wastes" and includes "household waste and similar commercial, industrial and institutional wastes including separately collected fractions". MSW is then divided into 3 main categories (i.e. separately collected fractions, garden and park wastes, and other municipal wastes) and 40 sub-categories (including 14 hazardous waste sub-categories).

This EU classification reveals one crucial fact about the nature of MSW: it is a very complex mixture, made of many different materials when it comes to nature, origin, composition and intrinsic and physical properties. Furthermore, modification in composition of MSW may be expected with factors such as wealth, season or consumer's habits, further complicating the task of waste managers. As a consequence, MSW can not be managed as one single entity but may require a battery of solutions, each one being appropriate for a sub-class of MSW.

The next section will present data about the detailed composition of MSW going from the main categories/materials to the intimate chemical structure and composition. N-functionalities will be dealt with in Chapter 6.

3 Composition and properties of MSW

In this section, the detailed composition of MSW will be presented. This will be achieved by going stepwise into the nature of MSW (categories, sub-categories, macromolecules, proximate and ultimate analyses) and its key properties. This is vital for management strategies in order to improve MSW treatment routes by identifying recycling opportunities, promoting waste abatement efforts or isolating specific fractions.

3.1 Main materials

Table 3.1 presents the main materials found in MSW according to the US EPA and EUROSTAT classifications. Analogue categories are presented side by side

Table 3.1. Main MSW materials.

EPA (USA)	EUROSTAT (EU)
Paper and paperboard	Paper, paperboard and paper products
Food scraps	Organic waste
Wood	
Yard trimmings	
Plastics	Plastics
Metals	Metals
Rubber, leather and textiles	Textiles
Glass	Glass
Other	Other

The origin of a given material can be very diverse and this complicates the picture. Some items, such as fridges or computers, are intricate machinery made of numerous components and many different materials (plastic, glass, metal, etc). Consequently, other categorising systems could be chosen such as listing of durable/non-durable goods or combustible/non-combustible matter. The classification system can and should be designed according to the needs of its user. It is obvious that MSW is a complex and heterogeneous mixture, made of materials with very different chemical structures and physical properties. However, a further obstacle is appearing: the category “other”. This category is far from minute and may represent a significant share of the total MSW amount and can therefore make difficulties for waste management handling. Figures 3.1 and 3.2 present the composition of MSW in the USA and Norway.

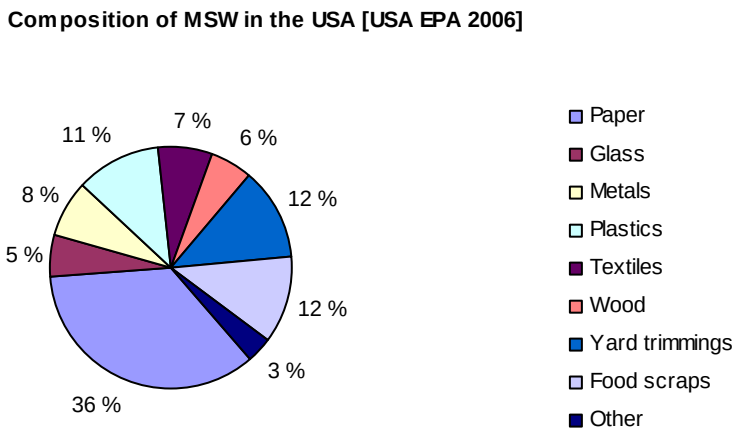

Figure 3.1. Composition of MSW per materials. USA 2003.

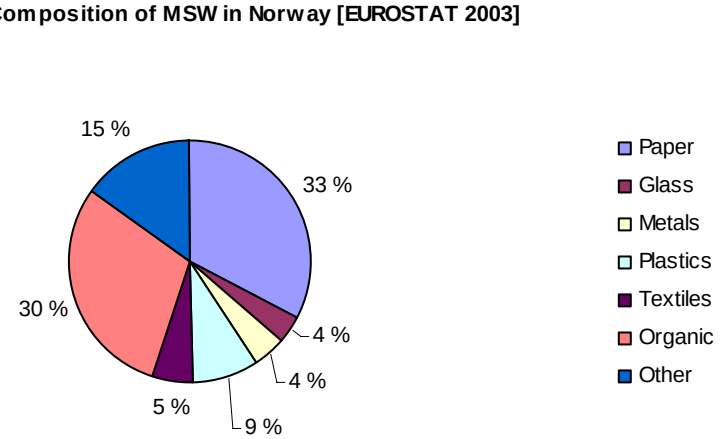

Figure 3.2. Composition of MSW per materials. Norway 2001. Only household waste.

The composition (by materials) is very similar for the USA and Norway, even though the statistics for Norway only includes household wastes. This similarity can be explained by the similar lifestyle and therefore consumption habits in these two industrialised countries. Comparison with developing countries would show major differences. The "organic" fraction in the Norwegian household wastes corresponds exactly to the sum of the "wood", "yard trimmings" and "food scraps" American categories. However, it does not mean that the same exact composition of the Norwegian organic fraction is to be expected. The "other" fraction represents in both cases several percent; a better characterisation of this fraction may yield more optimised treatment.

3.2 Sub-categories

Each of the afore-mentioned categories is made of several fractions which may exhibit significantly different composition and/or properties, the most important being amount and toxicity. A very extensive study carried out in Minnesota [Minnesota 2000] in 1992 and 1999 provides vital data about the main sub-categories in term of quantity and are listed in Table 3.2. Two extra categories, i.e. "problem materials" and "hazardous household wastes (HHW)", are used in this classification. It shows the variety of listing possibilities, usually chosen according to management challenges or specific legislation/requirements. The relative importance of a given sub-category is given into brackets; some minor contributors are not listed leading to sub-totals inferior to 100%. Each sub-category usually includes an "other" category. In spite of the very exhaustive work carried out, several percents of the total MSW remain poorly characterised.

Table 3.2. Main sub-categories of MSW.

MATERIAL	PROPORTION	MATERIAL	PROPORTION
Paper	**34.2% of MSW**	**Glass**	**3.0% of MSW**
Newsprint	12.6% of Paper	Glass containers	83.3%
Office paper	9%	**Organic materials**	**22.9% of MSW**
Old Corrugated Cardboard	15%	Yard Waste	7.9%
Magazines/catalogues (glossy paper)	8%	Food Waste	63.3%
Boxboard	8%	Wood waste	13.5%
Mixed Paper (non recyclable)	31.6%	**Other Waste**	**19.1% of MSW**
Plastic	**11.7% of MSW**	Rubber	3.7%
PET	7.7 %	Textiles	17.8%
HDPE	5.1%	Construction/Demolition	16.8%
Polystyrene	7.7%	Household bulky items	15.2%
Plastic Film (packaging, etc)	39%	Miscellaneous	35.1%
PVC	0.9%	**Problem Materials**	**2.0% of MSW**
Other (non container)	36%	Appliances	95%
Metal	**6.0% of MSW**	Batteries	5%
Aluminium Beverage cans	15%	**Hazardous Waste**	**1.0% of MSW**
Other aluminium	8.3%	Oil Paint	10%
Ferrous Containers	21.7%	Automobile used oil filters	10%
Other Ferrous	55%	Other	60%

3.3 Chemical structure (Nitrogenous compounds in Chapter 6)

Continuing our journey through the structure of MSW and looking further at the details, the next level is the macromolecules constituting the different materials found in MSW.

Paper products

Cellulose is the major constituent of paper. Cellulose is a material found in plant cell walls as microfibrils (2-20 nm in diameter and 100-40000 nm in length). Cellulose is a straight polymer (polysaccharide) made of β-1.4-linked glucose units, i.e. bonds that join 2 monomers via an oxygen atom (see Figure 3.3). This conformation favours hydrogen bonds between glucose units in the polymer but also with the adjacent polymers, building up a strong fibrous structure.

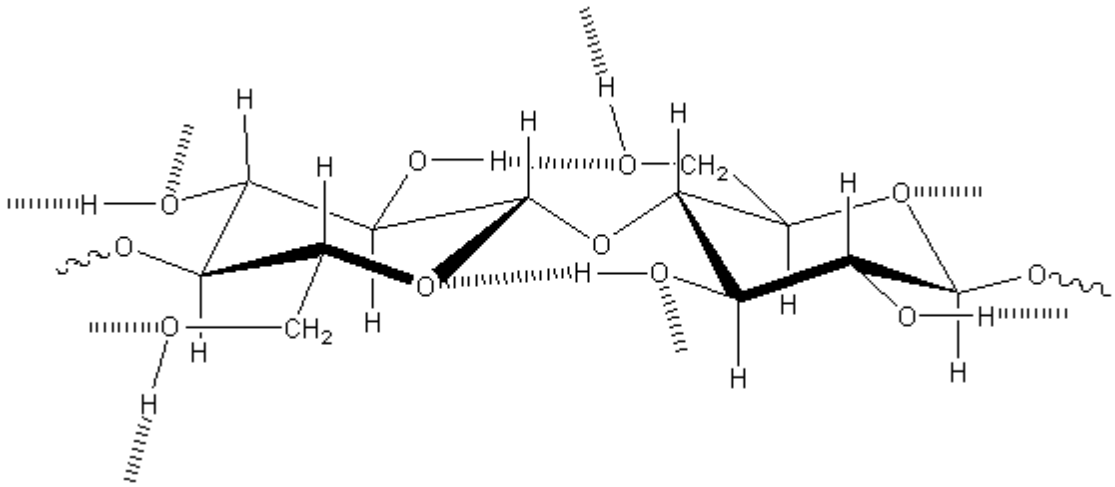

Figure 3.3. Cellulose unit. ıııııııı represents H bond.

Additional ingredients may be used to change the appearance and properties of the paper product. To mention the most common types of paper products, calcium carbonate is added to paper to produce glossy paper used for magazines, while Kraft paper (brown paper used for packaging) is treated with sodium sulphate. Moreover, no ingredient is adjoined in newsprint (the paper on which newspapers are printed), on the contrary, one plant constituent, i.e. the lignin fraction (see structure page 10 and 11), is not removed during the production process. The chemical composition of ink is very varied. The chemical bases of ink are water/petrochemical solvents/oil. The colorant is either dye or pigmentation (examples: calcium carbonate, titan oxide, barium sulphate, aluminium hydrate). Various additives (resin, humectant, etc) to change the ink properties complete this complex chemical makeup.

Yard trimmings and wood (biomass residues)

Yard trimmings are constituted of biomass residues of various sorts. In other words, trimmings include grass, leaves and woody materials (stem, branch, etc). Wastes like pallets or demolition wood are also present. The main biomass components are cellulose, hemicellulose and lignin (Table 3.3). As presented in the section (Figure 3.3) about paper, cellulose is a linear polymer of glucose units; hemicellulose is also a polymer of sugar units (mannose, galactose, 4-O-methyl-D glucuronic acid, xylose or arabinose) but it is shorter than cellulose (only 50-200 units) and branched. Hemicellulose is therefore more of a family of compounds rather than a well defined compound and is therefore often referred to as "hemicelluloses". One type, arabinoxylan, is presented in Figure 3.4. The third and last main component of biomass is lignin. Its structure, apparently random and unorganised, is an active field of research. Lignin is a complex aromatic polymer (Figure 3.5 presents the most common monomers) with a high degree of cross-linking. This gives birth to a very strong three dimensional structure and explains why lignin is not as degradable as cellulose and hemicellulose. Last but not least, extractives represent usually 1-5 wt% db of the wood matter. Extractives are natural products extraneous to a lignocellulose cell wall. Extractives are of two main sources [FPL 1979]: compounds directly involved in the metabolism of the plant and secondary products, products of further chemical modification by non-metabolic processes or from external sources. This fraction is extremely diverse and includes (not exhaustive): aromatic compounds, simple sugars, free amino acids, proteins, free fatty acids, resin (carboxylic) acids, chlorophyll, alkaloids (a vast family of natural compounds, see Chapter 6). Certain extractives are common to many different plants, while others are characteristic of a family, or even a species. Extracts may influence properties of the wood. For example, extractives can protect wood from degradation (anti microbial and anti fungal activity), add colour and odour to wood, and improve strength properties. Extractives may also cause problems in papermaking (resin acids); contribute to corrosion of metals in contact with wood; present health hazards, and affect colour stability of wood to light. The exact nature and concentration of N-compounds present in biomass will be discussed in Chapter 6.

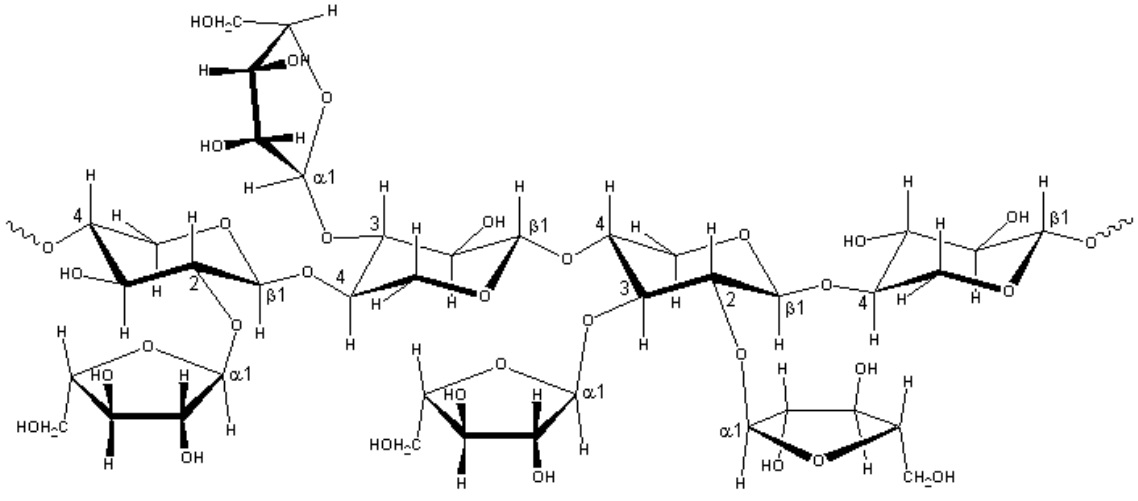

Figure 3.4. A hemicellulose: arabinoxylan.

Table 3.3. Typical composition of wood (% dry matter).

	Spruce [Grønli 1996]	Pine [Grønli 1996]	Wood [Stenseng 2001]
Cellulose (wt%)	43.1	40.9	40-45
Hemicellulose (wt%)	26.5	25.7	20-30
Lignin (wt%)	28.4	28.6	20-30
Extractives (wt%)	2.0	4.8	1-5 (up to 30)[a]

[a] For some tropical species.

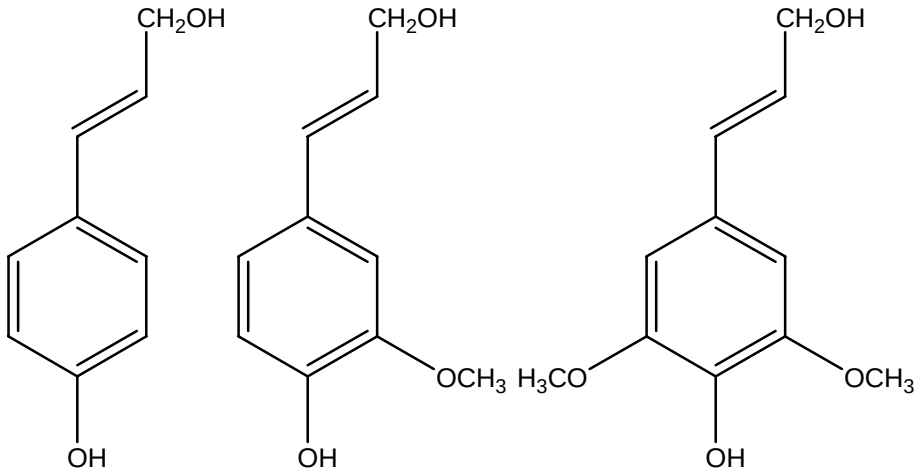

(a) (b) (c)

Figure 3.5. Most common monomers of lignin ("monolignols"). (a): p-coumaryl alcohol; (b): coniferyl alcohol (predominant lignin monomer in softwoods); (c): sinapyl alcohol. [DWB 2006].

Food

Food items can be of two origins: animal or vegetal. The main constituents of food are: proteins (polymers of amino acids, see Chapter 6), fat (a category of lipids, all fats are fatty acids, i.e. carboxylic acids with long aliphatic chains), carbohydrates (biological macromolecules used in the storage and transport of energy, they include mono-, di-, oligo- and polysaccharides) water, fibre (polysaccharides like cellulose or lignin), vitamins and minerals/inorganic matter (Ca, P, Fe, Na, K, Cu, Zn, Mg, Mn). The various proportions of the afore-mentioned components are depending greatly on the food item and a complete overview of the values is impossible. Three representative examples are briefly presented here:

Composition of bone: 65 to 70 percent of the bone is composed of inorganic substances. Almost all of this inorganic substance is a sole compound called hydroxyapatite, i.e. $Ca_{10}(PO_4)_6(OH)_2$. No vitamins, fatty acids, proteins or carbohydrates are present in this fraction. 30 to 35% of bone is composed of organic material (on a dry weight basis). Of this amount nearly 95 % is a substance called collagen. Collagen is a fibrous protein (see 3.5) found in connective tissue in animals. The amino acid composition of collagen is rather unusual with high levels of glycine, praline, hydroxyproline and hydroxylysine. The remaining organic fraction includes substances such as are chondroitin sulphate, keratin sulphate, and phospholipids [Samuel 1985].

Composition of meat (muscle): Meat is mostly made of muscle. The main components are: water (about 75%), protein (about 20%), fat (about 5%), and ash/minerals (about 1%) such as Ca, P, Na, K, S (main elements) and Fe, Cu, Zn, Mn, Al, Si and Mg.

Composition of a legume (potato): a raw potato is made of about 80% water. The rest is mostly carbohydrates (about 20%, including so-called “fiber”), followed by proteins, lipids, minerals (Fe, Ca, Mg, P, K, Na) and vitamins.

Plastics

Plastics are synthetic polymerisation products obtained by condensation reactions. Depending on their properties (plasticity, robustness, etc), plastics can be used for a variety of applications from films for food packaging to bullet proof vests (Kevlar). Figures 3.6-3.11 present the structures of some plastics commonly found in MSW:

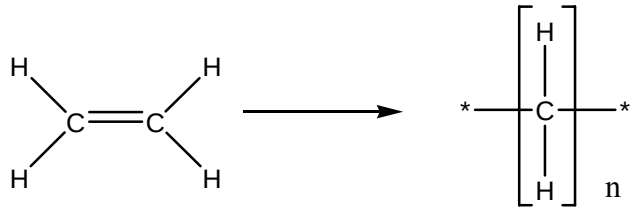

Figure 3.6. Polyethylene (PE).

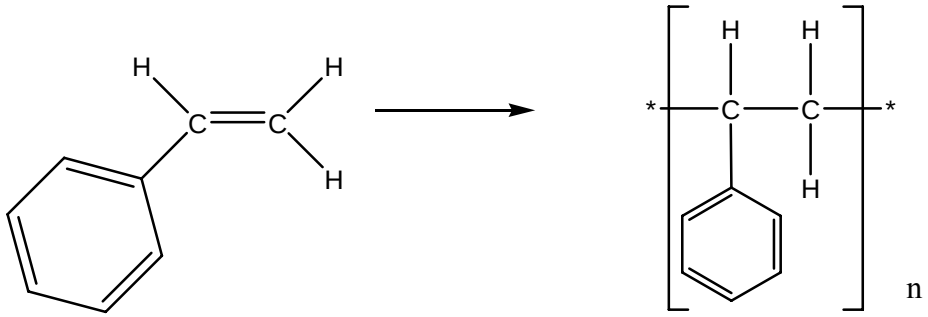

Figure 3.7. Polystyrene (PS).

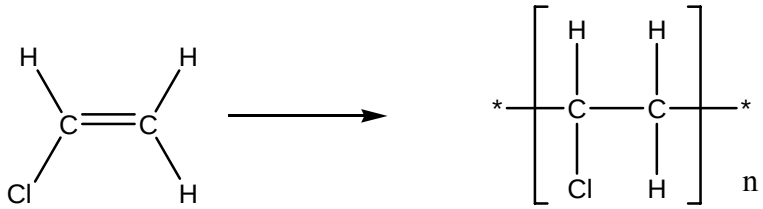

Figure 3.8. Polyvinyl chloride (PVC).

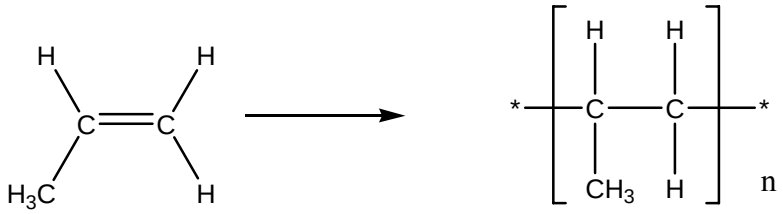

Figure 3.9. Polypropylene (PP).

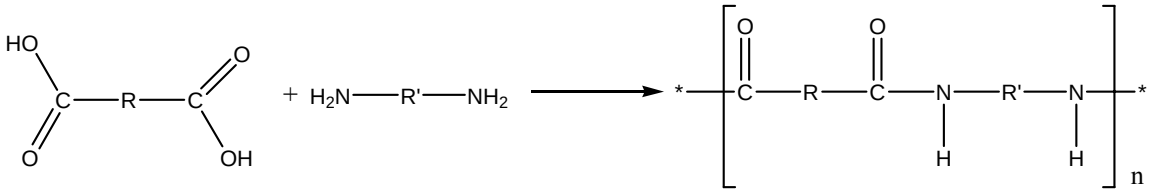

Figure 3.10. Polyamides (PA, general reaction).

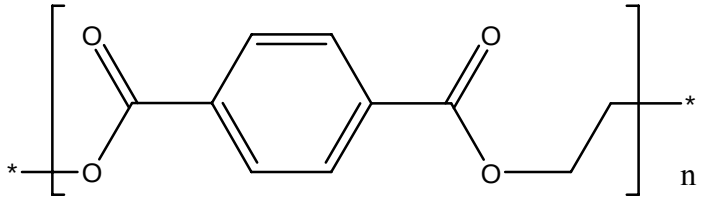

Figure 3.11. Polyester (PET here).

Metals

Ferrous metals represent more than 50% of the total metal products found in MSW [Minnesota 2000; Tchobanoglous 2002]. The other important metal is aluminium (cans, foils, etc). Another class of metals is particularly interesting as it is (considered) highly toxic: the so-called heavy metals. First, even though the term "heavy metals" is widely used it has recently been considered meaningless and even misleading by IUPAC [Duffus 2002] as no clear definition actually exists. The density (which has no significant meaning to assess the toxicity of a compound) has often been used to define heavy metals with lower limits for heavy metals ranging from 3.5 to 7 g/cm^3. Furthermore the actual toxicity of heavy metals and their products is often little documented. The debate about the scientific and chemical relevance of the term "heavy metals" is still open but its vagueness is problematic.

Heavy metals, as defined by the EU Directive 67/548/EEC, are antimony (Sb), arsenic (As), cadmium (Cd), chrome (Cr), copper (Cu), lead (Pb), mercury (Hg), nickel (Ni), selenium (Se), tellurium (Te), thallium (Tl), tin (Sn) and their compounds (oxides, chlorides, etc). Furthermore, manganese (Mn) and zinc (Zn) are often included. Heavy metals are often trace compounds (Table 3.4) but pose serious issues as their (sometime assumed) biological, ecological and human toxicity are very serious. The relative concentrations of heavy metals vary very much as they reflect the very different MSW compositions and definitions, thus very little consistency is found. Heavy metals can be found in all MSW fractions at various concentrations and are therefore difficult to sort out before MSW treatment (identification of major sources are important).

Table 3.4. Heavy metals in MSW (wet basis, ppmw).

	Zn	Pb	Cr^{III}	Cr^{VI}	Cr	Cu	Ni	Cd	As	Sb	Hg	Mn	References
Household waste	140-320	33-247			24-62	40-100	17-105	.4-1.9	1.8-10	.6-3.7	.02-.12	372-572	[NHWAP 1994]
MSW	172-606	136-426	0-193	.1-.5		79-158	18-27	7-9	0-7	0-2	1-1.5		[Morselli 1992]
Communal waste	290	110			35	1100		1.1	33		0.087		[SFT 1996]
MSW		12			6.5			.45			.12		[Kathirvale 2004]

Two important complementary data are important for heavy metals as they are hazardous: the MSW fractions (or even better, particular items) containing the highest concentrations of heavy metals and the MSW fractions contributing the most to the total amount of heavy metals. However, there is little agreement in the literature, due to the inconsistency of the MSW data quality [Sørum 2000; Jung 2006].

Nevertheless some hard facts exist: paper products do not contribute vastly to the total amount of heavy metals, even though pigments or coatings may contain (heavy) metal compounds [Sørum 2000]; virgin biomass and food scraps do not contain high levels of heavy metals but demolition wood is often contaminated by heavy metals found in treatment additives. Some types of plastic packaging contain high levels of heavy metals (Sb, Cr) and contribute heavily to their total output [Sørum 2000; Liou 2003; Jung 2006]. The metal fraction is, according to most sources, heavy contributors to the total output of several heavy metals [SFT 1996; Sørum 2000]. Glass may contain significant amounts of metals or metal oxides as colour additives (see glass); rubber and textiles are not major contributors. The "other" or rest fraction (especially HHW) contains some items with high concentrations of heavy metals: electronic appliances, paint pigments and batteries for example.

Tires/rubber

The increasing number of motor vehicles complicates the handling of used tires. Tires are made of synthetic rubber. Rubber is a polymer material obtained from polymerisation of a variety of monomers (or mixture of monomers), often with additives depending on the applications. Common monomers are presented on Figure 3.12.

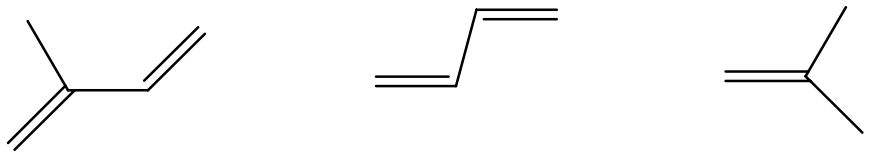

Figure 3.12. Isoprene, butadiene and methylpropene.

Textiles

Textiles are fibre-made material used in clothing, carpets, towels, tents, flags, industrial filters, etc. Textiles can be of animal origin such as wool, silk or cashmere, of vegetal origin such as cotton or linen, or of synthetic origin like acrylic, Nylon, polyester or Lycra. Wool is a natural protein (polypeptides chain, discussed in Chapter 6) fibre and like human hair it is composed of keratin-type protein. Cotton is a polysaccharide, a polymer of sugars like wood. Cotton is almost exclusively made of pure cellulose. Acrylic fibres (or polyacrylonitrile) are a synthetic polymer of acrylonitrile (C_3H_3N) used as a cheap alternative to natural fibres. Textiles can be treated in a variety of ways to modify their properties: flame retardation [Zhu 2004], waterproofing, etc.

Glass

"Common" glass contains 60-75% of silica (SiO_2), and the additional components are sodium (or potassium) carbonate Na_2CO_3 (12-18%) and calcium oxide CaO (5-12%) i.e. soda-lime glass, which represents 90% of the produced glass. Other ingredients are often added to change glass properties. The most common are lead oxide (at least 20%, lead glass also called crystal) or boric oxide (at least 5%, borosilicate glass withstanding high

temperatures). Coloured glass is obtained by adding metals or metal oxides (cobalt, tin oxide, copper oxide, selenium oxide, etc) in concentrations usually lower than 2-3%.

Other:

Construction/demolition

Sometimes mixed with MSW (depending on the collecting system), construction and demolition debris are mostly [Tchobanoglous 2002] made of bricks, stones (minerals), metals, wood wastes, plastics, fibreboard, textiles, concrete (mineral aggregates, generally gravel and sand, and water), asphalt (produced from petroleum products), soil, cardboard, steel and hazardous wastes among others. Heavy metals may also be present (paint, treated wood).

Bulky items and appliances

Durable goods (computers, washing machines, furniture, etc) are very complex manufactured items which contains almost all the fractions of MSW.

Household Hazardous Wastes (HHW)

Last but not least, HHW are a highly toxic family of compounds. The most prominent products found are paint (latex and oil), pesticides, cleaners, solvents, HHW containers (50% of total HHW), household and car batteries (Table 3.5) and automobile oil. Paint is composed of a binder (the film itself), a diluent (to adjust the viscosity) and additives. Typical binders include (synthetic or natural) resins such as acrylics, polyurethanes, polyesters, oils, or latex. Typical diluents include organic solvents such as alcohols, ketones, esters, glycol ethers or water. Typical additives include pigments, dyes, catalysts, thickeners and stabilisers. Chemical pesticides (herbicides, fungicides, insecticides, etc) are chemical compounds used to fight any type of pest attacking human food or propagating diseases.

Table 3.5. Household batteries: types and sales (USA EPA, 1992).

Type	Cathode	Anode	Electrolyte	Sales percentage
Alkaline	MgO	Zn	KOH and/or NaOH	63.5
Zn-C	MgO	Zn	NH_4Cl and/or $ZnCl_2$	19.7
HgO	HgO	Zn	KOH and/or NaOH	1.2
Zinc-air	Oxygen from air	Zn	KOH	3.4
Ag_2O	Ag_2O	Zn	KOH and/or NaOH	2.6
Li	Metal oxides	Li	Organic & salt solutions	0.2
Ni-Cd	NiO	Cd	KOH and/or NaOH	9.4

3.4 Proximate and elemental analyses (glass and metal not included)

C, H, O, N, S, Cl, Volatile Matter (VM), Fixed Carbon (FC), ash and moisture

The average proximate and elemental analyses are of interest but average values do not reflect/hide the huge variations from one fraction to another. In order to present a complete picture of the different fractions, a literature survey covering a very large number of products from all the MSW fractions have been achieved. Data collected from this literature search are presented in Appendix and are listed in 6 sections: paper, biomass, food, plastics and other (various materials).

The organic fraction of MSW (biomass residues and food scraps) has relatively high moisture content (10-20% in biomass, more in food waste). VM (dry basis) is high at about 60-80%, while the ash fraction rarely exceeds 10% except for some cases (bone, biomass husks). The level of FC is (by difference) about 10-20%. Paper has a VM above 70% and low ash content (less than 5%), except glossy, recycled and coated paper which exhibit high ash content (25-30%). Plastics have above 90% VM and no ash or moisture.

Even though the data are quite spread (see Table 3.6), an average ultimate MSW composition can be proposed (daf basis): 40-50% C; 25-35% O; 5-7% H; 0.5-2% N; 0.1-0.2% S; 0.1-0.2% Cl with a moisture content of 20-40% and an ash content of 15-30%. The differences observed can be attributed, not only to statistical differences but also consumption habits and the different "definitions" of MSW (household waste or inclusion of industrial and commercial wastes).

Table 3.6. MSW composition (wt%, daf or db basis) in literature (references in Appendix).

MSW	VM	Fix-C	Ash	Moisture	C	H	O	N	S/Cl	Ash
RDF	73.4	8.9	17.7	3.2	48.4	7.0	25.2	0.84	0.12/1.0	
MSW Thai db				(58.40)	37.14	5.41	24.93	0.22	0.09/0.8	32.2
MSW UK db	63	4	32.2	(32.43)	35.81	4.82	24.43	0.78	0.41/0.75	33.0
MSW Kuala L	31.36	4.37	9.26	55.01	46.11	6.86	28.12	0.23		17.1
MSW					52	8	38	0.5	0.3	
RDF-A	76.2	13.6	10.2	3.7	46.6	6.8	34.51	1.28	0.13/1.08	
RDF-B	72.5	3.9	12.5	11.1	41.7	5	36.3	0.75	0.17/1	
Typical MSW				25	25	3	20	0.5	0.2/0.2-0.6	25
MSW				15/35	15/30	2/5	12/24	.2/1	.02-.1	15/25
MSW					42.4	6.1	35.1	2.2	0.24/0.5	
MSW			6.9	19.2	35	11.7	30.2	?	1.9/0.25	

Ash composition

The inorganic fraction of MSW (bottom ash and fly ash from combustion) is mainly made of oxides of silica (Si), calcium (Ca), iron (Fe), sodium (Na), aluminium (Al), magnesium (Mg) and potassium (K). The average composition of ash may vary greatly (see Figures 3.13-3.15) with the changing nature of MSW and the combustion process conditions. For unsorted (or partly sorted) MSW, the concentrations of Fe and Al species may be significantly increased. Furthermore, trace metals (heavy metals) are present and represent about 1% of the total ash material [Tchobanoglous 2002].

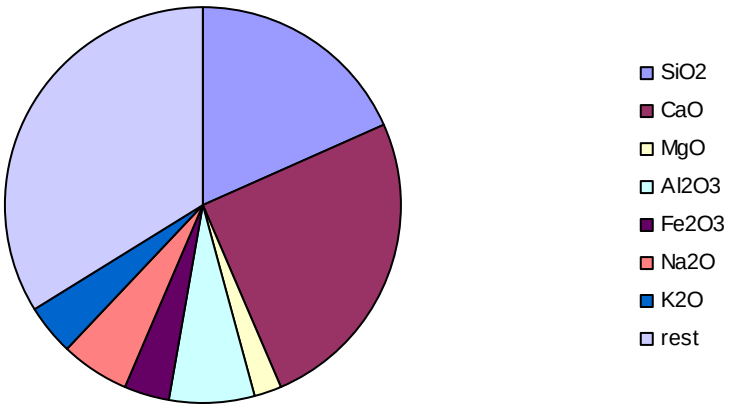

Figure 3.13. Fly ash composition. Rest: heavy metals, Cl, sulphur oxides. [Qian 2006].

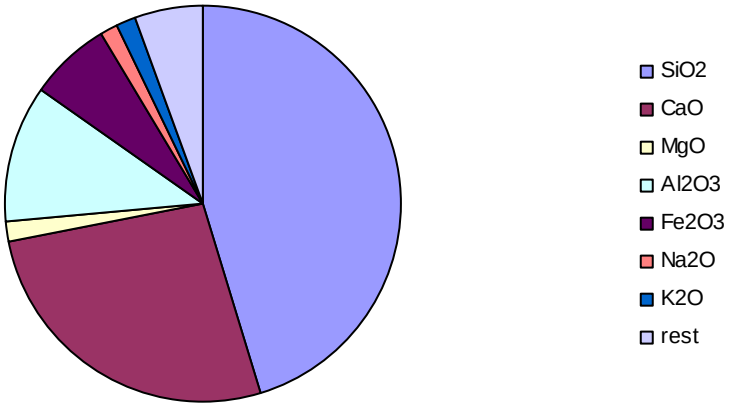

Figure 3.14. Bottom ash composition. Rest: heavy metals, Cl, sulphur oxides. [Qian 2006].

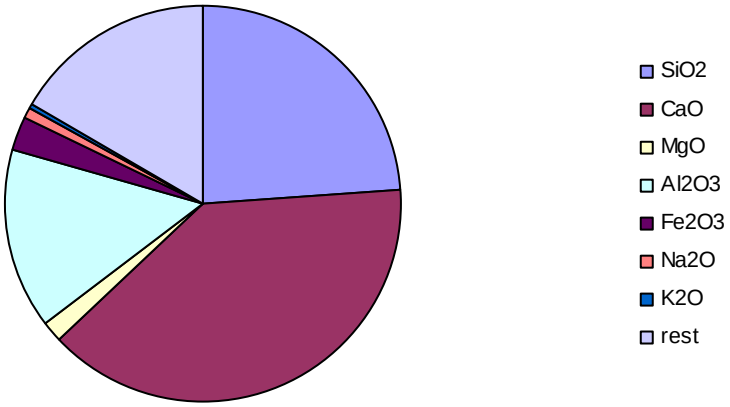

Figure 3.15. Bottom ash composition. Rest: heavy metals, Cl, sulphur oxides. [Jurič 2006].

Werther et al. [2000] review the ash composition of 15 biomass and biomass residues samples. Similarly to MSW SiO_2, CaO, Al_2O_3 and K_2O are the main identified components of ashes (origin not specified).

3.5 Other MSW properties

Apart from the composition and structure of MSW fractions, several other parameters are of importance in order to design or optimise waste management. Table 3.7 summarises the most important properties grouped into three categories.

Table 3.7. MSW properties.

Properties type	Method (example)	Significance
Physical properties	---	---
Apparent density	ASTM D1895	transport
Real density	n.f.	transport
Particle size distribution	microscopy	homogeneity
Field capacity	n.f.	landfilling
Permeability	n.f.	landfilling
Surface area	BET	treatment process
Porosity	water saturation	treatment process
Particle morphology	microscopy	burning
Thermal degradation characteristics	TGA DSC	kinetic data, degradation temperatures and rates
Chemical properties	---	---
Ash melting behaviour	ash melting microscope	ash treatment, burning
Energy content/HHV	calorimeter	burning
Nutrients content	ultimate analysis	composting
Biological properties	---	---
Biodegradability	n.f.	landfilling
Odours generation	---	public health

n.f.: not found.

4 Municipal Solid Waste management and treatment technologies: Situation and challenges

4.1 The situation in Europe and in the USA

Any waste management strategy should deal with waste in an acceptable manner in accordance with public health and safety, environmental regulations and long-term sustainability. The most widely used technologies carried out to dispose of waste throughout the world are: landfilling (included composting), recycling (also called reuse or recovery) and combustion with energy recovery.

It is important to remember that a good waste management should focus first on waste prevention (product substitution) and waste reduction (new packaging, etc) in order to reduce the stream of solid wastes at its source. These measures involve not only the consumers by the conscious choices they are taking (to privilege loose food items, limit the use of disposable items, etc) but also the industrials, who are using attractive (and therefore expensive and voluminous) packaging to sell a product (for mineral water the package represents 50% of the consumer price). They should "understand", through corporate social responsibility, public pressure and legislation, the benefits of waste prevention as they are the first and foremost actors of this strategy.

The most widely used waste treatments and their relative importance are summarised in Figure 4.1-4.3.

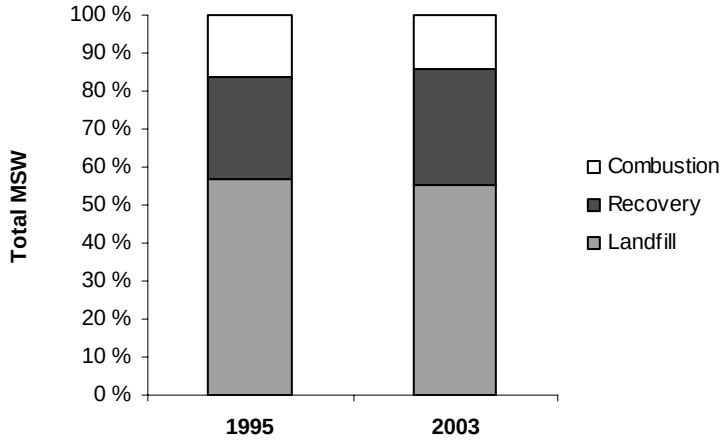

Figure 4.1. US Waste treatment technologies [US EPA 2006]. Remark: Terms used in 1995: *recovery for recycling (including composting)*, *combustion* and *landfill, other*; terms used in 2003: *recovery*, *combustion* and *land disposal*.

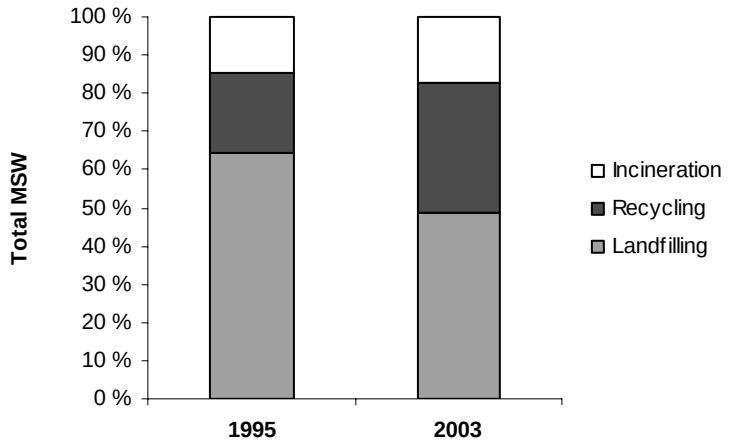

Figure 4.2. EU 25 Waste treatment technologies [EUROSTAT 2005]. Remark: incineration is with or without energy recovery.

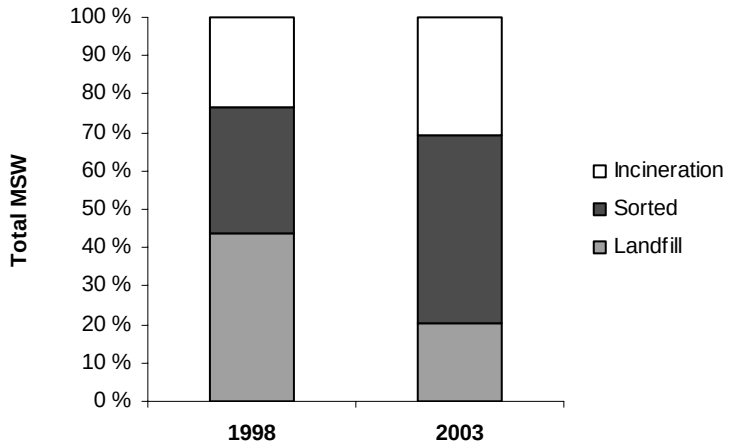

Figure 4.3. Waste treatment technologies in Norway [SSB 2006]. Remark: 75% of the "sorted" materials are recycled, 25% are incinerated, stored or unknown treatment; "other" represents less than 0.1%; household waste only; home composting not included.

The EU and Norway are showing significant strategy shift towards incineration and recycling while little changes are observed in the USA. The slowness of the US evolution might be due to the vast spaces available and a better acceptance of landfilling as a waste treatment solution. The share of landfilling in USA and EU25 is still predominant with around half of the total MSW generated disposed this way. However, the relative importance of landfilling is decreasing rapidly in the EU due to clear political targets. The goals established by the EU are to reduce landfilling to 75% of its 1998 level by 2010, 50% of 1998-level by 2013 and 35% of 1998-level by 2016. The national and local situations in the EU are extremely various due to political and technological factors. Only 1.1% of the MSW is landfilled in Trondheim (160000 inhabitants), Norway for example.

An interesting fact is the choice of words or the vague denominations sometimes used in presenting the situation often to embellish the broader picture. The term "recovery" is sometimes preferred to the term "recycling" and reminds us that a significant part of "recovered" material (often by selective sorting by people) may not be further used for recycling and/or reuse in another manner but rather incinerated and/or landfilled. Very few data are available about this non-recycled recovered fraction. This will depend on the facilities a community has and its ability (technological and economical) to implement recycling but also that some recovered material are un-recyclable. Recovery/recycling come second with a third of the total amount of MSW recovered/recycled. This concerns essentially paper, glass, metal and plastic (USA EPA data for 2003: 48% of paper and paperboard generated were recovered). Likewise, incineration/combustion with and without energy recovery are reported together. "Land disposal" is also replacing the term "landfilling". An "other" category is sometimes added or included in another category with no detail.

The observed trends are leading towards less landfilling in favour of recycling and incineration with energy recovery more and more often as they are (or seen as) more environmentally-friendly, cost-effective and are privileged by the EU legislation. However, other techniques are available/under development and may provide efficient solutions for some specific MSW fractions, i.e. niche applications. Diversification and flexibility of energy carriers, technologies and infrastructure for the production of heat, electricity and fuels is an important feature of an efficient waste management. The next section is going to briefly present the principles of the various chemical, biological and physical treatment technologies with emphasis on opportunities and constraints.

4.2 Thermal treatment

Combustion

In this process, the waste is burnt in a combustion chamber with air (oxygen) to form mainly CO_2 and H_2O. This is one of the most efficient techniques of dealing with solid wastes as it allows an immediate and important reduction of volume and mass together with conversion to energy and production of an inert solid residue (ash). Several MSW incinerators are currently available: mass burn incinerators (grate furnace/fixed bed), modular/controlled air units (two-chamber units) and RDF-fired incinerators (fluidised bed) are the most common [Morcos 1989; Saxena 1994; Obernberger 1998; Ruth 1998; IEA Task 32 2002]. The installation will be chosen mostly on the basis of the fuel properties (particle size, moisture content, etc) as good combustion conditions reduce the necessary post-combustion cleaning devices. The incinerator is followed by a series of cleaning techniques as this process is accompanied by production of harmful by-products.

The environmental challenges are associated with the various by-products:

- effluents (water from scrubber, slurry)
- emissions to air (volatile pollutants)
- solid residue (bottom ash and particles collected from the filtering system)

The emissions have to be monitored and follow regulations for a given installation to be allowed to function. Two types of measures can be taken to optimise the overall process, i.e. better energy output and less harmful emissions: primary measures, i.e. improvement of the burning unit and feedstock, and secondary measures, i.e. flue gas and residue cleaning and treatment. Table 4.1 summarises the situation (**EU Directive 2000/76/EC**).

Table 4.1. Main pollutants of concern from MSW incineration.

Nature	**Origin**	**Limits/regulations**	**Risks**	**Possible solutions**
Effluent	-	-	-	-
Water, slurries	Wet cleaning	pH, T, flow, contaminants concentration (see directive)	Water pollution	Scrubber design, post treatment
Solid residue	-	-	-	-
Bottom Ash	Grate	Heavy metals and TOC contents	-	Stabilisation, concrete industry
Fly ash	Filters	"	-	"
TOC (Total Organic Carbon)	Ash	3% in ashes	-	Operating conditions
Gas emissions *	-	-	-	-
Total dust	-	10	Breathing problem	collection device and further disposal
Heavy metals	-	See directive	Health hazard	collection, adsorption (Hg), further disposal
CO	-	50	Respiratory problems	Primary measures
NOx	-	200	Acid rain	Primary, de-NOx
SOx	-	50	Acid rain	Scrubbing, absorption
Dioxins, Furans	-	0.1 ng/m^3	Toxic (human food chain)	Primary measures, waste pre-treatment, adsorption
HCl,SO_2,HF	-	10/50/1	Respiratory problems	Scrubbing, adsorption

*mg/m^3 @ 273 K, 101.3 kPa, 11% O_2, dry gas. Daily average values. See directive for further details.

The air emission limit values include daily average, half-hourly average values together with other time-related constraints imposed on incinerators. Procedures and standards for the measurements are also included in the directive. Other terms are sometimes used to design classes of pollutants: CFC (ChloroFluoro Compounds), VOC (Volatile Organic Compounds), POP (Persistent Organic Pollutants), PAH (Poly Aromatic Hydrocarbons).

Pollution control can be achieved at two different levels: **prevention** of pollutants' production (by optimised process or fuel pre-treatment for example) or **capture** of the pollutant before further destruction, stabilisation or disposal (isolation). Two of the most demanding/acute challenges are heavy metals and dioxins/furans. ***Heavy metals*** (found mostly in ashes, except for Hg, which is collected in the flue gas cleaning system, [Sørum 2000]) can not be destruct during combustion and have to be disposed of in a proper way (controlled landfilling, etc) to avoid any contamination of the environment. Novel solutions propose stabilisation of residue containing heavy metals [Kuo 2004] and recovery [Izumikawa 1996]. ***Dioxins and furans'*** synthesis are depending on numerous factors (temperature, chlorine content, and surface reactions) and is therefore difficult to control. Even though they are produced at very low concentrations, their toxicity is acute and they concentrate in biological reservoirs of the human food chain (especially cow milk) with nocuous but difficult to predict chronic effects.

Further constraints include: BAT requirement (Best Available Technique) imposes constant improvement of the installation; technological challenges (fuel pre-treatment, optimal fuel quality, slagging, ash melting, corrosion, fouling, etc); costs (CO_2 tax); logistical issues (CO_2 emitted by transport); continuous monitoring; reporting to the public and the authorities.

Gasification

Even though incineration of MSW with energy recovery, air emission control and proper waste disposal (ash, particles, waste water) is the overwhelmingly used thermal treatment, two other thermal techniques are promising and currently under development/early stage of industrial scale use and interesting alternatives for MSW or at least some selected/sorted MSW fractions. Gasification is one of them. Gasification is a thermochemical conversion process where a solid fuel is transformed into a gaseous fuel that mainly contains H_2, CO and CH_4. This gas can be used for electricity and heat production. Figure 4.4 summarises the principle of gasification, the produced gas that then be used for electricity and heat production through turbine, engine or boiler.

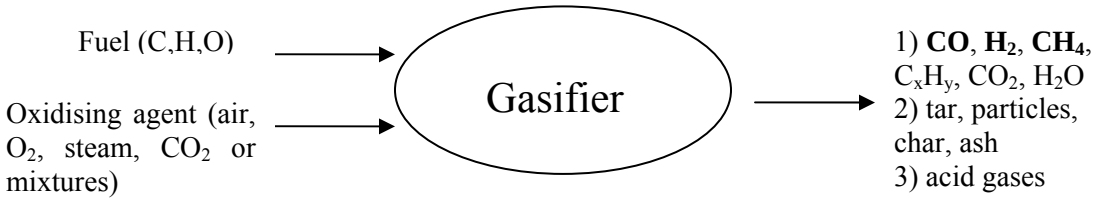

Figure 4.4. Gasification principle.

Gasification reactions: $C + H_2O + heat \rightarrow CO + H_2$

$$C + CO_2 + heat \rightarrow 2\ CO$$

The design principles of the gasifier unit are of three main kinds: fixed-bed gasifier (updraft or downdraft), fluidised bed gasifier (bubbling or circulating) and pressurised (fluidised bed) reactor which can be connected to gas turbine [Barrio 2002]. Waste can be used for gasification, it does not need specific sorting but it must be crushed and pelletised to increase the energy density. Produced gas composition depends on the biomass type and the gasifiying conditions (and the eventual presence of catalysts for reforming).

Gasification is of particular interest for the biomass fraction of MSW but also biomass residues and woody biomass after pre-treatment (drying, particle size, pelletising) but mostly on a small to medium scale. However several constraints associated with gas conditioning make gasification difficult and still not very attractive: hot gas cleaning (particle and H_2S removal, etc), H_2/CO ratio (quality of gas), CH_4 and tar reforming and first and foremost efficient and economical removal of tar [Barrio 2002]. Association of a gasifier to a turbine is particularly difficult as a turbine is an intricate and delicate machinery that require a very clean gas with low levels of contaminants (alkali, etc). Furthermore other technical problems are to be expected such as feeding difficulties, ash slagging and corrosion. Environmental aspects comparable to the one faced with combustion are also to be expected [Kwak 2006].

Pyrolysis

Pyrolysis is a thermochemical conversion process where a solid fuel is heated in the absence of an oxidising agent (in an inert atmosphere). Furthermore it is the initial step in combustion and gasification processes and can therefore bring useful information about the primary products of these processes. Pyrolysis, as a conversion process, yields 3 products: (i) a gas mixture; (ii) a liquid (bio-oil/tar); (iii) a solid residue (char). The proportion and composition of the various fractions will depend on a variety of parameters. Each fraction may have a commercial potential in spite of some limitations/constraints. Pyrolysis is of particular interest for the biomass fraction of MSW. Two technologies exist and differ on the method of heat transfer: fast pyrolysis for production of bio-oil and slow pyrolysis for production of charcoal.

For more about pyrolysis see **Chapter 7**.

4.3 Biological treatment of MSW

Biological treatment will require longer time than thermal conversion as biological processes takes days, weeks or even months to be carried out fully. These processes may be particularly suited for some MSW fractions i.e. niche applications and will therefore contribute to the expansion of the MSW treatment arsenal.

Composting

Composting of MSW has been defined as "the biological decomposition of the biodegradable organic fraction of MSW under controlled conditions to a state sufficiently stable for nuisance-free storage and handling for a safe use in land applications" [Tchobanoglous 2002]. Several specificities of composting are immediately arising from this definition: (1) this process is limited to the organic fraction of MSW and separation of other fractions is a prerequisite; (2) this process is carried out under controlled conditions and is not a mere dump; (3) the resulting decomposition product, i.e. compost or humus, has to comply with safety and quality standards before further agricultural use [Tchobanoglous 2002]. This technology will therefore achieve a twofold goal: reduction of waste volume and mass, and production of a valuable by-product.

Practically, various micro organisms (bacteria, fungi, etc) break down the organic matter to produce CO_2, water, heat and a stable and nutrient-rich organic product useable for soil amendment. The decomposition process goes through different phases with change in the micro organisms' population and activity of decomposition. The different phases can be followed by the temperature profile in the composting matter. To optimise the process (i.e. fast process), many parameters are of importance: C/N ratio (nutrition of the micro organisms), particle size/surface area exposed (the smaller the particle, the easier for micro organisms to work), oxygen/aeration, moisture content, pH level, temperature.

Different technical solutions exist for composting of vast amounts of waste. Traditionally, windrow systems (outdoor row of protected/unprotected waste) were used but today preference is given to in-vessel systems (i.e. large incubators) as they allow easier and more efficient control of the process [Iyengar 2006]. To ensure fast, efficient and safe decomposition, "active (or fast, hot) composting" operation is preferred to passive composting where no maintenance is applied. Active composting requires the follow-up and optimisation of aeration, moisture and C/N ratio throughout the composting matter.

On top of the care required for the optimisation of the process by providing ideal conditions for the microbial activity several problems are to be expected. The main challenges associated will be: pre-processing of the MSW, pathogen control (health hazard posed by the propagation of micro organisms into the air), leaching to underground water (need for an impermeable surface), odour control, fly and rodent attraction, fires risks (spark or self ignition), contaminants presence (heavy metals). Health and safety constraints are therefore a hindrance for the establishment of vast composting systems and their commercial viability. However, "backyard" composting remains a good waste treatment for organic wastes such as yard clippings or food scraps.

Anaerobic digestion

Anaerobic digestion can be described as composting in the absence of oxygen and require therefore a closed reactor system, i.e. a digester.

Anaerobic digestion is especially well adapted for high-moisture wastes. The products of anaerobic digestion are a biogas (CH_4, CO_2 and acid gases), a liquid ("oil") and a solid residue (mostly lignin and chitin). However, the energy density of the gas has to be increased (removal of CO_2) as well as to be cleaned before eventual use for electricity generation. The liquid fraction may be used as a fertilizer if it does not concentrate contaminants (pesticides, heavy metals), while the solid residue may be further composted. The obvious limitations make this technique little appealing and economically viable except in some specific niche applications such as wastewater treatment (sludge digestion) and farm slurries [Rodriguez Andara 2002].

Fermentation

Fermentation is of interest for the biomass fraction of MSW and more generally biomass residues. This process includes two steps: (1) lignocellulosic materials are first hydrolysed to sugars with the help of enzyme and/or acid hydrolysis [Xiang 2003] and thereafter (2) converted into ethanol through fermentation. Ethanol production from lignocellulosic materials (not only corn but woody biomass) is a hot topic as development of a car fuel blend including 85% of ethanol and 15% gasoline known as E85 is a serious alternative to conventional gasoline. The trend now is for the production of Flexible Fuel Vehicles that can function either on gasoline or on E85. An overview of ethanol production (potentials, constraints and technologies) from waste and biomass residues can be found in [Prasad 2006]

4.4 Physical treatment of MSW

Source reduction, recycling and separation

Efficient and responsible waste management strategies include several physical treatments. **Source reduction** is a pre-emptive measure aimed at lowering the amount of waste. This could be achieved by adopting various measures such as design of smaller, biodegradable packages, purchase of bulk products, reduce use of disposable items or lengthening the life of durable goods (less renewal, charities). Industrials and consumers can both act towards this goal but political involvement can fasten and improve the results. **Separation** consists in removing some fractions, especially problematic fractions (PVC, batteries, etc) in order to provide proper handling of these but also to prevent problems associated with them. For example, removal of PVC from MSW mainstream will greatly reduces production of Cl-containing compounds during combustion. **Recycling** is an important feature of waste management as it is a step towards a more sustainable society. Recycling consists in the re-use, after proper re-processing, of materials. Recycling allows a reduced use of natural resources and offers commercially viable opportunities. Recycling is mostly aimed at paper products, plastic, metal and glass but may apply to other products. Most of the recycled materials are obtained

through active sorting of the consumers but not always; big appliances have to be demounted, dangerous components removed and further treated before metal and plastic can be recuperated and re-used.

Landfilling

Landfilling is the process by which solid waste are placed/deposited in or on the surface soils. Modern landfilling has little to do with old-fashioned dumps where wastes were thrown with no consideration for the immediate and long-term environmental and public health consequences. Modern landfilling includes proper planning, design, monitoring and follow-up of the site after its closure.

Combustion and recycling are today seen as better alternatives even though landfilling with proper monitoring is considered by many (especially in the USA) as an economical and environmentally acceptable method (large area available, limited incineration capacity). However, landfilling is the main solution for solid residues, in other words residues collected after a previous treatment such as combustion.

Several configurations of landfilling exist and usually differ by the shape of the terrain. However, they all face the same environmental challenges, i.e. emission of gases to the atmosphere and leaching of contaminants to soils and water resources.

Generation of landfill gases includes CO_2, CH_4 but also trace gases (ammonia, sulphides, etc) with potential risks. This gaseous release to the atmosphere will also be accompanied by odours, which may be a major problem. That is why landfills are covered by a layer of fresh soil regularly. The nature, release rate and origins of the gases will evolve with time during the life of a landfilling site. Several technologies are available for management of landfill gas: capping/covering and extraction wells for collecting (and recovery eventually), vents for pressure release, burner for flaring. Leachate can be defined as the liquid produced in a landfill from the decomposition of waste within the landfill accompanied by water. Composition of the leachate is very complex and will change over time. This makes its management very complicated. Handling of the leachate consists in preventing its release outside the landfilling site. Physical barriers (liners) can be placed under the landfill and the leachate collected by channels and removed to be further treated or placed back at the surface of the landfill.

Continuous monitoring is necessary to ensure the safe operation and relative innocuousness of the landfill. Air quality (ambient air and landfill gas) and groundwater quality are monitored continuously.

4.5 Complete overview of waste management

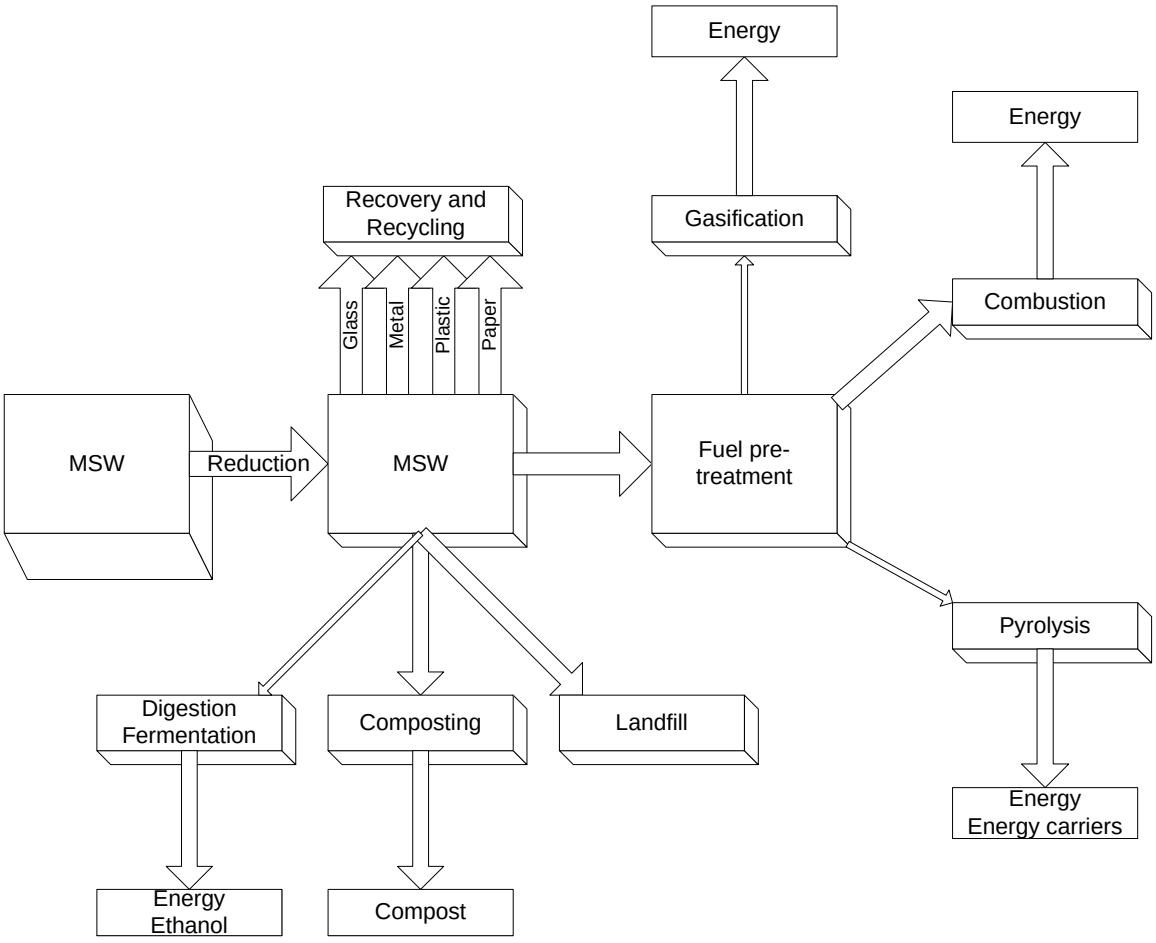

Figure 4.5. Waste treatment: a complete overview.

Figure 4.5 summarises the present waste treatment situation. Thin arrows represent emerging technologies.

5 Experimental section

5.1 Reactor and set-up

The set-up used is an in-house designed and fabricated "macro-TGA" (batch reactor) for experiments on samples up to about 100 grams. It is possible to measure gas concentrations and weight loss simultaneously while keeping good control of the operating parameters: reactor temperature, gas medium temperature, heating rate and inlet gas flow. Operating conditions of the reactor are flexible when it comes to gas nature (inert or active) and flow, temperature profile and range (up to 900°C) along the reactor, heating rate and sample size, weight and nature of the sample.

The reactor is a vertical stainless steel tube with an Al_2O_3 ceramic coating to minimise the catalytic reactivity of the walls. The reactor has an inner diameter of 0.1 meter and a height of 1 meter. It is heated by 5 independent heating elements with a total effect of 6 kW. Each heating element is regulated by 2 thermocouples installed at the surface of the tube reactor (diametrically opposed location). A pre-heater is used to heat the gas medium before entering the reactor. A suspension system holds a cylindrical-shaped wire mesh basket containing the sample. The basket is connected to a Sartorius CP 153 precision balance to record the weight loss of the sample during its thermal decomposition ("macro TGA" function). The fuel can also be placed directly on a grate (distribution plate) located right above the pre-heater. In this configuration, no weight loss can be recorded during the experiment but samples up to several hundreds grams can be loaded. A schematic diagram of the pre-heater, the reactor and the sampling line is shown in Figure 5.1.

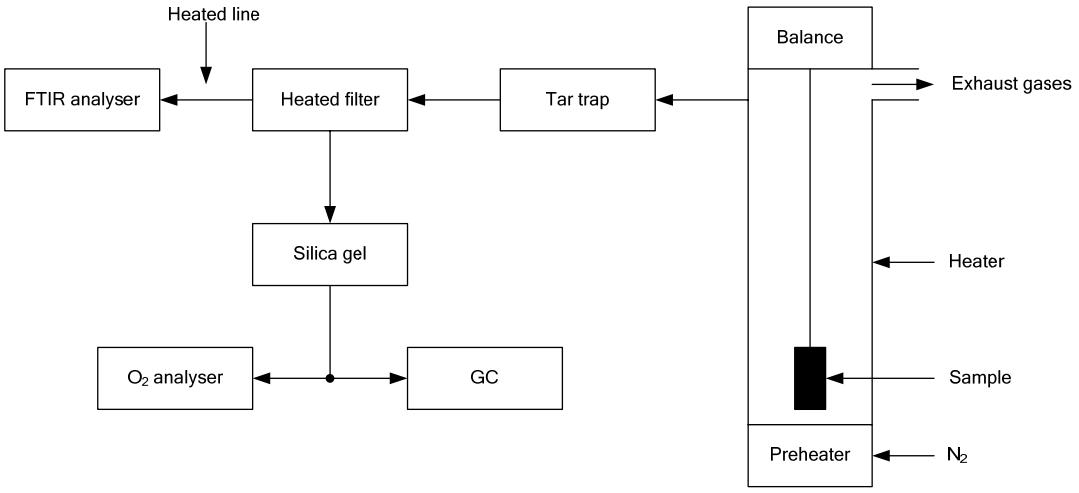

Figure 5.1. Reactor and gas sampling set-up.

Only a fraction of the exhaust gases (about 6 Nl/min) is extracted through a glass probe placed inside the reactor and going through a (ice+water)-cooled trap (glass bottles) and a filtering system (paper filter) before it is analysed by a FTIR analyser and a micro-GC. This prevents any deposition on the optical system of the FTIR analyser and pollution of the GC columns. A small amount of silica gel was also used to prevent any water from entering the GC columns.

Temperature measurements inside the sample were realised using up to 4 thermocouples. The detail concerning these intra-sample temperature measurements can be found in **[Becidan 2007d] (P-VI)**.

5.2 FTIR analysis

Principle of FTIR. FTIR (Fourier Transform Infra Red) analysis is an analytical method based on the interactions between IR light (i.e. wavelength range from 2.5 to 15 μm) and matter. Molecules are vibrating at characteristic frequencies. Exposed to IR radiations, a molecule will absorbed IR energy only at frequencies matching the molecule's natural frequency of vibration (resonant frequencies). As a consequence, the absorption pattern (frequencies and intensities) is unique for a given molecule. The frequencies of vibration of a molecule (subsequently the frequencies of the radiations absorbed) are directly related to the nature of the atoms and the structure of the molecule. The absorption intensity is correlated to the change of the dipole moment due to the vibration and to the concentration of molecules. Consequently, qualitative and quantitative results can be extracted. Almost all molecules can be identified by FTIR except for some symmetrical molecules (O_2, N_2, H_2, etc) and inert gases (Ar, He, etc) because they do not exhibit any change in their dipole moment.

Important general FTIR definitions.

$A(\lambda) = \varepsilon(\lambda) \cdot b \cdot c$; A: absorbance

$A = \log_{10} (I_0/I)$; I_0: light intensity before the absorbing sample; I: light intensity after the absorbing sample

$A = \log_{10} (1/T)$; $A = \log_{10} (100/\%T)$; $T = I/I_0$

T: transmittance; λ: wavelength; $1/\lambda$: wavenumber

b: the distance the light has to perform through the absorbing sample (pathlength)

c: concentration of the absorbing sample

$\varepsilon(\lambda)$ is the extinction (or absorptivity) coefficient, substance-specific and function of λ

Interferogram and Fourier Transform. During FTIR analysis, the specimen is subjected to a modulated IR beam. The heart of the FTIR analyser is the interferometer. This optical device converts the IR radiation from many waves with different frequencies to a single wave that varies over time and known as interferogram. This very conversion (or modulation) allows the FTIR to analyse all IR frequencies simultaneously, while previous FTIR apparatus had to scan over the whole IR spectrum. The Fourier Transform is the mathematical tool that finds back the frequencies information contained in the interferogram and reconstructs all the waves that constitutes it. By subjecting the interferogram to a Fourier transform, all the original frequencies are retrieved except those which were absorbed by the sample. The modulation is therefore reversed to get the IR spectrum. The IR spectrum usually presents the absorbance (see page 32 for definitions) as a function of wavenumber (1/wavelength).

$$f(t) = \mathcal{F}^{-1}(F)(t) = \frac{1}{\sqrt{2\pi}} \int_{-\infty}^{\infty} F(\omega) e^{i\omega t}\, d\omega. \qquad (1)$$

The continuous Fourier Transform mathematical expression (1)

Our FTIR. The FTIR analysis of the gases was performed with a Bomem 9100 analyser and GRAMS/32AI version 6.00 for spectrum analysis. The FTIR sampling line and cell (volume of 5 litres and optical path length of 6.4 m) were heated at 176°C. The instrument was equipped with a DTGS (Deuterated TriGlycine Sulfate) detector at the maximum resolution of 1 cm^{-1}. The FTIR was used to quantify CO_2, CO, CH_4, C_2H_2, C_2H_4, HCN and NH_3. The FTIR analyser gives one measuring point every minute (1 scan every 5 s, averaging value over 12 scans).

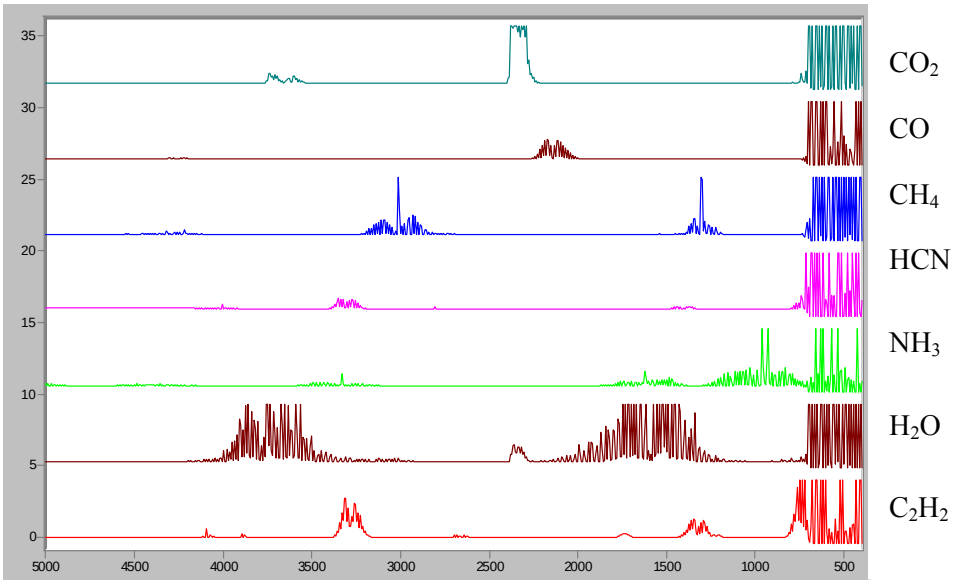

Figure 5.2. Stacked FTIR spectra of various gaseous species. Arbitrary unit versus wavenumber (cm^{-1}).

Qualitative analysis. Each gas has a unique IR absorption pattern, often referred to as a fingerprint or signature (see Figure 5.2). It can therefore be matched with known IR patterns of identified materials to perform a qualitative analysis. However, overlapping of IR spectra of different species in a mixture is a very common problem encountered during IR analysis. It does not mean that further analysis is not possible but it does often lead to further treatment of the data. Overlapping is not a critical problem when it comes to identify the various compounds present in an exhaust gas, but it can be a major problem when it comes to quantification of the various gaseous species.

Quantitative analysis. Quantitative analysis, in other words determination of concentration, with FTIR is based on the Beer-Lambert law (illustrated on Figure 5.3). The Beer-Lambert law is the linear relationship between absorbance (A, no unit) and concentration of an absorbing species. Absorbance is defined as the fraction of the initial radiation I_0 absorbed by the sample, i.e. $1-I/I_0$ (definitions page 32). Consequently, if all the light passes through a sample without any absorption, then absorbance is zero, and transmittance (definitions page 32) is 1. If all the light is absorbed, then percent transmittance is zero, and absorption is infinite.

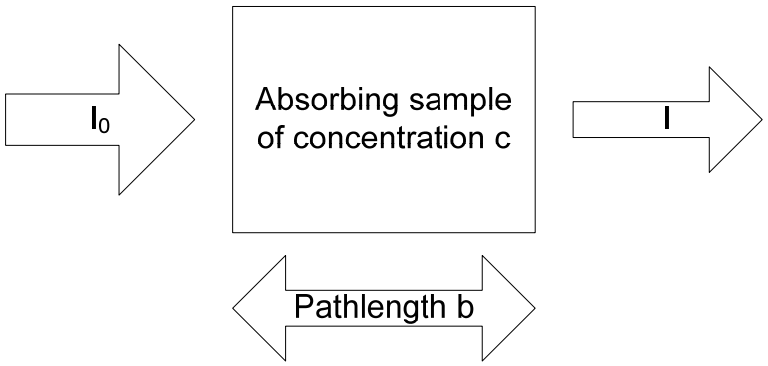

Figure 5.3. Illustration of the Beer-Lambert law (see page 32 for definitions).

Nevertheless, the Beer-Lambert law suffers several limitations. The linearity of the Beer-Lambert law is limited by both chemical and instrumental factors. The most common causes of non-linearity are, amongst others: deviations in absorptivity coefficients at "high" concentrations (several hundreds ppm typically) due to interactions between molecules in close proximity; scattering of light due to particles; fluorescence or phosphorescence of the sample.

Calibration. Because of this non-linearity it is vital to build good calibration curves, i.e. with a sufficient number of points covering the whole working range as intra- and extrapolation is delicate. Practically, to perform a calibration one has first to select a wavenumber (1/wavelength) zone where the species is absorbing, in other words where an absorption peak or series of peaks is visible (Figure 5.4). It is important to be sure that only the investigated component is absorbing at this wavenumber. If it is not possible (see HCN in **[Becidan 2007b] (P-IV)**), the data has to be further processed.

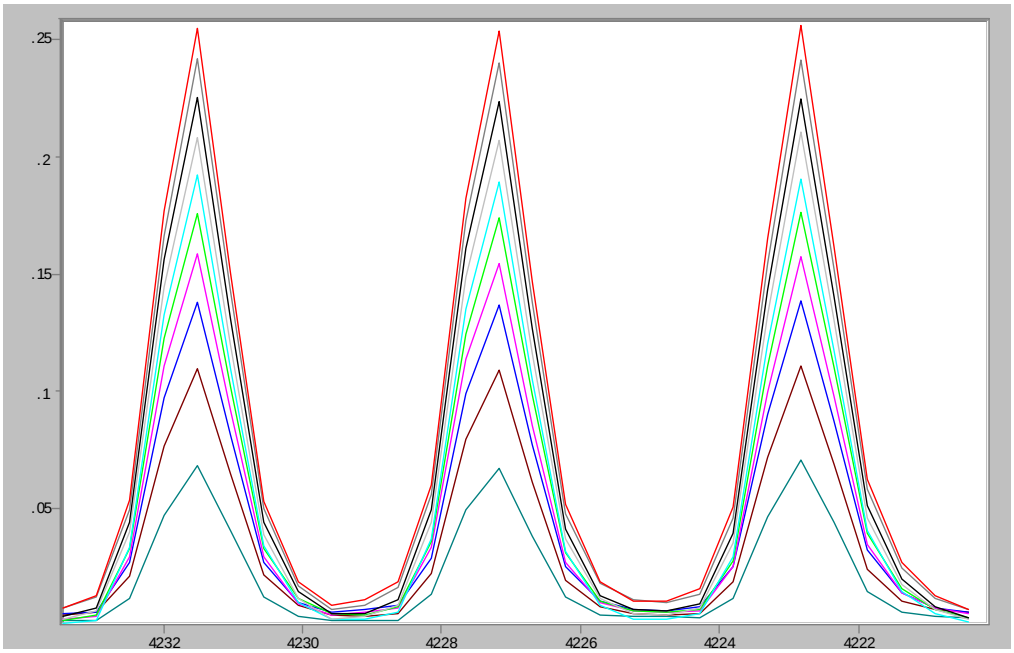

Figure 5.4. 10 CO calibration spectra (from 1.21% to 12.13%). Absorbance (no unit) against wavenumber (cm^{-1}).

Two parameters can be registered to build a calibration curve: the height of a peak and the area of a peak. Figure 5.5 presents the calibration curve for HCN between 0-300 ppm with use of the peak height at 3372.29-3374.7 cm^{-1}. The points are experimental points and the linear trendline (proposed by MS Excel) is shown, exposing the linear relationship between peak height and HCN concentration. However this linearity is not valid at high concentrations as shown in Figure 5.6 with the linear trendline calculated by Excel for HCN between 0-1990 ppm.

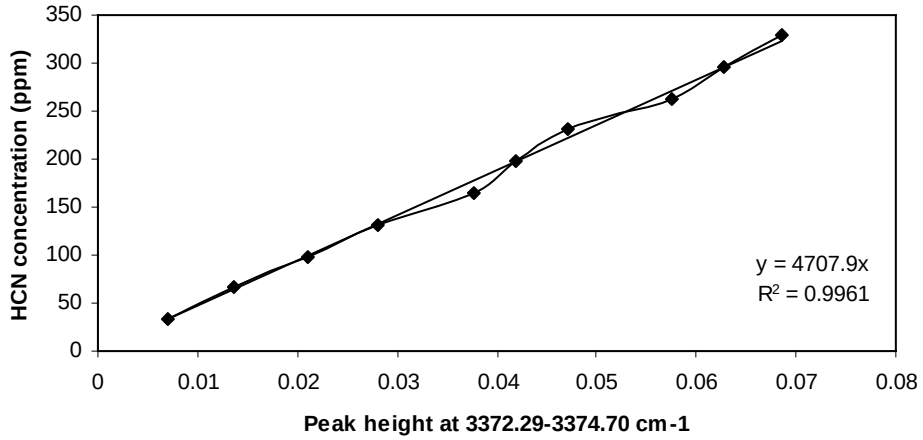

Figure 5.5. Calibration curve for HCN at 0-300 ppm (and linear trendline).

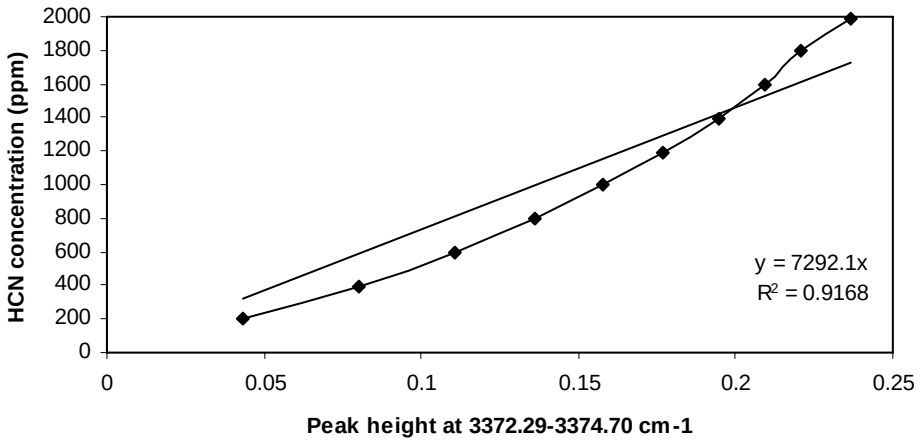

Figure 5.6. Calibration curve for HCN at 0-1990 ppm (and linear trendline).

Other constraints associated with FTIR analysis.

Baseline: the baseline (reference line to measure height and area) has to be similar for the calibrations and the experimental data. Disturbance of the baseline (background noise) by experimental factors can affect low concentrations measurements.

A>1: absorbance above 1 can not be used for quantification as this reflects the fact that all the light has been absorbed by the sample. Therefore one should choose a peak whose height is less than 1 for the whole measuring range. This problem may occur at high sample concentrations.

High concentrations: the non-linearity can have consequences at high concentrations. At high concentration the correlation between area and height values and concentration is such that a minor increase in absorbance can lead to a substantial increase in concentration. This sensibility makes quantification difficult as the slightest shift can influence substantially the calculated concentration.

Matrix effects: another type of interference is known as "matrix effects". This is similar to overlapping except that in this case the resulting spectrum (of the 2 or more interfering species) is not the addition of the spectra of the individual species. The shape and the area of the peaks are modified and new peaks may appear.

Overlapping and spectral subtract, the HCN example: ideally it is possible to find a unique wavenumber region where only the relevant species absorbs IR light but in practise there is no such region for HCN (pyrolysis experiments). Further treatment of the spectra is therefore necessary. The 3774.70-3372.29 cm^{-1} region (the less overlapped) is disturbed by C_2H_2 and NH_3. The 3774.70-3372.29 cm^{-1} region was corrected for the interferences from NH_3 and C_2H_2 whenever necessary. The high Signal-to-Noise-Ratio of the selected HCN bands, due mainly to the high N content (and the high (N/C) ratio) of the biomass samples, made absolute concentration measurement possible and accurate.

The procedure of "correction", in other words removal of interferences, is an operation performed with help of the FTIR software (GRAMS32 AI) and consists in electronically removing disturbances. This operation is called "spectral subtract" and can be described very simply as such (example in Figure 5.7, (1) before and (4) after spectral subtract):

Result file = Sample file – (Subtrahend file x Subtraction factor)

Result file = "Clean" spectrum where [HCN] can be determined, e.g. (4).

Subtrahend file = Interfering species X calibration spectrum (at a known concentration $[X]_0$ from a database of 10 spectra to limit non-linearity effects), e.g. NH_3 in (2).

Sample file = Raw spectrum from experiment (with calculated [X]), e.g. (1).

Subtraction factor = $[X] / [X]_0$; as the interferences are assumed to be linear.

The spectral subtraction operations were performed manually and 10 calibration spectra were available as subtrahend file per interfering species over the working range to reduce non-linearity effects between two calibration spectra. The subtraction factors were calculated by assuming linear interferences (matrix effects were assumed negligible).

(1) (2)

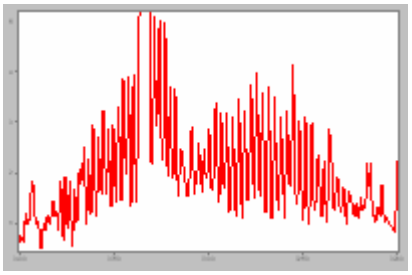

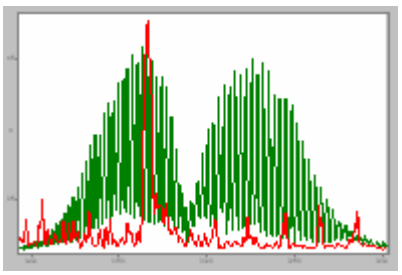

(3) (4)

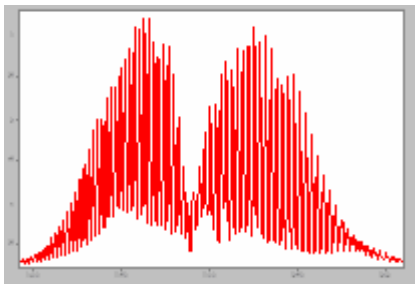

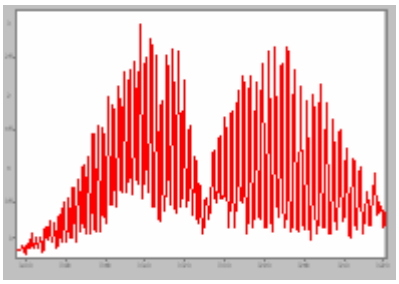

Figure 5.7. FTIR Spectra (absorbance versus wavenumber (cm^{-1})) at 3200-3400 cm^{-1}.

(1) Raw data: spectrum obtained during pyrolysis of BSG.

(2) Calibration spectra of HCN (green) and NH_3 (red) showing the overlaps.

(3) Calibration spectra of HCN (400 ppm).

(4) "(1) after spectral subtract": NH_3 interferences removed, HCN can be quantified.

Uncertainties calculation. Example with NH_3 [EURACHEM/CITAC 2000]. The combined uncertainty was obtained from the contribution from (1) the precision of the method, expressed as the relative standard deviation calculated from the FTIR heights and areas tabulated for a given point (experimental), (2) the trueness (accuracy) of the method, expressed as the relative uncertainty on the calibration method. Two "zones" are visible, one (low concentration) where uncertainty is not (little) dependent on the concentration and another (high concentration) where uncertainty is proportional to the concentration (Figures 5.8- 5.9).

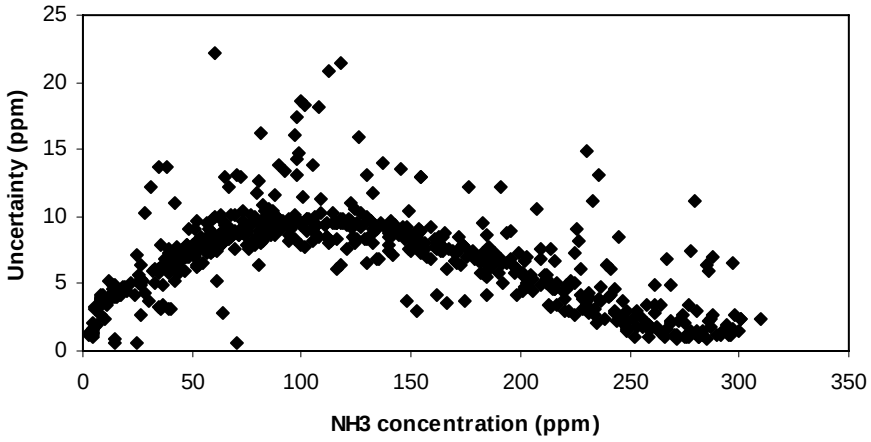

Figure 5.8. Experimental uncertainty at low levels for NH_3.

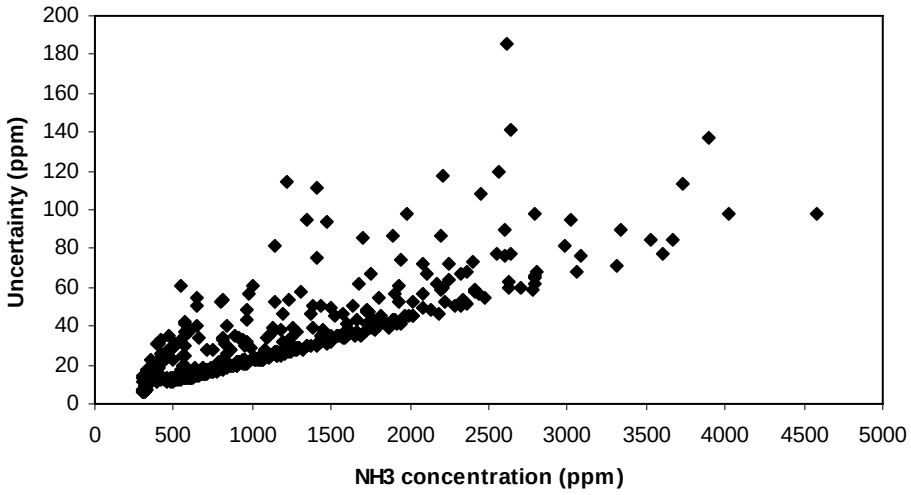

Figure 5.9. Experimental uncertainty high levels for NH_3.

The uncertainty at high concentrations (above 300 ppm) was reported as a relative standard deviation (in %) corresponding to the square root of the slope of the linear regression between squared uncertainty and squared concentration. The uncertainty at

low concentrations (below 300 ppm) was reported as a (minimum) standard deviation (same unit as concentration). The results can be found in the articles.

5.3 GC analysis

Principle. Gas Chromatography (GC) is an analytical method for analysis of complex mixtures. It is based on the different affinities of compounds between a stationary phase (inner coating of a column) and a moving phase (gas medium). Each constituent of a mixture will be separated (GC term: eluted) from one another and come out of the column (and reach the detector) after a characteristic duration (GC term: retention time). Detectors will also be able to determine the concentration of each species. Figure 5.10 illustrates the principle. Parameters such as column temperature, column pressure, stationary phase nature, column length and carrier gas can be adapted to optimise the separation between compounds.

Our GC. The gas samples were quantified online using a Varian CP-4900 micro gas chromatograph equipped with 2 TCD detectors and a double injector connected to two columns: a CP-PoraPLOT Q column (10 m length, 0.25 mm inner diameter and 10 µm film thickness) to separate and quantify CO_2, CH_4, C_2H_2+C_2H_4 (not separated) and C_2H_6 and a CP-MolSieve 5Å PLOT column (20 m length, 0.25 mm inner diameter and 30 µm film thickness) to analyse H_2, O_2, CH_4, CO and N_2. Helium and argon were used respectively as carrier gases in the two columns. TCDs (Thermal Conductivity Detector) were used. Calibration over the working ranges was realised with 3-5 points per compound. The response of the TCDs was linear for all compounds at the concentration ranges studied during the experiments.

Constraints associated with GC. The following problems can be mentioned: optimisation of the separation process may be complex and time-consuming; a given column can not detect all types of compounds, hence the need for multi-column devices; slow elution limits the number of experimental points; identification of unexpected compounds.

GC performance. The GC was able to provide one measurement every 2.5 minutes (2 min total elution time, 30 s sampling time). Results from GC and FTIR were most often in good accordance except for the fast heating rate experiments where significant differences could be observed due to the rapid completion of the experiment. GC results were therefore mainly used for comparison purposes with FTIR. The following figures present some results. Figure 5.11 and 5.12 show the good accordance between GC and FTIR results, while Figure 5.13 show the problems caused by the insufficient resolution of the GC. GC gives an “instant” value while FTIR gives an average value (1 point is the average of 12 5-second scans and gas is constantly travelling through the FTIR cell). Fast processes will therefore not be properly described by GC.

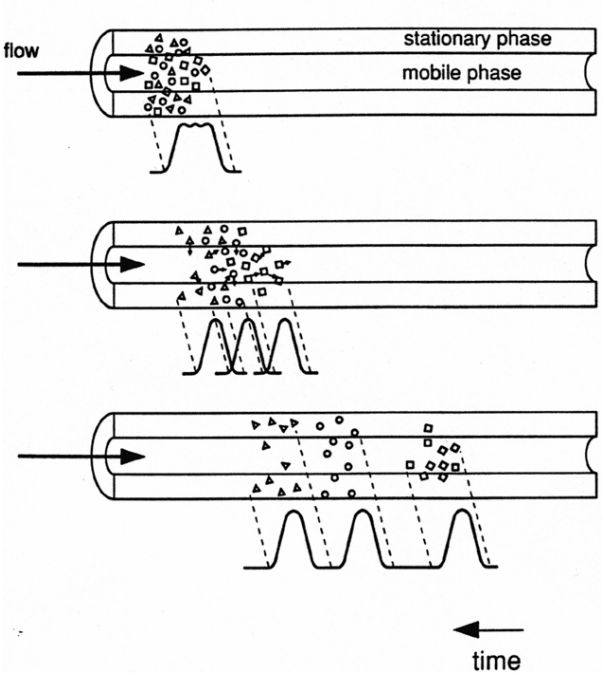

Figure 5.10. GC principle: separation of compounds in a column [Varian 2006].

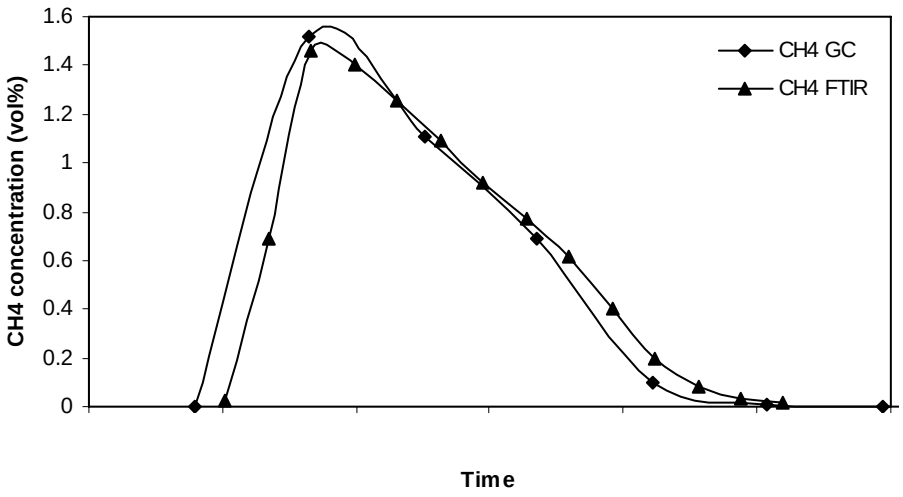

Figure 5.11. Comparison of GC and FTIR (pyrolysis of BSG at 700°C): good agreement.

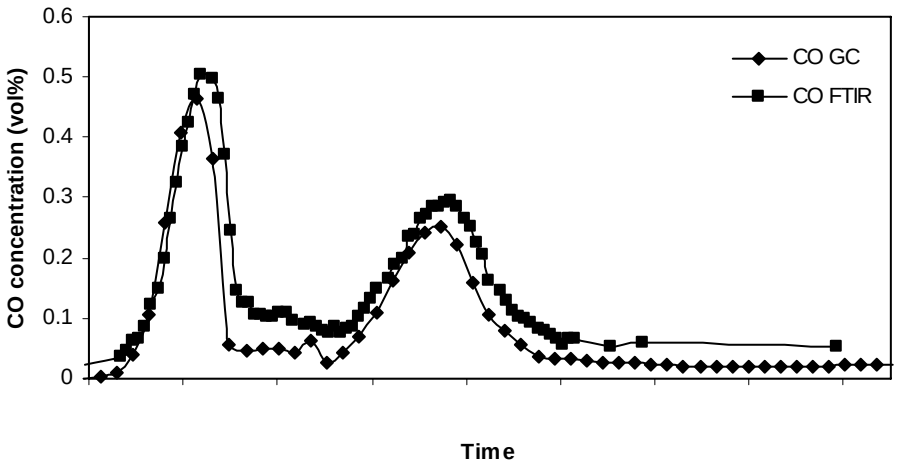

Figure 5.12. Comparison of FTIR and GC (pyrolysis of coffee waste, 10°C/min): good agreement.

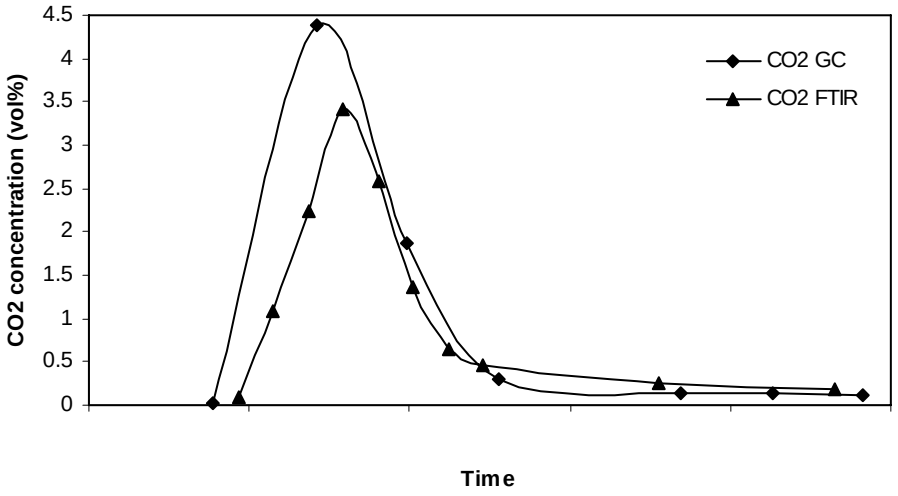

Figure 5.13. Comparison of FTIR and GC (pyrolysis of fibreboard at 900°C): very fast process, too few points for GC.

6 N-chemistry in biomass before and after thermal degradation

Abstract

During thermal conversion, a fraction of N will be released as NOx, a major pollutant. This section deals with N-chemistry before, during and after pyrolysis, the first step in combustion.

N-concentration in biomass. *Large variations occur from wood that contains about 0.1 wt% of N to leaves, seeds and biomass residues which contains several percents of N.*

N in biomass. *N-chemical structures in biomass are many and versatile. The detailed knowledge is often overseen by the bioenergy world, where N is considered vaguely as "mostly of proteinaceous origin". Reviewing plant physiology publications, it was shown in this study that this is an inaccurate approximation. N can be found in many other forms at significant levels and proportions. Significant Non-Protein-Nitrogen (NPN) contributors have been identified as: free amino acids, polypeptides, non-protein amino acids, nucleic acids and mononucleotides, alkaloids, inorganic nitrogen and chlorophyll.*

N-release from model compounds. *Chemical compounds depicting a single chemical function of N, i.e. model compounds, have been studied to determine the release pathways of N. Two classes have been under scrutiny in the literature: proteins /amino acids and N-aromatics. The main final product for amino acids/proteins is HCN in most cases. The primary and secondary pathways of decomposition identified are many. The main (out of 5) primary path is dehydration through formation of cyclic amides, the most common being 2,5-diketopiperazine (DKP). The DKP ring will then (secondary reaction) open/break, producing a variety of compounds, which will thereafter produce mostly HCN but also NH_3 and HNCO. Pyrrole and pyridine are the most common N-aromatic compounds. They almost exclusively produce HCN. The mechanism of decomposition of pyrrole and pyridine involves breaking of bonds in the ring and/or rupture of the C-N bond followed by random cleavage/recombination of the resulting diradical.*

New considerations. *The results obtained from model compounds should be looked upon carefully. Even if it is true that N is found in protein/amino acids and N-aromatic structures, it is also true that N-structures are only a part of the biomass matrix (cellulose, hemicellulose and lignin) and therefore N-compounds will not only be in the vicinity but also linked in a variety of ways to many different functional groups (containing N or not), which may significantly influence N-chemistry. This brings limitation to the validity of the results obtained through model compounds studies and their direct transfer to biomass. Model compounds can not portray fully biomass and its intricate makeup. This calls for the study of biomass itself even though its complex constitution has hindered mechanistic insights so far.*

N release from biomass. *(1) N-release in biomass. Experimental results from literature are often contradictory. NH_3 is often the main N-product but not always. HCN release is increasing with temperature and heating rate, while NH_3 release dependence is unclear but is most often increasing until a given temperature. The dependence on N-functionalities is still unclear. (2) Comparison with model compounds. Little mechanistic insight can be obtained from biomass studies and transfer of model compounds results is not straightforward as the interactions between N-compounds and non N-compounds are not known.*

It was concluded that the combined study of biomass and model compounds is the best approach to try to grasp a more complete picture of N-chemistry.

On the one hand, Nitrogen (N) can be considered a ***minor*** component of biomass when it comes to weight percentage, on the other hand when it comes to pollution potential N is a ***major*** challenge both ***directly*** through NOx emission and its consequences (acid rain, greenhouse effect intensification) and ***indirectly*** through its involvement in synthesis of ground-level ozone formation and stratospheric ozone destruction. In this section, an in-depth overview of N in biomass will be given. First the concentrations and chemical forms in which N can be found in biomass will be presented, and then a presentation of N-chemistry studies (NOx precursor's mechanistic considerations) during pyrolysis through model compounds and various biomass samples will be presented. This chapter shows that the bioenergy world often have a too simplified picture of the variety of chemical forms of N in biomass prior to pyrolysis. When it comes to N-chemistry during pyrolysis, it is suggested that model compounds studies should be looked upon carefully, while interpretation of the widespread biomass pyrolysis results is attempted.

6.1 Total-N (TN, [N], N-concentration)

N-concentration in biomass is usually determined according to the micro-Kjeldahl procedure and is referred to as "total-N" (TN). TN and N-functionalities in biomass may vary with numerous parameters (Figures 6.1-6.4) such as: biomass type [Stuart 1936; Cowling 1966; Yeoh 1994; Periago 1996 and Table in Appendix]; location in the plant (bark, stem, root, branch, leaf, cross-section, flower, etc) [Merrill 1966; Cowling 1970; Langlois 1976]; the season [Näsholm 1990; Billow 1994; Gomez 2002]; the age of the plant or the aging after cutting [Birecka 1984] ; the resources availability (water, fertiliser) [Langlois 1976; Billow 1994; Dong 2002; Meuriot 2003; Cheng 2004]; or the stage of growth [Sánchez 2005].

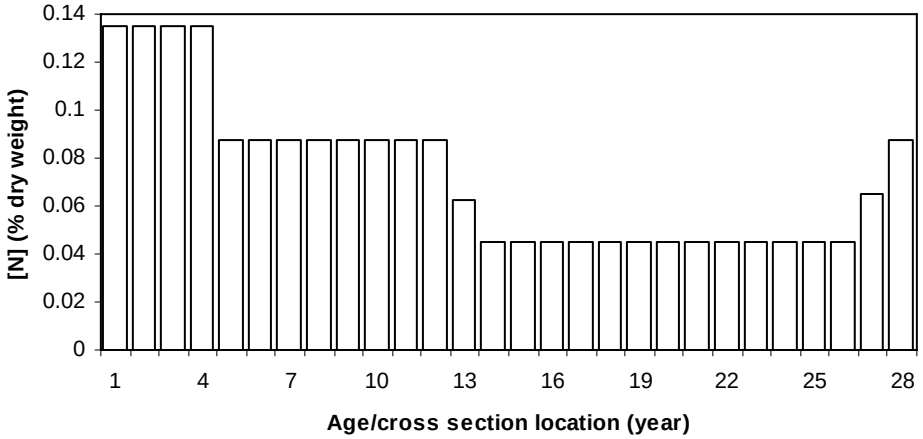

Figure 6.1. Cross-section of white pine. 1-13:sapwood, 14-27: heartwood, 28: pith. [Merrill 1966].

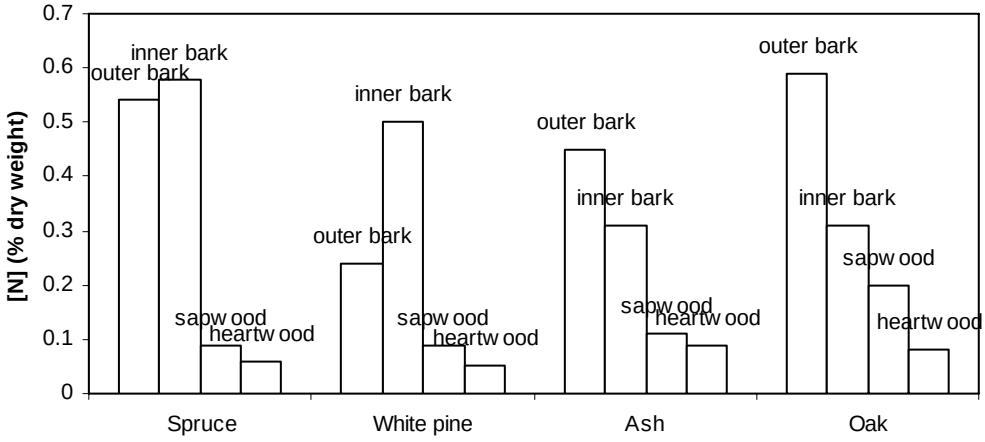

Figure 6.2. [N] in various tree sections. [Merrill 1996].

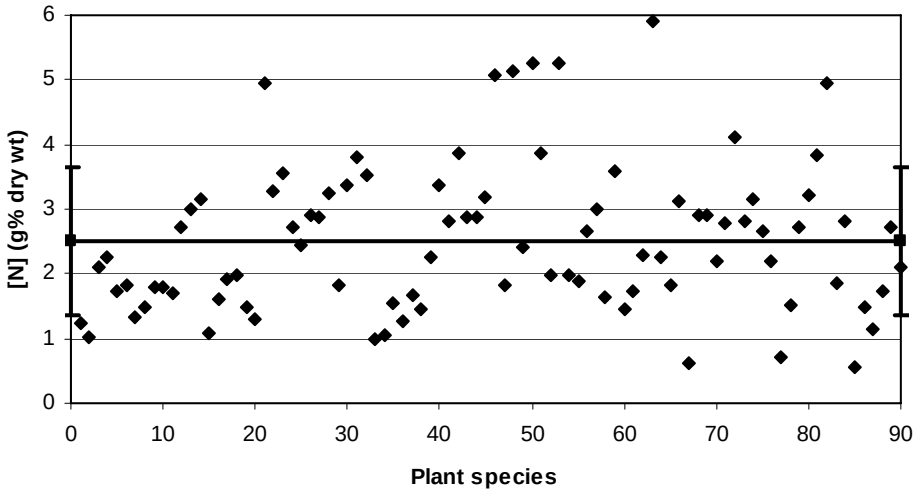

Figure 6.3. [N] in leaf of 90 plants from the 3 major plant phyla. Line: average value, 2.51 wt% (+/- 1.15 wt%). [Yeoh 1994].

The level of N in a plant can be explained by the biological roles played by N-species. The TN in wood will decrease as one is going deeper in the trunk (Figure 6.1) as a result of cell maturation [Cowling 1966; Merrill 1966; Cowling 1970]. Seeds have high [N] (Figure 6.4) as they contain nutritive and protective compounds (proteins for energy, alkaloids for antifungal activity) to nurture plant development. It can therefore be understood that the level but also the nature of N in biomass is directly related to the physiology of plants. However, the chemical structures in which N is found in biomass are many and their relative proportion is not well known in the bioenergy world.

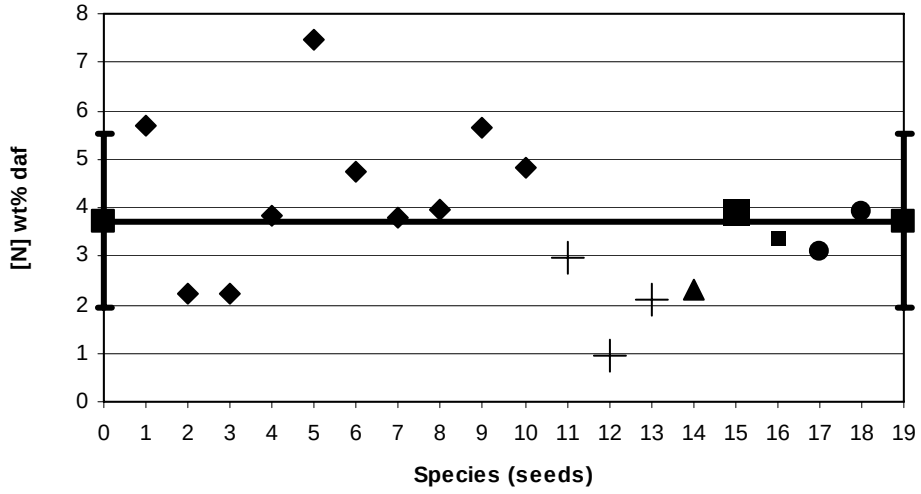

Figure 6.4. [N] in 6 seeds. Line: average value, 3.73 wt% (+/- 1.57 wt%). [Predel 1998; Onay 2001; Ezeagu 2002; Hansson 2003a; Acikgoz 2004].

6.2 Nature of N in biomass (N-functionalities)

The chemical structures in which N is found in biomass are many. However their variety and relative importance/concentration are not well known outside the plant physiology world. The detailed knowledge of the nature and relative amount of the many N-containing compounds is often overseen by researchers working in the field of bioenergy, describing the N-compounds vaguely as "mostly of proteinaceous origin" with very little or no further investigation. However a look at the physiology of plants (not discussed here) shows that this is unsatisfactory as plants have the ability to synthesize a myriad of N-containing compounds. Even though a clear correlation between N-functionalities in biomass and N-behaviour/chemistry during thermal degradation (pyrolysis, combustion, gasification) is yet to be clearly established, it is crucial to lay out an accurate picture of N in biomass.

It is possible to classify N compounds in 2 main groups: the protein-N (PN) and the non-protein-N (NPN).

6.2.1 Protein-N (PN)

A significant proportion of the nitrogen present in biomass is found in form of proteins (Figure 6.5). Proteins are bio-macromolecules that consist of amino acids (molecules that contain both amine and carboxylic acid functions) joined by peptide bonds (amide bond) and have a variety of biological roles (structural, storage of nutrients, etc). Some typical values of protein-N in biomass collected from the literature are presented in Table 6.1.

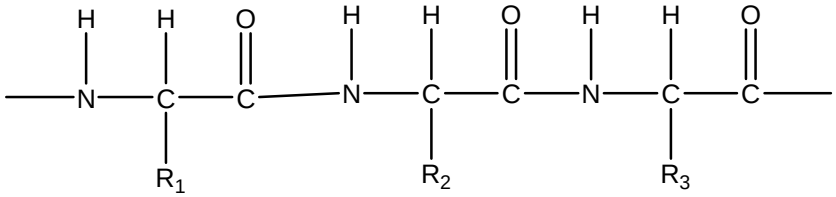

Figure 6.5. Protein sequence. R_n can contain a variety of functional groups.

Proteins are potentially made of 20 different naturally occuring α-amino acids (glycine, alanine, valine, leucine, isoleucine, methionine, proline, phenylalanine, tryptophan, asparagine, glutamine, serine, threonine, tyrosine, cysteine, aspartic acid, glutamic acid, lysine, arginine, histidine). The occurrence and nature of amino acids constituting a protein will form a unique makeup and will influence the properties of the protein (thermal behaviour, functional groups, etc). It is important to notice that the extractive methods used to determine PN are not perfect [Ezeagu 2002]. Amino acids may be destroyed or chelated, and amino acids might not yield the "expected" products (NH_3 and measured amino acids) or tightly bound proteins/amino acids with plant cell-wall matrix may not be released.

Several interesting results can be extracted from Table 6.1. First, it is true that PN represents the major single N-group. However, the relative importance of PN is highly variable, varying roughly from about 30% to more than 90% of TN. PN has always been seen as a good representation/picture of biomass-N and further used as a starting point for N-mechanistic studies. This generalisation is at the least inaccurate, at the most wrong for many biomass species or biomass fractions. The inadequacy of the assumption that N is only of proteinogenic nature in biomass is obvious from the knowledge of synthesis of plant tissues and tree physiology (not discussed here). Any study of N in biomass (NOx formation during combustion, etc) can not be pursued further without a definition as correct as possible of the nature of N-compounds.

Furthermore the protein composition is very complex as the nature of the proteins (amino acids composition) can vary greatly from one biomass species to another [Näsholm 1990]. Roots and fleshy storage organs (tubers, bulbs) generally contain smaller proportions of their total nitrogen in the form of protein than do leaves [Fowden 1980]; some protein amino acids contain non amino acid-N (tryptophan, asparagine, glutamine). All this complicates the establishment of an accurate N-compounds determination.

The remaining part of the nitrogen (non-protein nitrogen or NPN) contains a large variety of compounds which are often difficult to isolate, characterise and quantify. In the following section, a list of the known NPN compounds as complete as possible has been compiled with quantification information whenever possible.

Table 6.1. PN in % of TN.

Reference	Type of biomass	PN-average	PN-range	Comments
[Adelsberger 1976]	Scots pine sapwood/heartwood	-	66-71/68-71	+/-15%
[Laidlaw 1965]	Scots pine	87	-	9 months storage
[Periago 1996]	6 legumes	63.7	38.5-74.0	-
[Yeoh 1994]	90 plants (leaves)	76	55-90	-
[Ezeagu 2002]	13 tropical plant seeds	78	40-79	-
[Langlois 1976]	Tree (salicornia ramosissima)	-	Stem: 50-68 Branch: 46-71 Roots: 41-44	Different stage and conditions
[Langlois 1976]	Tree (salicornia stricta)	-	Stem: 44-57 Branch: 19-92 Roots: 55-59	Different stage and conditions
[Cheng 2004]	Bark tissue of apple trees	90	-	-
[Cheng 2004]	Whole-tree basis (apple trees)	60	-	-
[Cowling 1966]	Heartwood of English oak and eucalyptus	50	-	-
[Cowling 1966]	Sapwood of eucalyptus	75	-	-
[Fowden 1980]	Plant	80	-	Estimation
[Näsholm 1990]	Needles of Scots pine trees	70	-	-
[Leppälahti 1995a]	Peat (review)		28-58	Minimum values

6.2.2 Non-Protein-N (NPN)

The identification and quantification of NPN compounds is challenging as their detection and separation are complex and their concentration levels often rather low.

Free amino acids and polypeptides

Free amino acids (Figure 6.6) are said to be one of the main constituents of NPN [Periago 1996]. It was shown for 36 grass species that the free amino acids constituted 0.9 to 12% of the total leaf protein amino acid, and generally less than 5%. From the results presented in [Billow 1994; Curran 2001] it was possible to calculate that about 5% of total-N was of free amino acids origin in slash pine leaves and less than 10% of total-N in coniferous forest canopies (needles). Cheng et al. [2004] studied apple trees, the ratio between N-protein and N-free amino acids was between 27.1 and 3.2, confirming the fact that PN is the most important form of biomass-N but also that its relative proportion is variable (depending on season, growth, nutrients); arginine was the main free amino acid, containing from 50 to 80% of the free amino acid nitrogen (typical of some tree species). The nature of free amino acids is also varying as Näsholm et al. [1990] reported that the main free amino acids in needles of fertilized Scots pine are glutamine, glutamic acid, γ-aminobutyric acid, aspartic acid and proline (50-70% of the total free amino acids).

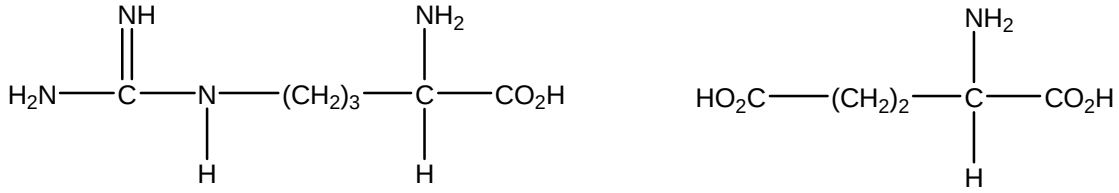

Figure 6.6. Two essential amino acids: arginine (left) and glutamic acid (right).

Non-protein amino acids

Only 20 different amino acids (the so-called essential α-amino acids) are naturally occurring in proteins of plants (and animals) but many more can be found in plants and are derived from the chemical modification of proteins (secondary compounds). Fowden [1980] evaluates at 200 the number of non-protein amino acids in plants; the concentrations of individual components may vary within wide limits, some occurring at several percents of the dry matter; as high as 10% have been recorded for DOPA in seeds of Mucuna species [Fowden 1980]. Ezeagu et al. [2002] reports that as many as 300 non-proteinogenic amino acids are derived from plants and characterizes their amounts in several seeds of leguminous family as "significant". The general structure of non protein amino acids can be written as $RCH(NH_2)COOH$ [Fowden 1980]; based on R nature, the compounds can be classified as alkyl, hydroxy, acidic, basic, sulphur-containing, aryl or heterocyclic amino acids.

Nucleic acids and mononucleotides

Nucleic acids are the biochemical macromolecules containing the genetical information of living cells. The most common are DNA and RNA. Nucleotides are the building bricks of this macromolecules and are constituted of a nucleobase (Figure 6.7; N-containing structures: purines or pyrimidines), a pentose (sugar) and a phosphate or polyphosphates. No data was found about the proportion of N found in nucleobases in biomass.

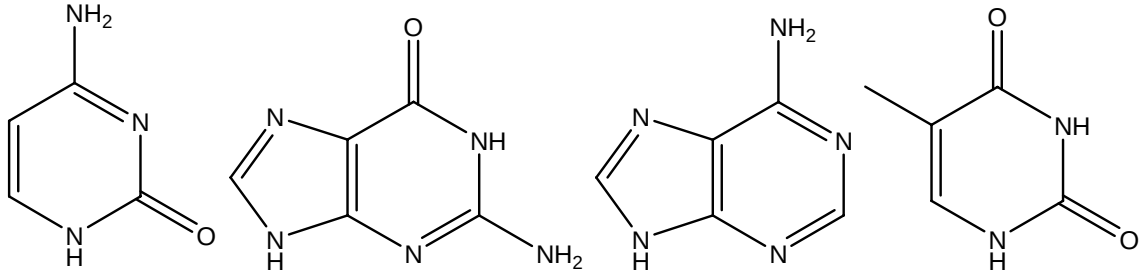

Figure 6.7. Cytosine, guanine, adenine and thymine.

Alkaloids (N functionality in *italic* and **bold**)

Alkaloid is a generic term covering a vast family of natural compounds estimated at roughly 10 000 [Hesse 2002]. This family includes some famous compounds like opium, nicotine or caffeine. Alkaloids may have numerous biological roles such as antifungal agent, protection against UV irradiation, insecticide, etc. Alkaloids frequently exhibit physiological activity and therefore newly discovered compounds are under the scrutiny of pharmaceutical industries.

Classification of alkaloids is a complicated task but the five main alkaloid classes [Hesse 2002], determined according to the position of the N-atom in the main structural element, are:

- Heterocyclic alkaloids (N can be found as pyrrolidine, indole, piperidine, pyridine, imidazole, quinoline, quinazoline, benzoamine, benzoxazole, pyrrolizidine, quinolizidine, indolizine, pyrazine, purine, pteridine, etc) = ***Cyclic N (aromatic or non aromatic)***

- Alkaloids with exocyclic N-atoms and aliphatic amines (benzylamine, phenylalkylamine, etc) = ***Amine***

- Putrescine, spermidine and spermine alkaloids (biogenic amines) = ***Amine***

- Peptide alkaloids = ***Amide***

- Terpene and steroid alkaloids (N-atoms may in principle be present either as parts of rings or attached on side chains) = ***Various N-functionalities***

When it comes to how much alkaloids are present in a sample, the values are variable going from barely detectable (less than 0.01% [Hiraoka 1974]) to significant. Up to 5% caffeine (Figure 6.8) can be found in leaf tea, up to 1.9% in coffee beans [Hesse 2002], 5% of the weight of the wood in certain tropical species [Cowling 1966]. The portion of N present as alkaloids is following the same behaviour. The highest values reported are 8-10% of total-N as alkaloids in lupin seeds [Sánchez 2005]; Birecka et al. [1984] measured that in the youngest organs of heliotropium plants, the pyrrolizidines alkaloids represented over 5% of the total nitrogen content.

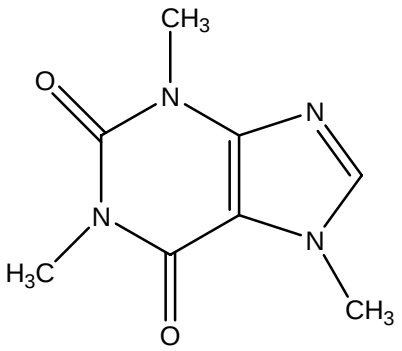

Figure 6.8. A famous alkaloid: caffeine.

Inorganic-N

The most common forms of inorganic nitrogen are nitrate (NO_3^-), nitrite (NO_2^-) and ammonium (NH_4^+). They are early forms of N-uptake by plants. Inorganic-N is then used by plants and incorporated in their tissues as plant protein (and other N-containing compounds). Gomez et al. [2002] measured that the contribution of nitrate to TN was 2-4% over the course of a year in peach trees.

Chlorophyll

Chlorophyll is the green photosynthetic pigment found in plants and is involved in the energy storage process. Several types of chlorophyll exist, the most universal being chlorophyll *a* with the molecular formula $C_{55}H_{72}O_5N_4Mg$. The basic structure where N is found in this pigment is a porphyrin macrocycle (Figure 6.9) with a magnesium ion (Mg^{2+}) in the central cavity and various side chains. The amount of N contained as chlorophyll-N is usually significant in plant foliage. It was calculated, from [Birecka 1984] measurements, that, in half-expanded leaves of heliotropium plants, about 7% of N was chlorophyll-N (highest value). The lowest value was found in the flowers of this plant where only about 0.3-0.4% of N was chlorophyll-N. Similar results were found by [Billow 1994] (0.9-2.5% chlorophyll-N in coniferous forest canopies) and [Curran 2001] (about 1% of chlorophyll-N in needles of slash pine).

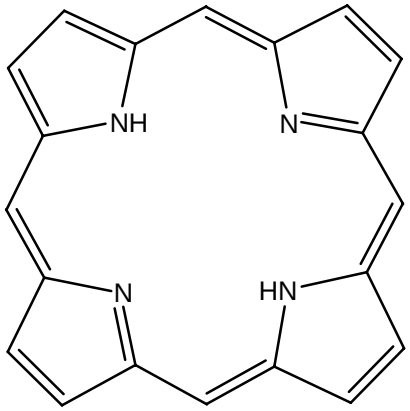

Figure 6.9. Porphyrin structure.

Quaternary-N (Q-N)

The ambiguous term "quaternary nitrogen" is often used to refer to an N-functionality. The exact nature of Q-N is still obscure and discussed. It is described as "pyridinic N that has been protonated, oxidised or otherwise subjected to electron withdrawal" [Hansson 2003b] or "N which substitutes for carbon in the graphene type structure" [Babich 2005] or "inorganic quaternary species (ammonium carboxylates)" [Keleman 1999]. However, it was shown [Keleman 1999] that XPS (used to determine the pyridinic-, pyrrolic-, amino-, amide-, Q-N) can not distinguish pyrrolic and amide nitrogen (in other words PN) or even low level of amines from pyridinic-N, which complicates the analysis of XPS measurements. Furthermore, a study [Hansson 2003b] showed that at room temperature XPS can not distinguish amino acids and Q-N, this fact leads to the hypothesis that Q-N might in fact be amines or amino acids as it might explain several features of the pyrolysis process of solid fuels. The debate is not yet over and requires further work.

Other minor N-compounds

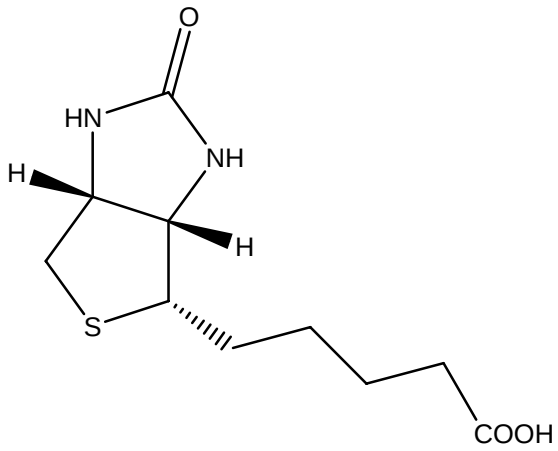

Figure 6.10. Biotin (vitamin H or B_7).

Vitamins are essential to human diet for synthesis of proteins [Damon 2005]. They are present in many edible plants, may contain N in a variety of compounds for example biotin (Figure 6.10). Vitamins are usually found at very low concentrations, typically in the order of milligrams per 100 g biomass [Damon 2005; Lebiedzińska 2006].

A glucoside is a compound that is derived from glucose and another substance (the bioactive part). Glucosides are common in plants, but rare in animals. Cyanoglucosides contain a cyano functional group (also called nitrile) that consists of a carbon atom joined to a nitrogen atom by a triple bond. Concentration of about 50 mg of cyanoglucoside per 100 g dry matter (in young curled fronds of bracken fern) is considered very high [Bennett 1968]. Amino sugars are alkali-insoluble polysaccharides (carbohydrates), another class of biomacromolecules than proteins [Leppälahti 1995a]. Three amino-sugars are common in nature: D-glucosamine, D-mannosamine and D-galactosamine. The polymer of glucosamine is chitin, a compound found in the cell walls of many lower plants.

This overview of the N-containing compounds in biomass shows that NPN is diverse and may represent a very substantial portion of the TN for many biomass samples. The most interesting/significant compounds to consider are: free and NP amino acids, alkaloids, inorganic nitrogen and chlorophyll. Their relative weight as N compounds will vary substantially depending on the species but also other biological factors. It may not be possible to give an exhaustive picture of biomass-N but this in-depth overview is a strong evidence of the crucial need for a detailed case-to-case knowledge of the nature of N-chemical forms in each biomass sample as the "N biomass equals PN" simplification is far from satisfactory to describe biomass-N in many cases.

6.3 NOx precursors: NH_3 and HCN

NH_3 and HCN release from biomass pyrolysis has been studied in two ways: study of biomass itself and study of model compounds, i.e. chemical compounds depicting a single chemical functionality of N. Pyrolysis of N-containing model compounds has been used to characterise the main decomposition products and elucidate the main degradation pathways by fragment identification.

6.3.1 N-model compounds: protein/amino acids/oligomers/polypeptides

Final products studies

The main classes of model compounds studied are amino acids (a.a.)/proteins and pyrrole/pyridine (aromatic N-heterocycles) as they are 2 representative biomass N-functionalities (discussed in section 6.1 and 6.2). The pyrolysis of these compounds at high temperatures (700-1000°C) and long residence time provide information about the main final N-products (see Table 6.2).

Table 6.2. Protein/amino acids (a.a.): pyrolysis final products studies.

N-compound	Conditions	HCN	NH_3	Reference
Alanine	850°C He	0.01 mol/mol a.a.	0.05 mol/mol a.a.	[Haidar 1981][9]
Glutamic acid[2]	850°C	0.33	0.01	"
Leucine	850°C	0.01	0.03	"
Lysine[3]	850°C	0.39	0.10	"
Phenylalanine	850°C	0.17	0.003	"
Proline[4]	850°C	0.31	0.02	"
Serine[5]	850°C	0.20	0.01	"
Tryptophan[6]	850°C	0.45	0.01	"
Valine	850°C	0.03	0.05	"
Glycine	1000°C He	0.32 mol per mol of N	n.a.	[Johnson 1971][9]
Alanine	1000°C	0.12	"	"
Leucine	1000°C	0.08	"	"
Isoleucine	1000°C	0.08	"	"
Serine[5]	1000°C	0.45	"	"
Phenylalanine	1000°C	0.43	"	"
Aspartic acid[2]	1000°C	0.35	"	"
Glutamic acid[2]	1000°C	0.71	"	"
Asparagine[7]	1000°C	0.21	"	"
Glutamine[7]	1000°C	0.46	"	"
Aspartic acid[2]	700°C	0.007	"	"
Glutamic acid[2]	700°C	0.14	"	"
Asparagine[7]	700°C	0.02	"	"
Glutamine[7]	700°C	0.10	"	"
Poly-L-leucine[1,8]	700°C N_2	1.7 NH_3	<--	[Hansson 2003a][10]
Poly-L-leucine[1,8]	800°C	2.2 NH_3	<--	"
Poly-L-proline[1,8]	800°C	9.5 NH_3	<--	"

n.a.: not analysed; [1]: N-conversion of 60-89%. Structural comments: [2]: dicarboxylic acid ; [3]: diamino; [4]: N is in a 5 member N-cycle; [5]: OH function; [6]: 2N, one is in a cycle; [7]: amino acid and amide (2N). [8]: HNCO was not quantified (minor component). Reactor type: [9]: Vycor tube; [10]: fluidised bed.

The results show that HCN is the predominant N-component in most cases. N-chemistry during pyrolysis is dependent on temperature and heating mode but the most influential parameter appears to be the structure/chemical properties of the reactant as this will influence the decomposition paths. However, those studies provide information about the final N-gaseous products NH_3 and HCN (and eventually HNCO) and very little about the decomposition mechanisms.

Mechanistic studies: pathways of decomposition

Nevertheless, pyrolysis carried out at low temperatures (300-500°C) can be used in order to provide mechanistic information through fragments analysis. This provides information about primary products of pyrolysis and the identification of fragmentation products (which would normally undergo further decomposition at higher temperatures) can be a direct experimental evidence of favoured pathways and directly related to starting materials via plausible mechanisms. The presence (or absence) of fragments can help in the insightful elucidation of the mechanisms which may have taken place in the thermal zone. The first and foremost result obtained by these low temperature studies is that (most of) **NH_3 and HCN are NOT primary products of model compounds pyrolysis but rather products of secondary decomposition** [Basiuk 1998a; Simmonds 1972; Johnson 1971; Ratcliff 1974]. Furthermore, during the pyrolysis of poly-L-valine (protein) at 500°C, Basiuk et al. [2001] identified **18** (less-volatile) fragments by GC/FTIR/MS: one isocyanate, one unsaturated carboxylic acid, two ketones, three unsaturated hydrocarbons, three nitriles, five amines, one linear amide and two cyclic amides. This abundance of compounds reveals the **multitude of reactions involved**. Under the same conditions, poly-L-alanine and poly-glycine will similarly produce a variety of compounds but the composition of the products is different [Basiuk 2000], further demonstrating that the original makeup of the N-compounds is of importance.

(1) Primary pathways of decomposition

The multitude of reactions involved presents a very complex picture of amino acids/proteins decomposition but some typical mechanisms may be extracted. **The two (plus three) main identified primary pathways of decomposition of amino acids/oligomers of amino acids/polypeptides/proteins are** (Figure 6.11)**:**

1. Dehydration through formation of cyclic amides, the most common being 2,5-diketopiperazine (also called DKP or DP) with consequent loss of water. [Johnson 1971; Simmonds 1972; Ratcliff 1974; Haidar 1981; Chiavari 1992; Voorhees 1994; Basiuk 1998a; Basiuk 1998b; Basiuk 2000; Basiuk 2001; Sharma 2004; Sharma 2006].

2. Decarboxylation with consequent amine formation. [Simmonds 1972; Ratcliff 1974].

Other (supposedly less important) primary decomposition pathways include:

3. (Intermediary) formation of α-lactam. [Simmonds 1972; Hansson 2003b].

4. Amide intermediaries formation. [Simmonds 1972; Samuelsson 2006].

A fifth path is also important as it produces char-N compounds:

5. **Cross-linking** of proteins'side groups (if present) to produce char-N and NH_3 [Hansson 2003a; Samuelsson 2006]. Reactants with no side groups will evidently not follow this path and therefore produce none or very little char.

Thermal loss of NH_3 (**deamination**) does not appear to be a significant decomposition pathway as the corresponding carboxylic acids are usually not found [Johnson 1971; Simmonds 1972; Ratcliff 1974; Basiuk 1998a; Sharma 2006]. The relative significance of each pathway depends on the nature of the reactant as it influences the stability of intermediate species.

(2) Secondary pathways of decomposition

The **secondary reactions** which may happen are numerous and pathways are versatile. A full understanding of the different degradation mechanisms for a given model compound is challenging and many aspects of N-pyrolysis remain obscure. As mentioned, it is often the presence or the absence of fragments which allow to speculate if a pathway is significant or not and act therefore as experimental confirmation. Focusing on the five primary products afore-mentioned, it is possible to predict the thermal decompositions predominantly occurring via logical mechanisms:

1. Cleavages (openings/breakings) of **DKP** (Figure 6.12)

Depending on the opening of the cycle and further recombination, these products may occur (not exhaustive):

(a) **Nitriles,** with one less carbon than the parent amino acid, the formation of **HCN** from glycine [Ratcliff 1974] being an evidence of this pathway.

(b) **Intermediary imines** (two different paths possible [Hansson 2003b]). These **imines** may react with **amines** (originating from primary decomposition through decarboxylation) to produce **NH_3** and **N-alkylaldimines** (identified by Ratcliff et al. [1974] and Chiavari et al. [1992]) or decompose at once to yield **HCN** and/or **nitriles** with consequent **H_2** creation [Johnson 1971; Haidar 1981].

(c) Release of **HNCO** and **pyrroline** [Haidar 1981; Basiuk 1998a; Hansson 2003b].

(d) Isomerisation to **hydantoins** (or imidazoledinediones, 5-membered cyclic amides) before further cleavages [Basiuk 2000; Basiuk 2001].

(e) Intermediary **α-lactam** [Simmonds 1972; Hansson 2003b].

The relative importance of a given DKP decomposition pathway will obviously vary with the nature of the original compound and the temperature. At sufficiently high temperatures, the secondary compounds will then decompose to HCN and to HNCO to a minor extent. N-conversion to HCN from 2,5-piperazinedione will vary from 38% at 700°C [Johnson 1971] to over 80% at 1000-1100°C [Johnson 1971; Hansson 2003b].

2. Reactions of (primary-formed) amines (Figure 6.13)

(a) Amines may, as previously mentioned, react with **imines** to yield **NH_3** and **N-alkylaldimines** or produce **nitriles** and/or **HCN** through an imine intermediate [Simmonds 1972; Hansson 2003b].

(b) Direct thermal loss of **NH_3** from aliphatic amines is considered a minor process [Johnson 1971; Simmonds 1972; Ratcliff 1974; Basiuk 1998b].

3. Reactions of α-lactam (primary and secondary) (Figure 6.14)

(a) Further reaction to **amide**, which can evolve to **nitrile** and/or **HCN** (at sufficiently high temperatures and residence times [Glarborg 2003]) with release of water.

(b) Further reaction to **intermediary imine** (see previous points).

4. Reactions of primary nitriles from intermediary amides (Figure 6.15)

(a) See previous points.

5. Reactions of N-containing char compounds (Figure 6.16)

(a) These compounds might react to form hydantoins (or imidazoledinediones, 5-membered cyclic amides), which can open to yield HNCO and/or HCN [Basiuk 2000; Basiuk 2001; Samuelsson 2006]

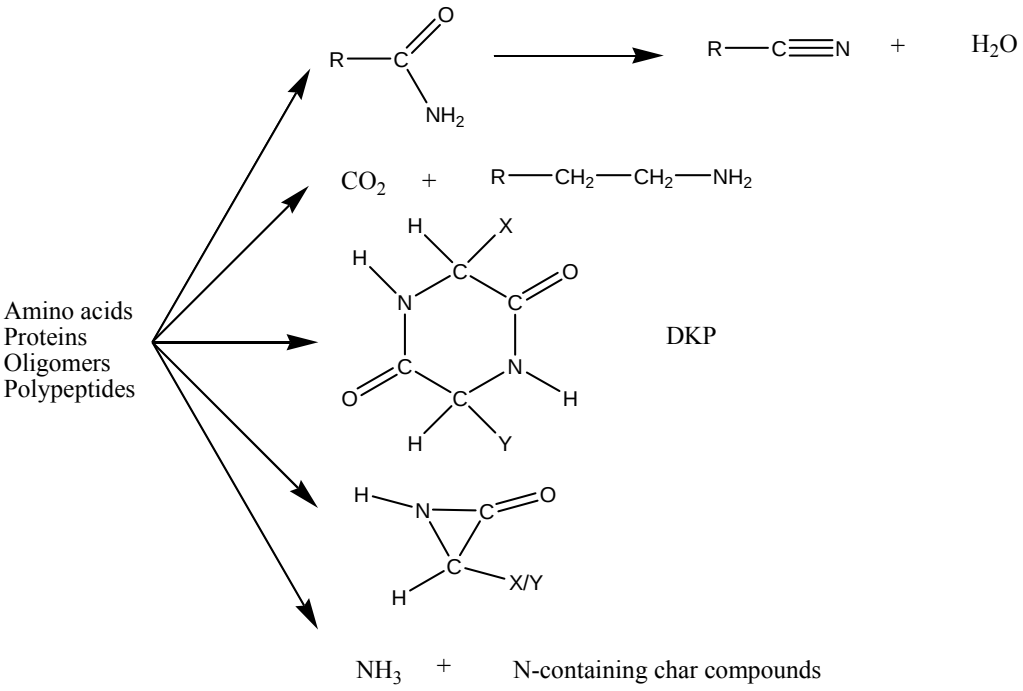

Figure 6.11. **Primary decomposition paths** of proteins / amino acids / oligomers / polypeptides.

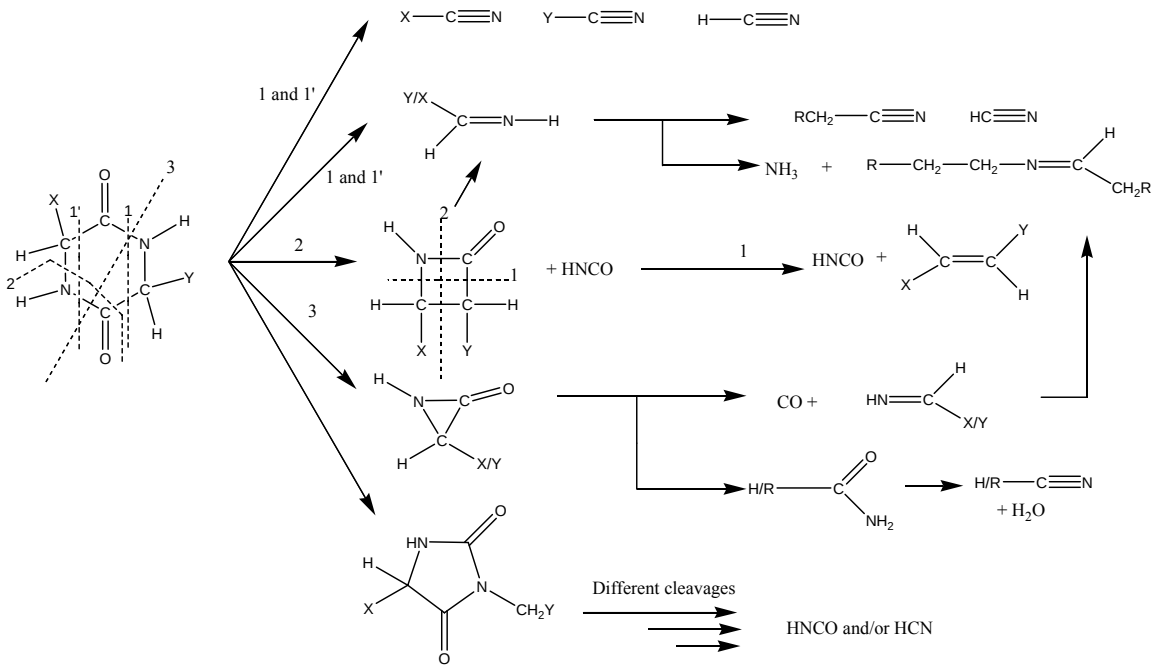

Figure 6.12. Secondary decomposition reactions of DKP. X and Y may be different and contain various functional groups. Dotted lines indicate opening of the cycle.

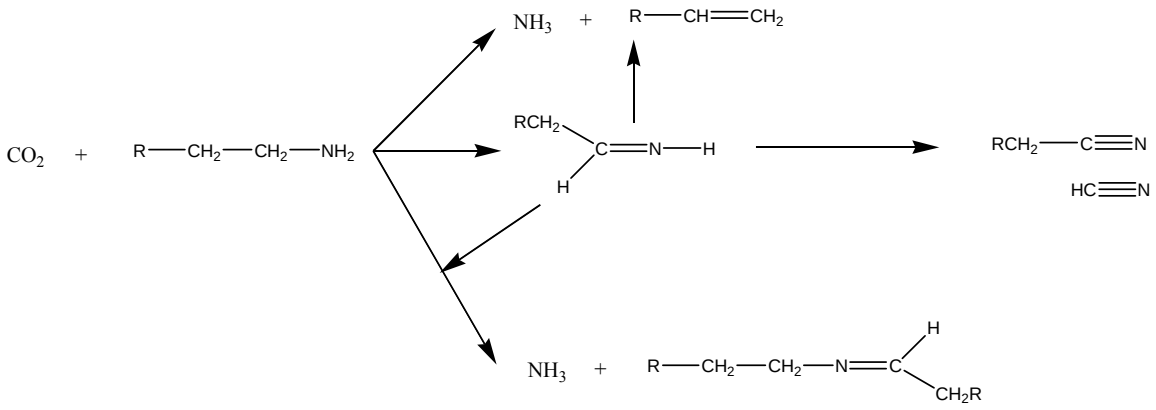

Figure 6.13. Secondary decomposition reactions of Primary-formed amines.

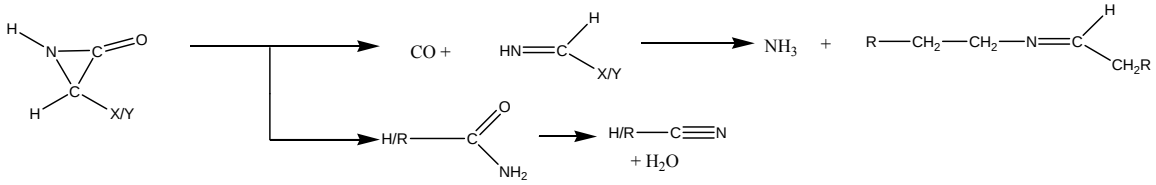

Figure 6.14. Secondary decomposition reactions of lactam.

Figure 6.15. Secondary decomposition reactions of nitriles.

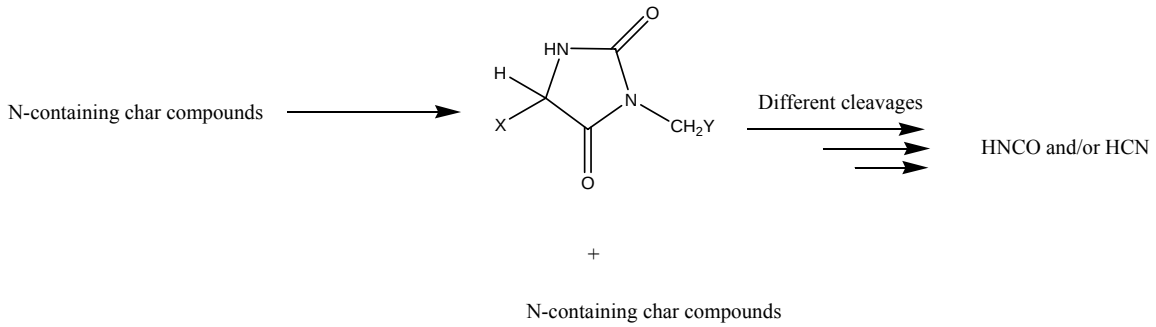

Figure 6.16. Secondary decomposition reactions of char-N compounds.

6.3.2 N-model compounds: N-heterocycles

Apart from proteins/amino acids, N in biomass is also found in a variety of functions (section 6.2). N is frequently included in various heterocycles. Table 6.3 presents studies of heterocyclic compounds with emphasis on pyrrole (5-member aromatic heterocycle) and pyridine (6-member aromatic heterocycle).

Table 6.3. N-conversion to HCN and NH_3 of various heterocycles.

References	Final products studies	Temperature	HCN (%)	NH_3 (%)
[Patterson 1968]	Pyrrole	850°C	49	little
[Hämäläinen 1994]	Acridine	800°C	1.1	1.8
Pyridine-type	1,2-bis(4-pyridyl)ethane		9.2	5.4
“	3-pyridol		18	9.1
“	Nicotinic acid		8.8	3.3
“	Orotic acid		19	42
“	Citrazinic acid		7.2	13
“	Dipicolinic acid		22	5.9
Pyrrole-type	Carbazole	800°C	2.4	1.4
“	Antipyrine		9.7	7.8
“	2-pyrrolecarboxylic acid		17	6.8
“	DL-pyroglutamic acid		10	5.0
[Axworthy 1978]	Pyridine	960°C	40%*	<5
“	* decomposed portion		49% residue*	
“	Pyridine	1100°C	102	0
[Johnson 1971]	Proline (700/800/1000°C)	<--	-/-/86	nm
“	4-hydroxyproline		-/-/90	nm
“	2-pyrrolidone		-/67/90	nm
“	Pyrrolidine		46/77/95	nm
“	Piperidine		33/47/62	nm
“	3-pyrroline		0/26/72	nm
“	pyrrole		0/22/87	nm
“	Piperazine		34/69/80	nm
“	2,5-piperazinedione		38/50/81	nm
“	2-oxohexamethylenimine		-/-/71	nm
“	N-methylpyrrole		-/-/40	nm
“	N-methylpyrrolidine		-/-/35	nm
	Kinetic studies	T	Yield (%): minT & maxT	
[Ikeda 1995]	Pyridine	1100-1220 K	0-17	Not reported
[Mackie 1990]	Pyridine	1300-1800 K	0-75	Not reported
[Houser 1980]	Pyridine	900-1000°C	.14-.52 mol per mol	Not reported
[Mackie 1991]	Pyrrole	1300-1800 K	<1%-75%	Not reported
[Lifshitz 1989]	Pyrrole	1050-1350 K	0-17%	Not reported

nm: not measured.

Pyridine. HCN and cyanoacetylene (H-C≡C-C≡N) were identified as the main volatile products. HCN predominating at the high end of the temperature range [Mackie 1990]. Cyanoacetylene has been identified as the primary N-containing product for pyridine decomposition [Ikeda 1995]. A wide range of other N-compounds were observed experimentally (benzonitrile, quinoline, fused ring heteroatomic compound, etc) demonstrating the complexity of pathways (see references from Table 6.3).

Pyrrole. Pyrrole's decomposition produced also a collection of N-containing compounds. Allylcyanide (H_2C=CH-CH_2-C≡N), crotonitrile (H_3C-CH=CH-C≡N), HCN, acetonitrile (H_3C-C≡N) and cyanoacetylene are among the major ones. The predominating products are varying with the temperature (see references from Table 6.3).

The mechanisms suggested for both pyridine and pyrrole involve the **breaking of bonds in the ring and/or rupture of the C-N bond** followed by **random cleavage/recombination of the resulting diradical** [Lifshitz 1989]. This aspect explains the large variety of observed products. HCN is the predominant (and almost the only) N-containing compound above 1000°C. It is due to the fact that, at sufficiently high temperatures and sufficiently long residence times, nitriles will largely converted to HCN and hydrocarbons [Glarborg 2003]. The mechanisms suggested consists usually of numerous steps (75 in [Mackie 1991] for pyrrole) where HCN is formed through a sequence of reactions and not during the initial steps [Houser 1980]. Johnson et al. [1971], studying various N-heterocycles, shows that not only the temperature but also the ring size, the ring unsaturation, the substitution of the ring-N and the substitution adjacent on the ring-N have an effect on N-chemistry during pyrolysis. Sadly no information about NH_3 at the low end of the temperature range studied is available.

A study on the decomposition of pyridinic- and pyrrole-**type** compounds ([Hämäläinen 1994], see Table 6.3 for results) reports significant amounts of NH_3. Hämäläinen et al [1994] states that the presence of –OH groups in the ring structure and adjacent to the N atom clearly increased the conversion to NH_3 at the expense of HCN, however the formation of NH_3 was not as strong when the –OH groups were coupled with C=O groups. The mechanism by which NH_3 is produced from these compounds is unclear. These results are very interesting as all N-compounds in biomass may be located in the vicinity of functional groups which may influence N-chemistry. This matter (intricate structure of biomass) and its implications for N-chemistry during pyrolysis are discussed in 6.3.5 and **[Becidan 2007b] (P-IV)**.

6.3.3 N-model compounds: tar and char compounds

Experimental studies ([Haidar 1981; Hansson 2003b], 700-850°C) show that the structure of the amino acid/protein has a significant effect on their transformation to gaseous products during pyrolysis. The smaller the compound and the less encumbered it is (no reactive side chains, no extra functional groups), the more it is converted to gases. For example [Haidar 1981], alanine will be converted at 95.0% at 850°C, leucine at 89.4% (longer and branched), lysine at 66.0% (extra functional group capable of H bonding) and phenylalanine at 27.7% (extra group which may create a stable aromatic nucleus). A connection between increasing char formation and increasing NH_3 formation was noticed. This is explained by a cross linking reaction between proteins' side groups which simultaneously yield char-N compounds and NH_3 ([Li 2000; Glarborg 2003; Hansson 2003c; Tian 2005a; Samuelsson 2006; **Becidan 2007b (P-IV)**]). Little data about the proportion of N in tar/char of model compounds was found. [Axworthy 1978] measured that 49% of N in the decomposed portion of the sample (65% at 960°C) was found in the "residue" (carbonaceous residue on the reactor walls, probably tarry and charry deposit). The structure of N-compounds in char and tar is a very complex issue. As mentioned earlier, the low temperature pyrolysis studies show a large number of compounds (18 main compounds in [Basiuk 2001]). During pyrolysis of glutamine, glutamic and aspartic acids (α-amino acids), the N-containing compounds in tar were identified as N-Polycyclic Aromatic Compounds [Sharma 2006], their nature changing with the nature of the original compound and the number of fused rings increasing with the temperature. Char-N are also included in complex systems, Sharma et al. [2006] shows that the char of aspartic acid contains polysuccinimide (polymer of N-cycles). Char- and tar-N are diverse and incorporated in multiple fused rings and/or polymer systems.

6.3.4 Comments about the validity of model compounds studies

Apart from the influence of operating parameters, release, distribution and nature of the N-compounds from pyrolysis are dependent on the structure of the N-containing model compounds. This fact shows the need for a detailed knowledge of the N-biomass nature in order to use appropriate model compounds. However, this may not be sufficient and the validity of the results obtained from model compounds should be looked upon carefully. Even if it is clear that N is found in protein/amino acids/cyclic structures/amines, it is also clear that these N-structures are only a part of the wider biomass macro-structure (cellulose, hemicellulose, lignin) and therefore N-compounds will not only be surrounded but also integrated/linked with many compounds (containing N or not) and a variety of other chemical functions which may significantly influence the final N-products **[Becidan 2007b] (P-IV)**. This brings limitation to the validity of the results obtained through model compounds and their direct transfer to biomass. Model compounds can not portray fully the structure and composition of biomass in its intricate complexity. However, the study of model compounds is a necessary step to understand, at least partly, $HCN/NH_3/HNCO$ precursors' formation and selectivity from biomass pyrolysis. Other limitations are evident (only gas-phase reactions for many model compounds while biomass pyrolysis involves devolatilisation, homogeneous gas-phase reactions and heterogeneous oxidation of char). All this calls for the study of biomass itself in spite of its complex constitution which hinders clear mechanistic insight.

6.3.5 Biomass pyrolysis and NOx precursors: status and new considerations

Pyrolysis of biomass is a more complex process than pyrolysis of a single N-model compound as biomass is made of an intricate architecture of various N-containing compounds but also cellulose, hemicellulose and lignin (which do not contain N). N-components represent only a minor part of the biomass matrix and their possible interactions/(cross-)linking/integration is complex. The results from biomass pyrolysis studies should be looked upon 2 axes:

(1) N-chemistry from biomass: amounts of NH_3, HCN, tar-N and char-N produced and their dependence on the operating parameters and the fuel properties (N-functionalities, physical and chemical) if possible. These factors are of major significance to understand pyrolysis as a thermal process but also for comprehension of NOx formation as pyrolysis is the primary step of gasification and combustion. The N-distribution is central since NO and N_2O formation from the fuel-N takes place through the combustion of the N-species released with the volatiles and the oxidation of the nitrogen retained in the char, which involves fuel devolatilisation, homogeneous gas-phase reactions and heterogeneous oxidation of char. The dominant volatile N-species are NH_3 and HCN. The different species are susceptible to produce different products during combustion: NH_3 may decompose to NO and N_2, HCN to N_2O and NO and char-N to NO, N_2O and N_2 (Fuel-N mechanism [Saenger 2001]). The partitioning of N into volatiles (light gases and tar) and char during pyrolysis but also the qualitative/quantitative composition of the different fractions (volatiles/tar-N/char-N) are crucial for NOx formation.

(2) Comparison with model compounds: by comparing alongside the results from biomass and model compounds and both the analogies and the discrepancies, it may be possible to have a full picture of the decomposition mechanisms of N which may take place during biomass pyrolysis.

Less is known about N-pyrolysis of biomass than N-pyrolysis of coal, which is often used to complete the knowledge about N biomass pyrolysis, even though their general properties (N-functionality, moisture content, density, ash content, VM, structure, ultimate analysis, etc) are rather different. N-biomass pyrolysis has not been as intensively studied as N-coal pyrolysis. N-fate is one of the most obscure features of biomass pyrolysis. This situation may be explained by several factors: (1) N is a minor component and its low concentrations in most of the biomass samples make it difficult to investigate; (2) the nature of N-containing compounds in biomass is various and versatile and not as well known as N in coal in the energy world; (3) the wet measuring techniques often used to measure N-compounds do not allow time-resolved measurements (and HNCO may be converted into NH_3); (4) the treatment of results obtained by FTIR analysis is not easy (especially for HCN); (5) it seems like N-release is extremely sensitive to the pyrolysis mode/set-up and the fuel properties both physical and chemical. All this may partly explain the discrepancies (or sometime conflicting results) reported in the literature. Table 6.4 shows the results of N-conversion (as NH_3, HCN and HNCO) from 12 studies covering 29 biomasses under various conditions (different pyrolysis mode, temperature, heating rate, pressure and sample size).

Table 6.4. N-conversion (as NH_3, HCN and HNCO) from 12 studies covering 29 biomasses (2 pages).

Fuel (N wt% daf)	Mass or Feeding	Heating mode	T (°C)	HCN (%)	NH_3 (%)	HNCO (%)	Reference
Bagasse (0.31)	n.f.	7°C /min	1000	7	1.5	-	[Li 2000]
Bagasse (0.31)	n.f.	iso.	800	53	12	-	"
Cane trash (0.31)	1.0g	5°C /min	700	8	6	-	[Tian 2005b]
Cane trash (0.31)	1.0g	iso.	400	2	5	-	"
Cane trash (0.31)	1.0g	iso.	500	5	5	-	"
Cane trash (0.31)	1.0g	iso.	600	12.5	6	-	"
Cane trash (0.31)	1.0g	iso.	650	-	12.5	-	"
Cane trash (0.31)	1.0g	iso.	700	-	18.3	-	"
Cane trash (0.31)	1.0g	iso.	800	33	33	-	"
Cane trash (0.31)	1.0g	iso.	900	42.5	31	-	"
Rape seed (3.4)	62g/h	n.f.	500	-	10.9	-	[Predel 1998]
Rape seed (3.4)	66g/h	n.f.	600	-	17.2	-	"
Rape seed (3.4)	63g/h	n.f.	700	-	26.6	-	"
Rape seed (3.4)	1030g/h	n.f.	600	-	7.5	-	"
Whey protein (15.3)	117-174mg	iso.	700	$0.6NH_3$	←	.45HCN	[Hansson 2004]
Whey protein (")	"	iso.	800	$1NH_3$	←	.27HCN	"
Whey protein (")	"	iso.	900	$1.2NH_3$	←	.17HCN	"
Whey protein (")	"	iso.	1000	$1.6NH_3$	←	.12HCN	"
Soya beans (6.8)	150-250mg	iso.	700	$0.3NH_3$	←	.31HCN	"
Soya beans (")	"	iso.	800	$0.4NH_3$	←	.24HCN	"
Soya beans (")	"	iso.	900	$0.7NH_3$	←	.13HCN	"
Soya beans (")	"	iso.	1000	$1.0NH_3$	←	.07HCN	"
Yellow peas (4.3)	240-270mg	iso.	900	$0.9NH_3$	←	.13HCN	"
Bark pieces	200-260mg	iso.	900	$0.8NH_3$	←	0	"
Bark pieces	"	iso.	1000	$1.2NH_3$	←	0	"
Miscanthus (0.64)	13-16mg	10°C/min	900	17.8	16.7	10.2	[Chiavari 1992]
Miscanthus (")	13-16mg	30°C /min	900	11.3	12.9	5.6	"
Miscanthus (")	13-16mg	100°C/min	900	8.9	14.2	3.6	"
Wood pellets (0.33)	13-16mg	10°C /min	900	14.1	0	10.9	"
Wood pellets (")	13-16mg	30°C /min	900	14.1	5	2	"
Wood pellets (")	13-16mg	100°C /min	900	7.9	7.5	4.9	"
Bagasse (0.31)	0.5g	iso.	800	53	12.5	-	[Tan 2000]
S peat (1.4)	20-30g	10°C /min	625	<1	13	-	[Leppälahti 1995b]
S peat (1.4)	20-30g	10°C /min	825	<1	14	-	"
S peat (1.4)	20-30g	10°C /min	925	2	12	-	"
C peat (2.8)	20-30g	10°C /min	625	1	19	-	"
C peat (2.8)	20-30g	10°C /min	825	3	18.5	-	"
C peat (2.8)	20-30g	10°C /min	925	3	24	-	"
Pine bark (0.4)	20-30g	10°C /min	825	<1	13.5	-	"
Pine bark (0.4)	20-30g	10°C /min	925	<1	13.5	-	"
C peat (2.8)	20-30g	Drop	885	9	24	-	"
S peat (1.4)	20-30g	Drop	885	6	22	-	"
CB peat (3.6)	0.3g/s	iso.	800	3.3	4.1	-	[Aho 1993]
C peat (2.6)	0.3g/s	iso.	800	2.2	5.2	-	"

Fuel (N wt% daf)	Mass or Feeding	Heating mode	T (°C)	HCN (%)	NH_3 (%)	HNCO (%)	Reference
S peat (1.9)	0.3g/s	iso.	800	1.2	3.9	-	"
LS peat (1.7)	0.3g/s	iso.	800	0.6	3.8	-	"
Birch bark (0.52)	0.3g/s	iso.	800	0.7	4.5	-	"
Fir bark (0.53)	0.3g/s	iso.	800	0.73	4.9	-	"
Pine bark (0.25)	0.3g/s	iso.	800	0.55	5.5	-	"
Miscanthus (0.68)	270-280g/h	iso.	700	0.01	27	-	[Vriesman 2000]
Miscanthus (")	"	iso.	800	n.a.	29	-	"
C peat (2.3)	.015-.095g/s	10^5 °C/s	847	-	65	-	[Hämäläinen 1996]
C peat (")	"	10^5 °C/s	847	-	75	-	"
Sewage sludge (5.47)	75g	drop	600	n.d.	36.5	-	**[Becidan 2004] (P-I)**
Sewage sludge (")	75g	drop	750	5.7	40.8	-	"
Sewage sludge (")	75g	drop	900	8.6	50.7	-	"
Brewer Spent Grain (4.15)	75g	"	700	5.9	21.5	-	**[Becidan 2007b] (P-IV)**
Brewer Spent Grain (")	75g	"	900	17.1-18.3	31.0-31.3	-	"
Brewer Spent Grain (")	75g	10°C/min	900	3.5	15.7	-	"
Fibreboard (3.6)	75g	drop	600	<0.5	18.2	-	"
Fibreboard (")	75g	drop	900	9.1-10.0	36.0-38.4	-	"
Fibreboard (")	75g	10°C/min	900	<1	11.5	-	"
Coffee waste (3.0)	75g	drop	600	1.1	15.7	-	"
Coffee waste (")	75g	drop	900	14.5	37.8	-	"
Coffee waste (")	75g	10°C/min	900	1	6.9	-	"

n.f.: not found. n.a.: not available. Iso.: isothermal.

[a] Total N-conversion: 60-89%.

Measurement method: [Chiavari 1992; Hansson 2004]: FTIR, others: wet collection .

Reactor type: fixed bed: [Leppälahti 1995b], [Li 2000], [Tan 2000], [**Becidan 2004**], [**Becidan 2007b**]; fluidised bed: [Predel 1998], [Vriesman 2000], [Hansson 2004], [Tian 2005b]; entrained flow reactor: [Hämäläinen 1996], [Aho 1993]; TG: [Chiavari 1992].

1. axis: N-chemistry during biomass pyrolysis

N-compounds, selectivity and dependence on temperature and heating rate (See Table 6.4). HCN, NH_3 and HNCO to a minor extent are the three N-gaseous products. HCN is sometimes reported to be the main N-product of biomass pyrolysis under all conditions and with increasing emissions with increasing heating rate and temperature. However, NH_3 has also been reported to be the main N-product of biomass pyrolysis for all conditions. Its dependency on increasing temperature has been reported as increasing, decreasing, indifferent or reaching a maximum. In other cases, NH_3 is the main product at low temperatures/low heating rates while HCN is the main product at high temperature and/or high heating rates or increasing at a faster rate than NH_3, leading to increasing HCN/NH_3 with temperature and/or heating rate. HNCO is considered a very minor N-compound and has seldom been reported.

Total N-conversion (NH_3+HCN+HNCO) (See Table 6.4). The total conversion of N to NH_3, HCN and HNCO is most often increasing with temperature, heating rate and pressure. The values (for temperatures from 400°C to 1000°C, heating rates from 5K/min to isothermal experiments, pressure from 1 atm to 8 bars) are ranging from 10-15% to 70-75%.

Tar-N and char-N: amount and nature. The remaining part of N is found in tar or retained in char. **Char-N**. The experimental results gathered from [Leppälahti 1995b; Hansson 2004; Lang 2005] reviewing numerous works and covering all types of biomass show that the amount of char-N during biomass pyrolysis is decreasing with temperature. However, the proportion of N retained in char varies from sample to sample. An indicative value is that above 400-500°C, char retains less than 50% of the original fuel-N present in the biomass. The large variations encountered from one biomass species to another call for a need to investigate on a case-to-case basis. **Tar-N**: Almost no reliable and consistent data is available concerning tar-N from biomass pyrolysis. This might be due to low N-concentrations or the tar-N collection/sampling methods. Hansson et al. [2004] reviews 10 studies (isothermal/low heating rate) mostly at 500-550°C. Most of the tar-N proportions are located around 20-50% of fuel-N. However the low N-concentrations of the majority of these studies may affect the reliability of the results. The **nature of char-N and tar-N** is complex but it is usually assumed that N is incorporated in fused-ring systems in char and in a variety of N-compounds in tar such as nitriles [Li 2000; Tan 2000; Glarborg 2003; Tian 2005b]. The fact that N is present in many other functionalities of "less-volatile" compounds (various heterocycles, N-alkylaldimines, amides, etc) is almost certain but no extensive study has been carried out so far.

N-functionalities dependence. This is one of the most debated aspects of biomass pyrolysis: to which extent can fuel-N functionalities be correlated to N-release? Several explanations to elucidate N-distribution during pyrolysis of biomass have been proposed [Aho 1993; Hansson 2004]. N-functionalities and fuel content (O/N ratio, etc) influence on N-chemistry have been discussed but no clear dependence could be established **[Becidan 2007b] (P-IV)**. This is without doubt due not only to the sensitivity of N-chemistry to operating parameters but also to the intricate nature of biomass.

2. axis: Comparison biomass-model compounds and mechanistic considerations for biomass

Mechanistic considerations. Before trying to get further into N-release mechanisms during pyrolysis of biomass, the results from N-compounds studies and from biomass studies should be compared alongside according to key-parameters/features in order to identify the similarities and differences. See Table 6.5.

Table 6.5. Results from literature: comparison model compounds-biomass.

	Model compounds	Biomass
Main N-components	HCN, NH_3 and HNCO	HCN, NH_3 and HNCO sometimes
Significant biomass parameters	The presence of functional groups favours the formation of NH_3	N-distribution dependence on fuel properties not clear
Mechanistic results	HCN, NH_3 and HNCO are mainly products of secondary reactions through a variety of intermediates, pathways highly dependent on original N-compound	Results are difficult to interpret because of the complexity of the biomass N-compounds and their possible interactions with the other components of biomass
Main N-component	HCN main product from protein, amino acid, amine, N-heterocycles	The main product is sometimes HCN, sometimes NH_3
Char production	Compounds with side-chains or extra functional side groups produce char	Significant amount of char produced
Biomass type importance	The initial structure of the compound has a major influence on the final distribution of N-products	The biomass type has a significant influence on the final N-distribution
NH_3-HCN release: operating parameters	Increasing N-release with increasing temperature and heating rates	Increasing release with increasing temperature and heating rates for HCN but conflicting results for NH_3
Biomass NH_3 release	Correlation between char and NH_3 production	Char formation appears to be important for NH_3 formation

The interesting results from this comparison are: (1) little mechanistic information is known about biomass N-pyrolysis primary decomposition steps. The knowledge is usually directly derived from model compounds' studies neglecting the possible importance of the biomass structure, or even based on coal studies and therefore assuming rather wrong N-functionalities and fuel properties; (2) biomass often produces significant amount of NH_3 (often related to char production). This is not the case for most model compounds.

As previously mentioned in 6.3.4, assuming that N-compounds in biomass are decomposing according exclusively to the paths available to N-model compounds does not withstand a careful analysis of biomass intricate makeup. The intertwined interactions between N-compounds and non N-compounds before and during pyrolysis have been given none or little attention. Based on a discussion on how N-compounds and non N-compounds may be bound and may interact in biomass, novel and plausible decomposition paths involving N- and non N-reactants have been proposed and discussed in **[Becidan 2007b] (P-IV)**. This not only acknowledges the very probable significance of biomass structure, it may also explain the "extra" biomass NH_3 often observed. The plausible occurrence of (N-compounds + non N-compounds) reactions during pyrolysis can not be ignored even though their relative importance on the global N-chemistry is

difficult to assess. The sources of NH_3 during biomass pyrolysis are in all probability originating from a variety of sources. Many sources have been suggested based on experimental observations, plausible mechanisms or chemical considerations [Phillips 1978; Aho 1993; Hämäläinen 1994; Li 2000; Schäfer 2000; Tan 2000; Tian 2005a; Tian 2005b]: HNCO reaction with water, gas-phase hydrogenation of HCN, char-surface hydrogenation of HCN, direct hydrogenation of fuel-N at the char surface. Nevertheless, none of these routes takes into account the main biomass compounds and are widely inspired by coal studies.

N-chemistry during biomass pyrolysis is a sophisticated subject. A combination of model compounds' study and "real" biomass experiments is the most appropriate approach to grasp a picture as correct as possible. It is important to highlight the very unique structure and properties of each and every biomass. This often requires a careful case-to-case analysis. The experimental work realised should and can be used for improved modelling of biomass-N conversion during pyrolysis, combustion and gasification.

6.4 Modelling: NOx formation and reduction

Fuel-N release during solid waste pyrolysis/devolatilisation can be used as input for detailed chemical kinetics of NOx formation, or more specifically, NOx reduction. However, the scarce and often contradictory experimental results from the literature (see Table 6.5) may be confusing as the quality of input data is vital to the quality of the results. However, for biomass/waste (organic fraction) applications, assuming a pyrolysis fuel gas composition containing NH_3 as the main N-species accompanied by some HCN (and eventually HNCO) seems to be appropriate as a base case. The main application is the study on NOx reduction. NH_3 (in the pyrolytic gas) may be converted to NO or to N_2 depending on the conditions (fuel-N mechanism). Studying the effect of these conditions (residence time, temperature, etc) in order to promote N_2 formation is a major field of modelling work. Gas phase models including subsets for N-chemistry have been built since the 1980s. The first model for N-chemistry was developed by Glarborg et al. [1986] and further developed by Miller et al. [1989], Kilpinen et al. [1999] and Glarborg et al. [1998]. Models upgrades/improvements (i.e. better prediction ability) happen through a greater number of reactions, new reactions and a wider base of experimental results. The latest updates about NOx precursors chemistry include:

- NH_3 oxidation study for biomass applications [Skreiberg 2004]

- "Advanced reburning" abatement technique [Han 2003]

- NOx reduction by staged air combustion **[Skreiberg 2004] (P-II)**.

- Selective oxidation of NH_3 over catalysts [Jones 2005]

7 Biomass and waste pyrolysis

The high level of present interest in biomass and biomass residues generated energy is the direct consequence of the increased awareness of the environmental, social and energy security challenges our world is confronting. The public wants its ever-growing need for energy to be fulfilled but is also demanding sustainable alternatives to the fast disappearing fossil fuels to protect the environment from harmful emissions and global warming, which may dramatically alter the climate with disastrous consequences.

Biomass is one of the most promising alternatives to fossil fuels, and different biochemical and thermochemical conversion technologies exist in order to produce energy from it. The most common thermochemical technologies are combustion, gasification and pyrolysis. This chapter will look at the broader picture about pyrolysis as a viable energy and energy carrier's production source.

7.1 Resources

Biomass wastes, but also municipal solid waste [Antal 1983], are a humongous and often cheap material source for pyrolysis. The biomass feedstocks available are diverse:

- Forest wood residues. About 60% of a harvested tree is left in the forest during logging [Parikka 2004]. However, collection may be a serious economical, logistical and environmental issue.

- Agricultural residues (rice husks, bagasse, animal manures, etc). The exploitation of biomass residues is of particular relevance in agricultural areas where the intensive production of a plant will generate huge amounts of by-products such as cherry stones in Spain [González 2003], coffee husks in Kenya [Saenger 2001], rice husks in China [Fang 2004], cottonseed cake in Turkey [Özbay 2001], coffee grounds in Brazil [Silva 1998] and grape residues in Italy [Di Blasi 1999].

- Urban and industrial wood waste (e.g. yard trimmings, pallets, demolition wood, etc). Residues from processing of biomass such as Brewer Spent Grains or coffee roasting waste **[Becidan 2007a] (P-III)** are widely available at food and beverage industries. In many cases the residues collection, and even direct use, can be done at the processing plants, reducing the transport and collection costs.

- The organic fraction of municipal solid waste (MSW) is also a possible source. However, variation in MSW properties and the presence of heavy metals may be an hindrance [Antal 1983].

Pre-treatment (drying, grinding, etc) may be necessary before further utilisation even though this will have a non-negligible economical and logistical cost.

7.2 Pyrolysis products: applications

Pyrolysis produces energy carriers in three forms: bio-oil (liquid), charcoal (solid) and gas. The potential utilisations of those products are diverse.

The **bio-oil**, composed of aliphatic and aromatic hydrocarbons along with more than 200 identified compounds [González 2003] is a very flexible energy carrier. It can be transported and stored for use in energy and heat generation in boilers as a fuel-oil substitute (or in co-firing) and has the potential to be employed as a liquid transportation fuel for internal combustion engines. However, several properties (see Table 7.1) of the bio-oils such as high water content, low pH, high viscosity, corrosiveness, poor ignition ability and instability due to the oxygen content have to be ameliorated or existing equipment have to be modified to meet competitive standards [Encinar 1996; González 2003; Czernik 2004]. The establishment of standards for the specification of bio-oil is an important step for its commercialisation.

Upgrading of the bio-oil can be done by different means [Oasmaa 1999]: deoxygenation (by high-pressure hydrogenation in the presence of metal catalysts for example) to increase the heating value, hot vapour filtration to remove char, solvent addition to homogenise and reduce viscosity, use of surfactants to allow bio-oil/hydrocarbon fuel emulsification. Novel concepts to improve bio-oil characteristics such as catalytic conversion with the help of mesoporous materials [Adam 2005] or mild oxidation with ozone are promising [TN 2006]. Upgrading of bio-oil has proven not economically sound so far.

Bio-oil also contains valuable chemicals such as acetic acid, levoglucosan, food flavourings (commercially available, i.e. barbecue sauce flavour), resins, adhesives, etc. Their recovery is technically feasible but problematic due to low concentrations [Encinar 1996; González 2003].

Table 7.1. Properties of bio-oil and Diesel oil.

	Bio-oil from wood [González 2003]	Bio-oil from wood [Bridgwater 2003]	Diesel no.2 [González 2003]
Moisture content	17.0-18.9	15-30	n.a.
pH	2.4-2.8	2.5	1
Specific gravity	1.20-1.25	1.20	0.847
Elemental analysis C (wt%)	44.0-46.5	55-58	86
H	6.9-7.2	5.5-7.0	11.1
O	46.1-49.0	35-40	0
N	n.d.	0-0.2	1
S	n.d.	n.d.	0.8
HHV (MJ/kg) as produces	10.0-13.9	16-19	44.7
Viscosity	13.5-28 cSt (50°C)	40-100 cp (40°C, 25% H2O)	<2.39 (50°C)

The **charcoal**, basically a carbon-rich solid residue, can be upgraded to activated carbon. Activate carbon is characterised by a very high surface area and has the ability to adsorb a vast array of components. It is widely used in metal extraction, water purification, medicine (poison absorption), gas cleanup (SO_2, dioxins and Hg removal), and food industry (organic impurities removal).

The dry **pyrolysis gas mixture** contains the main components CO_2, CO, CH_4, H_2 and C_2 hydrocarbons [Figueiredo 1989; Williams 1996; Encinar 2000; **Becidan 2007a (P-III)**] and can be used for heat production and power generation, but is usually used to produce energy to sustain the pyrolysis process in a biomass waste pyrolysis plant [Encinar 1996; González 2003] or to dry the feedstock.

Each fraction can have a commercially viable interest but a specific pyrolysis installation will almost always aim at the optimal production (yield, composition and properties) of only one of the principal products bio-oil or charcoal. However, it is important to keep in mind the inherent limitations associated with biomass use (costs associated with small- or medium scale power production, corrosion problems) [Leppälahti 1991].

7.3 Pyrolysis products: influence of operating parameters

Many studies have been carried out in order to determine the operating parameters influencing the product yields but also their composition, i.e. quality. Fuel type, temperature, heating rate, pressure, moisture content, initial sample weight and reaction time (residence time) are all variables that can affect the yields and properties of the products formed.

The most important parameters are temperature and heating rate. Under fixed bed conditions, with biomass as fuel, the **bio-oil** yield is exhibiting a peak value (55-75%) at moderate temperatures (400-550°C) and high heating rates [Encinar 2000; González 2001; Onay 2001; Acikgoz 2004; Schröder 2004]. **Char** formation is minimised by high heating rates and high temperature [Williams 1996; González 2003], while the carbon content in the charcoal and its heating value (based on the carbon content) are increasing with increasing temperature and slow heating rate [Encinar 2000]. The optimal conditions for char production will have to take into account the conflicting effect of temperature in order to produce a satisfying amount of charcoal with acceptable properties. The yields of each and every gas species of the pyrolysis **gas**-phase mixture are enhanced by increasing temperature and high heating rates [Zabaniotou 1994; Encinar 1996; Williams 1996; Barbooti 1998; Schröder 2004; **Becidan 2007a (P-III)**], except carbon dioxide which is often reported to reach a plateau at high temperatures (800-900°C) [Encinar 1996; **Becidan 2007a (P-III)**].

It is important to keep in mind that pyrolysis is not only a thermal conversion technique but also the preliminary step of combustion and gasification. Its investigation can therefore bring information about the early chemistry of these processes.

7.4 Technologies: situation and perspectives

Two classes of pyrolysis exist and differ by the heat transfer:

- **The slow heating rate pyrolysis**, aimed at producing charcoal (also referred to as carbonisation).

Charcoal production technology is of two kinds: batch process (brick kiln and rotary retort furnace, see Figures 7.1 and 7.2) and continuous carbonisation process [BioNett 2000].

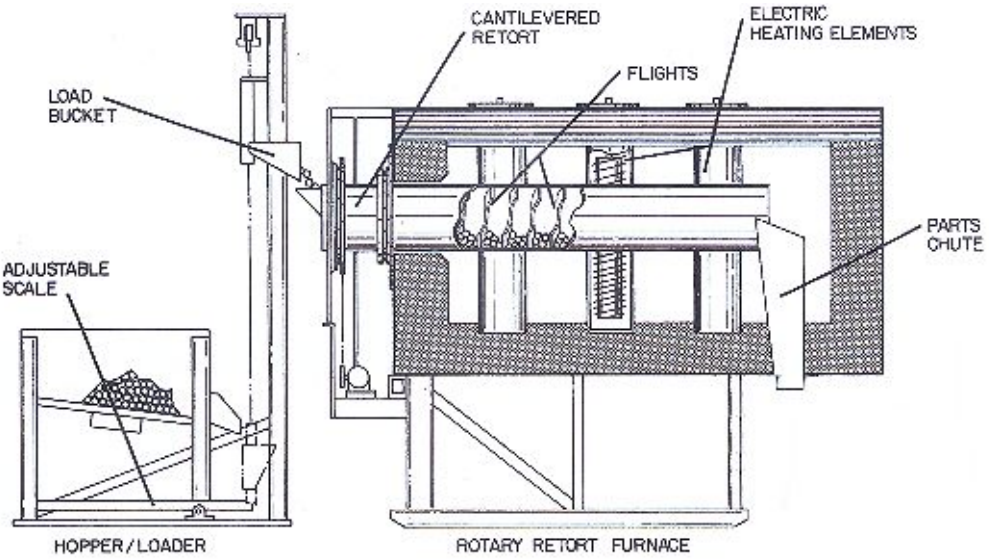

Figure 7.1. Rotary retort furnace [Secowarwick 2006].

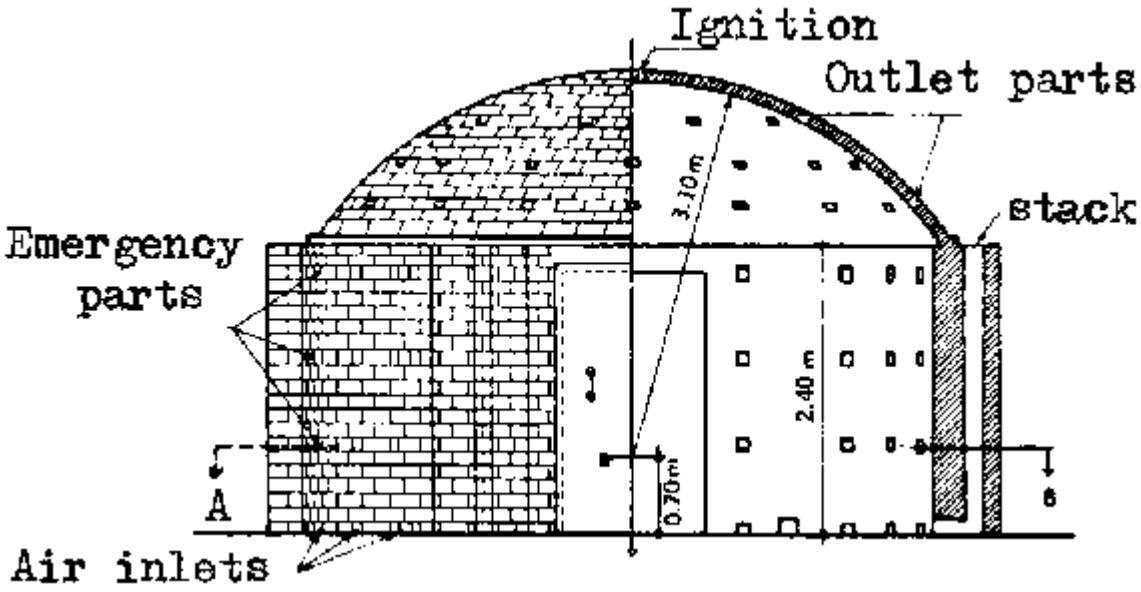

Figure 7.2. Brazilian beehive kiln [Fao 2006].

- **The flash/fast pyrolysis** where the sample is heated at high heating rates (typically several hundreds degrees per minute) or suddenly exposed to a high temperature in order to produce bio-oil.

Flash pyrolysis reactor designs include: Bubbling Fluidised Bed, Circulating Fluidised Bed, transported bed, ablative pyrolysis, entrained flow reactor and rotating cone (vortex) pyrolysis reactor [Bridgwater 2003]. The three most important features of these reactor systems are: prompt heat transfer from reactor to fuel (small particles are therefore necessary), followed by efficient char removal (by means of a cyclone), before rapid condensation of the vapours (bio-oil). All this is done in order to maximise bio-oil production (and its quality) and reduce cracking.

However, besides the previously mentioned issues surrounding pyrolysis products quality (including gas cleaning), several technical challenges such as system integration for energy production and the lack of experience due to few pilot plants have severely limited the market attractiveness of pyrolysis hitherto. It does not mean that pyrolysis does not have a potential, especially in niche applications. One concrete example of the feasibility and potential of biomass pyrolysis may be demonstrated by the recent construction of a Dutch-designed fast pyrolysis plant for the palm oil industry in Malaysia. With the capacity to process 50 tons of empty fruit bunches per day, it is one of the largest fast pyrolysis plants ever built [BI 2005].

8 Thermal degradation characteristics and kinetic study of MSW fractions and biomass by TGA

8.1 Presentation

Thermogravimetric Analysis (TGA) is a well know experimental technique in which the mass of the sample is recorded while the temperature of the sample, in a controlled atmosphere, is programmed.

The sample is no more than a few milligrams to ensure that decomposition is taking place in the kinetic regime. The sample is loaded in an inert crucible (platinum, alumina), placed on (or attached to) a balance. The experiment is usually carried out with a gas flow (inert or reactive). Different types of equipment exist with different positioning of the sample (holder and eventual reference holder) and different positioning of the thermocouples. The positioning of the thermocouple is a crucial feature of TGA as very significant temperature shifts/errors may occur [Stenseng 2001; Grønli 1999]. TGA coupled with analytical equipment such as FTIR or MS is increasingly common.

In order to investigate the **degradation characteristics** and **kinetic of decomposition** of MSW fractions and/or materials, pyrolysis conditions are used (N_2 or Ar gas flow) at a low heating rate (typically 1-40°C/min). It may be argued that these conditions (kinetic regime) do not correspond to realistic thermal conditions but this simplification are necessary to be able to **analyse, interpret and understand** the experimental results as the reality is far more complex **[Becidan 2007d] (P-VI)**. TGA is an essential first step to the thermal study of MSW materials.

In this section, an overview of the results for different materials relevant for MSW will be presented. Kinetic parameters are reported as E_a (activation energy) and log A (A is the frequency factor, specific to a reaction). Degradation characteristics are described in terms of characteristic temperatures and decomposition rates [Grønli 2002].

TGA studies have focused on three main groups of MSW products: the organic fraction (biomass residues and food waste), paper and plastics.

8.2 TGA study of the organic fraction of MSW

This study can be divided into two: (1) MSW organic compounds, i.e. cellulose, hemicellulose, lignin, and proteins/amino acids and (2) MSW fractions per say, i.e. paper products (paper, cardboard and food container) and plastics.

TGA pyrolysis study of cellulose

Grønli has extensively studied [Grønli 1999; Grønli 2002] cellulose pyrolysis under a variety of experimental conditions (different gas flow, sample mass, sample holder, TG equipment and heating rates). Cellulose decomposition can be described as a single peak. The maximum degradation intensity (rate of mass change as a function of time or temperature) and temperature occurrence are dependent mainly on the heating rate (as

long as the sample weight is small enough i.e. some milligrams depending on the set-up). Figure 8.1 shows the DTG curve of Avicel cellulose (5 mg) at a heating rate of 10°C/min (using a SDT 2960). Thermal degradation starts at about 280°C and ends at about 380°C, with the highest decomposition rate located at 337-338°C. With the same fuel and the same weight a Round-Robin study of cellulose pyrolysis located the peak temperature at 327°C (average of 8 laboratories) and 358°C (average of 8 laboratories) for respective heating rates of 5 and 40°C/min, clearly showing the shift towards higher temperature range with increasing heating rate. It is probably due to the fact that a high heating rate shortens the exposure of the sample to a given temperature [Grønli 1996].

It is important to notice that one can not talk of "one" cellulose but several celluloses, depending on its origin. Different celluloses will have slightly different degradation characteristics and therefore decomposition kinetics [Antal 1998; Yang 2006].

The cellulose pyrolysis kinetics is well described by a single-step, irreversible, first order rate law. The kinetic parameters of this reaction have been evaluated at 228 kJ/mol [Antal 1998], 222-244 kJ/mol [Grønli 1999], 216 kJ/mol [Grønli 1996] for the activation energy and 13.4-18.9 [Antal 1998], 17-19 [Grønli 1999] and 16.1 [Grønli 1996] for logA for a variety of celluloses at different conditions (sample weight and heating rates).

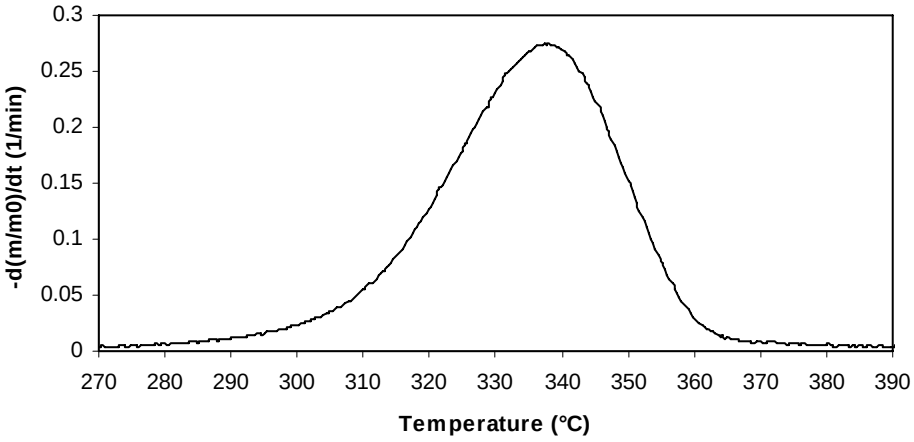

Figure 8.1. DTG curve of A-cellulose. 5mg, 10°C/min.

Cellulose pyrolysis will produce numerous volatile products and a carbonaceous residue. 59 volatile products were isolated and 37 identified by [Antal 1983]: aldehydes, ketones, furans, alcohols, phenols, etc. This reveals the complexity of its decomposition paths described as "complete series of concurrent and consecutive pyrolysis reactions". A review of cellulose degradation mechanisms can be found in [Antal 1983].

TGA pyrolysis study of hemicellulose

Like cellulose, one standard hemicellulose does not exist. Moreover, hemicellulose is more various and complex than cellulose and accurate elucidation of its complete structure is difficult. A TGA curve of hemicellulose (extracted from wood) exhibits several differences with cellulose: (1) hemicellulose starts to decompose at lower temperature (about 150-175°C at a heating rate of 5°C/min with a peak value at 250-275°C [Grønli 1996; Yang 2006]); (2) two overlapping peaks or a major peak and a minor one at higher temperature (400-450°C) are visible. However, kinetic data should be looked upon cautiously as its extraction induces structural changes [Grønli 1996; Stenseng 2001].

TGA pyrolysis study of lignin

Lignin decomposition occurs at a low rate over a wide temperature range, starting at about 150°C and continuing above 500°C [Grønli 1996; Yang 2006] with a (minor) peak value located around 300-400°C. Extraction of lignin, like extraction of hemicellulose, affects its chemical structure (hence decomposition), making it difficult to provide kinetic data for pure lignin.

TGA pyrolysis study of naturally occurring amino acids

Proteins are natural polymers of naturally occurring α-amino acids. The nature of proteins is therefore extremely diverse and is dependent on the amino acids composition. The decomposition patterns of proteins are also greatly affected by the amino acids makeup. This was clearly shown by the study of α-amino acids by Rodante [1992] and Rodante et al. [1992]: the decomposition ranges, peak temperatures, decomposition stage(s), char amounts and kinetics of decomposition are covering a very large scope of values.

TGA pyrolysis study of biomass

Biomass pyrolysis decomposition has been widely studied mainly because of the potential offered by bioenergy production through thermal methods (pyrolysis, combustion and gasification). Biomass is made of cellulose, hemicellulose, lignin, extractives and minerals. A look at a biomass DTG curve shows that the different constituents' decompositions are (partially) overlapping (Figure 8.2), complicating the kinetic analysis. The resulting biomass DTG curves have therefore to be decomposed into partial curves.

A successful method has been developed by Várhegyi [Várhegyi 1979; Várhegyi 1989; Várhegyi 1996; Várhegyi 1997; Várhegyi 2002] and is assuming parallel, independent reactions. It is assumed that the products from a reaction are originating only from one reactant. The overall reaction rate is a linear combination of these reactions. For each reaction (reactant) a conversion (reacted fraction) and a reaction rate are defined with their own kinetic equation with its own parameters. Overlapping of curves mean that more than one (mathematical) solution is possible; ambiguity can be reduced by evaluation of series of experiments under different experimental conditions (the same set of kinetic parameters should fit for all conditions) and/or proper input data such as known

kinetic parameters for single components or peak temperature values. The evaluation of the parameters is done by the method of least squares method (Hook-Jeeves) [Meszaros 2004]. An example of the decomposition into partial curves of a wood DTG curve is shown on Figure 8.3.

Biomass samples are all constituted of hemicellulose (often two types), cellulose, lignin, extractives and minerals (ash). It is therefore natural to expect each of this reactant to be attributed a decomposition reaction for the evaluation of DTG curves. However, severe overlapping (or complexity of the biomass structure) often calls for the use of the notion of pseudo-component, i.e. a group of reactants with similar reactivity, rather than component [Meszaros 2004].

Besides the pseudo-reactant concept, several approaches can be adopted to describe biomass decomposition but will not provide similar results and will have to be interpreted accordingly. The different kinetic evaluation methods include: determination of the number of partial reactions required, order of the reactions (first order, n^{th} order) and distributed reactivity models [Burnham 1999]. A kinetic study of complex biomass residues according to different models can be found in **[Becidan 2007c] (P-V)**.

The choice of the evaluation methods and its characteristics will be dictated by the nature of the biomass but also the desired accuracy. For example, assuming n^{th}-order decomposition reactions instead of first-order reactions requires fewer pseudo-components [Meszaros 2004].

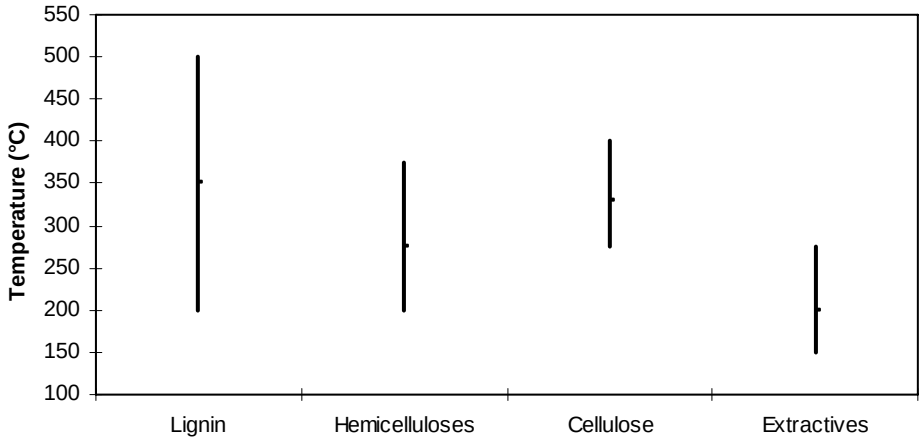

Figure 8.2. Main decomposition range of biomass constituents: overlapping [Grønli 1996; Yang 2006].

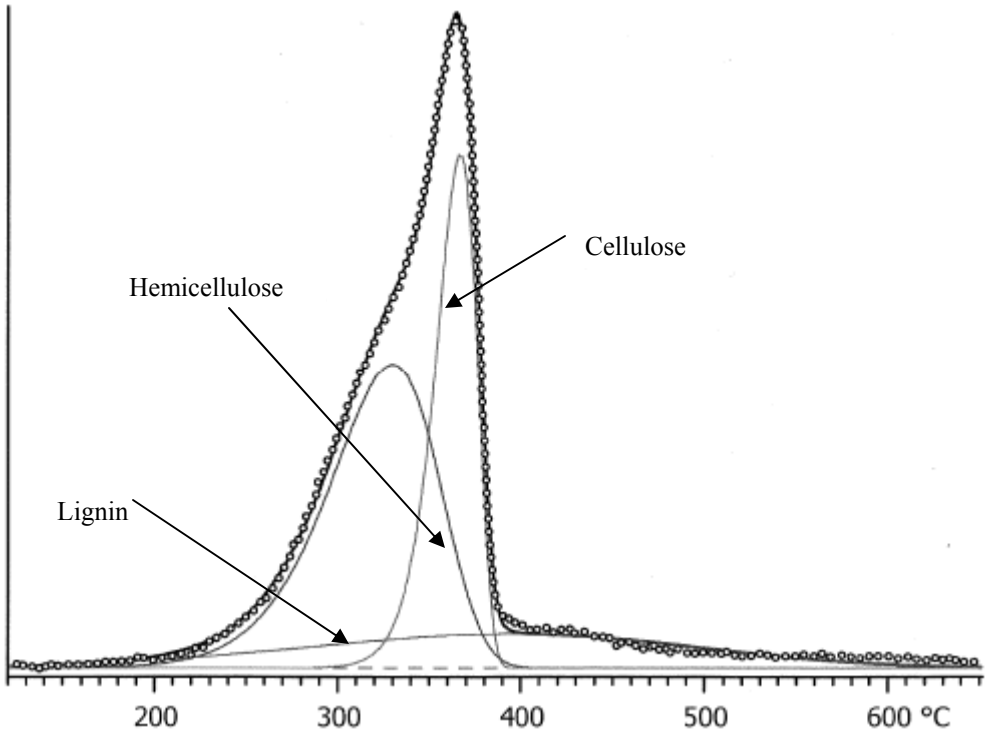

Figure 8.3. Partial curves constituting the DTG curve of pine (10°C/min, 5 mg, SDT 2960). Dotted line: experimental curve. Full line: simulated curve.

TGA pyrolysis study of paper

Paper is produced from wood but the different types of paper have significantly different compositions (cellulose, hemicellulose and lignin content, mineral content) due to different production processes. These different compositions respond to the specific applications of a given product. Sørum [2000] studied 4 types of paper products: newspaper, cardboard, recycled paper and glossy paper. TGA will evidently reveal those differences: newspaper has a low ash content and a (relatively) high lignin content (causing yellowing), recycled paper is made of a variety of waste paper and exhibit an intermediary thermal behaviour, glossy paper has a high mineral content influencing its decomposition pattern through catalytic effects. However, the different paper products all decompose between 200 and 450/500°C, like wood.

The major products from paper pyrolysis are CO, CO_2, H_2O, H_2 and hydrocarbons [Wu 2002].

8.3 TGA pyrolysis study of plastic

Thermal decomposition of most plastics (HDPE, LDPE, PS, PP) can be described by a single step reaction [Sørum 2001] occurring at 400-500°C (HDPE, LDPE, PP) or 350-450°C (PS). This simple thermal behaviour can be explained by the very homogeneous structure of plastics. PVC is of special interest as it represents a significant share of MSW plastic (about 1% [Minnesota 2000]) and is responsible for the formation of many chloro-

compounds during MSW incineration. Furthermore it exhibits a significantly different thermal behaviour. Two overlapping decomposition steps are observed at 225-350°C followed by a third peak at 350-550°C. The first steps were associated with chlorine and Cl-containing compounds release while the third one is mostly due to hydrocarbon decomposition. Pyrolysis of HDPE in a fluidised bed show that the main decomposition products are CH_4, C_2H_4, C_2H_6, C_3, C_4, aromatic and C_5-C_8 [Mastral 2003]

8.4 Other MSW fractions

The thermal behaviours (**kinetics** and/or **emissions**) of other MSW fractions have been studied: rubber, latex, tire, packaging film [Kim 1994; Lin 1998; Sørum 2001; Liou 2003]. Two important aspects are of interest: the degradation characteristics (temperature range, char amount, reactants identification, T_{peak}, etc) and the nature (chemical composition) of the different products in order to identify the potentially harmful or valuable chemical products.

Attempts have been made to study "simulated" MSW by blending 2 or more MSW fractions [Sørum 2000]. Possible interactions between MSW materials have been suggested but seem limited. RDF can be seen as a homogenised and pelletised version of MSW. Cozzani et al. [1995] and Lin et al. [1999] concluded that the pyrolysis rate could be predicted by the weighed sum method of the RDF components. This appears to confirm the limited effect of possible interactions between MSW fractions. However, it is not a definite piece of evidence as no chemical information is provided.

8.5 Non-kinetic regime

As previously mentioned, TGA is limited to the study of purely kinetic regime conditions. The reality encountered in industrial applications is far more complex with the occurrence of heat and mass transport phenomena. The effects of these phenomena on temperature profile in the sample and the degradation pattern have been investigated in our in-house designed macro-TGA (study of 75 g samples) and compared with TGA (to determine the so-called "scaling effect") **[Becidan 2007d] (P-VI)**.

9 Conclusions and recommendations for further work

MSW and biomass residues management. Waste management is a complex and growing issue because it involves a complex and heterogeneous product but also societal choices. Trends go towards more fraction-specific treatments together with development of technologies at a large industrial scale such as advanced combustion and gasification.

Pyrolysis. Knowledge of the pyrolysis process as the first step in combustion and gasification is of major importance. Furthermore, pyrolysis investigation of scarcely known biomass residues demonstrates their potential for energy production through this thermal process. This shows that no biomass resources should be overlooked and that tailor-made niche pyrolysis processes based on specific residues can be efficient.

Further work should focus on modifying the experimental set-up to obtain a complete picture of the amount and properties (physical and chemical) of tar and char but also to be able to operate with continuous feeding of the fuel, as done in most real systems.

N-chemistry before and after thermal degradation. Nitrogen in biomass is usually considered to be of protein origin by the bioenergy world. It was shown that this is quite inaccurate as non-protein nitrogen is diverse and may represent a substantial proportion of nitrogen for many biomasses. The most significant compounds are: free and non protein amino acids, alkaloids, inorganic nitrogen and chlorophyll. Their relative weight will vary substantially and depend on biological factors.
A discussion about the intricate biomass structure reveals that possible reactions/interactions/linkages between N-compounds and non N-compounds have to be taken into account to elucidate the biomass-N pyrolysis mechanisms. Model compounds studies can not render this complexity and should therefore be looked upon carefully.
Release trends of HCN and NH_3 were experimentally studied. It was shown that N-chemistry is a complex issue and that biomass pyrolysis studies do not provide clear mechanistic insights. Biomass compounds and model compounds studies should accordingly be studied hand in hand to obtain a more complete picture.

Further work should focus on comparative studies, in order to try to assess the N-chemistry during decomposition of biomass. For this purpose, “simulated biomass” (one main biomass compound + one N-functionality), N-model compound and main biomass component (with no N) should be studied alongside.

Degradation characteristics. Two different types of studies were carried out: a kinetic study of small particles and an investigation on thermally thick biomass samples.
TGA studies of small particles provide kinetic data about the decomposition of biomass materials. The evaluation method had to be adapted to the studied fuel. The biomass residues studied exhibited complex decomposition patterns due to their heterogeneous structure.
Macro-TGA studies of thermally thick particles show the complex temperature history inside large samples but also the exothermic step of pyrolysis. Study of the scaling effect (comparative study of TGA and macro TGA experiments) confirms the complexity of

heat and mass transport processes in industrial applications. They will have an effect on the main features (pyrolysis rate and pyrolysis time) of the thermal process.

Further work should aim at collecting more experimental data at various operating conditions and feedstock properties to thereafter use them for improved modelling of fixed-bed systems for conditions relevant for waste and biomass applications.

References

[Acikgoz 2004] Acikgoz C., Onay O., Kockar O.M. Fast pyrolysis of linseed: product yields and compositions. Journal of Analytical and Applied Pyrolysis 71 (2004) 417-429.

[Adam 2005] Adam J. Doctoral Dissertation 2005. NTNU, Trondheim, Norway.

[Adelsberger 1976] Adelsberger V., Petrowitz H. Gehalt und Zusammensetzung der Proteine Verschieden Lange Gelagerten Kiefernholzes (Pinus Sylvestris L.). Holzforschung 30 (1976) 109-113.

[Aho 1993] Aho M.J., Hämäläinen J.P., Tummavuori J.L. Importance of solid fuel properties to nitrogen oxide formation through HCN and NH_3 in small particle combustion. Combustion and Flame 95 (1993) 22-30.

[Antal 1983] Antal M.J.Jr. Biomass Pyrolysis: A Review of the Literature Part 1-Carbohydrate Pyrolysis (p.61-111). Advances in Solar Energy, 1983. American Solar Energy Society, Inc.

[Antal 1998] Antal M.J.Jr, Várhegyi G., Jakab E. Cellulose pyrolysis kinetics: revisited. Industrial and Engineering Chemistry Research 37 (1998) 1267-1275.

[Axworthy 1978] Axworthy A.E., Dayan V.H., Martin G.B. Reactions of Fuel-Nitrogen Compounds under Conditions of Inert Pyrolysis. Fuel 57 (1978) 29-35.

[Babich 2005] Babich I.V., Seshan K., Lefferts L. Nature of nitrogen specie in coke and their role in NOx formation during FCC catalyst regeneration. Applied Catalysis B: Environment 59 (2005) 205-211.

[Barbooti 1988] Barbooti M.M. Flash pyrolysis for the continuous conversion of reed into hydrocarbons. Journal of Analytical and Applied Pyrolysis 13 (1988) 233.

[Barrio 2002] Barrio M. Experimental investigation of small-scale gasification of woody biomass. Doctoral Dissertation 2002. NTNU, Trondheim, Norway.

[Basiuk 1998a] Basiuk V.A. Pyrolysis of valine and leucine at 500°C: identification of less-volatile products using gas chromatography-Fourier transform infrared spectroscopy-mass spectrometry. Journal of Analytical and Applied Pyrolysis 47 (1998) 127-143.

[Basiuk 1998b] Basiuk V.A., Navarro-González R., Basiuk E.V. Pyrolysis of alanine and α-aminoisobutyric acid: identification of less-volatile products using gas chromatography/Fourier transform infrared spectroscopy/mass spectrometry. Journal of Analytical and Applied Pyrolysis 45 (1998) 89-102.

[Basiuk 2000] Basiuk V.A., Douda J. Pyrolysis of poly-glycine and poly-L-alanine: analysis of less-volatile products by gas chromatography/Fourier transform infrared

spectroscopy/mass spectrometry. Journal of Analytical and Applied Pyrolysis 55 (2000) 235-246.

[Basiuk 2001] Basiuk V.A., Douda J. Analysis of less-volatile products pyrolysis of poly-L-valine by gas chromatography/Fourier transform infrared spectroscopy/mass spectrometry.

[Becidan 2004] (P-I) Becidan M., Skreiberg Ø., Hustad J.E. An experimental study of nitrogen species release during municipal solid waste (MSW) and biomass pyrolysis and combustion. Proceedings of the Science in Thermal and Chemical Biomass Conversion Conference, 30 August-2 September 2004, Victoria, BC, Canada, vol. 2, pp. 1443-1455. Edited by A.V. Bridgwater and D.G.B. Boocock. CPL Press, UK, 2006. Peer-reviewed.

[Becidan 2007a] (P-III) Becidan M., Skreiberg Ø., Hustad J.E. Products distribution and gas release in pyrolysis of thermally thick biomass residues samples. Journal of Analytical and Applied Pyrolysis 78 (2007) 207-213.

[Becidan 2007b] (P-IV) Becidan M., Skreiberg Ø., Hustad J.E. NOx and N_2O precursors (NH_3 and HCN) in pyrolysis of biomass residues. Energy & Fuels 21 (2007) 1173-1180.

[Becidan 2007c] (P-V) Becidan M., Várhegyi G., Hustad J.E., Skreiberg Ø. Thermal decomposition of biomass wastes. A kinetic study. Industrial & Engineering Chemistry Research 46 (2007) 2428-2437.

[Becidan 2007d] (P-VI) Becidan M., Skreiberg Ø., Hustad J.E. Experimental study on pyrolysis of thermally thick biomass residues samples: intra-sample temperature distribution and effect of sample weight ("scaling effect"). Accepted for publication 2 March 2007. Available online 2 April 2007. Fuel.

[Bennett 1968] Bennett W.D. Isolation of the cyanogenetic glucoside prunasin from bracken fern. Phytochemistry 7 (1968) 151-152.

[BI 2005] Bioenergy International No. 16, 5-2005.

[Billow 1994] Billow C., Matson P., Yoder B. Seasonal biochemical changes in coniferous forest canopies and their response to fertilization. Tree Physiology 14 (1994) 563-574.

[BioNett 2000] Norsk Bioenergi Nettverk, BioNett 1998-2000, Sluttrapport, Temablad 8.

[Birecka 1984] Birecka H., DiNolfo T.E., Martin W.B., Frohlich M.W. Polyamines and leaf senescence in pyrrolizidine alkaloid-bearing heliotropium plants. Phytochemistry 23 (1984) 991-997.

[Bridgwater 2003] Bridgwater A.V. Renewable fuels and chemicals by thermal processing of biomass. Chemical Engineering Journal 91 (2003) 87-102.

[Burnham 1999] Burnham A. K., Braun R. L. Global kinetic analysis of complex materials. Energy & Fuels 13 (1999) 1-22.

[Cheng 2004] Cheng L., Ma F., Ranwala D. Nitrogen storage and its interaction with carbohydrates of young apple trees in response to nitrogen supply. Tree Physiology 24 (2004) 91-98.

[Chiavari 1992] Chiavari G., Galletti G.C. Pyrolysis-gas chromatography/mass spectrometry of amino acids. Journal of Analytical and Applied Pyrolysis 24 (1992) 123-137.

[CIA 2003] CIA's World Factbook. www.cia.gov/cia/publications/factbook/index.html

[Cowling 1966] Cowling E.B., Merrill W. Nitrogen in wood and its role in wood deterioration. Canadian Journal of Botany 44 (1966) 1539-1553.

[Cowling 1970] Cowling E.B. Nitrogen in forest trees and its role in wood deterioration. Abstracts of Uppsala Dissertations in Science 164 (1970).

[Cozzani 1995] Cozzani V., Petarca L., Tognotti L. Devolatilization and pyrolysis of refused derived fuels: characterization and kinetic modelling by a thermogravimetric and calorimetric approach. Fuel 74 (1995) 903-912.

[Curran 2001] Curran P.J., Dungan J.L., Peterson D.L. Estimating the foliar biochemical concentration of leaves with reflectance spectrometry: testing the Kokaly and Clark methodologies. Remote Sensing of Environment 76 (2001) 349-359.

[Czernik 2004] Czernik S., Bridgewater A.V. Overview of applications of biomass fast pyrolysis oil. Energy & Fuels 18 (2004) 590-598.

[Duffus 2002] Duffus J.H. "Heavy Metals" – a meaningless term? IUPAC Technical Report. Pure Applied Chemistry 74 (2002) 793-807.

[DWB 2006] Website associated to the University of Nebraska-Lincoln. www.dwb.unl.edu. Visited in August 2006.

[Dong 2002] Dong S., Cheng L., Scagel C.F., Fuchigami L.H. Nitrogen absorption, translocation and distribution from urea applied in autumn to leaves of young potted apple (Malus Domestica) trees. Tree Physiology 22 (2002) 1305-1310.

[Damon 2005] Damon M., Zhang N.Z., Haytowitz D.B., Booth S.L. Phylloquinone (vitamin K_1) content of vegetables. Journal of Food Composition and Analysis 18 (2005) 751-758.

[Di Blasi 1999] Di Blasi C., Signorelli G., Di Russo C., Rea G. Product distribution from pyrolysis of wood and agricultural residues. Industrial and Engineering Chemistry Research 38 (1999) 2216-2224.

[Encinar 1996] Encinar J.M., Beltrán F.J., Bernalte A., Ramiro A., González J.F. Pyrolysis of two agricultural residues: olive and grape bagasse. Influence of particle size and temperature. Biomass and Bioenergy 11 (1996) 397-409.

[Encinar 2000] Encinar J.M., González J.F., González J. Fixed-bed pyrolysis of *Cynara cardunculus* L. Product yields and compositions. Fuel Processing Technology 68 (2000) 209-222.

[EPA-I 2002] European Waste Catalogue and Hazardous Waste List (2002). Published by the Environmental Protection Agency of Ireland. Available online.

[EURACHEM/CITAC 2000] EURACHEM/CITAC Guide. Quantifying uncertainty in analytical measurement, second edition 2000. Editors: SLR Ellison (LGC, UK), M Rosslein (EMPA, Switzerland), A Williams (UK). Available online.

[EUROSTAT 2003] EUROSTAT report. Waste generated and treated in Europe. Data 1990-2001. 2003 Edition. Available online. EUROSTAT is the statistical office of the European Communities.

[EUROSTAT 2005] EUROSTAT report. Waste generated and treated in Europe 1995-2003. 2005 Edition. Available online. EUROSTAT is the statistical office of the European Communities.

[Ezeagu 2002] Ezeagu I.E., Petzka J.K., Metges C.C., Akin soyinu A.O., Ologhobo A.D. Seed protein contents and nitrogen-to-protein conversion factors for some uncultivated tropical plant seeds. Food Chemistry 78 (2002) 105-109.

[Fang 2004] Fang M., Yang L., Chen G., Shi Z., Luo Z., Cen K. Experimental study on rice husk combustion in a circulating fluidized bed. Fuel Processing Technology 85 (2004) 1273-1282.

[Fao 2006] www.fao.org/docrep/X5328E/x5328e08.htm

[Figueiredo 1989] Figueiredo J.L., Valenzuela C., Bernalte A., Encinar J.M. Pyrolysis of holm-oak wood: influence of temperature and particle size. Fuel 68 (1989) 1012-1016.

[Fowden 1980] Fowden L. Non-protein amino acids of plants. Food Chemistry 6 (1980-81) 201-211.

[FPL 1979] Extractives in Eastern Hardwoods – A Review. General Technical Report, Forest Products Laboratory. FPL 18 (1979). Available online.

[Glarborg 1986] Glarborg P., Miller J.A., Kee R.J. Kinetic modeling and sensitivity analysis of nitrogen oxide formation in well-stirred reactors. Combustion and Flame 65 (1986) 177-202.

[Glarborg 1998] Glarborg P., Alzueta M.U., Dam-Johansen K., Miller J.A. Kinetic modeling of hydrocarbon/nitric oxide interactions in a flow reactor. Combustion and Flame 115 (1998) 1-27.

[Glarborg 2003] Glarborg P., Jensen A.D., Johnsson J.E. Fuel nitrogen conversion in solid fuel fixed systems. Progress in Energy and Combustion Science 29 (2003) 89-113.

[Gomez 2002] Gomez L., Faurobert M. Contribution of vegetative storage proteins to seasonal nitrogen variations in the young shoots of peach trees (Prunus Persica L. Batsch). Journal of Experimental Botany 53 (2002) 2431-2439.

[González 2003] González J.F., Encinar J.M., Canito J.L, Sabio E., Chacón M. Pyrolysis of cherry stones: energy uses of the different fractions and kinetic study. Journal of Analytical and Applied Pyrolysis 67 (2003) 165-190.

[Grønli 1996] Grønli M. A theoretical and experimental study of the thermal degradation of biomass. Doctoral Dissertation 1996. NTNU, Trondheim, Norway.

[Grønli 1999] Grønli M., Antal M.J.Jr, Varhegyi G. A Round-Robin study of cellulose pyrolysis kinetics by thermogravimetry. Industrial and Engineering Chemistry Research 38 (1999) 2238-2244.

[Grønli 2002] Grønli M., Várhegyi G., Di Blasi C. Thermogravimetric analysis and devolatilization kinetics of wood. Industrial and Engineering Chemistry Research 41 (2002) 4201-4208.

[Haidar 1981] Haidar N.F., Patterson J.M., Moors M., Smith W.T. Effects of structure on pyrolysis gases from amino acids. Journal of Agricultural and Food Chemistry 29 (1981) 163-165.

[Hämäläinen 1994] Hämäläinen J.P., Aho M.J., Tummavuori J.L. Formation of nitrogen oxides from fuel-N through HCN and NH_3: a model-compound study. Fuel 1994 (73) 1894-1898.

[Hämäläinen 1996] Hämäläinen J.P., Aho M.J. Conversion of fuel nitrogen through HCN and NH_3 to nitrogen oxides at elevated pressure. Fuel 75 (1996) 1377-1386.

[Han 2003] Han X., Wei X., Schnell U., Hein K.R.G. Detailed modeling of hybrid reburn/SNCR processes for NO_X reduction in coal-fired furnaces Combustion and Flame 132 (2003) 374-386.

[Hansson 2003a] Hansson K.-M. Principles of biomass pyrolysis with emphasis on the formation of the nitrogen-containing gases HNCO, HCN and NH_3. Doctoral Dissertation 2003. Chalmers University of Technology, Göteborg, Sweden

[Hansson 2003b] Hansson K.-M., Åmand L.-E., Habermann A., Winter F. Pyrolysis of poly-L-leucine under combustion-like conditions. Fuel 82 (2003) 653-660.

[Hansson 2003c] Hansson K.-M., Samuelsson J., Åmand L.-E., Tullin C. The temperature's influence on the selectivity between HNCO and HCN from Pyrolysis of 2,5-diketopiperazine and 2-pyridone. Fuel 82 (2003) 2163-2172.

[Hansson 2004] Hansson K.-M., Samuelsson J., Tullin C., Åmand L.-E. Formation of HNCO, HCN and NH_3 from pyrolysis of bark and nitrogen-containing model compounds. Combustion and Flame 137 (2004) 265-277.

[HDR 2003] Human Development Report 2003 (United Nations). Available online.

[Hesse 2002] Hesse M. Alkaloids nature's curse or blessing? Wiley-VCH 2002.

[Hiraoka 1974] Hiraoka N., Tabata M. Alkaloid production by plants regenerated from cultured cells of Datura Innoxia. Phytochemistry 13 (1974) 1671-1675.

[Houser 1980] Houser T.J., Hull M., Always R.M., Biftu T. Kinetics of formation of HCN during pyridine pyrolysis. International Journal of Chemical Kinetics XII (1980) 569-574.

[IEA Task 32 2002] Handbook of Biomass Combustion and Co-Firing. IEA Bioenergy Agreement. Task 32: Biomass Combustion and Co-Firing. February 2002.

[Ikeda 1995] Ikeda E., Mackie J.C. Thermal decomposition of two coal model compounds – pyridine and 2-picoline. Kinetics and product distributions. Journal of Analytical and Applied Pyrolysis 34 (1995) 47-63.

[Iyengar 2006] Iyengar S.R., Bhave P.P. In-vessel composting of household wastes. Waste management 26 (2006) 1070-1080.

[Izumikawa 1996] Izumikawa C. Metal recovery from fly ash generated from vitrification process for MSW ash. Waste Management 16 (1996) 501-507.

[Jung 2006] Jung C.H., Matsuto T., Tanaka N. Flow analysis of metals in a municipal solid waste management system. Waste Management (2006). Available Online 24 January 2006.

[Jurič 2006] Jurič B., Hanžič L., Ilić R., Samec N. Utilization of municipal solid waste bottom ash and recycled aggregate in concrete. Waste Management (2006). Available Online 31 January 2006.

[Johnson 1971] Johnson W.R., Kang J.C. Mechanisms of hydrogen cyanide formation from the pyrolysis of amino acids and related compounds. Journal of Organic Chemistry 36 (1971) 189-192.

[Jones 2005] Jones J.M., Pourkashanian M., Williams A., Backreedy R.I., Darvell L.I., Simell P., Heiskanen K., Kilpinen P. The selective oxidation of ammonia over alumina supported catalysts–experiments and modelling. Applied Catalysis B: Environment 60 (2005) 139-146.

[Kathirvale 2004] Kathirvale S., Yunus M.N.M, Sopian K., Samsuddin A.H. Energy potential from municipal solid waste in Malaysia. Renewable Energy 29 (2004) 559-567.

[Keleman 1999] Keleman S.R., Freund H., Gorbaty M.L., Kwiatek P.J. Thermal chemistry of nitrogen in Kerogen and low-rank coal. Energy and Fuels 13 (1999) 529-538.

[Kilpinen 1999] Kilpinen P., Leppälahti J.K., Zabetta E.G., Hupa M. Gas-phase conversion of NH_3 to N_2 in gasification. Part I: A kinetic modeling study on the potential of the method. IFRF Combustion Journal, art. Nr. 199901, 1999.

[Kim 1994] Kim J.R., Lee J.S., Kim S.D. Combustion characteristics of shredded waste tires in a fluidized bed combustor. Energy 19 (1994) 845-854.

[Kuo 2004] Kuo Y.-M., Lin T.-C., Tsai P.-J. Metal behavior during vitrification of incinerator ash in a coke bed furnace. Journal of Hazardous Materials 109 (2004) 79-84.

[Kwak 2006] Kwak T.-H., Maken S., Lee S., Park J.-W., Min B.-R., Yoo Y.D. Environmental aspects of gasification of Korean municipal solid waste in a pilot plant. Fuel 85 (2006) 2012-2017.

[Laidlaw 1965] Laidlaw R., Smith G. The proteins of the timber of Scots Pine (Pinus Sylvestris). Holzforschung 19 (1965) 129-134.

[Lang 2005] Lang T., Jensen A.D., Jensen P.A. Retention of organic elements during solid fuel pyrolysis with emphasis on the peculiar behavior of nitrogen. Energy & Fuels 19 (2005) 1631-1643.

[Langlois 1976] Langlois J., Ungar I.A. A comparison of the effect of artificial tidal action on the growth and protein nitrogen content of Salicornia Stricta dumort. and Salicornia Ramosissima woods. Aquatic Botany 2 (1976) 43-50.

[Lebiedzińska 2006] Lebiedzińska A., Szefer P. Vitamins B in grain and cereal-grain food, soy-products and seeds. Food Chemistry 95 (2006) 116-122.

[Leppälahti 1991] Leppälahti J., Simell P., Kurkela E. Catalytic conversion of nitrogen compounds in gasification gas. Fuel Processing Technology 29 (1991) 43-56.

[Leppälahti 1995a] Leppälahti J., Koljonen T. Nitrogen evolution from coal, peat and wood during gasification: literature review. Fuel Processing Technology 43 (1995) 1-45.

[Leppälahti 1995b] Leppälahti J. Formation of NH_3 and HCN in slow-heating-rate inert pyrolysis of peat, coal and bark. Fuel 74 (1995) 1363-1368.

[Li 2000] Li C.-Z., Tan L.L. Formation of NOx and SOx precursors during the pyrolysis of coal and biomass. Part III. Further discussion on the formation of HCN and NH_3 during pyrolysis. Fuel 79 (2000) 1899-1906.

[Lifshitz 1989] Lifshitz A., Tamburu C., Suslensky A. Isomerization and decomposition of pyrrole at elevated temperatures. Studies with a single-pulse shock tube. Journal of Physical Chemistry 93 (1989) 5802-5808.

[Lin 1998] Lin J.-P., Chang C.-Y., Wu C.-H. Pyrolysis kinetics of rubber mixtures. Journal of Hazardous Materials 58 (1998) 227-236.

[Lin 1999] Lin K.-S., Wang H.P., Liu S.-H., Chang N.-B., Huang Y.-J., Wang H.-C. Pyrolysis kinetics of refused-derived fuel. Fuel Processing Technology 60 (1999) 103-110.

[Liou 2003] Liou T.-H. Pyrolysis kinetics of electronic packaging material in a nitrogen atmosphere. Journal of Hazardous Materials B 103 (2003) 107-123.

[Mackie 1990] Mackie J.C., Colket III M.B., Nelson P.F. Shock tube pyrolysis of pyridine. Journal of Physical Chemistry 94 (1990) 4099-4106.

[Mackie 1991] Mackie J.C., Colket III M.B., Nelson P.F., Esler M. Kinetics of pyrolysis of pyrrole. International Journal of Chemical Kinetics 23 (1991) 755-760.

[Mastral 2003] Mastral F.J., Esperanza E., Berrueco C., Juste M., Ceamanos J. Fluidized bed thermal degradation products of HDPE in an inert atmosphere and in air-nitrogen mixtures. Journal of Analytical and Applied Pyrolysis 70 (2003) 1-17.

[Merrill 1966] Merrill W., Cowling E.B. Role of nitrogen in wood deterioration: amount and distribution of nitrogen in tree stems. Canadian Journal of Botany 44 (1966) 1555-1580.

[Meszaros 2004] Meszaros E., Varhegyi G., Jakab E., Marosvolgyi B. Thermogravimetric and reaction kinetic analysis of biomass samples from an energy plantation. Energy & Fuels 18 (2004) 497-507.

[Meuriot 2003] Meuriot F., Avice J.-C., Decau M.-L., Simon J.-C., Lainé P., Volenec J.J., Ourry A. Accumulation of N reserves and Vegetative Storage Protein (VSP) in taproots of non-nodulated Alfalfa (Medicago sativa l.) are affected by mineral N availability. Plant Science 165 (2003) 709-718.

[Miller 1989] Miller J.A, Bowman C.T. Mechanism and modeling of nitrogen chemistry in combustion. Progress in Energy and Combustion Science 15 (1989) 287-338.

[Minnesota 2000] Statewide MSW composition study. A study of discards in the state of Minnesota. Final report, March 2000. Available online.

[Morcos 1989] Morcos V.H. Energy recovery from municipal solid waste incineration – A review. Heat Recovery Systems and CHP 9 (1989) 115-126.

[Morselli 1992] Morselli L., Zappoli S., Tirabassi T. Characterization of the effluents from a municipal solid waste incinerator plant and of their environmental impact. Chemosphere 24 (1992) 1775-1784.

[Näsholm 1990] Näsholm T., Ericsson A. Seasonal changes in amino acids, protein and total nitrogen in needles of fertilized Scots Pine trees. Tree Physiology 6 (1990) 267-281.

[NEA 2006] National environmental agencies.

[NHWAP 1994] NHWAP Survey 1994 (National Household Waste Analysis Program).

[Oasmaa 1999] Oasmaa A., Czernik S. Fuel oil quality of biomass pyrolysis oils-State of the art for the end users. Energy & Fuels 13 (1999) 914-921.

[Obernberger 1998] Obernberger I. Decentralized biomass combustion: state of the art and future development. Biomass and Bioenergy 14 (1998) 33-56.

[Onay 2001] Onay Ô., Beis S.H., Koçkar Ô.M. Fast pyrolysis of rape seed in a well-swept fixed-bed reactor. Journal of Analytical and Applied Pyrolysis 58-59 (2001) 995-1007.

[Özbay 2001] Özbay N., Pütün A.E., Uzun B.B., Pütün E. Biocrude from biomass: pyrolysis of cottonseed cake. Renewable Energy 24 (2001) 615-625.

[Parikka 2004] Parikka M. Global biomass fuel resources. Biomass and Bioenergy 27 (2004) 613-620.

[Patterson 1968] Patterson J.M., Tsamasfyros A., Smith W.T.Jr. Pyrolysis of pyrrole (1). Journal of Heterocyclic Chemistry 5 (1968) 727-729.

[Periago 1996] Periago M.J., Ros G., Martinez C., Rincón F. Variations of non-protein nitrogen in six Spanish legumes according to the extraction method used. Food Research International 29 (1996) 489-494.

[Phillips 1978] Phillips L.F. Pressure dependence of the rate of reaction of OH with HCN. Chemical Physics Letters 57 (1978) 538-539.

[Prasad 2006] Prasad S., Singh A., Joshi H.C. Ethanol as an alternative fuel from agricultural, industrial and urban residues. Resources, Conservation and Recycling (2006). Available Online 3 July 2006.

[Predel 1998] Predel M., Kaminsky W. Pyrolysis of rape-seed in a fluidised-bed reactor. Bioresource Technology 66 (1998) 113-117.

[Qian 2006] Qian G., Song Y., Zhang C., Xia Y., Zhang H., Chui P. Diopside-based glass-ceramics from MSW fly ash and bottom ash. Waste Management (2006). Available Online 20 February 2006.

[Ratcliff 1974] Ratcliff M.A.Jr, Medley E.E., Simmonds P.G. Pyrolysis of amino acids - mechanistic considerations. Journal of Organic Chemistry 39 (1974) 1481-1490.

[Rodante 1992a] Rodante F. Thermodynamics and kinetics of decomposition processes for standard α-amino acids and some of their dipeptides in the solid state. Thermochimica Acta 200 (1992) 47-61.

[Rodante 1992b] Rodante F., Marrosu G., Catalami G. Thermal analysis of some α-amino acids with similar structures. Thermochimica Acta 194 (1992) 197-213.

[Rodriguez Andara 2002] Rodriguez Andara A., Lomas Esteban J.M. Transition of particle size fractions in anaerobic digestion of the solid fraction of piggery manure.Biomass and Bioenergy 23 (2002) 229-235.

[Ruth 1998] Ruth L.A. Energy from municipal solid waste: a comparison with coal combustion technology. Progress in Energy and Combustion Science 24 (1998) 545-564.

[Saenger 2001] Saenger M., Hartge E.-U., Werther J., Ogada T., Siagi Z. Combustion of coffee husks. Renewable Energy 23 (2001) 103-121.

[Samuel 1985] Samuel L., Turek M.D., Lippincott J.B. Orthopaedics: principles and applications. Second edition (1985). Pages 113 and 136.

[Samuelsson 2006] Samuelsson J.I. Conversion of nitrogen in a fixed burning biofuel bed. Licentiate Thesis 2006. Chalmers University of Technology, Göteborg, Sweden.

[Sánchez 2005] Sánchez M.d.C., Altares P., Pedrosa M.M., Burbano C., Cuadrado C., Goyoaga C., Muzquiz M., Jiménez-Martínez C., Dávila-Ortiz G. Alkaloid variation during germination in different Lupin species. Food Chemistry 90 (2005) 347-355.

[Saxena 1994] Saxena S.C., Jotski C.K. Fluidized-bed incineration of waste materials. Progress in Energy and Combustion Science 20 (1994) 281-324.

[Schäfer 2000] Schäfer S., Bonn B. Hydrolysis of HCN as an important step in nitrogen oxide formation in fluidised combustion. Part 1. Homogeneous reactions. Fuel 79 (2000) 1239-1246.

[Schröder 2004] Schröder E. Experiments on the pyrolysis of large beechwood particles in fixed beds. Journal of Analytical and Applied Pyrolysis 71 (2004) 669-694.

[Secowarwick 2006] www.secowarwick.com/thermal/bulleting/rotaryretort.htm

[SFT 1996] SFT (Statens Forurensningstilsyn) Report. Utslipp ved Håndtering av Kommunalt Avfall. Report Number 96-3318.

[Sharma 2004] Sharma R.K., Chan W.G., Wang J., Waymack B.E., Wooten J.B., Seeman J.I., Hajaligol M.R. On the role of peptides in the pyrolysis of amino acids. Journal of Analytical and Applied Pyrolysis 72 (2004) 153-163.

[Sharma 2006] Sharma R.K., Chan W.G., Hajaligol M.R. Product compositions from pyrolysis of some aliphatic α-amino acids. Journal of Analytical and Applied Pyrolysis 75 (2006) 69-81.

[Silva 1998] Silva M.A, Nebra S.A., Machado Silva M.J., Sanchez C.G. The use of biomass residues in the Brazilian soluble coffee industry. Biomass and Bioenergy 14 (1998) 457-467.

[Simmonds 1972] Simmonds P.G., Medley E.E., Ratcliff M.A.Jr, Shulman G.P. Thermal decomposition of aliphatic monoamino- monocarboxylic acids. Analytical Chemistry 44 (1972) 2060-2066.

[Skreiberg 2004] Skreiberg Ø., Kilpinen P., Glarborg P. Ammonia chemistry below 1400 K under fuel-rich conditions in a flow reactor. Combustion and Flame 136 (2004) 501-518.

[Skreiberg 2004] (P-II) Skreiberg Ø., Becidan M., Hustad J.E., Mitchell R.E. Detailed chemical kinetics modelling of NOx reduction by staged air combustion at moderate temperatures. Proceedings of the Science in Thermal and Chemical Biomass Conversion Conference, 30 August-2 September 2004, Victoria, BC, Canada, vol. 1, pp. 40-54. Edited by A.V. Bridgwater and D.G.B. Boocock. CPL Press, UK, 2006. Peer-reviewed.

[SSB 2006] SSB (Statistisk Sentralbyrå/Statistics Norway) website. www.ssb.no.

[Stenseng 2001] Stenseng M. Pyrolysis and combustion of biomass. Doctoral Dissertation 2001. Technical University of Denmark.

[Stuart 1936] Stuart N.W. Adaptation of the micro-Kjeldahl method for the determination of nitrogen in plant tissues. Plant Physiology 11 (1936) 173-179.

[Sørum 2000] Sørum L. Environmental aspects of municipal solid waste combustion. Doctoral Dissertation 2000. NTNU, Trondheim, Norway.

[Sørum 2001] Sørum L., Grønli M.G., Hustad J.E. Pyrolysis characteristics and kinetics of municipal solid wastes. Fuel 80 (2001) 1217-1227.

[Tan 2000] Tan LL, Li C-Z. Formation of NO_x and SO_x precursors during the pyrolysis of coal and biomass. Part I. Effects of reactor configuration on the determined yields of HCN and NH_3 during pyrolysis. Fuel 79 (2000) 1883-1889.

[Tchobanoglous 2002] Tchobanoglous G., Kreith F. Handbook of solid waste management, Second Edition (2002). McGraw-Hill Handbooks.

[Tian 2005a] Tian F.-J., Wu H., Yu J.-I., Mc Kenzie L.J., Konstantinidis S., Hayashi J.-i. Chiba T., Li C.-Z. Formation of NOx precursors during the pyrolysis of coal and biomass. Part VIII. Effects of pressure on the formation of NH_3 and HCN during the pyrolysis and gasification of Victorian brown coal in steam. Fuel 84 (2005) 2102-2108.

[Tian 2005b] Tian F-J, Yu J-l, Mckenzie LJ, Hayashi J-i, Chiba T, Li C-Z. Formation of NOx precursors during the pyrolysis of coal and biomass. Part VII. Pyrolysis and gasification of cane trash with steam. Fuel 84 (2005) 371-376.

[TN 2006] Thermal Net Newsletter, PyNe/GasNet/CombNet, July 2006, Issue 2.

[US EPA 2006] US Environmental Protection Agency website. www.epa.gov.

[Varian 2006] Varian's documentation.

[Várhegyi 1979] Várhegyi G. Kinetic evaluation of non-isothermal thermoanalytical curves in the case of independent reactions. Thermochimica Acta 28 (1979) 367-376.

[Várhegyi 1989] Várhegyi G., Antal Jr M. J., Székely T., Szabó P. Kinetics of the thermal decomposition of cellulose, hemicellulose and sugar cane bagasse. Energy & Fuels 3 (1989) 329-335.

[Várhegyi 1996] Várhegyi G., Szabó P., Jakab E., Till F., Richard J.-R. Mathematical modelling of char reactivity in Ar-O_2 and CO_2-O_2 mixtures. Energy & Fuels 10 (1996) 1208-1214.

[Várhegyi 1997] Várhegyi G., Antal Jr M. J., Jakab E., Szabó P. Kinetic modelling of biomass pyrolysis. Journal of Analytical and Applied Pyrolysis 42 (1997) 73-87.

[Várhegyi 2002] Várhegyi G., Szabó P., Antal Jr M. J. Kinetics of charcoal devolatilisation. Energy & Fuels 16 (2002) 724-731.

[Voorhees 1994] Voorhees K.J., Zhang W., Hendricker A.D., Murugaverl B. An investigation of the pyrolysis of oligopeptides by Curie-point pyrolysis-tandem mass spectrometry. Journal of Analytical and Applied Pyrolysis 30 (1994) 1-16.

[Vriesman 2000] Vriesman P., Heginuz E., Sjöström K. Biomass gasification in a laboratory-scale AFBG: influence of the location of the feeding point on the fuel-N conversion. Fuel 79 (2000) 1371-1378.

[Werther 2000] Werther J., Saenger M., Hartge E.-U., Ogada T., Siagi Z. Combustion of agricultural residues. Progress in Energy and Combustion Science 26 (2000) 1-27.

[Williams 1996] Williams P.T., Besler S. The influence of temperature and heating rate on the slow pyrolysis of biomass. Renewable Energy 7 (1996) 233-250.

[Wu 2002] Wu C.-H., Chang C.-Y., Tseng C.-H. Pyrolysis products of uncoated printing and writing paper of MSW. Fuel 81 (2002) 719-725.

[Xiang 2003] Xiang Q., Lee Y.Y., Pettersson P.O., Torget R.W. Heterogeneous aspects of acid hydrolysis of α-cellulose. Applied Biochemistry and Biotechnology 105-108 (2003) 505-514.

[Yang 2006] Yang H., Yan R., Chen H., Zheng C., Lee D.H., Liang D. T. In-depth investigation of biomass pyrolysis based on three major components: hemicellulose, cellulose and lignin. Energy & Fuels 20 (2006) 388-393.

[Yeoh 1994] Yeoh H.-H., Wee Y.-C. Leaf protein contents and nitrogen-to-protein conversion factors for 90 plant species. Food Chemistry 49 (1994) 245-250.

[Zabaniotou 1994] Zabaniotou A.A., Gogotsis D., Karabelas A.J. Product composition and kinetics of flash pyrolysis of *Erica arborea* (biomass). Journal of Analytical and Applied Pyrolysis 29 (1994) 73-87.

[Zhu 2006] Zhu P., Sui S., Wang B., Sun K., Sun G. A study of pyrolysis and pyrolysis products of flame-retardant cotton fabrics by DSC, TGA, and PY-GC-MS. Journal of Analytical and Applied Pyrolysis 71 (2004) 645-655.

Appendix

Biomass and waste composition table

Sample	Proximate analysis (wt%)				Ultimate analysis (wt%)						HHV MJ/kg	Reference
	VM	FC	Ash	Moisture	C	H	O	N	S/Cl	Ash		
PAPER												
Cardboard					39.5	5.8	44.3	0.2	0.3			Fuel 81 (2002) 2277-2288
Newspaper	88.5	10.5	1.0		52.1	5.9	41.86	0.11	0.03		19.3	Fuel 80 (2001) 1217-1227
Cardboard	84.7	6.9	8.4		48.6	6.2	44.96	0.11	0.13		16.9	Fuel 80 (2001) 1217-1227
Recycled paper	73.6	6.2	20.2								13.6	Fuel 80 (2001) 1217-1227
Glossy paper	67.3	4.7	28.0		45.6	4.8	49.41	0.14	0.05		10.4	Fuel 80 (2001) 1217-1227
Juice carton	86.0	6.1	7.9								24.4	Fuel 80 (2001) 1217-1227
Coated paper			27.7	0.9	30.5	4.6	37.7	2.9	1.5/1.5		12.2	Fuel 76 (1997) 1151-1157
Paper and card	76-81	8-12	2-5	5-10							15.7-18.6	www.capenhurst.com
Cartons	90.9	4.5	1.2	3.4							16.4	www.capenhurst.com
Newspaper	85.9	10.7	3.5		44.7	5.8	49.4	0.1	<0.02			This study
Glossy paper	70.6	4.5	24.8		31.5	4.0	64.4	0.08	<0.02			This study
BIOMASS												
Pine branch big					47.87	6.23	45.64	0.08	0.17			Biomass and Bioenergy 27 (2004) 385-391
Pine branch small					45.42	6.81	47.42	0.24	0.10			Biomass and Bioenergy 27 (2004) 385-391
Needles					46.93	6.74	44.65	1.47	0.37			“
Mbuni husks	64.6	20.0	4.1	11.4	43.9	4.8	49.6	1.6	0.1		16.1	Renewable Energy 23 (2001) 103-121
Parchment husks	72.0	17.0	0.9	10.1	46.8	4.9	47.1	0.6	0.6		18.2	Renewable Energy 23 (2001) 103-121
Palm fibre	46.3	12.0	5.3	36.4	51.5	6.6	40.1	1.5	0.3			“
Wood chips	82		0.5	40.8	50.6	6.3	43	0.14				Fuel 78 (1999) 1065-1072
Pinewood			0.3		50.7	6.3		0.15	0.02			Fuel 82 (2003) 1591-1604
Wood chip	81.13	8.52	3.86	6.49	48.9	10.61	40.13	0.21	0.15			Fuel Process. Technol. 84 (2003) 13-21
Rice husk	55.12	19.37	18.87	6.64	45.2	15.6	38.91	0.2	0.09			“
Sawdust			0.73	15.9	45.1	6.66	47.3	0.19	0.02			Applied Energy 74 (2003) 383
Manure	40.4	10.5	42.3	6.8	23.9	3.57	20.3	2.30	0.90		9.65	Fuel 82 (2003) 1183-1193
Manure dry	50.2		40.4		29.6	3.35	23.30	2.55	0.81		13.4	Fuel 82 (2003) 1167-1182
Olive cake	68.82	15.64	9.01	6.53	46.80	6.07	36.69	0.68	0.12	9.64	19.81	Fuel 83 (2004) 859-867

Sample	Proximate analysis (wt%)				Ultimate analysis (wt%)						HHV MJ/kg	Reference
	VM	FC	Ash	Moisture	C	H	O	N	S/Cl	Ash		
Hazelnutt shell	76.3	21.2	1.5		52.8	5.6	42.6	1.4	0.04			Prog. Energy Comb. Sci. 30 (2004) 219-230
Sawdust	82.2	15.0	2.8		46.9	5.2	37.8	0.1	0.04			“
Corn stover	84.0	10.9	5.1		42.5	5.0	42.6	0.8	0.2			“
Poplar		16.4	1.3		18.4	5.9	39.6	0.4	0.01			“
Rice husk	61.0	16.7	22.6		47.8	5.1	38.9	0.1	-			“
Cotton gin					42.8	5.4	35.0	1.4	0.5			“
Sugarcane bag.		15.0	11.3		44.8	5.4	39.6	0.4	0.01			“
Peach pit		19.9	1.0		53.0	5.9	39.1	0.3	0.05			“
Alfafa stalk	76.1	17.4	6.5		45.4	5.8	36.5	2.1	0.09			“
Switchgrass	76.7	14.4	8.9		46.7	5.9	37.4	0.8	0.19			“
Red oak wood					50.0	6.0	42.4	0.3	-/-			“
Wheat straw	66.3	21.4	13.7		41.8	5.5	35.5	0.7	-/1.5			“
Olive husk	77.5	18.4	4.1		49.9	6.2	42.0	1.6	0.05/0.2			“
Beech wood	82.5	17.0	0.5		49.5	6.2	41.2	0.4	--			“
Spruce wood	80.2	18.1	1.7		51.9	6.1	40.9	0.3	--			“
Corncob	87.4	11.5	1.1		49.0	5.4	44.5	0.5	0.2/-			“
Tea waste	85.5	13.0	1.5		48.0	5.5	44.0	0.5	0.06/0.1			“
Walnut shell	59.3	37.9	2.8		53.5	6.6	45,4	1.5	0.1/0.1			“
Almond shell	74.0	22.7	3.3		47.8	6.0	41.5	1.1	0.06/0.01			“
Sunflower shell	76.2	19.8	4.0		47.4	5.8	41.3	1.4	0.05/0.1			“
Beech wood bark	65.0	29.3	5.7									“
Oak wood	77.6	21.9	0.5									“
Colza seed	78.1	15.4	6.5									“
Cotton refuse	81.0	12.4	6.6									“
Olive refuse	66.1	24.7	9.2									“
Sunflower shell	76.4	12.2	3.3	8.1							16.21 GCV	Energy Conversion and Management 44 (2003) 155
Colza seed	70.0	15.8	5.8	8.4							19.38	“
Pine cone	69.0	20.9	0.7	9.4							18.65	“
Cotton refuse	75.8	12.3	6.5	5.4							18.83	“

Sample	Proximate analysis (wt%)				Ultimate analysis (wt%)						HHV MJ/kg	Reference
	VM	FC	Ash	Moisture	C	H	O	N	S/Cl	Ash		
Olive refuse	56.0	8.1	20.3	15.6							15.77	“
Peat slightly dec					48-53	5-6.1	40-46	.5-1	0.1-0.2			Fuel Process. Technol. 43 (1995) 1
Peat highly dec.					56-58	5.5-6	34-39	.8-1	0.1-0.3			“
BSG Ca Mg												Biological Wastes 34 (1990) 335
Beech wood					49.5	6.3	44.0	0.149	0.018	0.5		Energy Fuels 19 (2005) 1631-43
Waste wood					50.0	6.3	42.0	1.50	0.089	3.1		“
Fibreboard					48.6	6.3	41.6	3.50	0.034	1.2		“
Carinata					48.2	6.3	44.0	1.12	0.322	5.2		“
Rape					49.3	6.4	44.0	0.328	0.060	3.1		“
Cane trash					49.5	6.1	44.0	0.31	0.08			Fuel 84 (2005) 371-376
Bagasse	82.4		9.7		47.6	5.5	46.3	0.31	0.28			Fuel 79 (2000) 1883-1889
S peat	70.6		3.7		50.7	5.8		1.4	0.12			Fuel 74 (1995) 1363-1368
C peat	71.1		2.8		54.2	6.0		2.8	0.19			“
Pine bark	69.4		1.2		53.8	5.7		0.4	0.02			“
Birch bark	83.6		2.2		61.6	8.4	28.9	0.52	<0.1			Combust. Flame 95 (1993) 22-30
Fir bark	73.1		3.3		54.1	6.1	39.0	0.53	<0.1			“
Pine bark	70.5		2.2		56.4	5.8	37.5	0.25	<0.1			“
Miscanthus					48.4	6.0	41.5	0.68		2.7		Fuel 79 (2000) 1371-1378
Fir bark	73.1	26.9	3.5		54	6.1	40	0.5				Fuel 75 (1996) 1377-1386
Sod peat	71.1				57.2	5.8	35.5	1.5	0.15		21.8	Fuel Process. Technol. 29 (1991) 43
O. tobacco					50.35	6.28	45.53	2.78	0.60			Fuel 80 (2001) 1765-1786
Bright tobacco					51.09	6.36	43.38	3.09	0.69			“
Burley tobacco					45.03	6.06	42.94	5.22	0.76			“
Sunflower husk	69.1	19.9	1.9	9.1	51.4	5.0	43.0	0.6	0.0			Prog. Energy Comb. Sci. 26 (2000) 1-27
Cotton husk	73.0	16.9	3.2	6.9	50.4	8.4	39.8	1.4	0.0			“
Mustard husk	68.6	22.0	3.9	5.6	46.1	9.2	44.7	0.4	0.2			“
Palm fibre	46.3	12.0	5.3	36.4	51.5	6.6	40.1	1.5	0.3			“
Pepper waste	58.4	24.4	7.4	9.7	45.7	3.2	47.0	3.4	0.6			“

Sample	Proximate analysis (wt%)				Ultimate analysis (wt%)						HHV MJ/kg	Reference
	VM	FC	Ash	Moisture	C	H	O	N	S/Cl	Ash		
Soya husk	69.6	19.0	5.1	6.3	45.4	6.7	46.9	0.9	0.1			“
Groundnut shell	68.1	20.9	3.1	7.9	50.9	7.5	40.4	1.2	0.02			“
Coconut shell	70.5	22	3.1	4.4	51.2	5.6	43.1	0.0	0.1			“
Malt waste	67.4	15.5	6.0	11.1	47.98	6.64	40.01	4.99	0.38			Bioresour. Technol.
Straw	65.4	19.7	6.8	8.1	49.04	5.65	44.82	0.43	0.06			70 (1999) 39-49
Alder wood	82.3	14.0	0.3	3.4	49.95	5.72	44.02	0.26	0.05			“
Cottonseed cake	78.7	10.3	4.9	6.1	52.0	5.9	40.8	1.3				Renewable energy 24 (2001) 615
Rice husk	51.98	25.1	16.92	6	37.6	4.89	32.61	1.888				Fuel Process. Technol. 85 (2004) 1273
Erica arborea					51.0	6.2	41.9	1.0		0.6	20.6	J. Anal. Appl. Pyrolysis 29 (1994) 73-87
C. cardunculus L	77.3	14.3	8.4		46.7	4.8	47.7	0.7	0.1		18.2	Fuel Process. Technol. 68 (2000) 209
Grape bagasse	64.8	27.1	8.1		47.6	5.6		1.6			17.2	Biomass & Bioenergy
Olive bagasse	77.7	20.2	2.1		51.5	6.0		1.0			18.2	11 (1996) 397
Cherry stones	73.9	25.9	0.2		51.08	6.49	42.03	0.38	0.02		22.5	J. Anal. Appl. Pyrolysis 67 (2003) 165-190
Wood chips					46.4	5.9		0.085	0			Ind. Eng. Chem. Res.
Wheat straw					43.6	6.2		0.30	0.08			38 (1999) 2216-2224
Olive husks					50.9	6.3		1.37	0.03			“
Grape residues					47.9	6.2		2.11	0.09			“
Rice husks					40.3	5.7		0.30	0.03			“
Whey					50.9	6.8	22.26	14.7	1.24			K-M Hansson’s thesis (2003)
Shea					49.3	5.1	36.64	2.7	0.26			Chalmers, Sweden
Bark					53.2	6.0	37.08	0.39	0.03			“
Grass	18.7	4.5	1.6	75.2							4.8	www.capenhurst.com
Wood	67.9	11.3	0.8	20							19.6	“
Wood					47.6	6.4	45.3	0.2	0.2			Fuel 81 (2002) 2277-2288
Spruce	89.6	10.2	0.2		47.4	6.3	46.2	0.07			19.3	Fuel 80 (2001) 1217-1227
Green coffee	81.2	14.9	3.9		52.24	7.73	37.14	2.79	0.1			This study
-	-	-	-		-	--	-	-	-		-	-

Sample	Proximate analysis (wt%)				Ultimate analysis (wt%)						HHV MJ/kg	Reference
	VM	FC	Ash	Moisture	C	H	O	N	S/Cl	Ash		
FOOD												
Wheat 2000					49.1	6.5	43.6	0.634	0.202	5.1		Energy & Fuels
Wheat 2001					48.8	6.4	44.3	0.394	0.076	4.2		19 (2005) 1631-1643
Linseed seed	77.0	10.7	5.6	6.7	61.0	8.5	28.2	2.3				J. Anal. Appl. Pyrolysis 71 (2004) 417-429
Rape seed	81.7	7.9	5.5	4.9	62.1	9.1	24.9	3.9				J. Anal. Appl. Pyrolysis 58-59 (2001) 995
Rape-seed					56.0	8.2		3.4	-/0.01			Bioresour. Technol. 66 (1998) 113
Pea					45.1	6.4	41.54	4.2	0.16			K-M Hansson's thesis (2003)
Soya					51.8	7.2	29.16	6.5	0.34			Chalmers, Sweden
Food waste	17.1	3.5	1.1	78.3							4.2	www.capenhurst.com
Fried fats	97.6	2.4	0.0	0.0							38.3	"
Bone meal A	58.20	11.40	25.90	4.50	52.68	6.78	27.03	11.08	0.34/0.55		18.03	SINTEF report (confidential)
Bone meal B					51.28	7.97	30.63	9.52	0.61/-		19.56	Project number 844027.00
Fat					76.23	12.12	11.55	0.00	0.025/0.019		39.56	"
Soy protein	84.3	11.7	4.0		52.24	7.43	25.04	14.73	0.56			This study
PLASTICS												
PUF	88.2 d	11.5 d	0.3 d	1.8 rec.	63.2 d	6.7 d	13.5 d	6.6 d	0.01/9.6 d		27MJ/kg dry LH	Zevenhoven et al., presented at the 39th IEA FBC meeting, 1999
PA6/PE	99.8	<0.2	0.1	0.8	79.7	13.3	4.2	2.6	<0.01/<0.01		39.5	"
Polyethylene	100	0	0	1.1	85.7	13.9	0	0	0			Fuel 78 (1999) 301-307
PET					62	4.2	33.2	0.1	0.3			Fuel 81 (2002) 2277-2288
Polyamide					62.4	9.8	15.7	12	0.1			"
Polystyrene	99	1	0		92	8	0	0	0.04		44.5	Fuel 77 (1998) 183-196
Polyethylene	100	0	0		86	14	0	0	0		40.5	"
Polypropylene	100	0	0		86	14	0	0	0		43.4	"
PMMA	100	0	0		60	8	32	0	0		25.8	"
PVC	91	9	1		38	5	0	0	0/57		19.2	"
HDPE	100	0	0		86.1	13.0	0.90				46.4	Fuel 80 (2001) 1217-1227
LDPE	100	0	0		85.7	14.2	0.05	0.05	0		46.6	"
PVC	94.8	4.8	0.4		41.4	5.3	5.83	0.04	0.03/47.7		22.8	"
NILAMID					63.1	9.8	15.0	12.1				J. Anal. Appl. Pyrolysis 55 (2000) 255-268

Sample	Proximate analysis (wt%)				Ultimate analysis (wt%)						HHV MJ/kg	Reference
	VM	FC	Ash	Moisture	C	H	O	N	S/Cl	Ash		
OTHER												
Waste tire	67.3	28.5	3.7	0.5	83.8	7.6	3.1	0.4	1.4	3.7	8500kcal/kg	Energy 19 (1994) 845-854
UF glue	87.4	12.6	0.1	32.8	32.5	5.8	24.1	37.4	0.01/<0.01		13.4	Zevenhoven et al., presented at the 39th IEA FBC meeting, 1999
Scrape tyre	61.9	29.5	8.0	0.7	86.7	8.1	1.3	0.4	1.4	2.1	36.2	J. Anal. Appl. Pyrolysis 58-59 (2001) 667-683
Tire	52.3	21.7	13.7		71.9	4.7	7.0	1.36	1.36		29.2	Fuel 77 (1998) 183-196
Electronic packaging					15.95	1.98	1.68	0.17		80.2		J. Hazard. Mater. 103 (2003) 107
Polybutadiene rubber			0.08		88.72	11.17	<0.1	0	2.04/0.36		45.7	J. Hazard. Mater. 58 (1998) 227
Styr-butene rubber			0.15		87.58	10.41	0.84	0	1.91/0.27		43.4	"
Vacuum cleaner dirt	55.7	8.5	30.3	5.5							14.8	www.capenhurst.com
Leather	75.3	11.8	12.9		53.01	7.74	27.75	9.94	1.56			This study
MSW												
RDF	73.4	8.9	17.7	3.2	48.4	7.0	25.2	0.84	0.12/1.0		19.1	Zevenhoven et al., presented at the 39th IEA FBC meeting, 1999
MSW Thai db				(58.40)	37.14	5.41	24.93	0.22	0.09/0.8	32.2	6.5/15.6 dry	Energy Conversion and Management 43 (2002) 2329
MSW UK db	63	4	32.2	(32.43)	35.81	4.82	24.43	0.78	0.41/0.75	33.0	10.3/15.2 d	"
MSW K-L	31.36	4.37	9.26	55.01	46.11	6.86	28.12	0.23		17.1		"
MSW					52	8	38	0.5	0.3			Fuel 81 (2002) 2277-2288
RDF-A	76.2	13.6	10.2	3.7	46.6	6.8	34.51	1.28	0.13/1.08		20.64	Waste management
RDF-B	72.5	3.9	12.5	11.1	41.7	5	36.3	0.75	0.17/1+ Ca		18.39	20 (2000) 443-447
Typical MSW				25	25	3	20	0.5	0.2/0.2-0.6	25	1.1 J/g	Prog. Energy Comb. Sci. 24 (1998) 545
MSW				15/35	15/30	2/5	12/24	.2/1	.02-.1	15/25	7-14	Heat. Rec. Syst. & CHP 9 (1989) 115
MSW					42.4	6.1	35.1	2.2	0.24/0.5		17.2	SINTEF report (confidential) Project number 844027.00
MSW			6.9	19.2	35	11.7	30.2	?	1.9/0.25			[Tchobanoglous 2002]

Paper I

An experimental study of nitrogen species release during municipal solid waste (MSW) and biomass pyrolysis and combustion.

Becidan M., Skreiberg Ø., Hustad J.E.

Proceedings of the Science in Thermal and Chemical Biomass Conversion Conference, 30 August-2 September 2004, Victoria, BC, Canada, vol. 2, pp. 1443-1455. Edited by A.V. Bridgwater and D.G.B. Boocock. CPL Press, UK, 2006. Peer-reviewed.

An experimental study of nitrogen species release during municipal solid waste (MSW) and biomass pyrolysis and combustion

Michaël Becidan, Øyvind Skreiberg and Johan E. Hustad
Norwegian University of Science and Technology
Department of Energy and Process Engineering
N-7491 Trondheim, Norway

ABSTRACT: In this paper an experimental set-up and preliminary experimental results are presented. The set-up is composed of a fixed bed reactor with heaters, a quartz-made probe and a FTIR analyser. The release rate of CO, CO_2, NO, NO_2 and N_2O has been measured during combustion of MSW fractions and biomass species; the release rate of NH_3 and HCN has been studied during pyrolysis of sewage sludge. The parameters studied in this paper are final reactor temperature and fuel nitrogen content (fuel type). The main results from this study are: the higher the fuel-N content, the lower the N-conversion to NO_x and N_2O during combustion; NH_3 is the main N-containing pyrolysis product at all temperatures; conversion of fuel-N to NH_3 and HCN increases with increasing temperature; and, the NH_3/HCN ratio increases with decreasing temperature.

INTRODUCTION

Combustion, eventually with energy recovery, is one of the MSW conversion methods very common today. However, combustion leads to harmful emissions, NO_x involved in the formation of photochemical smog and acid rain being one of them. A detailed knowledge of the release rate of nitrogen species from MSW fractions and various biomass species during pyrolysis is important in connection with improved strategies for NOx emission reduction. MSW management is an increasing challenge as waste production per inhabitant is steadily growing all over the world. However, greater ecological awareness amongst the population has led to implementation of complex waste management systems by the authorities in many countries. One of the most important features of those systems is the separate collection of reusable waste, i.e. glass, paper, cardboard and textiles, and dangerous toxic waste. The remaining combustible waste is most often combusted. The main advantages of this technique are [1]:

1) The reduction of 70-75% of the mass of the waste.
2) The reduction of 90% of the volume of the waste.
3) A sustainable alternative to fossil fuels as a source of energy.

However, combustion will produce a variety of gaseous emissions that can have a negative impact on our environment (water, air and soil) if not avoided in the combustion process (by primary measures) or cleaned by secondary measures. Together with dioxins, heavy metals, chlorine compounds and carbon dioxide, N-containing compounds (NO, NO_2 and N_2O) are amongst the most harmful emissions from waste combustion as they are involved in:

1) The generation of ground-level ozone (O_3). This ozone has a noxious effect on the human respiratory system and the ecosystem development.
2) The formation of acid rain that damage forests and also human and animal health.
3) The depletion of Earth's protective ozone layer. N_2O is a key intermediate in the ozone destruction cycle in the stratosphere. This ozone is protecting the Earth from aggressive UV solar radiation.
4) The increase in the greenhouse effect known as global warming. N_2O is a very powerful greenhouse gas as it is about 310 times more powerful than carbon dioxide on a per molecule basis [2].

The requirements for waste combustion NOx emissions control have become stricter recently; the European Union Standard emissions limit (EU directive 2000/76/EC) was 500 mg/Nm^3 (at 11% O_2, dry flue gas, 24 hour average) in 1986 and is now 200 mg/Nm^3 (at 11% O_2, dry flue gas, 24 hour average). This waste combustion emissions directive is more draconian than for any other fuel like natural gas, oils and virgin biomass. To control and reduce efficiently NOx (NO and NO_2) and N_2O emissions, it is primordial to understand the mechanisms leading to their formation and the parameters influencing their yields.

Numerous studies have been carried out to study nitrogen release during pyrolysis and combustion of waste fractions, biomass or model compounds under various conditions. A brief review of the studies relevant in nitrogen release during combustion or pyrolysis of waste fractions and biomass under fixed-bed/grate conditions will be presented.

LITERATURE REVIEW

For the combustion conditions studied (low temperature (i.e. 600-900°C), waste fractions and biomass combustion) NOx is almost exclusively formed through the fuel-NOx mechanism [3]. Nitrogen contained in the fuel is primarily released during pyrolysis as NH_3 and HCN. NH_3 and HCN may then be oxidised to NO, NO_2, N_2O and N_2 through a number of reaction paths. A simplified description of this mechanism is shown in Fig. 1, which also includes NO and N_2 formation from the char fraction of a solid fuel. Several theoretical studies [4] show that the main oxidation routes of NH_3 lead to NO and N_2 while HCN is the main precursor for N_2O. The operating parameters having an influence on N-release are: pyrolysis temperature, excess air ratio, heating rate, fuel-N content, nitrogen functionality and residence time in the pyrolysis/combustion zone in addition to pressure.

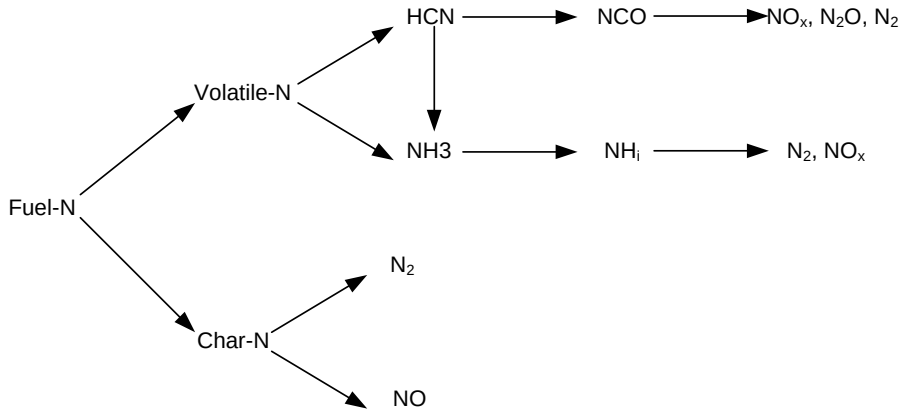

Fig.1 The fuel-N mechanism (simplified).

The experimental data from literature concerning NH_3 and HCN level, and NH_3/HCN ratio, in the pyrolysis gases are quite diverse. NH_3 is often reported [5, 6, 7] to be the main N-containing component in the pyrolysis gas. However in other studies [8, 9, 10] HCN appears to be released in equal amounts as NH_3 or even to be the main N-compound in the pyrolysis gas.

The main parameters controlling the composition of pyrolysis gas are temperature and heating rate. They not only have a significant effect on the yield of NH_3 and HCN but also on the NH_3/HCN ratio. An increase in heating rate will induce a higher yield of release of both NH_3 and HCN [9, 11]. Higher temperatures will lead to increasing levels of HCN [10, 12] while reports on the NH_3 behaviour seem to vary: NH_3 release is reported to be insensitive to temperature changes [13] but a decrease is sometimes reported with increasing temperature [12]. This observed different thermal behaviour may be explained by the nitrogen functionality in the fuel: HCN is mainly originating from pyridine and pyrrole (cyclic compounds) while NH_3 is released from proteins and amino acids (non-cyclic compounds); those different chemical compounds are known to have different thermal behaviour [14]. Consequently the NH_3/HCN ratio will also vary with the thermal history of the fuel. Low heating rate will promote NH_3 formation while HCN will be predominant when the heating rate is high [11, 12]. The effect of temperature is also significant: it has been reported decreasing NH_3/HCN ratio with increasing pyrolysis temperature [12]. It seems that NH_3/HCN ratio is a function of H/N ratio: it has been observed for a variety of fuels that an increasing H/N ratio in the fuel increases the NH_3/HCN ratio [12]. This phenomenon has been explained so [15]: HCN is the primary product and NH_3 is originating from two sources, the direct evolution from the fuel-N and the secondary conversion from evolved HCN (primary HCN that has reacted with the fuel-H to give NH_3). Furthermore the importance of HNCO in the pyrolysis gas has recently been demonstrated in an experimental study of model compounds of biomass fractions [14].

Final N-compounds from combustion are NO_x (NO and NO_2), N_2O and N_2. The most important factors controlling NOx formation are excess air ratio and temperature [16]. NOx emissions increase with increasing excess air ratio [1, 4, 16, 17] and increasing temperature [1, 3, 4, 6]. However, NOx is sometimes reported to show a

maximum value with temperature [12, 16]. A higher O_2 concentration will also promote NOx formation. On the other hand, higher fuel-N will usually result in lower fuel-N conversion to NO_x [18]. This decrease indicate that the presence of other N-compounds act to reduce NO_x as in the Selective Non Catalytic Reduction where ammonia reacts with NO to give N_2, although this phenomenon is not always observed experimentally [19].

The emissions of N_2O are predominantly very low in biomass combustion applications, e.g. wood stoves [20]. The main factor influencing N_2O emissions is temperature as N_2O is destroyed at high temperature [12].

EXPERIMENTAL SET-UP AND PROCEDURES

TEST FUELS

In this study glossy paper, birch wood and sewage sludge pellets were selected as fuels. The elemental analysis of these materials is presented in Table 1.

The glossy paper was taken from the same issue of a magazine. The paper was cut as a 4 cm by 4 cm square.

Wood samples were taken from a single plank to ensure a N-content as stable as possible. Pieces of 4 by 4 by 7 cm were used.

Sewage sludge pellets is produced from communal and small industries sewage sludge, pre-processed by drying and pelletised into a cylinder-like shape, even though the distribution in sizes is quite wide and the shapes diverse and irregular.

Table 1. Ultimate analysis of the fuels (dry ash free basis) and the ash content (dry basis), performed at Vienna University of Technology (Institut für Physikalische Chemie – Mikroanalytisches Laboratorium) and the moisture content of the fuels.

	Birch wood	Glossy paper [b]	Sewage sludge
C (wt%)	48.57	45.60	49.18
H (wt%)	6.31	4.80	8.46
N (wt%)	0.114	0.070	5.47
S (wt%)	<0.02	<0.05	1.31
O [a] (wt%)	44.99	49.48	35.38
Cl (wt%)	n.m.	n.m.	<0.10
Ash (wt%)	n.m.	28.0	46.7
Moisture (wt%)	13.1	8.0	22.0

[a] Oxygen is calculated by difference
[b] From [3]
n.m.: not measured

APPARATUS AND PROCEDURE

A schematic diagram of the reactor is shown in Fig. 2. The experimental set-up is presented in Fig. 3. The reactor is made of a stainless tube with a lining of Al_2O_3 ceramic to prevent catalytic reactions. The inner dimensions of the tube are a height of 1000 mm and a diameter of 100 mm. The reactor body is placed inside an electric heating furnace constituting of 5 independent heating zones. The air (or any other gases/mixtures of gases) is introduced into the reactor from the bottom through a grid distribution plate. The inlet gas can be preheated. The maximum operative temperature of the reactor and its pre-heater is 900°C.

Five thermocouples positioned in the middle of each heating zone are recording the temperature profile along the wall of the reactor. The temperature of the inlet gas is also recorded.

The sample can be placed on the grid plate or in a small basket (with a diameter of 65 mm and a length of 130 mm) made of an inconel alloy netting. This basket is hanging below a precision balance (Sartorius Competence-CP Series) to record mass loss during the experiment ("macro-TGA"). A pressurised-air elevator moves the system "balance-reactor top-basket" upwards and downwards.

Two types of experiments were carried out: "flash" experiments (or fast heating rate) and slow heating rate (from 7.5 to 15 K/min) experiments (not presented in this paper). During the "flash" experiments, the reactor and the gas stream were heated to the set temperature before the rapid introduction of the sample from the top with the elevator.

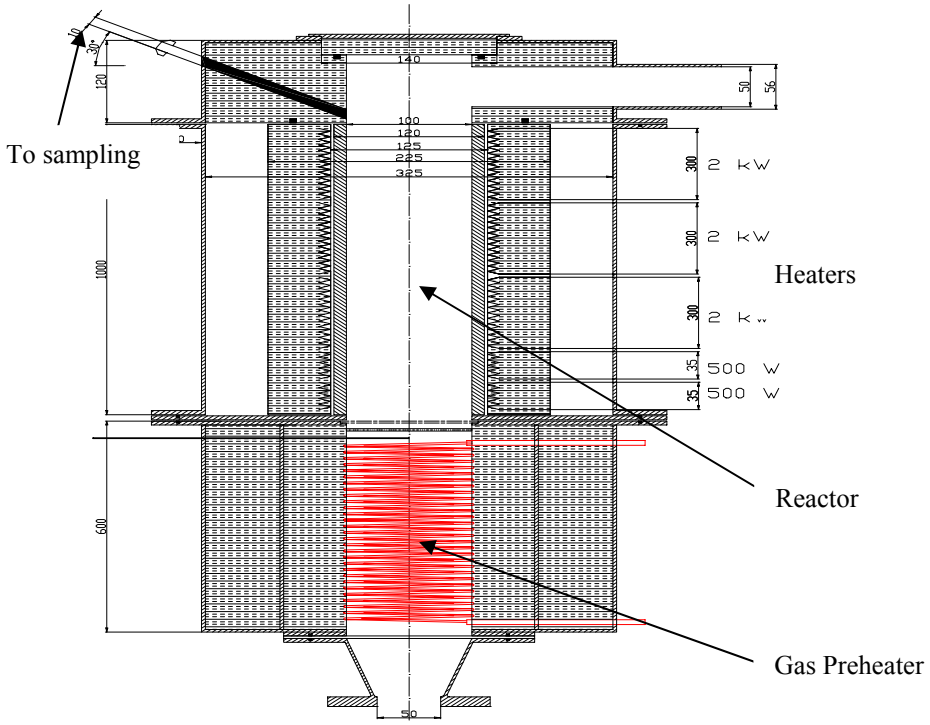

Fig. 2 The reactor, with heaters (dimensions in mm).

MEASUREMENTS AND CHEMICAL ANALYSIS

Only a slipstream of the volatiles is analysed (Fig. 3). After passing through a quartz glass pipe, the heavy tar compounds present in the volatiles are removed by using a tar trap constituted of a 3-extraction bottle system (one filled with glass spheres, one empty and one filled with fine glass wool). The exhaust gases are then filtered through a heated metal filter (SP 210-H from M&C). A part of the gas is then dried by passing through a U-tube containing silica gel before going to an online O_2 analyser (Servomex Oxygen Analyser 570 A). The rest of the sampled flue gases is being injected through a heated Teflon line (176°C) into the heated cell (176°C, path length of 6.4 m, DTGS detector, resolution of $1cm^{-1}$) of an FTIR spectrometer (BOMEM Model 9100). The levels of CO, CO_2, NO, NO_2 and N_2O has been measured during the combustion experiments; the release rate of NH_3 and HCN was studied during pyrolysis experiments. Analyses results were logged every minute approximately (56-59 seconds). To reach the best accuracy 12 scans are performed, each taking 4.5 to 5 seconds.

Absolute yields of compounds were calculated from their concentrations and the total gas flow.

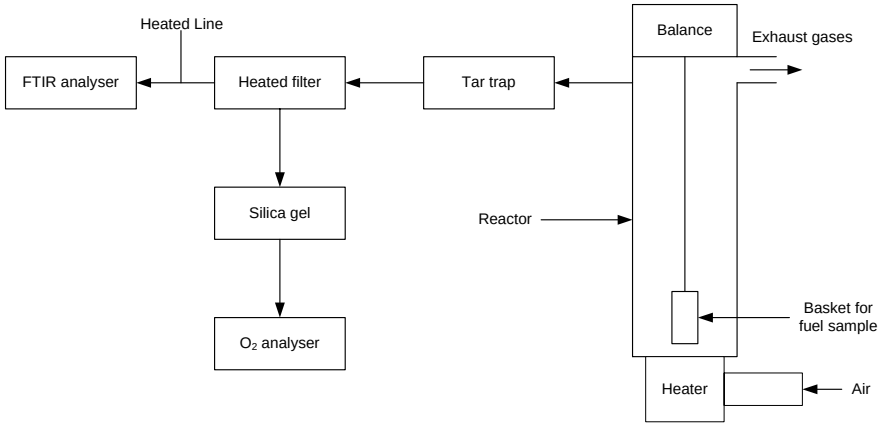

Fig. 3 The experimental set-up.

EXPERIMENTAL RESULTS

This section present preliminary experimental results and is intended to illustrate the possibilities and limitations of the experimental set-up.

TEMPERATURE HISTORY DURING COMBUSTION

Temperature measurements were performed by six sets of two diametrically opposed thermocouples at the wall of the reactor, and not directly at the sample surface where the flame temperature may be significantly higher.

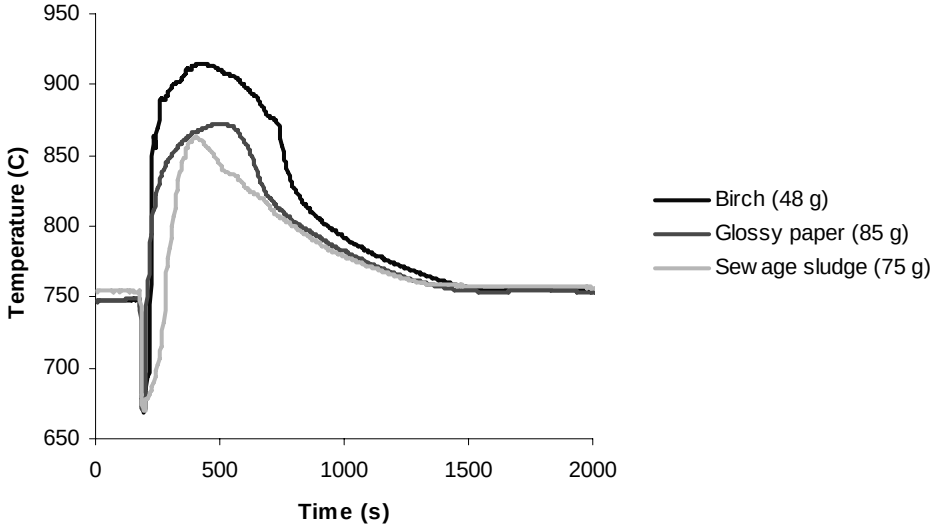

Fig. 4 Temperature history (average wall temperature) during combustion for the set of two opposing thermocouples located closest to the sample.

After an initial decrease in temperature of 70-80°C due to the introduction of the fuel (and the basket), a rapid augmentation corresponding to the ignition can be observed. The characteristics of the profile will depend on the fuel at otherwise equal initial conditions.

Temperature profiles measured at combustion conditions for three fuels at an initial reactor temperature of 750°C are presented in Fig. 4. The time necessary to reach the peak temperature (from the lowest temperature) is respectively 210 seconds for sewage sludge pellets, 225 seconds for birch and 290 seconds for glossy paper.

The wall temperature approaches its initial value of 750°C after 21 to 22 minutes for all fuels studied.

MACRO-TGA

The experimental set-up allows the reactor to be used as a macro-TGA (Thermo Gravimetric Analyser) with a sample mass of up to 150 grams, with simultaneous gas analysis.

The mass loss profile for a given fuel depends on the temperature and the heating rate. Figs. 5, 6 and 7 present selected results.

Combustion

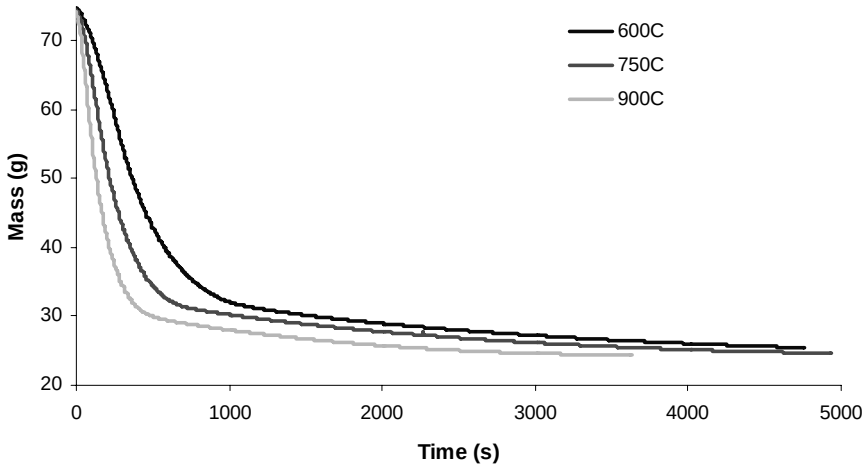

Fig. 5 Mass loss curves for sewage sludge pellets (75 g) at three temperatures.

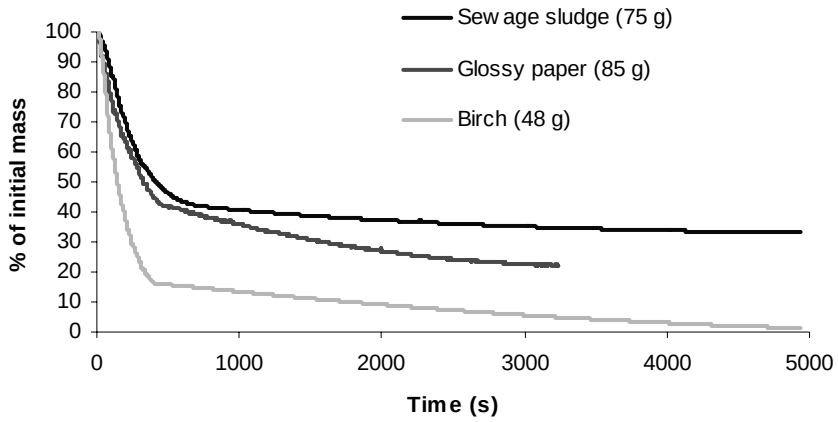

Fig. 6 Mass loss curves for the three fuels at 750°C (initial reactor temperature, the corresponding temperature profiles are shown in Figure 4).

Pyrolysis

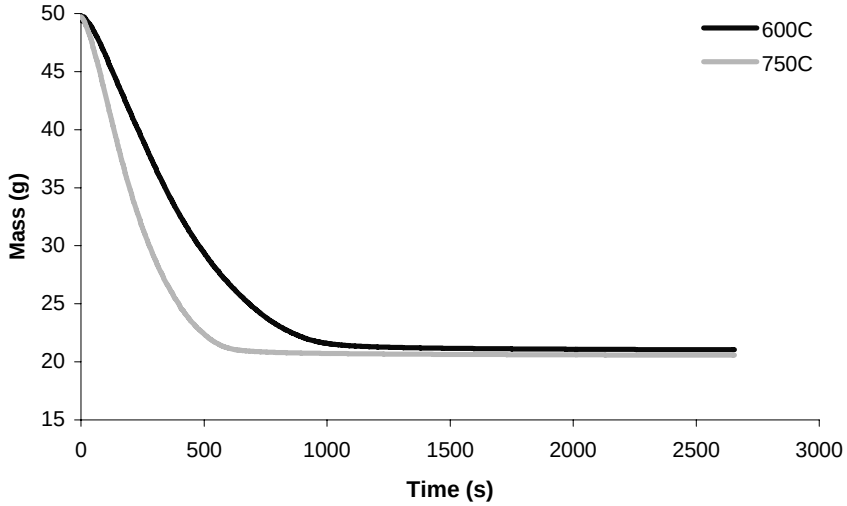

Fig. 7 Mass loss curves for sewage sludge pellets pyrolysis at two initial reactor temperatures.

At both combustion and pyrolysis conditions an increase in temperature will promote a higher mass loss rate, as shown in Figs. 5 and 7. The temperature also, to a small degree, influences the amount of char remaining in the basket in the pyrolysis experiments, with increasing char fraction with decreasing temperature.

Every fuel has a unique mass loss profile under given conditions because of its unique physical properties (particle size, particle shape, density, porosity, specific area, ignition temperature) and chemical properties (elemental composition, heating value, moisture content, volatile fraction, fixed carbon fraction and ash amount and composition). The samples studied are rather large particles where a substantial temperature gradient may occur inside the particle during heating and conversion. At these conditions the mass loss rate is mainly controlled by heat and mass transfer. This study is therefore relevant for grate/fixed bed combustion/pyrolysis of waste and biomass as those fuels are rarely used in the form of very small particles having no heat and mass transfer limitations.

During pyrolysis, the fuel will undergo different processes. First, the water present in the fuel is evaporated, afterwards the temperature of the surface of the fuel will reach a critical value where thermal decomposition will start and propagate inside the particle. This will induce release of volatiles and formation of char. The structural changes of the fuel result in an increase of porosity, increase of specific surface area, decrease of bulk density and modification of the chemical composition. The proportion and the composition of the volatiles are typically used to characterise the pyrolysis process. The reactor can be used to test and develop models for drying and pyrolysis of large biomass particles in grate/fixed bed combustion.

To analyse the mass loss rate both for combustion and pyrolysis, t_{50} (the time in seconds for conversion of 50% of the dry ash free fraction of the fuel) has been calculated. The results, presented in Table 2, show that increasing temperature will

increase the mass loss rate at both combustion and pyrolysis conditions as mentioned earlier; furthermore the mass loss rate of pyrolysis and combustion of sewage sludge pellets are rather close at the same temperature, while for glossy paper, combustion has a mass loss rate nearly 1.9 times higher than for the pyrolysis experiments at the same temperature.

Table 2. Time (s) for 50% mass conversion, t_{50} (P: pyrolysis, CB: combustion). No data available at pyrolysis conditions at 900°C.

	CB 600°C	P 600°C	CB 750°C	P 750°C	CB 900°C
Glossy paper	280	n.a.	215	395	n.a.
Sewage sludge	365	385	220	220	135
Birch	n.a.	n.a.	145	n.a.	n.a.

n.a.: not available

GASEOUS EMISSIONS

Gaseous emissions were measured with an FTIR analyser (Bomem 9100) that was calibrated for the measurements of waste combustion emissions by the manufacturer. However the built-in calibrations could not be used for the study of pyrolysis because of interferences by typical pyrolysis compounds in the IR region. Therefore, calibration curves were made to quantify NH_3 and HCN. The wave number ranges selected for NH_3 quantification were 1142.26-1138.88 cm^{-1} and 1124.30-1120.00 cm^{-1} while HCN quantification was performed at 3374.70-3372.29 cm^{-1}. At these wave numbers no major interference from other gas species occurred in the sewage sludge pellets experiments, due to the high N-content. An IR-spectrum from the pyrolysis at 600°C using sewage sludge pellets is presented in Fig. 8.

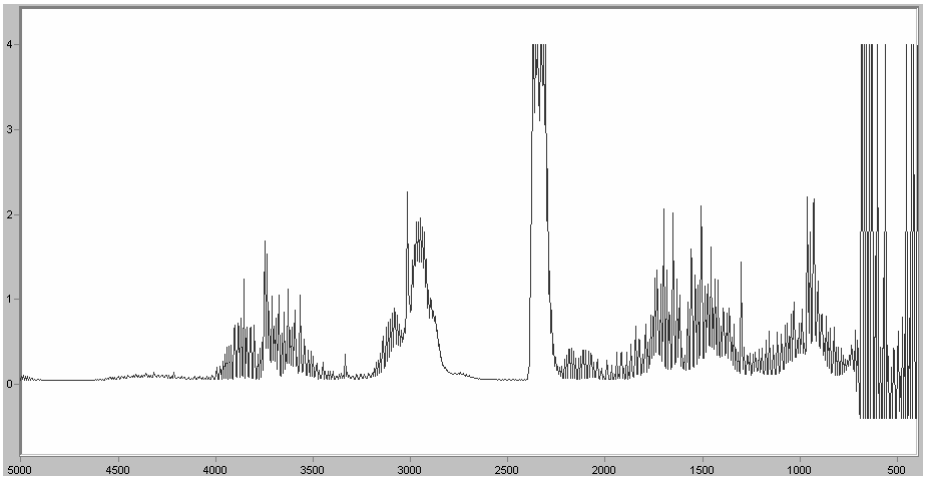

Fig 8 IR-spectrum: Pyrolysis at 600°C of sewage sludge pellets (absorbance against wave number in cm^{-1}).

Combustion

Flash combustion of glossy paper has been performed at three temperatures (600°C, 750°C and 900°C). During combustion fuel-N was released as NO, N_2 and to a minor extent NO_2 and N_2O. Fig. 9 presents the N-conversion to NO_x and N_2O against the C-conversion to CO and CO_2. It can be seen only a small difference in the conversions between 600 and 750°C: 38 to 44 % of the initial fuel-N is released as NO_x and N_2O. However when the reactor temperature is 900°C, the N-conversion decreases to 25-29%. This is in accordance with the results from [3] where for the same fuel the conversion factor of fuel-N to NO was 26% at 850°C. The decrease in the N-release between 750°C and 900°C can be explained by the fact that N-conversion is showing a maximum value with temperature, this phenomenon has already been observed [12] for several biomass fuels like alder wood, peat or malt waste where the maximum conversions were observed at approximately 800°C.

The N-conversions measured were 17% for birch and 7% for sewage sludge pellets at 750°C. As commonly observed, the higher the fuel-N content, the lower the N-conversion to NO_x and N_2O.

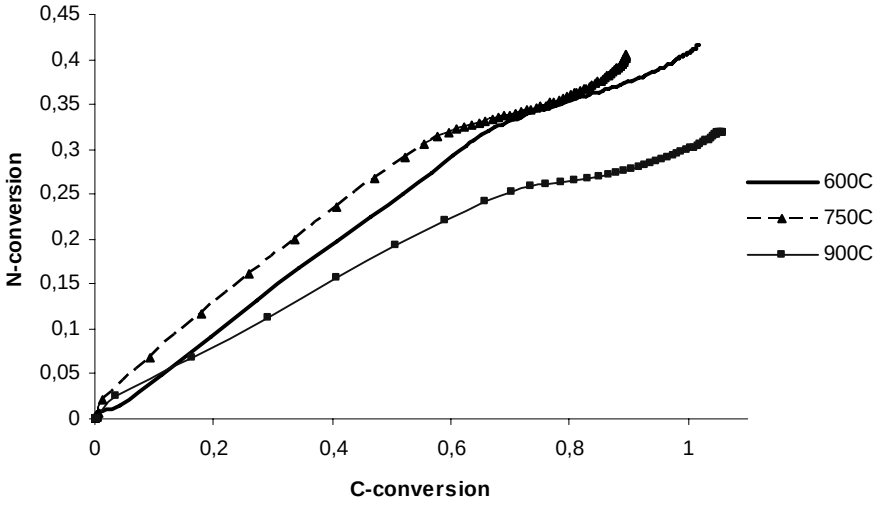

Fig. 9 N-conversion against C-conversion for glossy paper at three different initial reactor temperatures (C-conversion not equal to 1 because of experimental uncertainties)

Pyrolysis

The pyrolysis study has been carried out using sewage sludge pellets because of their high nitrogen content (5.47 wt%, dry ash free basis). Nitrogen was released as NH_3 and HCN during the pyrolysis, with conversion factors and NH_3/HCN ratios according to Table 3.

Table 3. Conversion factors of fuel-N to NH_3 and HCN, and NH_3/HCN ratios, during pyrolysis of sewage sludge pellets.

	900° C	750° C	600° C
NH_3	0.507	0.408	0.365
HCN	0.086	0.057	n.d.
NH_3/HCN	5.90	7.16	-
NH_3+HCN	0.593	0.465	-

n.d.: not detectable

The main experimental results are:

(1) NH_3 is the main N-containing pyrolysis product at all temperatures.
(2) Conversion of fuel-N to NH_3 and HCN increases with increasing temperature.
(3) The NH_3/HCN ratio increases with decreasing temperature.

After pyrolysis, char (7.5-8% of the initial mass) combustion was carried out. At all temperatures the conversion of the char-N to NO and N_2O was less than 1% of the initial fuel-N, indicating that a very small fraction of the initial fuel-N remained in the char after pyrolysis. This is in accordance with [21]. The part of the sewage sludge nitrogen released during pyrolysis reported in the literature (for the temperature range 600-900°C) varies from 27% to 90% depending on the temperature, the type of sewage sludge and the heating rate [10, 22, 23]. The remaining part of the nitrogen is found in the tar fraction (not analysed) and NH_3 may also be found in the product water (not analysed) as reported by [24, 25].

CONCLUSION

This preliminary study has shown that the reactor can be used as a macro TGA, providing valuable data for mass loss rate studies of thermally thick biomass particles. Furthermore the FTIR has been successfully used in combination with the reactor to investigate combustion of sewage sludge and biomass. However, the pyrolysis study appeared to be possible exclusively for fuels with high N-content (the lower limit is not yet established). The mass loss curves show a clear dependence on the temperature in the reactor, with increased mass loss rate as the temperature in the reactor increases, both for the combustion and for the pyrolysis experiments. The remaining ash content in the combustion experiments confirms the laboratory proximate analysis. The N-conversion to NO_x and N_2O show expected results based on earlier literature data,

which implies that, an increased N-content in the fuel decrease the conversion factor for fuel-N to NO_x and N_2O.

The results obtained for pyrolysis of sewage sludge pellets have shown the presence of NH_3 and HCN in the pyrolysis gas, and a clear temperature dependence of the release of these two fuel-N species.

The experimental set-up is currently under improvement. A micro-GC (Gas Chromatograph) will be installed to measure new species (N_2 and H_2) and will also provide a second set of results for some other species.

Further plans include the study of the release of fuel-N compounds at various conditions for a large variety of fuels. This experimental study and further planned studies will provide important input for gas-phase modelling.

ACKNOWLEDGEMENTS

This work is part of the "Environment and Process Management" research program, and is funded by the Research Council of Norway.

REFERENCES

1 Rogaume T., Auzonneau M., Jabouille F., Goudeau J.C. & Torero J.L. (2002) The effects of different airflows on the formation of pollutants during waste incineration. Fuel, 81, 2277-88.

2 IPPC (1996) Climate Change 1995: The Science of Climate Change – Contribution of Working Group I to the 2nd Assessment Report of the IPPC.

3 Sørum L., Skreiberg Ø., Glarborg P., Jensen A. & Dam-Johansen K. (2001) Formation of NO From Combustion of Volatiles From Municipal Solid Wastes. Combustion and Flame, 123, 195-212.

4 Löffler G., Winter F. & Hofbauer H. (2001) Parametric Modelling Study of Volatile Nitrogen Conversion to NO and N_2O during Biomass Combustion. Progress in Thermochemical Biomass Conversion (Ed. by A. V. Bridgewater), 1, 642-55.

5 Nielsen M., Jurasek P., Hayashi J. & Furimsky E. (1995) Formation of toxic gases during pyrolysis of polyacrylonitrile and nylons. Journal of Analytical and Applied Pyrolysis, 35, 43-51.

6 Keller R. & Nussbaumer T. (1994) A new method to analyse the nitrogen content and investigations of the conversion to nitric oxides during combustion. Advances in Thermochemical Biomass Conversion (Ed. by A. V. Bridgewater), 1, 549-62.

7 Leppälahti J. & Koljonen T. (1995) Nitrogen evolution from coal, peat and wood during gasification: Literature Review. Fuel Processing Technology, 43, 1-45.

8 De Jong W., Pirone A. & Wójtowicz M.A. (2003) Pyrolysis of Miscanthus Giganteus and wood pellets: TG-FTIR analysis and reaction kinetics. Fuel, 82, 1139-47.

9 Li C-Z & Tan L.L. (2000) Formation of NOx and SOx precursors during the pyrolysis of coal and biomass. Part III. Further discussion on the formation of HCN and NH_3 during pyrolysis. Fuel, 79, 1899-1906.

10 Tian F.-J., Li B.-Q., Chen Y. & Li C.-Z. (2002) Formation of NOx precursors during the pyrolysis of coal and biomass. Part V. Pyrolysis of a sewage sludge. Fuel, 81, 2203-08
11 Leppälahti J. (1995) Formation of NH_3 and HCN in slow-heating-rate inert pyrolysis of peat, coal and bark. Fuel, 74, 1363-68.
12 Winter F., Wartha C. & Hofbauer H. (1999) NO and N_2O formation during the combustion of wood, straw, malt waste and peat. Bioresource Technology, 70, 39-49.
13 Leichtnam J.-N., Schwartz D. & Gadiou R. (2000) The behaviour of fuel-nitrogen during fast pyrolysis of polyamide at high temperature. Journal of Analytical and Applied Pyrolysis, 2000, 255-68.
14 Hansson K.-M. (2003) Principles of Biomass Pyrolysis with Emphasis on the Formation of the Nitrogen-Containing Gases HNCO, HCN and NH_3. Dphil thesis, Chalmers University of Technology.
15 Wartha, C. (1998) An experimental study on Fuel-Nitrogen Conversion to NO and N_2O and on Carbon Conversion under Fluidized Bed Conditions, Dphil thesis, Vienna University of technology.
16 Skreiberg Ø., Glarborg P., Jensen A. & Dam-Johansen K. (1997) Kinetic NOx modelling and experimental results from single wood particle combustion. Fuel, 76, 671-82.
17 Stenseng M. (2001) Pyrolysis and Combustion of Biomass. Dphil thesis, Technical University of Denmark.
18 Aho M. (1987) Pyrolysis and Combustion of Peat and Wood as Single Particles and as a Layer. Journal of Analytical and Applied Pyrolysis, 11, 149-62.
19 Skreiberg Ø. Hustad J. E. & Karlsvik E. (1997) Empirical NOx-modelling and experimental results from wood stove combustion. In Developments in Thermochemical Biomass Conversion, Blackie Academic & Professional.
20 Karlsvik E., Hustad J. E., Skreiberg Ø. & Sønju O. K. (1997) In Combustion Technologies for a Clean Environment, Gordon and Breach Science Publishers.
21 Rumphorst M.P. & Ringel H.D. (1994) Pyrolysis of sewage sludge and use of pyrolysis coke. Journal of Analytical and Applied Pyrolysis 28:137-155.
22 Ogada T. & Werther J. (1997) Sewage sludge combustion. Progress in Energy and Combustion Science 25:55-116.
23 Fullana A., Conesa J. A., Font R. & Martín-Gullón I. (2003) Pyrolysis of sewage sludege : nitrogenated compounds and pretreatment effects. Journal of Analytical and Applied Pyrolysis 68-69:561-575.
24 Kaminsky W. & Kummer A.B. (1989) Fluidized bed pyrolysis of digested sewage sludge. Journal of Analytical and Applied Pyrolysis 16:27-35.
25 Inguanzo M., Domínguez A., Menéndez J.A., Blanco C.G. & Pis J.J. (2002) Journal of Analytical and Applied Pyrolysis 63:209-222.

Paper II

Detailed chemical kinetics modelling of NOx reduction by staged air combustion at moderate temperatures

Skreiberg Ø., Becidan M., Hustad J.E., Mitchell R.E.

Proceedings of the Science in Thermal and Chemical Biomass Conversion Conference, 30 August-2 September 2004, Victoria, BC, Canada, vol. 1, pp. 40-54. Edited by A.V. Bridgwater and D.G.B. Boocock. CPL Press, UK, 2006. Peer-reviewed.

Detailed Chemical Kinetics Modelling of NOx Reduction by Staged Air Combustion at Moderate Temperatures

Øyvind Skreiberg, Michaël Becidan and Johan E. Hustad
Norwegian University of Science and Technology, Department of Energy and Process Engineering, N-7491 Trondheim, Norway
Reginald E. Mitchell
Stanford University, Mechanical Engineering Department, Thermosciences Division, Stanford, California, 94305-3032, USA

ABSTRACT: Staged air combustion is a well known method for reducing NOx (primarily NO) to molecular nitrogen, either integrated in a combustion chamber by separating primary and secondary air addition, or by applying a separate reduction chamber. However, the details of the chemical kinetics responsible for the NOx reduction are less well known, especially at moderate temperatures (below 1400 K), e.g. in most biomass combustion applications. Several reaction paths are involved in the reduction of NOx to molecular nitrogen, and a number of parameters influence the relative importance of the various reaction paths and the final degree of NOx reduction. Parameters of special importance are temperature, primary excess air ratio, residence time in the reducing zone and the fuel-N content and N-species distribution. However, also the overall excess air ratio and the final temperature level are of importance if intermediate N-species, mainly NH_3 in biomass combustion applications, exits the reducing zone. Additionally, the C/H/O pyrolysis/gasification gas composition and speciation will to some degree influence NOx reduction by staged air combustion, mainly through its influence on the radical pool.

In this paper a recently developed detailed chemical kinetics NOx mechanism, regarded as especially suitable for biomass combustion applications, has been used in a parametric study to reveal the influence of the most important parameters influencing the NOx reduction by staged air combustion at moderate temperatures. Plug flow reactor and perfectly stirred reactor conditions are used, representing two extremes of mixing conditions. Detailed reaction path analysis is also carried out to explain the influence of the parameters on the detailed chemical kinetics. From the parametric study, recommendations on how to achieve an optimum NOx reduction by staged air combustion at moderate temperatures are drawn.

INTRODUCTION

Staged air combustion has been identified as a primary NOx reduction measure with a high NOx reduction potential [1, 2, 3], comparable to that of staged fuel combustion, at optimum conditions. However, to achieve these optimum conditions there is a need for a well controlled combustion process according to [1]. In reality the optimum

conditions may vary significantly depending on the fuel and the operating conditions of the application in question. It is therefore interesting to reveal to what extent general optimum conditions can be stated, if at all. It is also interesting to reveal the influence of the fuel gas composition and the fuel-N speciation on the NOx reduction potential by staged air combustion. Significant research effort is directed towards identification and quantification of primary fuel-N species within the biomass research community today [4, 5]. Hence, an important question is to which extent the fuel-N speciation may influence the choice of optimum operating conditions.

The fuel-N release from solid biomass devolatilisation has traditionally been thought to consist mainly of NH_3, and to a lesser extent HCN, but the results reported in the literature are scarce and partly contradictory. However, recent findings show that the amount of HCN may be quite significant [4, 6, 7, 8, 9], and also that HNCO [4, 6, 7, 8] may be a significant fuel-N species. The ratio between these fuel-N species will be dependent on the nitrogen functionality in the fuel and on different operational parameters for the devolatilisation process, where temperature and heating rate are two important parameters [4]. Karlsson et al. [7] found a HNCO/HCN ratio of about 0.3 at 700°C, decreasing to about 0.1 at 1000°C for three biomass species. They also found a HCN/NH_3 ratio of about 0.3 at 700°C, increasing to about 1.0 at 1000°C for the same three species in the same experiments, and for two additional biomass species.

If the devolatilisation occurs without externally supplied oxygen, e.g. a pyrolysis process, different fuel-N speciation in the pyrolysis gas can be expected compared to a gasification process. For real biomass combustion units, as for grate combustion, it is not necessarily easy to distinctly separate the processes occurring, and also fuel-N species released from char oxidation will to some degree mix with the gas formed from the volatile fraction of the fuel, which is especially important if a separate NOx reduction chamber is applied. Hence, a fuel gas from a primary combustion chamber may consist also of fuel-N contributions from the char oxidation phase, e.g. NO, and also N_2O, which will influence the nitrogen chemistry in the NOx reduction chamber, and therefore also the NOx reduction potential.

METHODS

Detailed chemical kinetics modelling has been performed using a recent chemical kinetics mechanism [10] regarded as especially suitable for biomass combustion applications, e.g. moderate (below 1400 K) to low temperatures, fuel-rich conditions and with NH_3 usually as the main primary nitrogen species released from the pyrolysis. The mechanism is to a large extent based on the mechanism by Glarborg et al. [11], but with major updates to their NH_3 subset. The mechanism has been verified against an extensive set of experimental data on NH_3 oxidation [12]. See [10] for further detailed information about the details in the chemical kinetics mechanism used.

Two different ideal flow reactors have been used in this modelling study, a plug flow reactor (PFR) and a perfectly stirred reactor (PSR). These reactors represent two extremes of mixing conditions, and will as such give outer limit predictions compared to real mixing conditions. However, the ideal flow reactors are useful tools in analysing the influence of various process parameters on the degree of NOx reduction at different conditions. The SENKIN code [13] and the AURORA code [14] within the CHEMKIN Collection [15, 16] were used for respectively PFR and PSR modelling.

The modelling matrix carried out in this work has been extensive, covering a temperature range from 873-1373 K, using adiabatic and fixed temperature reactors; a primary excess air ratio range of 0-1.5; overall excess air ratios of 1.5, 2.0 and 2.5; single reactor residence times of 0.1, 0.5 and 1 s, and 2 s total residence time; and fuel-N levels in the pyrolysis gas of 100, 500, 1000, 5000 and 10000 ppm. The initial fuel-N species investigated includes NH_3, HCN, HNCO and NO, alone or mixed with each other in different fractions. The base case pyrolysis fuel gas composition used, excluding the fuel-N species, is given in *Table 1*. It is an average of the pyrolysis gas compositions measured by Chan [17], who performed pyrolysis experiments on Oregon lodgepole pine wood pellets. The tar fraction is assumed to crack and give a secondary gas composition equal to the primary gas composition. Measured pyrolysis gas compositions for wood only includes the direct formation of pyrolysis gases, and not the gases formed from secondary tar cracking. The pyrolysis gases accounted for 11-27 wt% in the study of Chan [17] while the tars accounted for 33-52 wt%. Grønli [18] reported 30-50 wt% pyrolysis gases and 25-40 wt% tars (including water). Finally, Di Blasi [19] reported a wide range of pyrolysis gas and liquid yields, for different wood species and as a function of heating rate. However, in this work the influence of each fuel gas species (except CO_2 and H_2O), and in addition H_2, was investigated by mixing one fuel gas species alone with respectively NH_3, HCN and HNCO. Also the effect of multiple air stages was analysed with respect to achieving an optimum degree of NOx reduction.

NOx reduction in this work means reduction of fuel-N to molecular nitrogen, N_2. This can be described by TFN/Fuel-N, which is the mass ratio between the nitrogen content in the predicted total fuel-N emissions (excluding N_2) and the content of nitrogen in the initial fuel gas (excluding any N_2).

The modelling results have been analysed mainly through rate of production analysis, showing the reaction path from fuel-N to final emissions, or N_2. However, through the modelling matrix TFN/Fuel-N sensitivities with respect to fuel gas species selection and fuel-N species selection have been analysed. Radical availability is a key factor in explaining the behaviour of TFN/Fuel-N at various conditions, and also for explaining the difference in TFN/Fuel-N between a PFR and a PSR.

Table 1. Base case pyrolysis gas composition, excluding N-species.

Species	CO	CO_2	CH_4	C_2H_2	C_2H_6	C_2H_4	H_2O
Volume fraction	0.4474	0.2661	0.0893	0.0016	0.0111	0.0202	0.1643

RESULTS AND DISCUSSION

Fig. 1 shows TFN/Fuel-N as a function of primary excess air ratio in a PFR and a PSR at a temperature of 1173 K and a residence time of 1 s for 1000 ppm NH_3 mixed with different fuel gas species.

As can be seen, both the trends and the quantitative TFN/Fuel-N values depend very much on the fuel gas species selection and on the mixing conditions. While TFN/Fuel-N in general stays high for hydrocarbon fuel gas species, CO and H_2 as fuel gas species yield very low TFN/Fuel-N values, especially for the PSR conditions. The optimum primary excess air ratio in the PFR is about 0.8 for hydrocarbon fuel gas species, while it is below 0.1 for CO and H_2. In the PSR the optimum primary excess air ratio is close to 1 for hydrocarbon fuel gas species, while

low TFN/Fuel-N values can be seen for a wide primary excess air ratio range for CO and H_2. For the PFR conditions the low values lies in a narrow primary excess air ratio range, and CO gives a narrower range than H_2. These results change as a function of temperature, as illustrated in *Fig. 2* for 1000 ppm NH_3 mixed with CO in a PFR and a PSR at a residence of 1 s. For the PFR the lower temperatures of 973 K and 1023 K give the widest operation window with respect to primary excess air ratios. For the PSR the highest temperatures of 1173 K and 1223 K give the optimal conditions. This picture will be different for other fuel gas species. In general, the presence of hydrocarbon species in the fuel gas lowers the NOx reduction potential by staged air combustion, while large amounts of CO, in pyrolysis gas, and additional H_2 in gasification gas, increase the NOx reduction potential.

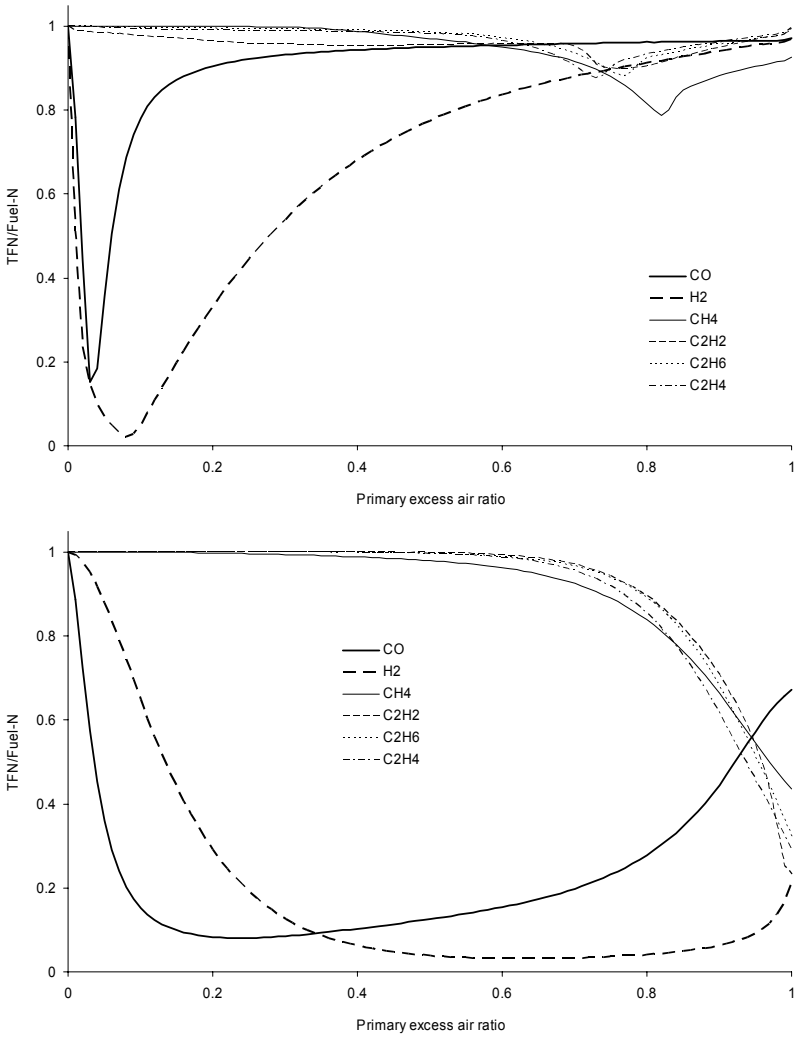

Fig. 1 TFN/Fuel-N as a function of primary excess air ratio in a PFR (upper half) and a PSR (lower half) at a temperature of 1173 K and a residence time of 1 s for 1000 ppm NH_3 mixed with different fuel gas species.

For HCN or HNCO as fuel-N species the picture is similar. However, TFN/Fuel-N is much higher for HCN with H_2 as fuel gas species, and also somewhat higher for the other fuel gas species. Hence, the NOx reduction potential is lower. For HNCO TFN/Fuel-N is rather similar to that of NH_3, for all fuel gas species. Hence, HNCO closely follows the fate of NH_3. As for NH_3 as fuel-N species, the results for HCN and HNCO change with temperature.

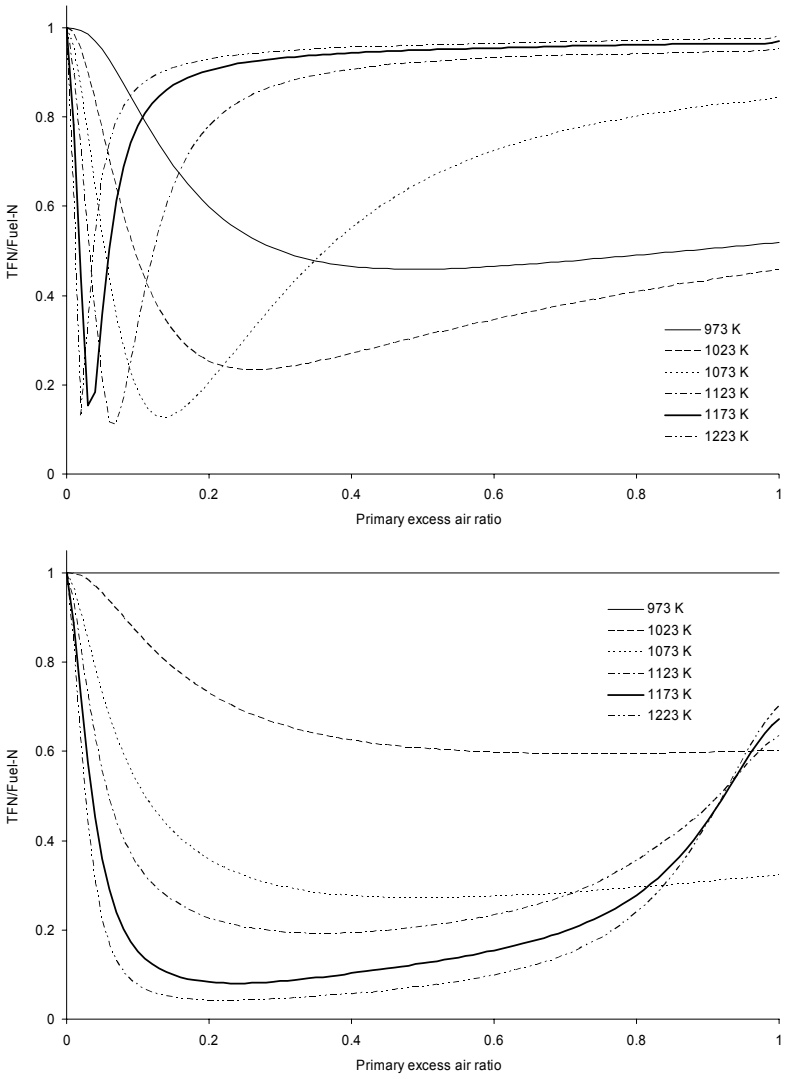

Fig. 2 TFN/Fuel-N as a function of primary excess air ratio and temperature in a PFR (upper half) and a PSR (lower half) at a residence time of 1 s for 1000 ppm NH_3 mixed with CO.

Fig. 3 shows TFN/Fuel-N as a function of primary excess air ratio in a PFR and a PSR at a temperature of 1173 K and a residence time of 1 s for 1000 ppm fuel-N species mixed with the base case pyrolysis fuel gas composition.

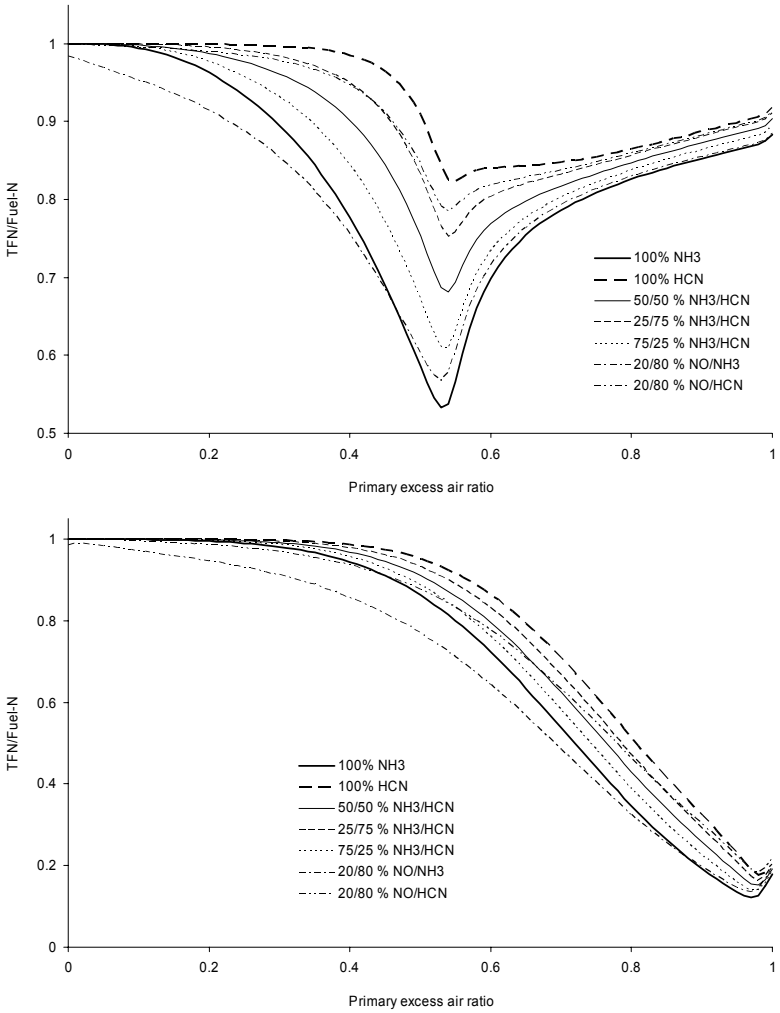

Fig. 3 TFN/Fuel-N as a function of primary excess air ratio in a PFR (upper half) and a PSR (lower half) at a temperature of 1173 K and a residence time of 1 s for 1000 ppm fuel-N species mixed with the base case pyrolysis fuel gas composition.

TFN/Fuel-N decreases with increasing NH_3 fraction in the fuel-N content, and increases with increasing HCN fraction. The difference is more significant in a PFR than in a PSR. Addition of NO to the fuel-N content enhances TFN reduction at lower primary excess air ratios, but slightly decreases TFN reduction at the optimum primary excess air ratio. Also for the base case pyrolysis fuel gas composition there is a significant influence of temperature on the TFN/Fuel-N trend as a function of primary excess air ratio and the predicted NOx reduction degree. The optimum primary excess air ratio lies somewhat below 0.6 in the PFR, and close to unity in the PSR. This behaviour is closely connected to the hydrocarbon content of the fuel gas, and its influence on the radical pool. At a primary excess air ratio of 0.6 in the PFR all hydrocarbon species will be converted, while in the PSR this happens at a primary excess air ratio close to unity. Hence, the amount of hydrocarbons present in the fuel

gas controls to a great extent the optimum primary excess air ratio and the NOx reduction potential, together with the flow/mixing conditions. In the PFR a typical high radical peak occurs when the hydrocarbons are completely converted, giving a rapid reduction in TFN/Fuel-N until the radical pool is close to consumed, where after the radical level stays very low and no significant further reduction of TFN/Fuel-N occurs. In the PSR radicals will be available continuously, but in much lower amounts compared to the radical peak levels in a PFR. Hence, both the main chemistry and the fuel-N chemistry become more sensitive to residence time in a PSR compared to a PFR, and this result in a significantly higher NOx reduction potential in a PSR compared to a PFR. For HNCO as fuel-N species instead of NH_3, alone or in the mixtures, the picture is similar as for NH_3. Hence, HNCO closely follows the fate of NH_3.

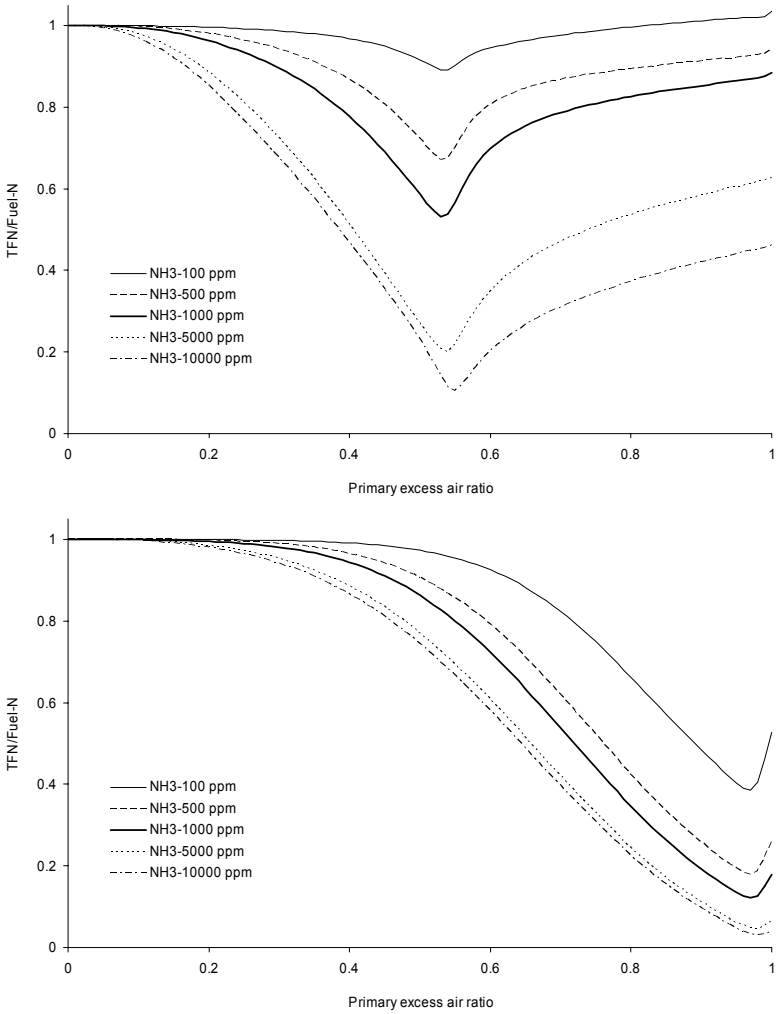

Fig. 4 TFN/Fuel-N as a function of primary excess air ratio and fuel-N level in a PFR (upper half) and a PSR (lower half) at a temperature of 1173 K and a residence time of 1 s for NH_3 mixed with the base case pyrolysis fuel gas composition.

Fig. 4 shows TFN/Fuel-N as a function of primary excess air ratio and fuel-N level in a PFR and a PSR at a temperature of 1173 K and a residence time of 1 s for NH_3 mixed with the base case pyrolysis fuel gas composition. As can be seen, TFN/Fuel-N decreases with increasing NH_3 level, which is mainly an effect of an increasing reaction rate, due to the increasing fuel-N concentrations, for the reactions involved in the reduction of intermediate fuel-N species to N_2.

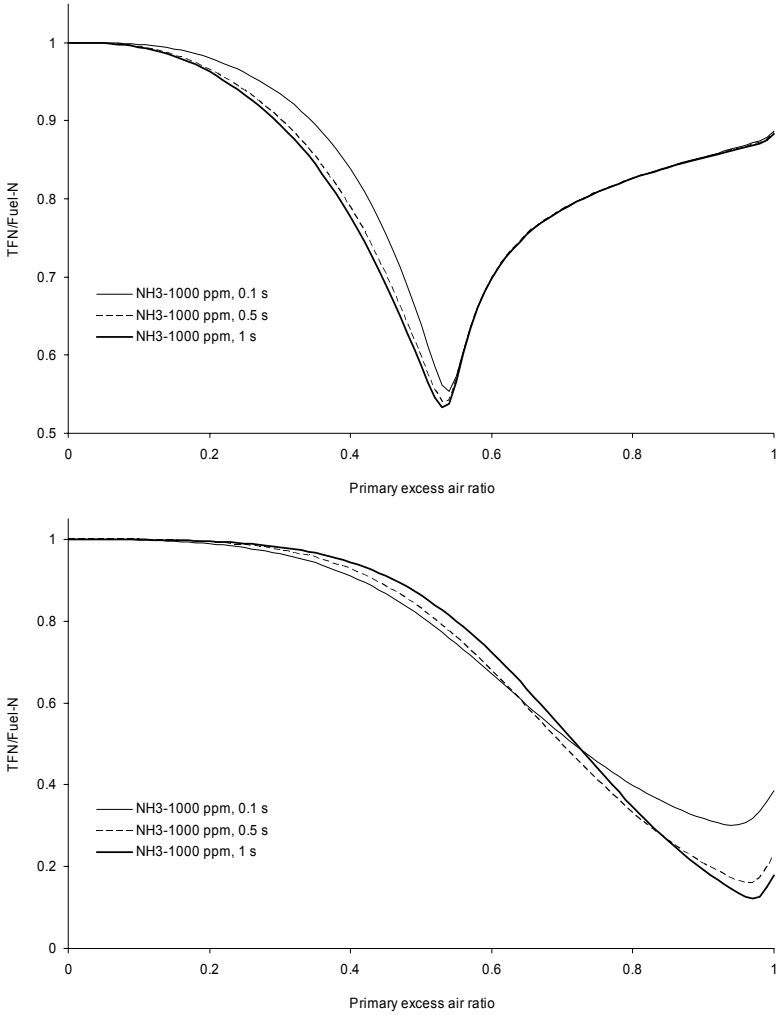

Fig. 5 TFN/Fuel-N as a function of primary excess air ratio and residence time in a PFR (upper half) and a PSR (lower half) at a temperature of 1173 K for NH_3 mixed with the base case pyrolysis fuel gas composition.

Fig. 5 shows TFN/Fuel-N as a function of primary excess air ratio and residence time in a PFR and a PSR at a temperature of 1173 K for 1000 ppm NH_3 mixed with the base case pyrolysis fuel gas composition. An increasing residence time will to some extent decrease TFN/Fuel-N, and the effect of an increasing residence is most pronounced in

a PSR reactor at optimum conditions. This is connected to radical availability, as already discussed. For practical purposes the residence time needed for NOx reduction by staged air combustion is rather short at higher temperatures, especially in a PFR, and increases with decreasing temperatures.

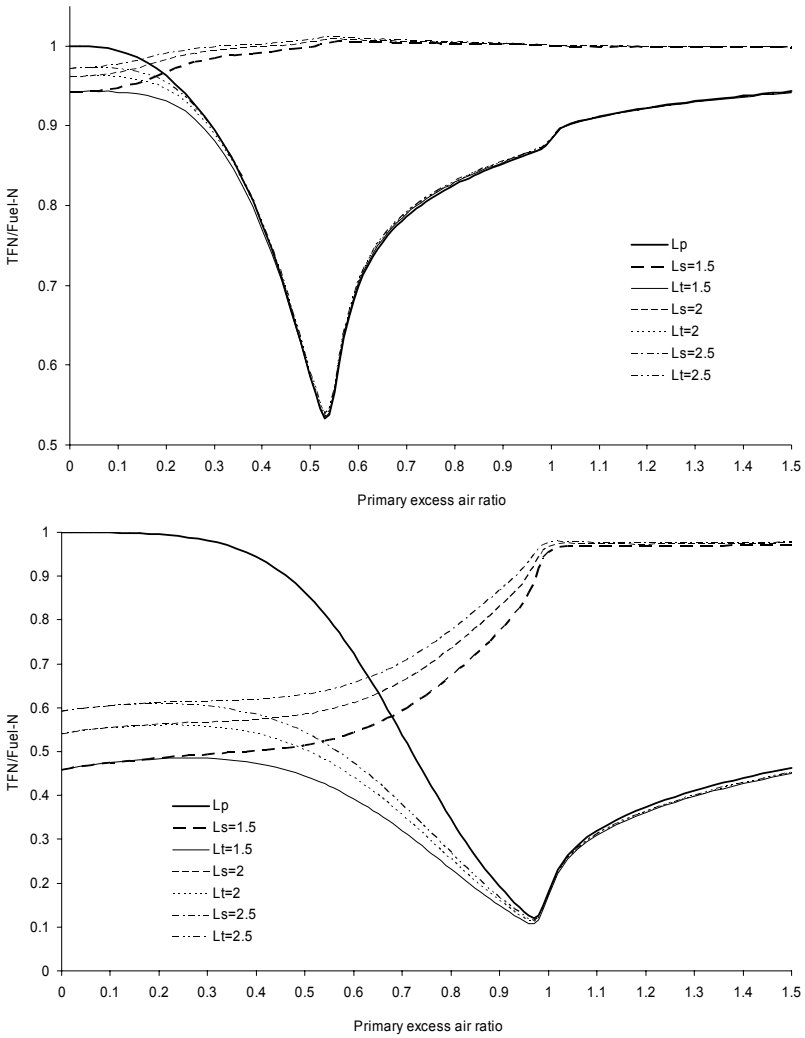

Fig. 6 TFN/Fuel-N as a function of primary and overall excess air ratio in a PFR (upper half) and a PSR (lower half) at a temperature of 1173 K for 1000 ppm NH_3 mixed with the base case pyrolysis fuel gas composition. Lp: TFN/Fuel-N after primary air addition only, residence time = 1 s; Ls: TFN/Fuel-N, based on remaining inlet fuel-N, in the second reactor for an overall excess air ratio of 1.5, 2 and 2.5, residence time = 1 s; Lt: total TFN/Fuel-N for the overall excess air ratio of 1.5, 2 and 2.5 and a total residence time of 2 s.

Fig. 6 shows TFN/Fuel-N as a function of primary and overall excess air ratio in a PFR and a PSR at a temperature of 1173 K for 1000 ppm NH_3 mixed with the base case

pyrolysis fuel gas composition. Some degree of TFN reduction may occur also when adding the secondary air for final burnout. In the PFR this happens to a significant degree if the primary excess air ratio is very low, while in the PSR this happens in the whole primary excess air ratio range below unity. Increasing the overall excess air ratio increases TFN/Fuel-N, hence reducing the NOx reduction potential. Even without air staging PSR conditions gives rather low TFN/Fuel-N, and significantly lower than for the PFR. Even though a significant additional NOx reduction may occur when adding secondary air for final burnout the optimum primary excess air ratio remains quite distinct, and no significant further decrease in TFN/Fuel-N occurs at the optimum primary excess air ratio.

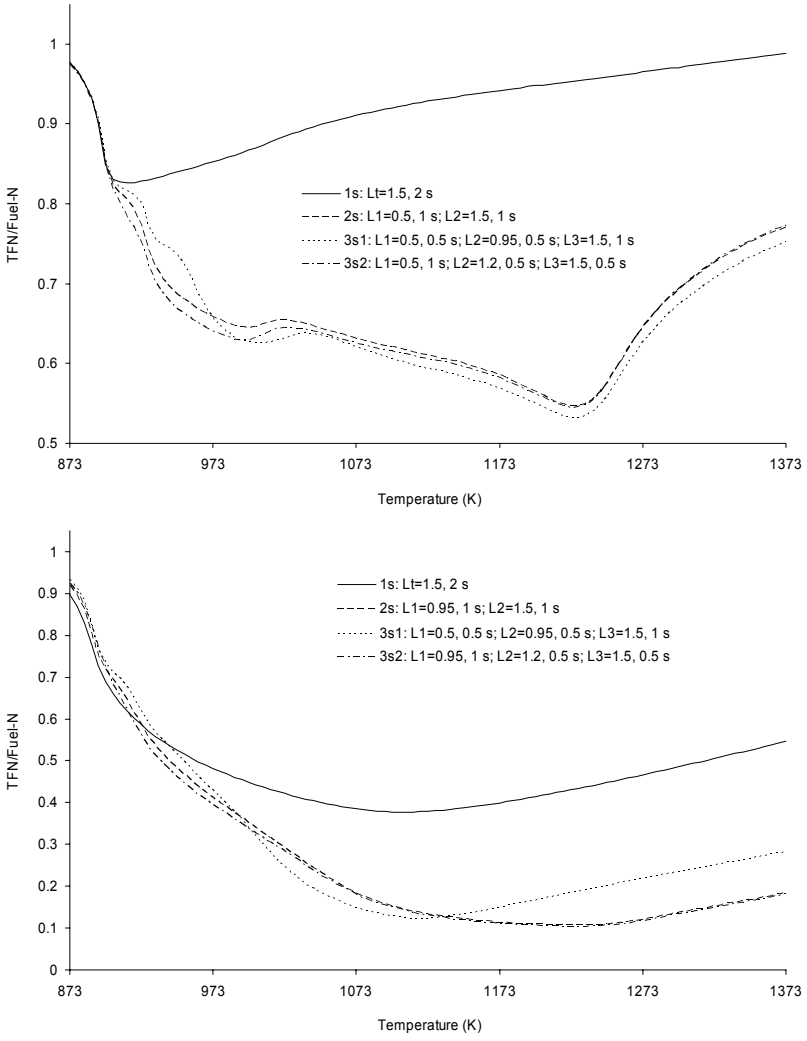

Fig. 7 TFN/Fuel-N as a function of temperature and number of air stages in a PFR (upper half) and a PSR (lower half) for 1000 ppm NH_3 mixed with the base case pyrolysis fuel gas composition.

Fig. 7 shows TFN/Fuel-N as a function of temperature and number of air stages in a PFR and a PSR for 1000 ppm NH_3 mixed with the base case pyrolysis fuel gas composition. In the PFR air staging very much decreases TFN/Fuel-N in a wide temperature range compared to no staging. However, it is not obvious that using two primary air stages will improve the degree of NOx reduction. This can be clearly seen for the PSR where one primary air stage is more optimal than two at higher temperatures. As the degree of NOx reduction is sensitive to a number of not necessarily independent factors the optimum procedure with regards to NOx reduction for addition of air in two or more air stages depends very much on the combustion application in question, and its operational characteristics. An extensive optimisation procedure is in reality needed for each single application to achieve as low as possible final TFN/Fuel-N.

Reaction Path Analysis (RPA) is a very helpful tool when analysing detailed chemical kinetics mechanisms, revealing the main reactions paths and the most important single reactions at the various conditions. In this work a large number of conditions have been investigated and it is out of the scope of this work to discuss the main chemical kinetics at all these conditions due to space limitations. However, the main reaction paths at optimum conditions using the base case pyrolysis gas composition mixed with NH_3, HCN or HNCO at a temperature of 1173 K and a residence time of 1 s are discussed below for both PFR and PSR conditions.

For NH_3 88.9% of the initial NH_3 is converted mainly through the reaction path $NH3 \xrightarrow{+OH} NH2 \xrightarrow{+HO2} H2NO \xrightarrow{+HO2} HNO \xrightarrow{+H,+O2} NO \xrightarrow{+NH2} N2$ in the PFR, yielding a TFN/Fuel-N of 0.53. The main reaction path in the PSR is $NH3 \xrightarrow{+OH} NH2 \xrightarrow{+H} NH \xrightarrow{+H} N \xrightarrow{+OH,+O2} NO \xrightarrow{+N} N2$, converting 99.2% of the initial NH_3 and yielding a TFN/Fuel-N of 0.12. This is shown in *Fig. 8*, which clearly illustrates the complexity of fuel-N chemistry, and the many reaction paths that may be involved in the conversion of fuel-N to emissions, or N_2.

For HCN 43.4% of the initial HCN is converted mainly through the reaction path $HCN \xrightarrow{+O} NCO \xrightarrow{+C2H6} HNCO \xrightarrow{+H} NH2 \xrightarrow{+H} NH \xrightarrow{+O,+O2} NO \xrightarrow{+N} N2$ in the PFR yielding a TFN/Fuel-N of 0.82. However, the reaction path picture is more complex for HCN compared to NH_3, and H_2, OH and CH_4 are almost as important as C_2H_6 for the conversion of NCO to HNCO in this specific case. Conversion of HCN to HOCN by reaction with OH was not found to be important. The main reaction path in the PSR is the same as in the PFR, converting 92.6% of the initial HCN and yielding a TFN/Fuel-N of 0.18. Also in the PSR the reaction path picture is more complex for HCN compared to NH_3.

For HNCO 99.5% of the initial HNCO is converted mainly through the initial reaction path $HNCO \xrightarrow{+H} NH2$ in the PFR, and then goes through the same main reaction paths as for NH_3, yielding a TFN/Fuel-N of 0.55. Some of the NH_2 is net converted to NH_3 by reaction with H_2, and the NOx reduction potential for HNCO therefore becomes rather similar to NH_3. The main initial reaction path in the PSR is as in the PFR, and the fuel-N then goes through the same main reaction paths as for NH_3, converting 99.7% of the initial HNCO and yielding a TFN/Fuel-N of 0.12.

The relative importance of the various reaction paths at other conditions will change quite significantly, making it impossible to propose general main reaction paths for a wide range of conditions. Hence, global and reduced fuel-N chemistry often used

in combination with CFD will be valid only at specific and limited conditions, e.g. only the conditions the simplified chemistry was developed, or optimised, for.

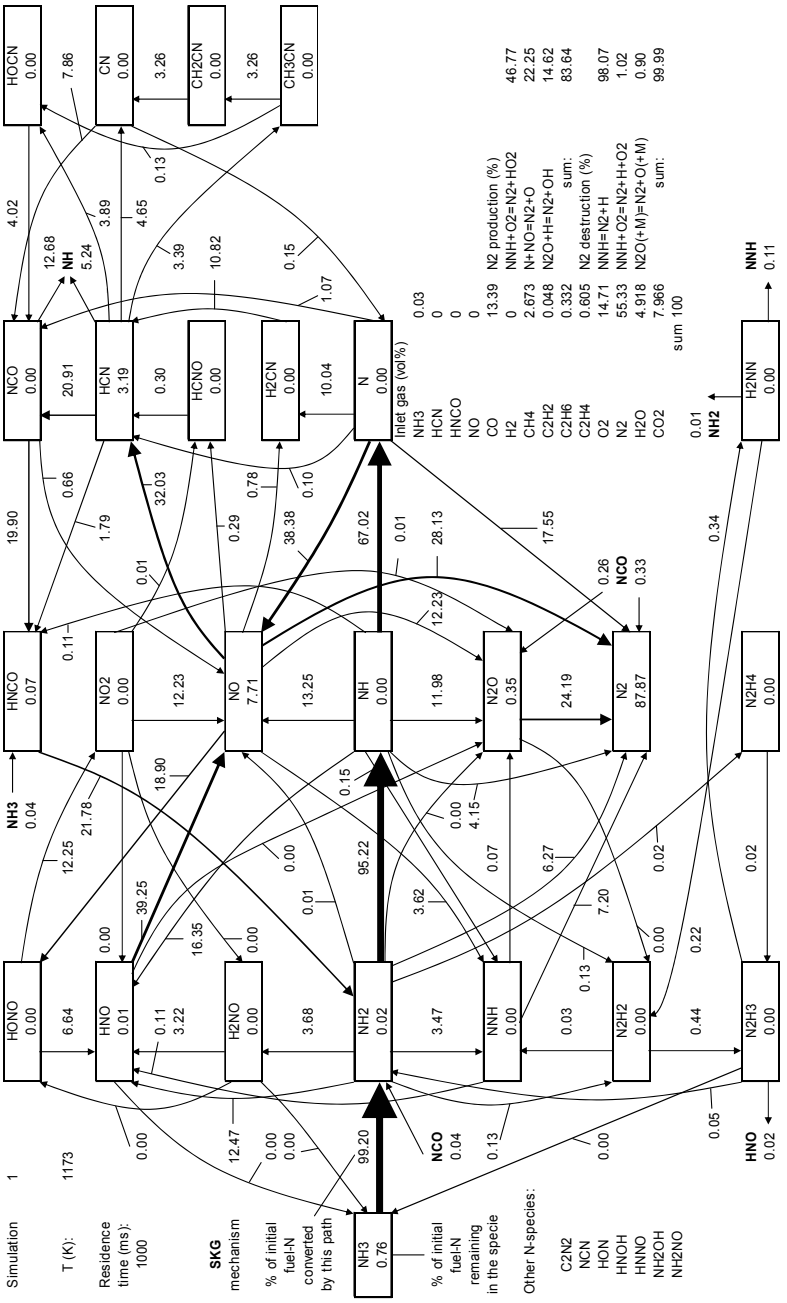

Fig. 8 Reaction path diagram at optimum primary excess air ratio in the PSR at a temperature of 1173 K and a residence time of 1 s for 1000 ppm NH_3 mixed with the base case pyrolysis fuel gas composition.

CONCLUSIONS

The potential for reduction of NOx emission formed from the nitrogen content in the fuel by applying staged air combustion is significant. However, this potential is also very dependent on a number of operational factors, which will vary from application to application. Hence, it is not possible to state general optimum conditions, and an extensive optimisation procedure is in reality needed for each single application to achieve as high as possible NOx reduction.

Calculations, as performed in this study, can be used as guidelines in an optimisation process, and the reason for a reduced NOx level can be explained through chemical kinetics analysis. However, the flow conditions will influence the chemistry, mainly through its influence on the radical pool, and will therefore also influence the degree of NOx reduction achievable. Computational Fluid Dynamics (CFD) calculations is needed for the best possible representation of the flow field in a real application. However, the combination of detailed chemical kinetics and CFD demands today very long calculation time, and even then a number of assumptions and simplifications must be made. Reactor network modelling, using a number of ideal reactors (PFR or PSR) can be used as a simplified CFD approach. However, as this study shows, these two reactors behave quite different. Great care should therefore be put on the proper selection of both the location and the number of ideal reactors to use in such a simplified CFD approach. A combination of calculations and experiments, and a detailed understanding of the chemistry involved, is potentially the most cost-effective method of achieving a highest degree of NOx reduction by staged air combustion as possible for a specific application. However, one also needs to keep in mind that uncertainties are connected to the detailed chemistry also.

Changes with respect to fuel composition and fuel-N composition will change the optimum conditions, while changes in the fuel-N level alone will change the degree of NOx reduction achievable. Further complications are introduced in batch combustion applications, where most of the fuel and operational parameters will change as a function of time.

Even though, the following general recommendations are proposed as guidelines to how to achieve a highest degree of NOx reduction possible by applying staged air combustion:

- PSR mixing conditions are favourable compared to PFR flow, at optimum conditions, in most cases. Increasingly well mixed conditions will shift the optimum primary excess air ratio closer to unity
- Increasing fuel-N content will significantly increase the percentage NOx reduction potential
- Increasing fuel-N fraction of NH_3, or HNCO, compared to HCN will increase the NOx reduction potential.
- Increasing amounts of CO, and H_2, compared to hydrocarbons in the fuel gas will increase the NOx reduction potential, but it depends also on the fuel-N speciation
- One primary air stage is for practical purposes sufficient, unless also the fuel supply is staged. It is theoretically possible to further increase the NOx reduction somewhat with more primary air stages at some conditions, but the increase is rather limited
- Increasing overall excess air ratio will decrease the NOx reduction potential

- Increasing residence time will only significantly increase the NOx reduction potential until the main chemistry is, from a practical point of view, completed. However, the time for completion of the main chemistry is significantly longer in a PSR compared to a PFR, and the effect of an increasing residence time is much more pronounced at optimum conditions in a PSR
- Temperature is an important parameter. However, for a specific set of other parameters there exists an optimum temperature. The temperature in the primary air stage should be high enough to, from a practical point of view, complete the main chemistry. The temperature needed to complete the main chemistry, and the fuel-N chemistry, in a PSR is higher than in a PFR for the same residence time. The temperature in the secondary air stage should be as low as possible, but high enough to ensure complete combustion.
- Finally, fuel-NOx reduction by staged air combustion is very application dependent, and no general optimum conditions can be defined which cover all applications, or all conditions. However, staged air combustion will always contribute to reduced NOx emissions to some degree, a degree which through optimisation can become very significant

REFERENCES

1 Nussbaumer T. (1997) Primary and secondary measures for the reduction of nitric oxide emissions from biomass combustion. In "Developments in Thermochemical Biomass Conversion", Blackie Academic & Professional, pp. 1447-1461.

2 Skreiberg Ø., Glarborg P., Jensen A. & Dam-Johansen K. (1997) Kinetic NOx modelling and experimental results from single wood particle combustion, Fuel 76:671-682.

3 Zabetta E.C., Kilpinen P., Hupa M., Ståhl K., Leppälahti J., Cannon J. & Nieminen J. (2000) Kinetic modeling study on the potential of staged combustion in gas turbines for the reduction of nitrogen oxide emissions from biomass IGCP plants. Energy and Fuels 14:751-761 and addition in p. 1335.

4 Hansson K.-M. (2003) Principals of biomass pyrolysis with emphasis on the formation of the nitrogen-containing gases HNCO, HCN and NH_3. Ph.D. Thesis, Chalmers University of Technology.

5 Glarborg P., Jensen A.D. & Johnsson J.E. (2003) Fuel nitrogen conversion in solid fuel fired systems, Progress in Energy and Combustion Science 29:89–113.

6 Hansson K.-M., Åmand L.-E., Habermann A. & Winter F. (2003) Pyrolysis of poly-L-leucine under combustion-like conditions, Fuel 82:653–660.

7 Hansson K.-M., Samuelsson J., Tullin C. & Åmand L.-E. (2004) Formation of HNCO, HCN and NH_3 from pyrolysis of bark and nitrogen containing model compounds, Combustion and Flame 137:265-277.

8 Hansson K.-M., Samuelsson J., Åmand L.-E. & Tullin C. (2003) The temperature influence on the selectivity between HNCO and HCN from pyrolysis of 2,5-diketopiperazine and 2-pyridone, Fuel 82:2163-2172.

9 Winter F., Wartha C. & Hofbauer, H. (1999). NO and N_2O formation during the combustion of wood, straw, malt waste and peat, Bioresource Technology 70:39-49.

10 Skreiberg Ø., Kilpinen P. & Glarborg P. (2004) Ammonia chemistry below 1400 K at fuel-rich conditions in a flow reactor. Combustion and Flame 136:501-518.

11 Glarborg P., Alzueta M.U., Dam-Johansen K. & Miller J.A. (1998) Kinetic modeling of hydrocarbon/nitric oxide interactions in a flow reactor, Combustion and Flame 115:1-27.
12 Hasegawa T. & Sato M. (1998) Study of ammonia removal from coal-gasified fuel. Combustion and Flame 114:246–258.
13 Lutz A.E., Kee R.J., Miller J.A. (1987), Senkin: a Fortran program for predicting homogeneous gas phase chemical kinetics with sensitivity analysis, Technical Report SAND87-8248, Sandia National Laboratories.
14 Meeks E., Moffat H.K., Grcar J.F. & Kee R.J. (1996) A program for modeling well stirred plasma and thermal reactors with gas and surface reactions in steady or transient conditions, Technical Report SAND96-8218, Sandia National Laboratories.
15 Kee R.J., Rupley F. & Miller J.A. (1989) Chemkin II: a Fortran chemical kinetics package for the analysis of gas phase chemical kinetics, Technical Report SAND89-8009, Sandia National Laboratories.
16 Kee R.J., Rupley F.M., Miller J.A., Coltrin M.E., Grcar J.F., Meeks E., Moffat H.K., Lutz A.E., Dixon-Lewis G., Smooke M.D., Warnatz J., Evans G.H., Larson R.S., Mitchell R.E., Petzold L.R., Reynolds W.C., Caracotsios M., Stewart W.E., Glarborg P., Wang C. & Adigun O. (2001) CHEMKIN Collection, Release 3.6, Technical Report, Reaction Design, Inc., San Diego, CA.
17 Chan, W.-C.R. (1989) Analysis of chemical and physical processes during the pyrolysis of large biomass pellets. Ph.D. Thesis, University of Washington.
18 Grønli M. (1996) A theoretical and experimental study of the thermal degradation of biomass. Ph.D. Thesis, Norwegian University of Science and Technology.
19 Di Blasi C. Branca C., Santoro A., Hernandez E.G. (2001) Pyrolytic behaviour of some wood varieties. Combustion and Flame 124:165-177.

Paper III

Products distribution and gas release in pyrolysis of thermally thick biomass residues samples

Becidan M., Skreiberg Ø., Hustad J.E.

Journal of Analytical and Applied Pyrolysis 78 (2007) 207-213.

Available online at www.sciencedirect.com
ScienceDirect
J. Anal. Appl. Pyrolysis 78 (2007) 207–213
JOURNAL of ANALYTICAL and APPLIED PYROLYSIS
www.elsevier.com/locate/jaap

Products distribution and gas release in pyrolysis of thermally thick biomass residues samples

Michaël Becidan *, Øyvind Skreiberg, Johan E. Hustad

NTNU, Department of Energy and Process Engineering, Kolbjørn Hejes vei 1A, NO-7491 Trondheim, Norway

Received 30 January 2006; accepted 9 July 2006
Available online 17 August 2006

Abstract

The pyrolysis of thermally thick (approximately 75 g) biomass residues samples (i.e. brewer spent grains, fibreboard and coffee beans waste) has been investigated in an in-house designed and fabricated macro-TGA both by rapid sample introduction at reactor temperatures from 600 to 900 °C and by applying a constant heating rate of 10 K/min. The composition of the product gas is determined by simultaneous online use of a micro-GC and a FTIR analyser. The product yields (liquid, char and gas) and the gas composition show a clear dependence on temperature and heating rate. The main gas products are CO_2, CO, CH_4, H_2, C_2H_2, C_2H_6 and C_2H_4. The results show that a rise in temperature leads to increasing gas yields and decreasing liquid and char yields. Lower heating rates favour liquid and char yields. The release patterns of the gaseous species are also greatly affected by the temperature history of the sample.

Keywords: Thermally thick particles; Pyrolysis; Biomass residues; FTIR; GC

1. Introduction

The present interest in biomass and biomass residues generated energy is the consequence of the increased awareness of the environmental, social and energy security challenges our world is facing. The public is demanding sustainable alternatives to the fast disappearing fossil fuels. Biomass is a promising alternative to fossil fuels. The most common thermochemical technologies for biomass conversion are combustion, gasification and pyrolysis.

Pyrolysis produces energy carriers in three forms: bio-oil, charcoal and gas. The utilisations of those products are diverse. The bio-oil, composed of aliphatic and aromatic hydrocarbons along with more than 200 identified compounds [1], can be used in electricity generation as a fuel-oil substitute. However, several properties of the bio-oils such as high water content or poor ignition ability have to be ameliorated or existing equipment modified to meet competitive standards [1–3]. Bio-oil also contains valuable chemicals but their recovery is problematic [1,2]. Charcoal, a carbon-rich solid residue, can be upgraded to activated carbon for use in chemical-, pharmaceutical- and food industries, or as domestic fuel for cooking. The dry pyrolysis gas mixture contains the main components CO_2, CO, CH_4, H_2 and C_2 hydrocarbons [4–6] and can be used for heat production and power generation, but is often used to sustain the pyrolysis process in a biomass waste pyrolysis plant [1,2] or to dry the feedstock. A specific pyrolysis installation will aim at the optimal production (yield, composition and properties) of one of the products. However, it is important to keep in mind the limitations associated with biomass use (small- or medium scale power production, corrosion problems) [7].

Fuel type, temperature, heating rate, pressure, moisture content, initial sample weight and reaction time may affect the yields and properties of the products formed. The most important parameters are temperature and heating rate. Two classes of pyrolysis exist: the slow heating rate pyrolysis and the flash/fast pyrolysis where the sample is heated at high heating rates or suddenly exposed to a high temperature. Under fixed bed conditions, with biomass as fuel, the liquid yield is exhibiting a peak value (55–75%) at moderate temperatures (400–550 °C) and high heating rates [1,5,8–10]. Char formation is minimised by high heating rates and high temperature [1,4], while the carbon content in the charcoal and its heating value are increasing with increasing temperature and slow

* Corresponding author. Tel.: +47 73 59 37 30; fax: +47 73 59 83 90.
E-mail address: michael.becidan@ntnu.no (M. Becidan).

0165-2370/$ – see front matter © 2006 Elsevier B.V. All rights reserved.
doi:10.1016/j.jaap.2006.07.002

heating rate [5]. The yields of all the gas species are enhanced by increasing temperature and high heating rates [2,4,9,11,12], except CO_2 which is often reported to reach a plateau at high temperatures (800–900 °C) [2].

Most studies have been focusing on small samples where the heating of the biomass is assumed to be instantaneous [1,2,5]. However, the conditions encountered in industrial processes are different and it is therefore important to investigate the thermal decomposition of thermally thick samples to simulate practical conditions better. In those "large" samples, heat and mass transport mechanisms will influence the amount and the composition of the gaseous components leaving the bed [9,13–15]. The present investigation is therefore of substantial interest to gather experimental data about the influence of temperature and heating rate on pyrolysis of biomass residues, and especially gas composition. Furthermore, pyrolysis is more than just a conversion method as devolatilisation is a key step of the gasification and combustion processes. These pyrolysis experiments were carried out to investigate what may take place in the fuel-rich zone of a gasifier or a combustor. This study of thermally thick samples will therefore be relevant for industrial processes such as biomass waste incineration and biomass gasification.

The exploitation of biomass residues is of particular relevance in agricultural areas where the intensive production of a plant will generate immense amounts of waste/by-products such as cherry stones [1], coffee husks [16], rice husks [17], cottonseed cake [18], coffee grounds [19], grape residues [14] or fruit bunches [20].

The biomass residues in this study have been selected because they cause problems for their producers for a variety of reasons (huge volumes, costs of treatment, non-satisfying present management).

Brewer Spent Grains (BSG) is the most abundant by-product of the beer brewing industry. Every litre of beer produced generates 0.03 kg of BSG (dry matter) [21]. The water content of BSG is typically 70–90% [21]. In this wet form, BSG deteriorates fast and is given away to farmers as cattle feed, but breweries are looking for more reliable and profitable solutions.

Green coffee beans are covered by a thin skin until it is blown away during roasting as the beans expand. This waste (designated here as "coffee waste") represents 1.5 wt% of the green coffee beans. In the example studied, coffee waste is roughly pelletised before being thrown away as household waste.

The last selected biomass fuel is an urban wood waste, fibreboard. Fibreboard is a processed biomass material commonly used in furniture. The sample studied is composed of spruce and pine with a urea–formaldehyde (UF) resin as binder.

The present study focuses on the temperature and heating rate dependence of the products yields and gas composition during pyrolysis of thermally thick biomass residues samples in an in-house designed and fabricated macro-TGA.

2. Apparatus and experimental procedure

2.1. Reactor

The reactor is basically a vertical stainless steel tube with an Al_2O_3 ceramic coating to minimise the catalytic reactivity of the walls. The reactor has an inner diameter of 0.1 m and a height of 1 m. It is heated by five independent heating elements; each heating element is regulated by two thermocouples installed at the surface of the tube reactor (diametrically opposed location). A pre-heater is used to heat the inert gas medium before entering the reactor. A suspension system holds a cylindrical-shaped wire mesh basket containing the sample. The basket is connected to a Sartorius CP 153 precision balance to record the weight loss of the sample during its thermal decomposition (not in focus in this article). A schematic diagram of the pre-heater, the reactor and the sampling line is shown in Fig. 1.

2.2. Procedures

Two types of experiments were carried out: "fast" heating rate pyrolysis experiments and "slow" heating rate pyrolysis experiments.

In the slow heating rate experiments, the basket, loaded with the sample, is first placed in the cold reactor. Then a N_2 (carrier

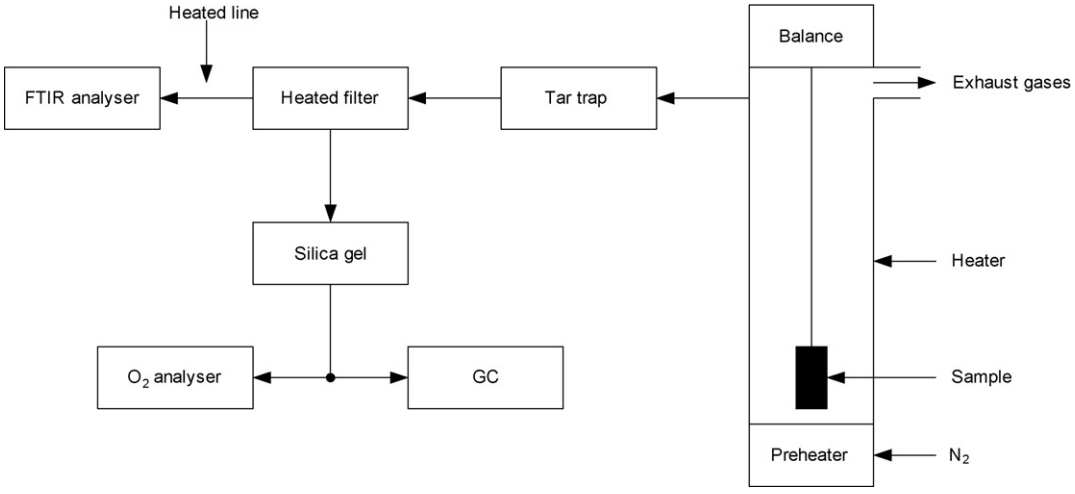

Fig. 1. Schematic diagram of the macro-TGA and the sampling line.

gas) flow of 40 Nl/min is established and is maintained at least 70 min to remove air from any part of the system. After this flushing period, the heating system is started (start of the run) to reach the final reactor temperature (900 °C) at the pre-designated heating rate (10 K/min). The final temperature is then held until no significant gas release is measured (about 30 min).

In the fast heating rate experiments, the procedure is quite different. A gas flow of nitrogen (40 Nl/min) is started to remove any air from the system while the heating system is connected to reach the appropriate reactor temperature. When the set reactor temperature is attained and the reactor has been flushed with nitrogen for at least 70 min, the basket containing the sample is rapidly lowered into the pre-heated reactor.

2.3. Sampling and analysis

Only a fraction of the exhaust gases (about 6 Nl/min) is going through a tar and water (ice + water)-cooled trap and a filtering system before it is analysed by a FTIR analyser and a micro-GC.

The FTIR analysis of the gases was performed with a Bomem 9100 analyser (sampling line and cell heated at 176 °C with a volume of 5 l and an optical path length of 6.4 m). The instrument is equipped with a DTGS detector (and a MCT detector, not used in this study) at the maximum resolution of 1 cm^{-1}. The FTIR was used to quantify CO_2, CO, CH_4, C_2H_2, C_2H_4 (and HCN and NH_3, not presented here).

The gas samples were also quantified online using a Varian CP-4900 micro-gas chromatograph equipped with two TCD detectors and a double injector connected to two columns: a CP-PoraPLOT Q column (10 m length, 0.25 mm inner diameter and 10 μm film thickness produced by Varian, Inc.) to separate and quantify CO_2, CH_4, C_2H_2 + C_2H_4 (not separated) and C_2H_6 and a CP-MolSieve 5 Å PLOT column (20 m length, 0.25 mm inner diameter and 30 μm film thickness produced by Varian, Inc.) to analyse H_2, O_2, CH_4, CO and N_2. Helium and argon were used, respectively, as carrier gases in the two columns. Nitrogen (used as inert medium during the pyrolysis) was also quantified so that the volumetric flow rate of the other gas components at the exit could be determined by relative comparison.

Table 1 summarises the characteristics of the two measurement techniques used.

Complementary comments concerning FTIR and GC measurements:

- Whenever possible more than one IR-wavenumber was used for every species.
- FTIR gives one measuring point every minute (1 scan every 5 s, averaging value over 12 scans).
- GC gives one measuring point every 2.5 min approximately.
- Error calculation according to Ref. [22].

2.4. Temperature in the sample

Four k-type thermocouples were placed in the sample in order to measure the vertical (axial) and radial temperature gradients in the biomass sample (separate runs from the gas emission and weight loss experiments, not in focus in this study). The temporal and spatial evolution of the temperature is

Table 1
FTIR and GC characteristics

Species	CO_2	CO	CH_4	C_2H_2	C_2H_4	C_2H_6	H_2	O_2	N_2
Detected by	FTIR GC	FTIR GC	FTIR GC	FTIR GC	FTIR GC	GC	GC	GC	GC
Range FTIR	0–9 vol%	0–12 vol%	0–6 vol%	0–8000 ppm	0–2.1 vol%	–	–	–	–
Range GC	0–100 vol%	0–32.1 vol%	0–14.1 vol%	0–3.02 vol%	0–3.02 vol%	0–1.51 vol%	0–45.8 vol%	0–5.66 vol%	0–100 vol%
Wave number (cm^{-1}) FTIR	3664.55–3662.55 2 baselines	2006.00–2001.00	>2713.17–2710.25 >2744.00–2740.16	>4090.72	>1081.85–1078.12 >1857.31–1855.38	–	–	–	–
Quantification methods FTIR	Height and area	Height and area	Height and area	Only height	Height and area	–	–	–	–
Comments GC	–	Slight interference with CH_4	2 columns used	Measured with C_2H_4	Measured with C_2H_2	–	–	O_2 analyser too	–
Relative standard deviation[a] (%)	4.7	8.5	2.2	n.a.	n.a.	–	–	–	–
Minimum standard deviation[a] (vol%)	0.04	0.08	0.01	0.02[b]	0.02[b]	–	–	–	–

n.a.: Not applicable.
[a] For FTIR analyser only.
[b] Standard deviation up to 1 vol%. Covers all the experimental points.

Table 2
Thermal history of coffee waste

	Fast heating rate (600 °C)	Fast heating rate (900 °C)	Slow heating rate
Average sample temperature (°C)	258	555	495
Average sample heating rate (°C/min)	40	115	8.3
Sample temperature at pyrolysis' start (°C)	[a]	[a]	131
Sample temperature at pyrolysis' end (°C)	460	850	859

[a] Pyrolysis process starts instantly after introduction. Not possible to determine a start temperature.

an important aspect of the pyrolysis process. The temperature profile inside thermally thick samples will depend on the physical and chemical properties of the sample and the temperature of the gas medium (reactor temperature). Some typical characteristic temperatures and heating rates are presented in Table 2 for coffee waste. Average sample temperature is the temperature between introduction of the sample in the pre-heated reactor (or start of the weight loss for slow heating rate experiments) and the end of the pyrolysis process (determined by the end of weight loss). Average heating rates are calculated similarly.

2.5. Biomass characteristics

The experimental setup aforementioned was used to study the pyrolysis of three different biomass residues: BSG, coffee waste and fibreboard. Table 3 shows the proximate analysis, the ultimate analysis and the gross calorific values of the samples, measured according to ASTM standards. The proximate analysis reveals that the three selected residues are quite similar except for the low ash content and higher volatile matter of the fibreboard. The ultimate analysis shows a slightly lower carbon and hydrogen content (and higher oxygen content) in fibreboard compared to BSG and coffee waste. Furthermore, the biomass residues studied have a very high nitrogen content (3–4 wt%) compared to most biomass samples. The N-content of wood stems is about 0.1 wt%, bark exhibits N-concentrations up to 0.5 wt% and fresh peat up to 1 wt%.

Table 3
Proximate analysis, ultimate analysis and heating values of the samples

	BSG	Coffee waste	Fibreboard
Proximate analysis (wt%, dry basis)			
Volatile matter	78.75	76.67	81.95
Fixed carbon	16.22	16.75	17.61
Ash	5.03	6.58	0.44
Ultimate analysis (wt%, dry ash free basis)			
Carbon	51.59	51.33	48.80
Hydrogen	7.07	6.79	6.33
Nitrogen	4.15	3.02	3.62
Sulfur	0.23	0.21	<0.02
Oxygen (by difference)	36.96	38.65	41.25
Gross calorific value (MJ/kg)	20.83	19.82	19.81

Table 4
Physical properties of the biomass samples

Biomass	Bulk density (kg/m^3)	Particle size (mm)	Sample height (mm)
BSG	188	0.06–1	120
Coffee waste	283	up to 15 × 15 × 5	80
Fibreboard	226	10 × 10 × 100	100

Table 4 presents the main physical characteristics of the samples studied: bulk density, particle size and height. The BSG was acquired from a Danish brewery. Except oven-drying, no pre-treatment before pyrolysis was applied. The coffee waste was collected from a local roasting company and dried. The sample size (diameter) was up to 15 mm and retains the lamellar structure of the original collected material. The fibreboard was collected from a local furniture store. It was cut into a 10 mm × 10 mm × 100 mm parallelepiped and oven-dried.

3. Results and discussion

3.1. Product yields and GCV: influence of temperature

Fig. 2 presents the total mass yield of the pyrolysis products and the mass yields of the main gaseous products for the fast heating rate experiments at different reactor temperatures. Only FTIR results were used for integration of the gas measurement results. GC results were not used for integration purposes because of insufficient resolution.

In accordance with the literature [6,14,15,23], an increase in temperature induces an increase in gas yield: from 30–35 wt% for all biomass residues to 52–57 wt% for BSG and fibreboard and 65 wt% for coffee waste.

Furthermore, temperature has not only a positive effect on the total amount of gas generated but also on the individual gases production. This behaviour reflects the fact that the main pyrolysis gases are formed through thermally favoured reactions such as cracking, depolymerisation, decarboxylation or oxidation [1]. CO_2 and CO are always the main pyrolysis products (CO contribution represents 45.9 wt% of the total amount of gas released and CO_2 37.2 wt% for fibreboard at 750 °C) but their temperature dependence differs. The CO yield is increasing 2–3 fold between 600 and 900 °C from 5.7–19.2 wt% for coffee waste for example, while the CO_2 yield is only slightly increasing or stabilising at high temperature (825–900 °C); e.g. the CO_2 yield is 18 wt% at 825 °C and 18.5 wt% at 900 °C for BSG. The tendency of the CO_2 yield to stabilise or decrease at high temperature has often been reported and attributed to the fact that CO_2 is a product of the pyrolysis of cellulose and hemicellulose by a path less favoured by increasing temperature [14].

CH_4, C_2 hydrocarbons and H_2 are the minor products. Methane yields range from 2.4 wt% (coffee waste and fibreboard) at 600 °C to around 6% at 900 °C. C_2 yields are

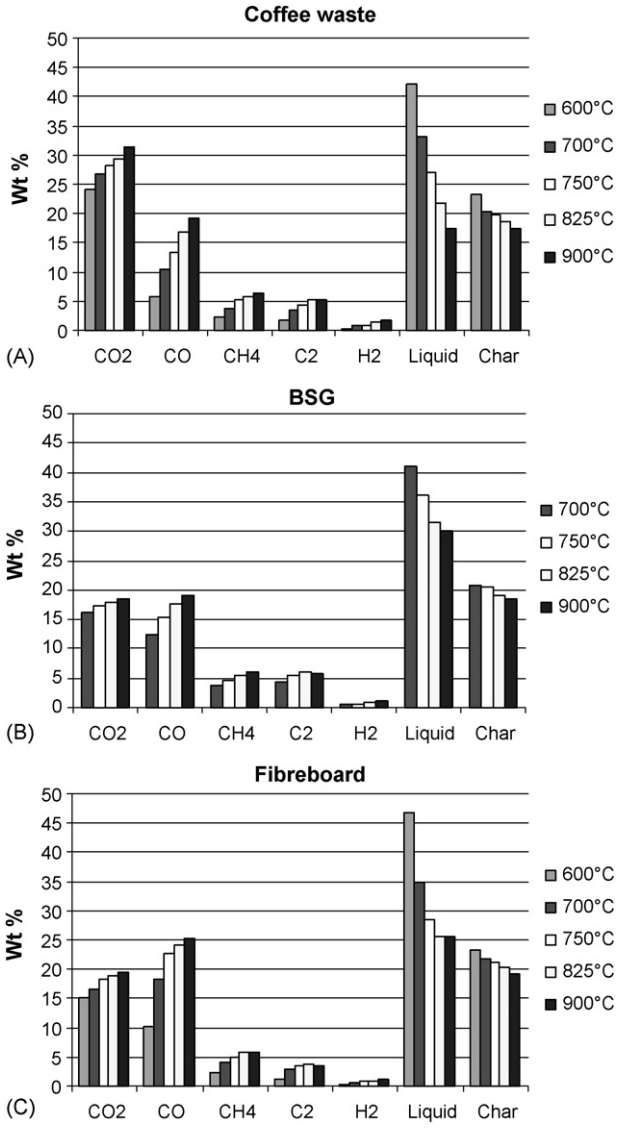

Fig. 2. Wt% of the various fractions at different temperatures (fast heating rate experiments). Dry ash free basis. Liquid calculated by difference.

also increasing greatly with temperature from 1.6 wt% at 600 °C to 5.2 wt% at 900 °C for coffee waste. However, it is important to notice that CH_4 yields reach a plateau, slightly increase or slightly decrease depending on the fuel at 825–900 °C because of increasing cracking at high temperature. Between 825 and 900 °C, C_2 yields are: stable at 5.2 wt% for

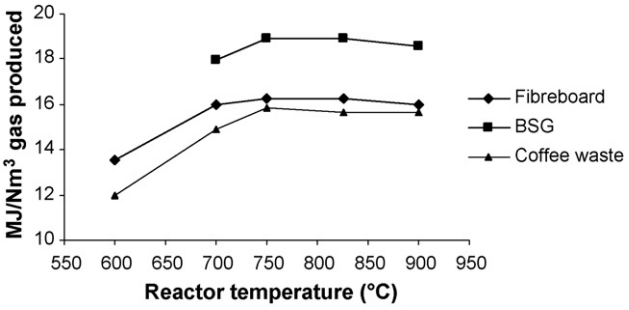

Fig. 3. Calculated GCV of the pyrolysis gas at different temperatures.

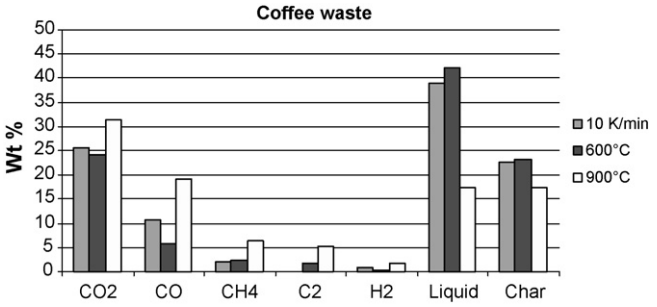

Fig. 4. Wt% (dry ash free basis) of the various fractions for coffee waste (slow and fast heating rate experiments).

coffee waste, decreasing moderately from 3.9 to 3.6 wt% for fibreboard and from 6.1 to 5.9 wt% for BSG. The H_2 yield, a product of cracking, is increasing sharply with temperature from less than 0.5 wt% at 600 °C to approximately 1.1–1.2 wt% for BSG and fibreboard and 1.7 wt% for coffee waste at 900 °C.

The increase in gas yield with temperature is coinciding with a decrease in char and liquid yields. The results obtained show a definite tendency of decreasing char yield with increasing temperature. All the residues have comparable char amounts. Char production will decrease from about 23 wt% at 600 °C to 17–19 wt% at 900 °C for the biomass residues studied.

The maximum liquid yield has usually been evaluated to be located in the temperature range 500–550 °C, so the liquid yield measured in this study at 600 °C is probably not the highest value accessible with this setup; however, the optimisation of the liquid yields was not in the focus of this study. The liquid yield generated from fibreboard decreases from 47 wt% at 600 °C to around 25 wt% at 900 °C.

The trends concerning the different products yields are similar and the range of the results is in agreement with literature [6,14,15,23].

Fig. 3 presents the gross calorific values (GCV) of the pyrolysis gas (based on the gross heat of combustion of the individual gases) for the ''fast'' pyrolysis experiments. This gas can be considered of low to medium heating value. As mentioned earlier, it can be used for heat production (feedstock drying), power generation or to provide the energy necessary to support the pyrolysis process.

The GCV of the pyrolysis gas is increasing with temperature between 600 and 750 °C before reaching a plateau to attain approximately 19 MJ/kg for BSG, 15.7 MJ/kg for coffee waste and 16.3 MJ/kg for fibreboard.

3.2. Product yields: influence of heating rate

Figs. 4–6 show the results obtained for the slow heating rate experiments and the fast heating rates experiments at the two extreme values of 600 and 900 °C (700 and 900 °C for BSG).

The integrated results obtained with the slow heating rate are quite similar to those obtained at 600 °C with sudden introduction of the sample in a pre-heated reactor, especially when it comes to products distribution. However, compared to

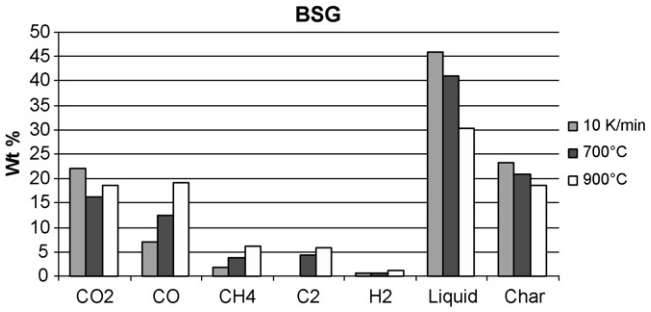

Fig. 5. Wt% (dry ash free basis) of the various fractions for BSG (slow and fast heating rate experiments).

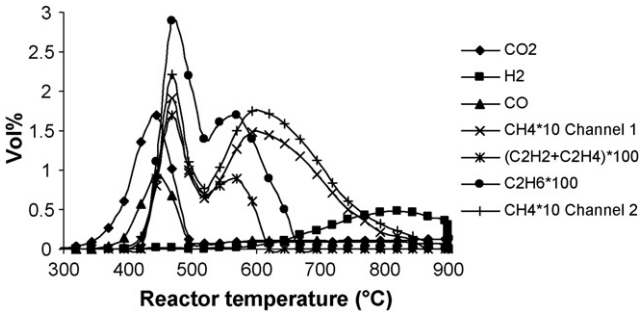

Fig. 7. Gas release profiles for fibreboard (slow heating rate).

the results obtained at 900 °C with rapid introduction, it can be seen that the slow heating rate promotes char and liquid yields as gas formation is a thermal process [1]. The gas yield is 38.3 wt% at slow heating rate for coffee waste, while it is 65.3 wt% at 900 °C (fast sample introduction).

3.3. Gas dynamics (release profiles)

3.3.1. Slow heating rate (10 K/min)

Detailed studies of the gas release dynamics are important to understand the processes going on during thermal decomposition of the residues. All the main components (CO_2, CO, CH_4, H_2 and C_2 hydrocarbons) exhibit a double-maxima release profile or a main release peak followed by a shoulder or lower emissions over a long period of time (Fig. 7). This pattern can be explained by the biomass structure [1,4].

The main constituents of biomass are lignin, hemicellulose and cellulose [14,24,25], the proportion of each constituent differs with the species. Moreover, BSG contains proteins (21–32 wt%) [21,26] while the N-containing fraction of coffee waste is not accurately identified, it includes proteins and alkaloids residues [27]. Lignin is a very complex aromatic structure, hemicellulose is a polymer of 5- and 6-carbon sugars and cellulose is a polymer of glucose [24]. Those structural differences have an influence on the thermal decomposition behaviour of the biomass. TGA studies [1,4,14,23] have shown that the decomposition of biomass components is happening at different temperatures: hemicellulose is decomposing between 200 and 375 °C, cellulose is decomposing at slightly higher temperatures, between 275 and 380 °C, leading to the double-maxima release profile observed. Lignin is decomposing gradually over a wide range of temperatures (180–550 °C), and is therefore producing low gas yields over a long period of time often referred to as a tail [1]. The multi-stage evolution of products for fibreboard can be characterised by the early release of CO_2 and CO starting around 270–295 °C and reaching a first peak around 445–460 °C, followed by the release of hydrocarbons starting around 420–445 °C with the first peak around 470–495 °C, then lower concentrations of CO and CO_2, originating from lignin, are observed during the remaining time of the heating period. The second small CO_2 peak is located at 900 °C and the second CO peak occurs at approximately 670 °C. Hydrogen is released at high temperature because it is originating from cracking of volatiles and therefore requires high temperatures (no significant release before a reactor temperature of 600 °C) and exhibits its peak value at approximately 820 °C; long after all the other gas species. Furthermore, a very small hydrogen release maximum, also observed by others, is visible around 470 °C [1]. The three samples exhibit very similar release patterns except for the fact that the main CH_4 peak of fibreboard happens earlier and faster than for BSG and coffee waste.

3.3.2. Fast heating rate

At high heating rates (‘‘fast’’ pyrolysis), the release patterns (Fig. 8) of the main gases differ noticeably from the experiments at slow heating rates; no double-maxima release patterns is observed as decomposition of hemicellulose, cellulose and lignin is occurring almost simultaneously.

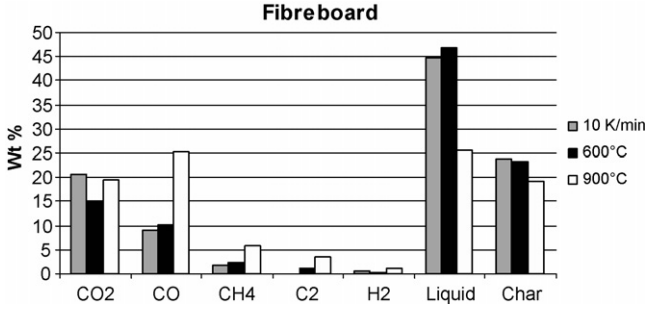

Fig. 6. Wt% (dry ash free basis) of the various fractions for fibreboard (slow and fast heating rate).

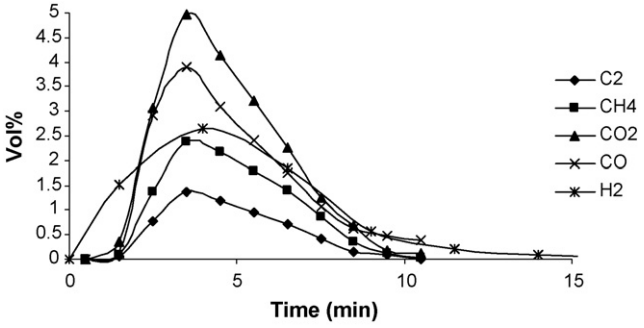

Fig. 8. Gas release at fast heating rate for coffee waste at 750 °C.

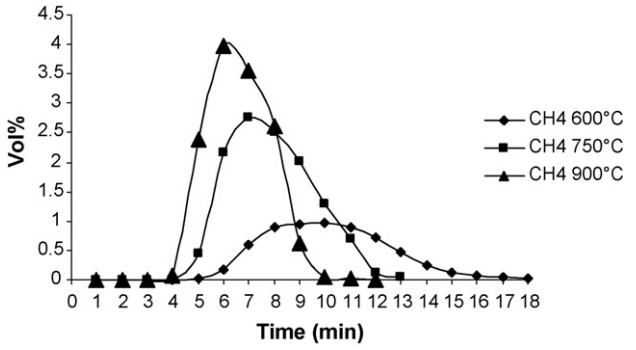

Fig. 9. CH_4 release during fast heating rate experiments at different reactor temperatures for fibreboard.

The gas production release pattern of each gas is greatly affected by the reactor temperature. The higher the reactor temperature the higher is the maximum concentration and the shorter is the time necessary to reach this maximum. The release time of the gas is also drastically reduced by increasing temperature; Fig. 9 shows CH_4 release at different temperatures for fibreboard; its release is taking approximately 6 min at 900 °C, 8 min at 750 °C and 13 min at 600 °C.

4. Conclusions

Pyrolysis of thermally thick samples of three biomass residues has been investigated. For all fuels, higher temperatures favour gas yield at the expense of char and liquid yields. High heating rate also promotes gas yield.

The main gas components, identified and quantified online with the use of an FTIR analyser and a micro-GC, were CO_2, CO, CH_4, H_2, C_2H_2, C_2H_6 and C_2H_4. An increase in temperature and heating rate leads to increasing yields for all the gases up to 825–900 °C where CO_2 and hydrocarbons yields show a clear tendency to stabilise, increase slightly or decrease slightly depending on the fuel.

The gas release dynamics reveal important information about the thermal behaviour of the various components (cellulose, hemicellulose and lignin) of the biomass and are consistent with previous literature studies using TGA. The gross calorific value of the gas produced increases with increasing temperature reaching a plateau at 750–900 °C. This study provides valuable data of the thermal behaviour of thermally thick biomass samples which is of interest for further work in the area of combustion, gasification and pyrolysis in fixed beds. The study confirms the potential of those unexploited residues for production of energy carriers through pyrolysis.

Acknowledgements

This work has been part of the ‘‘Environment and Process Management’’ research program, funded by the Research Council of Norway. The main author also expresses his gratitude to the Nordic Graduate School of Biofuels Science and Technology (biofuelsGS) for providing financial support.

References

[1] J.F. González, J.M. Encinar, J.L. Canito, E. Sabio, M. Chacón, J. Anal. Appl. Pyrolysis 67 (2003) 165.
[2] J.M. Encinar, F.J. Beltrán, A. Bernalte, A. Ramiro, J.F. González, Biomass Bioenergy 11 (1996) 397.
[3] S. Czernik, A.V. Bridgwater, Energy Fuels 18 (2004) 590.
[4] P.T. Williams, S. Besler, Renewable Energy 7 (1996) 233.
[5] J.M. Encinar, J.F. González, J. González, Fuel Process. Technol. 68 (2000) 209.
[6] J.L. Figueiredo, C. Valenzuela, A. Bernalte, J.M. Encinar, Fuel 68 (1989) 1012.
[7] J. Leppälahti, P. Simell, E. Kurkela, Fuel Process. Technol. 29 (1991) 43.
[8] C. Acikgoz, O. Onay, O.M. Kockar, J. Anal. Appl. Pyrolysis 71 (2004) 417.
[9] E. Schröder, J. Anal. Appl. Pyrolysis 71 (2004) 669.
[10] Ö. Onay, S.H. Beis, Ö.M. Koçkar, J. Anal. Appl. Pyrolysis 58–59 (2001) 995.
[11] M.M. Barbooti, J. Anal. Appl. Pyrolysis 13 (1988) 233.
[12] A.A. Zabaniotou, D. Gogotsis, A.J. Karabelas, J. Anal. Appl. Pyrolysis 29 (1994) 73.
[13] R. Bilbao, J. Arauzo, M.B. Murillo, M.L. Salvador, J. Anal. Appl. Pyrolysis 43 (1997) 27.
[14] C. Di Blasi, G. Signorelli, C. Di Russo, G. Rea, Ind. Eng. Chem. Res. 38 (1999) 2216.
[15] S.M. Andersen, S.T. Pedersen, B. Gøbel, N. Houbak, U. Henriksen, J.D. Bentzen, in: S. Kjelstrup, J.E. Hustad, T. Gundersen, A. Røsjorde, G. Tsatsaronis (Eds.), Shaping Our Future Energy Systems, Proceedings of ECOS 2005, Trondheim, Norway, June 20–22, (2005), p. 1657.
[16] M. Saenger, E.-U. Hartge, J. Werther, T. Ogada, Z. Siagi, Renewable Energy 23 (2001) 103.
[17] M. Fang, L. Yang, G. Chen, Z. Shi, Z. Luo, K. Cen, Fuel Process. Technol. 85 (2004) 1273.
[18] N. Özbay, A.E. Pütün, B.B. Uzun, E. Pütün, Renewable Energy 24 (2001) 615.
[19] M.A. Silva, S.A. Nebra, M.J. Machado Silva, C.G. Sanchez, Biomass Bioenergy 14 (1998) 457.
[20] Bioenergy International No. 16, 5-2005 www.bioenergyinternational.com.
[21] J. Grøndal, in: United Milling Systems A/S, Technical University of Denmark, Carlsberg Research Laboratory (Eds.), Utilization of Brewers Spent Grains Fractions as Ingredients in the Food and Feed Industry, An Industrial Research Education Programme under the Danish Academy of Technical Sciences, project no. 244, 1990.
[22] S.L.R. Ellison (LGC, UK), M. Rosslein (EMPA, Switzerland), A. Williams (UK) (Eds.), EURACHEM/CITAC Guide, Quantifying Uncertainty in Analytical Measurement, second ed., 2000 http://www.measurementuncertainty.org/mu/QUAM2000-1.pdf.
[23] M. Grønli, A Theoretical and Experimental Study of the Thermal Degradation of Biomass, Ph.D. Thesis NTNU (Norwegian University of Science of Technology), 1996.
[24] M. Stenseng, Pyrolysis and Combustion of Biomass, Ph.D. Thesis DTU (Technical University of Denmark), 2001.
[25] K.-M. Hansson, Principles of Biomass Pyrolysis with Emphasis on the Formation of the Nitrogen-Containing Gases HNCO, HCN and NH_3, Ph.D. Thesis, Chalmers University of Technology, 2003.
[26] M. Santos, J.J. Jiménez, B. Bartolomé, C. Gómez-Cordovés, M.J. del Nozal, Food Chem. 80 (2003) 17.
[27] M.C. Baquero, L. Giraldo, J.C. Moreno, F. Suárez-García, A. Martínez-Alonso, J.M.D. Tascón, J. Anal. Appl. Pyrolysis 70 (2003) 779.

Paper IV

NOx and N_2O precursors (NH_3 and HCN) in pyrolysis of biomass residues

Becidan M., Skreiberg Ø., Hustad J.E.

Energy & Fuels 21 (2007) 1173-1180.

Paper IV is not included due to copyright.

Paper V

Thermal decomposition of biomass wastes. A kinetic study.

Becidan M., Várhegyi G., Hustad J.E., Skreiberg Ø.

Industrial & Engineering Chemistry Research 46 (2007) 2428-2437.

Paper V is not included due to copyright.

Paper VI

Experimental study on pyrolysis of thermally thick biomass residues samples: intra-sample temperature distribution and effect of sample weight ("scaling effect")

Becidan M., Skreiberg Ø., Hustad J.E.

Accepted for publication 2 March 2007. Available online 2 April 2007. Fuel.

Available online at www.sciencedirect.com
ScienceDirect
Fuel xxx (2007) xxx–xxx
FUEL
www.fuelfirst.com

Experimental study on pyrolysis of thermally thick biomass residues samples: Intra-sample temperature distribution and effect of sample weight (“scaling effect”)

Michaël Becidan *, Øyvind Skreiberg, Johan E. Hustad

NTNU, Department of Energy and Process Engineering, Kolbjørn Hejes vei 1A, 7491 Trondheim, Norway

Received 8 October 2006; received in revised form 19 January 2007; accepted 2 March 2007
Available online 2 April 2007

Abstract

This study on thermally thick biomass residues (brewer spent grain, fibreboard and coffee waste) pyrolysis has been investigating two aspects: temperature history and weight loss characteristics. Significant temperature gradients were measured and will affect the pyrolysis chemistry. Three temperature regimes have been identified: (1) exponentially increasing temperature, (2) linearly increasing temperature and (3) 2-slope increasing temperature with a flattening period. The regime at a given point will depend on the sample weight, the reactor temperature and the location in the sample. The exothermic step of pyrolysis was shown. The comparative study of weight loss curves obtained in a TGA and a macro-TGA shows that pyrolysis rate and duration are affected.

Keywords: TGA; Biomass pyrolysis; Temperature

1. Introduction

Thermal gravimetric analysis (TGA) is an experimental technique recording continuous data of weight loss as a function of time as the sample is heated at a given rate. When studying samples of a few milligrams, the thermal processes undergone by the material are controlled by chemical kinetics. TGA studies are useful for the comprehension of pulverised fuel thermal conversion and to acquire knowledge about the chemical structure and stability of materials. Biomass thermal decomposition in an inert atmosphere can be described as the sum of the decomposition of its main components, i.e. cellulose, hemicellulose and lignin [1–3]. Calculation of reliable kinetic parameters requires complex models. This is due to the complexity and heterogeneity of biomass [4]. The fuels studied in this article are biomass residues. When the samples studied are large samples (thermally thick samples), a substantial temperature gradient within the particle occurs during conversion. The study of thermally thick particles is therefore relevant for industrial fixed bed thermal conversion of biomass as industrial applications rarely use solid fuels in the form of small particles. Knowledge about the thermal behaviour of large biomass samples is a key element to optimise thermal treatment [5]. The set-up employed allows the investigation of thermally thick samples while having good control and monitoring the conditions. Modelling of the thermally thick regime [1,6–9] requires the coupling of chemical kinetics and transport phenomena. Pyrolysis is of special relevance as it is a conversion technology and an important phase in combustion and gasification. The two goals of this study are to investigate: (1) temperature history: (a) qualitative and quantitative effect of temperature (fast heating rate), (b) interpretation in terms of chemistry of pyrolysis (slow heating rate); and (2) weight loss and effect of sample weight: comparison between TGA and

* Corresponding author. Tel.: +47 73 59 29 11; fax: +47 73 59 83 90.
E-mail address: michael.becidan@ntnu.no (M. Becidan).

0016-2361/$ - see front matter © 2007 Elsevier Ltd. All rights reserved.
doi:10.1016/j.fuel.2007.03.007

macro-TGA to expose the practical effect of transport phenomena (“scaling effect”). This has never been done before to our knowledge.

2. Experimental

2.1. Sample properties

Pyrolysis experiments were performed with about 75 g of dry biomass residues (brewer spent grain (BSG), fibreboard (FB) and coffee waste (CW) [10]) in nitrogen. The chemical and physical properties of the samples are shown in Table 1. Except oven-drying at 105 °C no pre-treatment was applied to study the samples “as received”.

2.2. The macro-TGA reactor (and procedures)

The experiments were carried out in an in-house designed and fabricated macro-TGA [10]. A suspension system holds the cylindrical wire mesh basket (diameter: 6.5 cm, height: 11.5 cm). The basket is connected to a Sartorius CP 153 precision balance.

Two procedures were carried out and described in [10]: “fast/high” heating rate pyrolysis (sudden introduction in a hot reactor) and “slow/low” heating rate pyrolysis (application of a 10 °C/min heating rate at the reactor walls). To measure the temperature history, separate runs were necessary as the thermocouples disturbed the weight loss recording. Four *k*-type thermocouples with a diameter of 0.5 mm were placed in the sample to measure the vertical (axial) and horizontal (radial) temperature gradients (based on the discrete temperature measurements). Their location is shown in Fig. 1. Placing the thermocouples was done manually each time and their location may vary slightly.

Table 1
Chemical and physical properties of the samples

	BSG	Coffee waste	Fibreboard
Proximate analysis (wt%, dry basis)			
Volatile matter	78.75	76.67	81.95
Fixed carbon	16.22	16.75	17.61
Ash	5.03	6.58	0.44
Ultimate analysis (wt%, dry basis)			
Carbon	51.59	51.33	48.80
Hydrogen	7.07	6.79	6.33
Nitrogen	4.15	3.02	3.62
Sulfur	0.23	0.21	<0.02
Oxygen (by difference)	36.96	38.65	41.25
Physical properties			
Bulk density (kg/m^3)	188	283	226
Particle size (mm)	0.06–1	up to $15\times15\times5$	$10\times10\times100$
Sample height (mm)	120	80	100
Main N-compounds	Proteins	Alkaloids, proteins	UF resin
N-compounds concentration (wt%, dry basis)	~26 [11–13]	Not found	~10 [14]

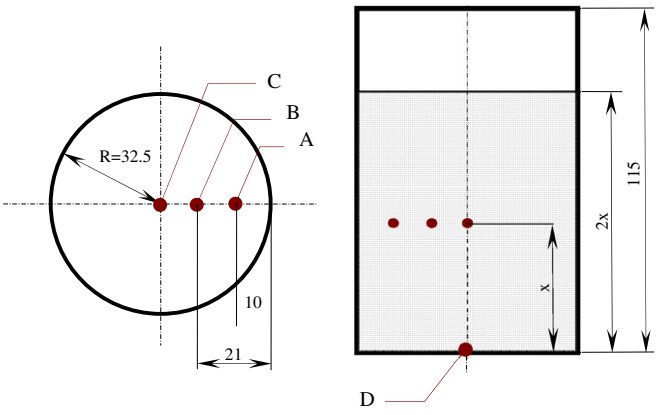

Fig. 1. Top view (left) and side view (right) of the basket sample and location of the four thermocouples (A, B, C and D). Grey shade represents the sample (Coffee waste, CW). Dimensions in mm (2*x* represents the total height of the sample).

3. Results and discussion

3.1. Temperature history

3.1.1. Fast heating rate experiments: qualitative and quantitative influence of temperature

The temperature history inside thermally thick samples is, apart from weight loss, the most important characteristic of pyrolysis. The temperature history is related to the properties (physical and chemical) of the sample and its interaction with the hot gas medium and the reactor. As the conditions are not isothermal, temperature distribution may reveal important gradients, which may affect fundamental features of the pyrolysis process, i.e. weight loss and products distribution and composition [7,15].

Fig. 2 shows the temperatures measured at three locations (see Fig. 1 for exact location) in CW during fast heating rate experiments at 600 and 900 °C. At 900 °C, the temperatures A, B (and D, not shown) are increasing very sharply/exponentially right after introduction in the hot reactor. However, deep in the sample (location C), the temperature profile reaches a plateau, before increasing at a heating rate close to the one at the outer locations. At 600 °C, in the innermost part of the sample (location C), temperature flattens over a long period of time (longer period than at 900 °C) before increasing vigorously. Tempera-

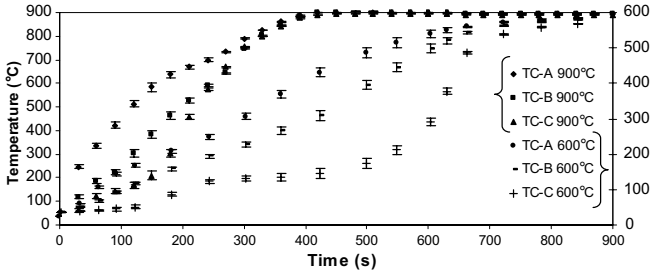

Fig. 2. Fast heating rate: temperature distribution. Coffee waste (CW). Bars show uncertainty. TC: thermocouple.

tures A, B (and D, not shown) are increasing linearly, which represent an intermediate case between the exponentially increasing temperature of the outer part of the sample and the 2-slope (plateau and increase) temperature profile, since the heat flux from the gas medium is smaller at 600 than at 900 °C. The 2-slope temperature profile behaviour observed deep in the sample can be explained by the thermal history of the outer regions of the sample (retardation due to endothermic decomposition) and by the different thermal conductivities and heat capacities of the charring layer and the unreacted substrate: the effective thermal conductivity of the inner regions of the sample is changing as the pyrolysis front is progressing [1,6,8,15].

Three main temperature regimes may be distinguished, the importance of each regime depending on the external temperature and the sample properties: (1) exponentially increasing temperature (outer regions of the sample at sufficiently high temperature), (2) linearly increasing temperature (at intermediate depths or lower temperatures) and (3) 2-slope increasing temperature (inner regions of the sample) with a flattening period/plateau for a duration increasing with decreasing temperature.

In order to quantitatively describe the temperature history, several parameters were compiled in Table 2 and gradients presented in Fig. 3. A maximum radial gradient of 167 °C/cm is observed at a reactor temperature of 900 °C. The higher the temperature, the higher the gradients in the sample but the difference (peak value) is not significant as an increase of 50% of the reactor temperature only provokes an increase of about 10% for the gradient peak value. Furthermore, the higher the reactor temperature, the steeper the increase and the shorter the total duration of the gradient, i.e. less time is necessary to "balance" the temperature in the sample. The end of the pyrolysis process (determined by the end of weight loss) is accompanied by an abrupt fall of the gradient at 600 °C while at 900 °C the sample temperature is homogeneous before the pyrolysis process is over.

In order to study further the thermal history of the sample, a novel parameter was investigated: *the intra-sample heating rate* which corresponds to the heating rates at the locations A, B and C, i.e. dT_A/dt, dT_B/dt and dT_C/dt. By studying the actual thermal field *inside* the sample, internal phenomena may be disclosed. Fig. 4 presents the results for CW at 600 and 900 °C. At 600 °C, several events can be listed: very fast heating of the outer regions of the sample (location A) to attain a heating rate of about 150 °C/min, thereafter successive smaller "introduction peaks" can be observed at locations B and C. However, the heating rate at location B is stable (at 50 °C/min) until increasing to almost 100 °C/min after 480 s, as the pyrolysis front is reaching this point. As the pyrolysis front is propagating deeper in the sample, the heating rate at C (centre of the sample) is exhibiting a steep increase and reaches 250 °C/min (after 630 s) for a short time. Fig. 4 also presents the intra-sample heating rates at a reactor temperature of 900 °C. The general temperature profiles are similar to the experiment at 600 °C. The intra-sample heating rates observed at 900 °C are fourfold higher than at 600 °C. The experimental noise is due to movements in the sample (fall of matter, shrinking).

Table 2
Pyrolysis temperature history parameters (radial)

	600 °C	900 °C
Fuel	CW	CW
Total duration of gradient (s)	1340	454
Average temperature during pyrolysis (°C)	241 (25)	523 (29)
Gradient: increase/decrease (s)	497/843	144/268
Max gradient (°C/cm)	143 (20)	167 (24)
Heating rate (°C/min)	40	121
Gradient: maximum (s)	513	150
Gradient: start/end (s)	16/1356	6/460
Duration of pyrolysis (s)	600	415

Fast heating. Uncertainty given in brackets.

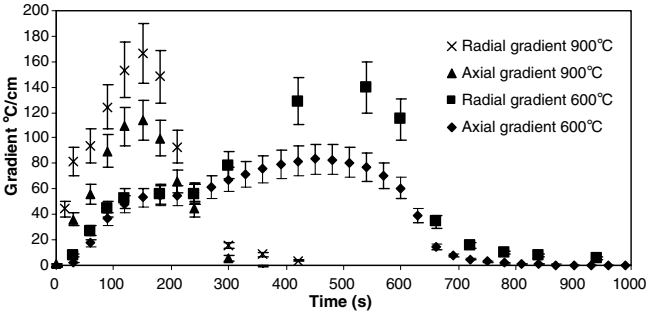

Fig. 3. Fast heating rate: temperature gradients at different temperatures. Coffee waste (CW). Bars show uncertainty.

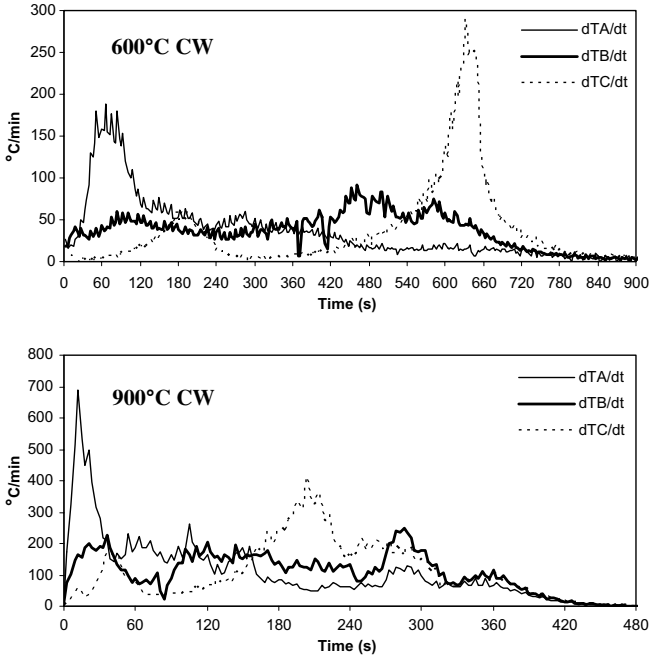

Fig. 4. Fast heating rate: intra-sample heating rates.

Please cite this article in press as: Becidan M et al., Experimental study on pyrolysis of thermally thick biomass ..., Fuel (2007), doi:10.1016/j.fuel.2007.03.007

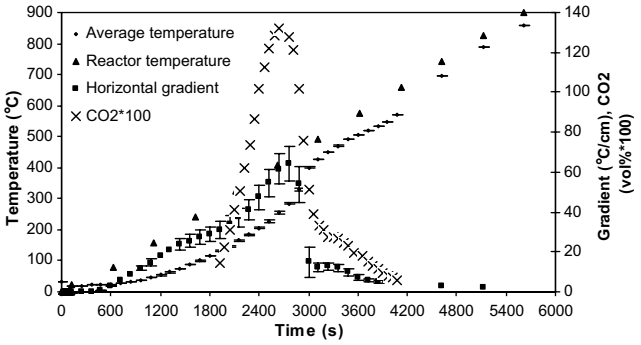

Fig. 5. Slow heating rate. Coffee waste (CW). Bars show uncertainty.

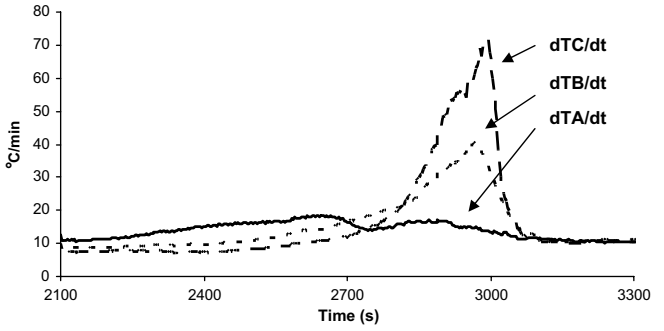

Fig. 6. Slow heating rate: intra-sample heating rate. Coffee waste (CW). Detail of the endothermic/exothermic pyrolysis. Trendlines (moving average).

3.1.2. Slow heating rate (10 °C/min) experiments: chemistry of pyrolysis

Just like "traditional" TGA, macro-TGA studies at a moderate heating rate provides more information than fast heating rate experiments as the processes (drying, start of pyrolysis, progression of the reacting front, decomposition) are not happening (too) fast and/or simultaneously but, at least partly, successively and may therefore be characterised (start and end, peak values, etc.) [1,2].

To describe the temperature history during slow heating rate experiments, Fig. 5 shows the reactor temperature, the average sample temperature (based on thermocouples A, B and C), the horizontal gradient and CO_2 release (to show pyrolysis advancement). The average temperature inside the sample is significantly lower than the reactor temperature (measured at the reactor wall), the maximum difference is reached at a reactor temperature of about 370 °C with a value of 170 °C. While the reactor temperature is following a linear profile, the shape of the average temperature in the sample exhibits different slopes (i.e. varying intra-sample heating rates) during the heating period, revealing the heat transfer limitations. The different heating rates were caused, as previously mentioned, by the changing thermal properties of the sample during the progression of the pyrolysis front and the thermal history of the outer regions of the sample. Moreover the intra-sample heating rates expose the steps of the pyrolysis process (quantitative description in Table 3) which may be correlated to pyrolysis chemistry. Pyrolysis (of CW) may be described as follows:

1. No process detectable (0–300 s).
2. Linear heating of the sample, no weight loss yet (300–1800 s).
3. Weight loss is starting together with CO_2 release (Fig. 5) as the *endothermic pyrolysis* is taking place. The heating rate at the outermost thermocouple (A) is exceeding the heating rate of the reactor after about 2100 s as *exothermic pyrolysis* is commencing at this location (2100–2400 s, see Fig. 6) but not yet at locations B and C.
4. Progressive increase of the intra-sample heating rates at the other locations after about 2400 s (B and C, see Fig. 6) as the *exothermic pyrolysis* has now propagated inwardly. Pyrolysis is, overall, an endothermic process. However, two distinct pyrolysis steps have been characterised through DSC studies. The first step, or primary pyrolysis, is endothermic and is characterised by the release of volatiles. The second pyrolysis step has an exothermic heat of reaction and is associated with char-forming processes and/or further reactions of the primary char [16–19]. A linear relationship between increasing exothermicity and increasing final char yield has been observed [16,18]. T_{shift}, i.e. the turning point from endo- to exothermic pyrolysis, was located at around 380 °C by [20]. T_{shift} was evaluated at 350–400 °C (2400–2700 s after start) for CW in the present experiments. *To our knowledge, it is the first time that the exothermic pyrolysis is exposed experimentally through intra-sample temperature measurements.*

Table 3
Steps of the pyrolysis of a thermally thick sample

Step no. and fuel	Step description	Time (s)	Average temperature (A, B and C)[a] (°C)	Reactor temperature (°C)	Intra heating rate A/B/C (°C/min)	Reactor heating rate (°C/min)
1 CW	Start period	0–300	(21)	25–43 (30)	0	3.5
2 CW	Linear heating	300–1800	21–131 (60)	43–293 (167)	5.8/4.2/3.1	10.0
3 CW	Endothermic pyrolysis	1800–2400	131–228 (176)	293–392 (342)	12.6/9.2/7.4	9.9
4 CW	Exothermic pyrolysis[b]	2400–3000	228–428 (320)	392–491 (441)	15/20.7/24.3	9.9
5 CW	Exothermic pyrolysis end	3000–3100	428–446 (437)	491–508 (500)	11/10.9/10.6	10.0
6 CW	Linear heating	3100–5400	446–859 (644)	508–885 (698)	10.4/10.8/11.1	9.8
7 CW	End process	5400–6000	859–883 (875)	885–898 (896)	2.3/2.5/2.5	1.3

[a] Average temperature for a period given into brackets.
[b] Exothermic pyrolysis is starting at location A (outermost) after 2100 s but is starting after 2400 s at locations B and C.

Please cite this article in press as: Becidan M et al., Experimental study on pyrolysis of thermally thick biomass ..., Fuel (2007), doi:10.1016/j.fuel.2007.03.007

5. Abrupt end of the exothermic pyrolysis, the intra-sample heating rates go back to 10 °C/min (3000–3100 s, see Fig. 6).
6. A heating rate of about 10 °C/min is persisting as gases are still released (3100–5400 s).
7. Pyrolysis is completed, the reactor temperature is about 850–880 °C (5400–6000 s).

The same steps are present in FB with changes in time of occurrence, duration and intensity.

3.2. Weight loss: comparison of TGA and macro-TGA (10 °C/min), the "scaling effect"

The different thermal behaviours exhibited by a fuel heated at the "same" heating rate (applied at the reactor walls for the macro-TGA) at different sample scales show that the pyrolysis processes are different and/or controlled differently. On the one hand, pyrolysis of small (powdered) samples are strictly controlled by chemical kinetics, on the other hand pyrolysis of thermally thick samples are limited by transport phenomena. The kinetic investigation of the fuels can be found in [21] and the study of gas release in [10].

However, to our knowledge, no work has been done to *examine TGA results alongside macro-TGA results*. It may be argued that the different processes are complex and different but this study is limited to comparing and translating general differences into practical outcomes. The different phenomena occurring in thick and non-thick samples and their practical effect will be discussed. This study is aimed at supporting modelling approaches of thermally thick samples. Two series of experiments were carried out: (1) experiments in the macro-TGA, with the three biomass samples presented in Table 1; (2) experiments in a "traditional" TGA (SDT 2960 from TA Instruments). The sample weight was about 5 mg with a particle size of 43–65 μm. A heating rate of 10 °C/min was applied up to 900 °C in high purity N_2.

In this study, the weight loss curves were synchronised according to the measured temperature in the TGA and the reactor temperature measured at the reactor walls in the macro-TGA. The reactor temperature (rather than intra-sample temperatures) was chosen because it translates the effective heat effect provided by the reactor. In order to describe and compare the TGA and macro-TGA weight loss curves, 10 parameters commonly used to evaluate TGA curves [2] were listed (Tables 4 and 5): characteristic reaction temperatures, devolatilisation rates (dY/dt) and mass fractions (Y).

3.2.1. TGA experiments – comparison of the fuels

The degradation and kinetic investigation of the fuels were done in [21]. Some further remarks can be proposed here. The *degradation temperature ranges* are very similar (200–500 °C) for the three fuels as they all are lignocellulosic materials. The different concentrations and compositions of the various components will then affect the *pattern of the weight loss curves* (devolatilisation rates, number of peaks, T_{peak}).

3.2.2. Macro-TGA experiments – comparison of the fuels

The factors influencing decomposition are not only the operating conditions but also the intrinsic and physical properties of the fuel, such as density, thermal conductivity, heat capacity, porosity and particle size [6,7,15,20,22]. These properties change as decomposition occurs and will not be identical all over the sample.

The most significant difference for the decomposition patterns is the peak devolatilisation rates ($(dY/dt)_{peak}$; Y is the rest mass fraction) with a ratio of 2 between BSG and FB (Table 5). This may be due to the fact that FB exhibits larger particles than BSG and the hot gas medium can access them easier, accelerating the decomposition. However, TGA experiments show that FB also exhibits the highest $(dY/dt)_{peak}$ (Table 5) at the kinetic regime too; the respective influence of intrinsic and physical prop-

Table 4
Conversion characteristics: temperatures (°C)

Parameters	CW		FB		BSG	
	Macro	TGA	Macro	TGA	Macro	TGA
$T_{initial}$[a]	265	220	288	220	271	228
T_{start}[b]	220	173	252	170	236	169
$T_{shoulder}$	–	275	–	–	–	293
T_{peak}	360	329	364	362	360	351
$T_{5\%}$[c]	563	523	430	458	603	560

[a] $T_{initial}$ corresponds to a rest mass fraction of 0.975.
[b] T_{start} is the temperature at which $dY/dt = 2\%$ of (dY/dt) peak.
[c] Temperature at which dY/dt is back to a value of 5% of (dY/dt) peak.

Table 5
Conversion characteristics: mass fractions and devolatilisation rates

Parameters	CW		FB		BSG	
	Macro	TGA	Macro	TGA	Macro	TGA
$Y_{shoulder}$[a]	–	0.83	–	–	–	0.77
Y_{peak}	0.63	0.57	0.63	0.38	0.69	0.49
Char fraction	0.28	0.23	0.25	0.16	0.28	0.21
$(dY/dt)_{peak}$	0.0010 s^{-1}	0.0010 s^{-1}	0.0016 s^{-1}	0.0014 s^{-1}	0.0008 s^{-1}	0.0010 s^{-1}
$(dY/dt)_{shoulder}$	–	0.0006 s^{-1}	–	–	–	0.0009 s^{-1}

[a] Y: rest mass fraction.

Please cite this article in press as: Becidan M et al., Experimental study on pyrolysis of thermally thick biomass ..., Fuel (2007), doi:10.1016/j.fuel.2007.03.007

erties cannot be separated. Furthermore, the lower the $(dY/dt)_{peak}$, the broader the decomposition range.

3.2.3. Comparison of fuels – macro-TGA/TGA

The foremost difference is the shape of the DTG curves (not shown). While TGA-DTG reveals the composition of the fuels (presence of a shoulder for example), macro-TGA-DTG exhibit a simple bell shape. The macro-TGA curve represents the kinetic phenomena combined with the transport processes. Fig. 7 shows the degree of conversion $(1 - Y)$ as a function of time for both scales ($t = 0$ when heating is starting) for CW. It can be said that TGA studies yield *successive component-decompositions* (according to their respective intrinsic properties), while macro-TGA-DTG studies yield *successive fuel-layer-decompositions*: while some parts of a thermally thick sample will be pyrolysing, others will be unreacted and some others already charred with a variety of intermediary states. T_{start} and $T_{initial}$ (Table 4) for a given fuel are shifting towards lower values in TGA as devolatilisation is starting earlier (Fig. 7). T_{peak} are not shifting very significantly. The peak devolatilisation rates (Table 5) are not influenced by the change in scales and are sensibly the same in TGA and macro-TGA for a fuel. The char fraction increases from TGA to macro-TGA scales (see Table 5), showing that larger particles favour char-forming reactions. It also appears that materials in the TGA have reacted to a greater extent when T_{peak} has been reached compared to macro-TGA (Table 5). For example, 51% of the BSG has been vaporised in the TGA when T_{peak} is attained, while only 31% of BSG has done so in macro-TGA. This is a direct consequence of transport processes which are retarding decomposition towards higher reactor temperatures (see also Fig. 7). Completion of the degradation at thermally thick conditions is therefore more time-consuming.

3.2.4. "Scaling effect" – quantification

It can be assumed that the differences observed on the weight loss curves are directly due to the heat and mass transport phenomena. The "scaling effect" was investigated for two central pyrolysis features: *pyrolysis rate* and *pyrolysis time* (*duration*).

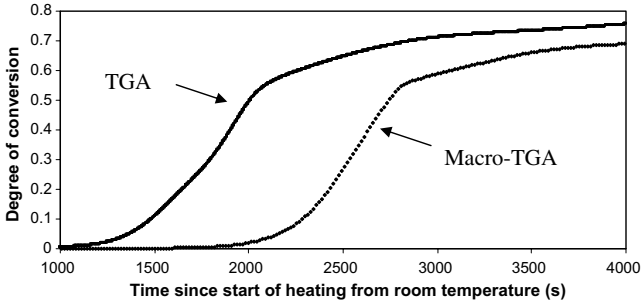

Fig. 7. Degree of conversion as a function of time for coffee waste (CW). Heating rate: 10 °C/min.

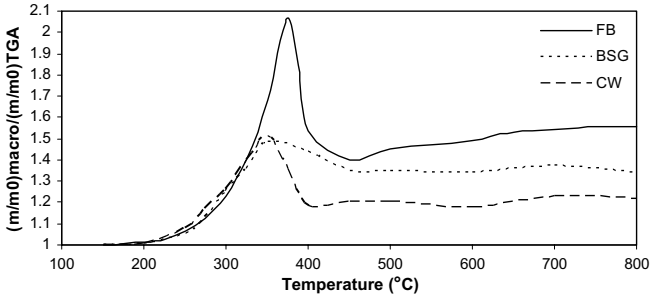

Fig. 8. Ratio of (m/m_0) ratios at the two scales for the three samples. Heating rate: 10 °C/min.

Fig. 8 shows the ratio of (m/m_0) ratios for macro-TGA and TGA experiments and is therefore a quantification of the *differential pyrolysis rate*: a ratio higher than 1 shows that the pyrolysis rate is lower in macro-TGA than in TGA. The higher the ratio, the bigger the differential. The profile exhibited in Fig. 8 is similar for BSG and CW with a top value of about 1.5. FB exhibits a higher differential peak value, most probably because of its large particle size. The highest differentials occur between 300 and 400 °C.

Fig. 9 shows the temperature difference (between TGA temperature and reactor temperature for macro-TGA) to reach a given degree of conversion $(1 - Y)$. The temperature difference is equivalent to a time difference and is therefore a way of quantifying the differential pyrolysis time (time necessary to reach a certain degree of conversion) at the two scales. The "temperature difference" curves of the fuels are similar. During the main part of the pyrolysis, the temperature difference between the two scales is stable at about 50 °C (i.e. 5 min) until a degree of conversion of 0.6. After this point, the temperature difference/time difference to reach the same degree of conversion increases strongly. This shows that completion of pyrolysis in the macro-TGA takes a longer period of time compared to TGA. To reach a degree of conversion of 0.7, BSG and CW in macro-TGA exhibit a time difference of 18–19 min with TGA, while this difference was only 6–7 min to reach a degree of conversion of 0.6. This translates the important slowing down of pyrolysis conversion in macro-TGA compared to TGA.

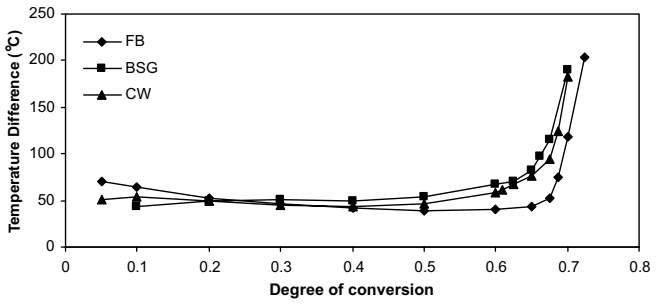

Fig. 9. Temperature difference (macro-T – TGA-T) versus degree of conversion. Heating rate: 10 °C/min.

4. Conclusion

The main findings of this study can be summarised as follows:

(a) Qualitative evaluation of the thermal history – three temperature regimes have been identified: (1) exponentially increasing temperature, (2) linearly increasing temperature and (3) 2-slope increasing temperature with a flattening period. The regime at a given point will depend on the sample weight, the reactor temperature and the location in the sample.
(b) Quantitative evaluation of the thermal history: significant temperature gradients were measured, with a maximum radial gradient of 167 °C/cm for coffee waste at a reactor temperature of 900 °C. This will affect the pyrolysis process.
(c) The step-by-step pyrolysis chemistry was described and discussed (10 °C/min heating rate). By use of a novel concept, i.e. intra-sample heating rate, the exothermic step of pyrolysis was shown. It is related to char and/or char-forming reactions.
(d) The comparative study of weight loss in TGA and macro-TGA (10 °C/min heating rate) was performed to investigate the ''scaling effect''. Pyrolysis time and pyrolysis rate differences were characterised and quantified.

Acknowledgements

This work has been part of the ''Environment and Process Management'' research program, funded by the Research Council of Norway. The main author expresses his gratitude to the Nordic Graduate School of Biofuels Science and Technology (biofuelsGS) for providing financial support.

References

[1] Grønli M. A theoretical and experimental study of the thermal degradation of biomass. PhD dissertation, NTNU, Norway; 1996.
[2] Grønli MG, Várhegyi G, Di Blasi C. Thermogravimetric analysis and devolatilization kinetics of wood. Ind Eng Chem Res 2002;41:4201–8.
[3] Várhegyi G, Antal Jr MJ, Jakab E, Szabó P. Kinetic modeling of biomass pyrolysis. J Anal Appl Pyrolysis 1997;42:73–87.
[4] Mészaros E, Várhegyi G, Jakab E. Thermogravimetric and reaction kinetic analysis of biomass samples from an energy plantation. Energy Fuels 2004;18:497–507.
[5] Bridgwater AV. Renewable fuels and chemicals by thermal processing of biomass. Chem Eng J 2003;91:87–102.
[6] Bryden KM, Ragland KW, Rutland CJ. Modeling thermally thick pyrolysis of wood. Biomass Bioenergy 2002;22:41–53.
[7] Di Blasi C. Influences of physical properties on biomass devolatilisation characteristics. Fuel 1997;76:957–64.
[8] Babu BV, Chaurasia AS. Parametric study of thermal and thermodynamic properties on pyrolysis of biomass in thermally thick regime. Energy Convers Manage 2004;45:53–72.
[9] Galgano A, Di Blasi C. Modeling wood degradation by the unreacted-core-shrinking approximation. Ind Eng Chem Res 2003;42:2101–11.
[10] Becidan M, Skreiberg Ø, Hustad JE. Products distribution and gas release in pyrolysis of thermally thick biomass residues samples. J Anal Appl Pyrolysis 2007;78:207–13.
[11] Grøndal J. Utilization of brewer spent grains fractions as ingredients in the food and feed industry. An industrial research education programme under the Danish academy of technical sciences, Project No. 244; 1990.
[12] Mussatto SI, Dragone G, Roberto IC. Brewer's spent grain: generation, characteristics and potential applications. J Cereal Sci 2006;43:1–14.
[13] Santos M, Jiménez JJ, Bartolomé B, Gómez-Cordovés C, del Nozal MJ. Variability of brewer's spent grain with a brewery. Food Chem 2003;80:17–21.
[14] Zevenhoven R, Axelsen EP, Kilpinen P, Hupa M. Nitrogen oxides from nitrogen-containing waste fuels at FBC conditions – Part 1. Presented at the 39th IEA FBC meeting, Madrid, Spain; November 2–24, 1999.
[15] Bilbao R, Arauzo J, Murillo MB, Salvador ML. Gas formation in the thermal decomposition of large spherical wood particles. J Anal Appl Pyrolysis 1997;43:27–39.
[16] Rath J, Wolfinger MG, Steiner G, Krammer G, Barontini F, Cozzani V. Heat of wood pyrolysis. Fuel 2003;82:81–91.
[17] Ahuja P, Kumar S, Singh PC. A model of primary and heterogeneous secondary reactions of wood pyrolysis. Chem Eng Technol 1996;19:272–82.
[18] Milosavljevic I, Oja V, Suuberg EM. Thermal effects in cellulose pyrolysis: relationship to char formation processes. Ind Eng Chem Res 1996;35:653–62.
[19] Strezov V, Moghtaderi B, Lucas JA. Computational calorimetric investigation of the reactions during thermal conversion of wood biomass. Biomass Bioenergy 2004;27:459–65.
[20] Schröder E. Experiments on the pyrolysis of large beechwood particles in fixed beds. J Anal Appl Pyrolysis 2004;71:669–94.
[21] Becidan M, Várhegyi G, Hustad JE, Skreiberg Ø. Thermal decomposition of biomass residues. A kinetic study. Ind Eng Chem Res 2007;46:2428–37.
[22] Bouvier JM, Charbel F, Gelus M. Gas–solid pyrolysis of tire wastes – kinetics and material balances of batch pyrolysis of used tires. Resour Conserv 1987;15:204–14.